EXPOSURE MATTERS: EFFECTS OF ENVIRONMENTALLY REALISTIC EXPOSURE CONDITIONS ON TOXICITY OF MODEL NANOMATERIALS TO DAPHNIA MAGNA

By

Fatima Nasser

A thesis submitted to the University of Birmingham

for the degree of Doctor of Philosophy

UNIVERSITY OF BIRMINGHAM

School of Geography, Earth and Environmental Science

College of Life and Environmental Sciences

University of Birmingham

July 2017

'There's plenty of room at the bottom' – Richard Feynman

Abstract

Nanomaterials (NMs) can be defined as having at least one external dimension between 1-100nm. Due to their small size, NMs have a large surface area giving them characteristics that differ from bulk material. NMs are incorporated into numerous applications making environmental exposure to NMs likely. Increased reliance on plastic results in accumulation of nano-plastics in fresh waters. Polystyrene (PS) acts as a representative of both nano-plastic and NMs. The deposition of gold (Au) NMs is also likely due to their use in medical applications so that both PS and Au have a potential to interact with environmental organisms. *Daphnia manga (D. magna)* is an ideal candidate in fresh water toxicity testing. Toxicity, uptake and retention of NMs by organisms is dependent on several factors such as NM charge, shape, chemical composition and the absorption of natural biomolecules binding to the surface of the NM creating an eco-corona, altering stability of the NMs thereby changing their toxicity. This work investigates the toxicity of PS and Au NMs and explores the effects of charge, shape, presence of a corona and the impact of realistic modes of presentation of NMs to *D. magna* and how these factors impact toxicity, uptake, retention and depuration.

Research Summary

Nanomaterials (NMs) can be defined as having at least one external dimension between 1-100nm. Due to their small size, NMs have a large surface area to volume ratio giving them unique characteristics that differ from bulk material of the same chemical composition. As a result, these novel materials have found numerous applications in medical and industrial fields with the result that environmental exposure to NMs is increasingly likely. In parallel, increased reliance on plastic, which degrades extremely slowly in the environment, is resulting in increased accumulation of micro- and nano-plastics in fresh and marine waters, whose ecotoxicological impacts are as-yet poorly understood. Polystyrene (PS) can act as a useful representative of nano-plastic and NMs. The deposition of gold (Au) NMs is also likely due to their wide use in medical applications. Thus, both PS and Au NMs have a large potential to interact with environmental compartments and organisms.

Daphnia magna (D. magna) is a fresh water organism that takes up material via filter feeding, making it an ideal candidate in fresh water toxicity testing. Toxicity, uptake and retention of NMs by organisms is highly dependent on several factors such as NM charge, shape, chemical composition as well as exposure related factors such as the absorption of natural biomolecules binding to the surface of the NM creating an eco-corona which can alter the stability of the NMs thereby changing their toxicity, and the presence or absence of other food sources during uptake of NMs.

The aim of this work was to investigate the toxicity of PS and Au NMs and explore the effects of NM charge, shape, the presence of a corona and the impact of realistic modes of presentation of NMs to *D. magna* and to understand how these factors impact NM toxicity, uptake, retention and depuration.

Positive and negative charged PS NMs were used to investigate the impact of charge on *D. magna* survivorship. The release of proteins by *D. magna* was also quantified and it was found that both types of charged PS NPs agglomerated in protein containing medium, with longer incubation times leading to a greater degree of agglomeration. The increase in size due to the destabilization of the NMs by the proteins present in the conditioned medium caused both types of NMs to become a more attractively sized food source for *D. magna* and therefore the release of proteins by *D. magna* into the medium decreases survivorship in the presence of NMs, with longer incubation times leading to a more detrimental effect. Positively charged NMs were overall more toxic than negatively charged ones. *D. magna* were also exposed to negatively charged fluorescent PS NMs, and steadily uptake the NMs during their exposure time (1-3 hours). After 6 hours of post-exposure, *D. magna* were able to remove the majority of PS NMs, though approximately 15% remained in the gut. PS NMs that had been previously incubated in protein contained medium before exposure had a greater retention, with 20% of the corona-coated PS NMs remaining within the gut, suggesting the presence of an absorbed corona increases retention. The corona-bound PS NPs NMs remaining within the gut subsequently decreased the grazing of *D. magna* on algae *C. vulgaris* for at least 6 hours. Both positively charged 'bare' and 'corona-coated' PS NMs caused no delay ($p > 0.05$) in the moulting pattern of *D. magna.* This work provides a significant insight into how naturally released proteins radically impact the stability, toxicity and retention by *D. magna* of NMs that are released into environmental waters.

Gold NMs of different charge (positive and negative) and shape (sphere, short rod, long rod) were investigated in terms of toxicity to *D. Magna*, with positively charged NMs being substantially more toxic than negative. With regards to shape, the ranking of toxicity to *D. magna* was spheres being most toxic, followed by short rods and then long rods when assessing mass concentration exposure. Assessment of survivorship based on number concentration was especially insightful when considering NMs of different size and shape and showed that toxicity results were strikingly different with long rods being the most toxic,

followed by short rods then spheres. Charge per surface area also showed to be an important modulator of toxicity. Gold NMs were also assessed in terms of reactive oxygen species (ROS) formation and recovery where negatively charged NMs only prompted minimal amount of ROS. At high exposure concentrations (EC_{40}), positively charged spheres prompted a high degree of ROS though *D. magna* were able to return to steady-state levels within 8 hours, whereas comparatively, when exposed to positively charged rods *D. magna* also prompted a similar high degree of ROS though were unable to recover fully from the stress, in agreement with survivorship results. *D. magna* that had been exposed to high concentrations (EC_{40} for positively charged and EC_{10} for negatively charged NMs) of NMs that had been previously incubated in protein contained medium showed a similar recovery pattern from ROS for all shapes and charges of NMs compared to those without an incubation step, except for *D. magna* that had been exposed to positively charged spheres which had significant death and did not reach the recovery phase due to spherical NMs agglomerating in protein contained medium, increasing their size causing an increase in uptake and consequently toxicity towards *D. magna.* Both positively charged spheres and rods caused a partial inhibition of moulting indicating that mechanisms of Au toxicity may be chemical (ROS formation) and physical (moulting).

Presentation mode of two differently sized PS NMs (small, 50 nm and large, 500 nm) to *D. magna* was assessed to determine if the presence of the algal *C. vulgaris* food source during different stages of the feeding cycle impacted uptake and depuration of NMs. *D. magna* were able to clear the majority of large NMs with only a residual amount remaining within the gut (approximately 10%) at 6 hours of post-exposure, which is accounted for by a minimal amount of NMs becoming trapped in the gaps of the bush border within the gut. Particles that get trapped in the bush boarder are not easily brushed away by microvilli. A higher amount (approximately 45%) of the smaller NMs was retained within this same time span. *D. magna* that were fed *C. vulgaris* during the excretion phase increased the clearance of both types of NMs at 1 hour post-exposure though ultimately the same amount of NMs remained within

the gut at 6 hours of post-exposure compared to the organisms with no feeding step, indicating that the presence of incoming food pushes out previously ingested material though this depends on the location of the NMs within the gut. NMs existing within the lumen may easily be pushed out by subsequently ingested food, while NMs located in the gaps of the bush border are more prone to retention and that larger NMs were more heavily located in the lumen whilst smaller NMs were located more in the gaps of the bush border. Both types of NMs, when incubated in the algal food source before exposure, have an increased uptake by *D. magna* as NMs are incidentally ingested along with the food source. Smaller NPs are cleared more effectively when travelling along the gut with the food source as they have a decreased likelihood of becoming stuck in the gaps of the bush boarder, though both large and small NMs still have a residual amount remaining within the gut after 6 hours of post-exposure. *D. magna* that had previously been fed on the algal food source showed a decrease in uptake of the larger PS NMs though uptake the same amount of the smaller PS NMs occurred, indicating that larger NMs are actively taken up while smaller NMs may have a passive uptake that happens even when the organisms are not actively feeding. Smaller PS NMs also show a strong tendency to agglomerate in protein contained medium only at longer incubation times while larger PS NMs remain stable. It was also confirmed that *D. magna* released a minimal amount of carbohydrates into their surrounding medium compared to a much larger concentration of proteins.

Graphical Abstract

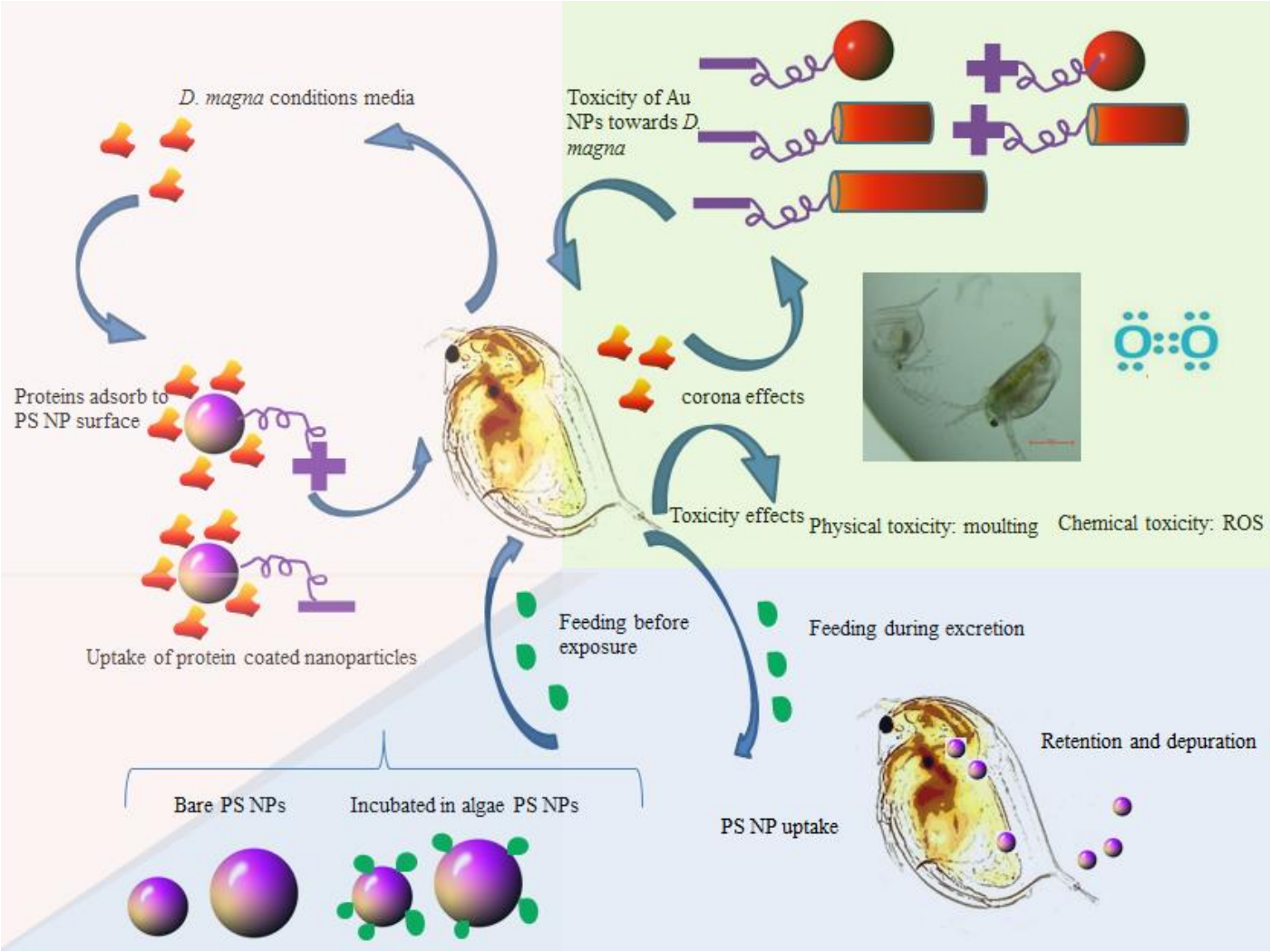

Acknowledgements

I would like to thank my supervisor Professor Iseult Lynch for being a pillar of support, for her enthusiasm throughout my project, her encouragement with paper writing and for consistently enhancing my career development with award applications.

I would also like to thank my co-supervisor Professor Eugenia Valsami-Jones for her support and interest in my work.

I gratefully acknowledge EU FP7 project FutureNanoNeeds which provided the funding for this project which opened a plethora of opportunity for me. I would also like to extend my thanks to the College of Life and Environmental Sciences Daphnia facility where parts of the research were undertaken and for the invaluable training with daphnia that I have received. I would like to thank Paul Stanley for the preparation of the epoxy-resin embedment samples via the electron microscopy facility. Thank you to Dr. Alessandro Di Maio for his training on the confocal microscope. I would also like to extend my gratitude to Dr. Jinglei Yu for analysis of the proteomics mass spectrometry samples.

I would like to thank several members of the lab who have become wonderful friends, for their incredible amount of support and who have made WG1 a fun place to work, including Laura Ellis, Sophie Briffa, Emily Guggenheim, Maria Thompson, Tassos Papadiamantis and Christine Elgy.

Last but not least, my heartfelt thanks go to Adam- my eternal cheerleader- for your patience and for being a source of unwavering support in every aspect.

Table of Contents

List of Figures

List of Tables

List of Abbreviations

ADP	Adenosine diphosphate
APS	ammonium persulphate
Au	Gold
ATP	Adenosine triphosphate
BCA	Bicinchoninic acid
BSA	Bovine serum albumin
BSI	British standards institution
C. vulgaris	*Cholera vulgaris*
CIT	Citrate
COOH	Carboxylic acid
CTAB	Cetyl trimethylammounium bromid
CM-H_2DCFDA	Chloromethyl-dichlorodihydrofluorescein diacetate
CNT	Carbon nanotubes
DCS	Disc centrifugation sedimentation
DI	Deionized
DLS	Dynamic light scattering
D. magna	*Daphnia magna*
D. pulex	*Daphnia pulex*
EC_{50}	Half-maximal effective concentration
EU	European union
EPS	Extracellular polymeric substances
FNN	Future nano needs

g	Grams
h	Hour
H_2O_2	Hydrogen peroxide
H_2SO_4	Sulfuric acid
HAS	Human serum albumin
HH	High-Hardness
kDa	Kilodalton
L	Litre
LSCM	Laser scanning confocal microscopy
mg	milligram
mL	Millilitre
MP	Microplastic
MPA	Mercaptopropionic acid
n	moles
NH_2	Amino
NM	Nanomaterial
nm	nanometer
NOM	Natural organic matter
$OH^{\cdot}$	Hydroxyl radical
$O_2^{\cdot-}$	Superoxide anion
NP	Nanoparticle
OECD	Organization for Economic Cooperation and Development
PAGE	Polyacrylamide gel electrophoresis

PAH	Poly(ally amine) hydrocholride
PBS	Phosphate buffered saline
PDI	Polydispersity index
PE	polyethylene
PES	polyester
PEG	Polyethylene glycol
PET	Polyethylene terephthalate
PS	Polystyrene
RB-ITC	Rhodamine B- Isothiocynate
RI	Refractive index
ROS	Reactive oxygen species
SDS	Sodium Dodecyl Sulphate
SOD	Superoxide dismutase
SOP	Standard operating procedure
SPR	Surface Plasmon Resonance
SSA	Specific surface area
TEM	Transmission electron microscopy
TEMED	tetramethylethylenediamine
t	time
UV-Vis	Ultra-violet Visual
WWTP	Waste-water treatment plant

1

Introduction

Nanoparticles (NPs) can be described as having each of their dimensions between 1-100 nm as described by the British Standards Institution (BSI), whereas nanomaterials (NMs) are described as having at least one dimension less than 100 nm (BSI, 2007) so that NPs are a sub-set of NMs. Due to their small size NMs have a large surface area to volume ratio, giving them unique properties that differ from those of bulk material of the same chemical composition. NMs provide novel characteristics that can be used in many fields of research such as drug delivery and electronics, although limited research has been conducted on the effect NMs may have on environmental species once deposited into environmental waters from industrial effluent and from consumer products. A fundamental point to consider is the fate and transport of NMs through the environment and how different biological molecules naturally existing in environmental waters may adsorb to NM surfaces, ultimately changing their identity, stability, and toxicity to organisms. It is equally as important to study the format and presentation of NMs to organisms and how diverse exposure scenarios may lead to different effects. In this thesis, the model organism utilized to address some of these questions is the freshwater indicator species *Daphnia magna (D. magna)*. The focus of the thesis is to gain new insights into the stability, uptake and depuration of NMs, and their toxicity to *D. magna* as a basis to understand their transformation in the environment. *D. magna* are model organisms prone to take up a range of particulate in the water column as a result of their filter feeding mechanism, and are known to be highly sensitive to toxicants making them an ideal organism for nano-ecotoxicological studies.

1.1 Nanomaterials and their Importance as a key enabling technology

NMs are described as having at least one external dimension less than 100 nm (Auffan et al., 2009). The small size of NMs provides a high specific surface area which in turn gives NMs many unique characteristics that differ from bulk material. These exclusive properties make NMs ideal candidates to be used in areas such as drug delivery where the small size and high surface area allows for a high amount of drug loading and potential for targeting (Tong et al., 2012) and in cosmetics where NMs such as zinc oxide provide UV deflection properties (Pardeike et al., 2009). Given their enormous range of application areas, the European Union (EU) considers NMs a priority investment area and has established the Nanosciences, Nanotechnologies, Materials and New Production technologies (NMP) theme within the 7th Framework Programme (FP7) funding projects addressing nanosafety. The FutureNanoNeeds (FNN) project, which supported the work undertaken in this thesis and aims to create a gold-standard in NM safety assessment based on state-of-the-art research, was funded via FP7. The EU FP7 also provides an opportunity for EU-USA transatlantic research collaboration and thus has largely capitalized on research investment in NM safety (Xing et al., 2016). Horizon2020 projects will provide further funding of € 77 billion dedicated to NMs research (Winkelmann and Bhushan, 2016).

While many of the most-used NMs currently (the so-called legacy NMs) are smaller forms of existing well-regulated spherical micron particles such as titanium dioxide (used in many food products and sun creams) and silicon dioxide (as an additive in food) (Yang et al., 2014), there has been an increasing interest in different shaped and charged NMs for future applications including in energy capture conversion and storage. These structurally and compositionally complex NMs provide a variety of morphologies and surface functionalities which in turn display properties that are not as apparent in spherical legacy NMs. These new characteristics have caused differently shaped NMs to be a fascinating new field of scientific and regulatory research as they are the focus of many new scientific-based products and future product developments, though these same properties need to be investigated in terms

of toxicity. For example, differently shaped NMs may have differential interactions with protein receptors on cells so that only specific shapes may prompt internalization or of varying degrees, where the order of NM uptake by shape, for identical composition, has been shown to be rods, spheres, cylinders and finally cubes though this order is dependent on aspect ratio of NMs, ligand type and NM (Albanese et al., 2012).

Due to the increased use of NMs, their deposition into the environment is inevitable and limited research has been conducted on the effects of NMs on environmental organisms and even less has been conducted under realistic environmental scenarios. The FutureNanoNeeds project through which the work for this thesis was funded, was tasked with assessing the applicability of current regulatory approaches for these so called 'future NMs'. The work in this thesis focuses specifically on the ecotoxicity of NMs with various properties such as charge (positive and negative) and shape (sphere or rod) and composition (polystyrene and gold) on the model organism *D. magna* under realistic environmental conditions, which include the presence of food and biomolecules and how this influences NM stability, toxicity and retention of NMs by *D. magna*.

1.2 Descriptions and Types of Nanomaterials

NMs can be generated in three different ways; naturally occurring are those that are produced in nature; incidental NMs are the by-product of other reactions; and manufactured (or engineered) NMs are purposely made in industry such as legacy and future NMs. The international organization for standardization (ISO) has described manufactured NMs as those purposely produced to have specific properties for commercial use (Hatto, 2011) and will be the type of NMs investigated throughout this thesis.

1.2.1 Naturally Occurring NMs

Naturally occurring NMs are created by the environment and are a subcategory of colloids where they can consist of various biological and physical entities (Baalousha and Lead,

2007). Natural NMs are found frequently in natural waters and can be produced by the environment itself or secreted by organisms (Buffle et al., 1998). With regards to NMs existing biologically, essential building blocks of organelles within cells such as polypeptides and polysaccharides exist within nano-dimensions. Many bacteria have been shown to precipitate extracellular NMs as a means to reduce the toxicity of high ion concentrations as seen with *S. oneidensis* producing 30 nm spherical gold NMs and *E. coli* precipitating 20 nm triangular and hexagonal gold NMs (Li and Hu, 2011). Viruses are commonly found in the environment and transfer DNA into a host genome for protein expression and are of different sizes in the nano-sized range (Gelderblom, 1996). NMs are also produced environmentally though physical means where natural volcanic eruptions and the crystallization of Calcite rock release nano-dimensional ash (Hochella, 2002). Clay particles have also been shown to have a stable and monodisperse nano-fraction under 100 nm (Dominika Dybowska et al., 2015) along with water vapour from oceans releasing aerosols under 80 nm before forming into cloud droplets (Lawler, 2014). The length of time in which natural NMs remain in nano-sized dimension depends on their environmental surroundings where the dynamic nature of environmental niches can influence NM size and stability. Saturated environmental fluids often have solutes precipitating out of solution that are nano in size though these NMs quickly grow to the micron range. The presence of naturally occurring NMs can lead to significant challenges in terms of distinguishing manufactured NMs against a high background of naturally occurring nano-scale materials.

1.2.2 Incidental NMs

NMs can also be made incidentally as a by-product in processes through combustion (Dunphy Guzman et al., 2006). Incidental NMs are also formed through exhaust from vehicles and by methods such as welding (Biswas and Wu, 2005) and cooking (See and Balasubramanian, 2006). These NMs can be released into the atmosphere and it is widely recorded that incidentally created particles less than 10 μm can lead to a detrimental effect

on the respiratory system (Soto et al., 2005). It has also been noted that ultra-fine NMs (less than 100 nm) causes increased pulmonary damage compared to fine particles (less than 2.5 μm) (Renwick et al., 2001) as the smaller ultrafine NMs can travel deeper into the lungs and (i) trigger an immune response by white blood cells causing inflammation; (ii) adsorb a greater quantity of proteins on their surface which allow the NMs to be transported across cell membranes and; (iii) prompt the production of lethal substances such as reactive oxygen species (ROS), of which more detail will be given later in this chapter, which can lead to cell death via necrosis (Borm and Müller-Schulte, 2006). On average about 50,000 kg of NMs are released into the atmosphere each year incidentally as a by-product of combustion reactions, including coarse particulate ranging from 2.5-10 μm (particle mass fraction (PM_{10}) (Borm and Müller-Schulte, 2006). An important incidental NM to consider is the formation of micro and nano plastics resulting from the degradation of larger plastics deposited into the environment. Polystyrene (PS) can act as a model to mimic microplastics which will also be the focus of two results chapters where chapter 3 will address toxicity of differently charged PS NMs and how natural biomolecules present in the water alter this, and their subsequent uptake and release by *D. magna* and chapter 5 will investigate realistic exposure scenario presentation modes of different sized PS NMs to *D. magna.* PS can be conveniently labelled with fluorescent tags so that they can be visualized, and their surface can be functionalised easily making them useful for assessment within assays.

1.2.2.1 Micro and nano plastics in environmental waters

An incidental type NM of great and increasing importance is the plastic NMs created from the degradation of larger plastics deposited into environmental waters as a result of the rapid increase of plastic production, which reached 230 million tonnes in 2009. While the benefits of plastic production are undeniable, the deposition of these plastics into the environment is a growing concern (Cole et al., 2011). Manufactured plastics released into environmental waters undergo a very slow degradation process of over a hundred years (Gewert et al.,

2015), causing plastic to be an internationally documented contaminant (Cole et al., 2011). The eventual degradation of larger plastics results in the accumulation of microplastics (MPs) (< 5 mm) who's further wearing is likely to result in NM plastic debris, although limitations in detection capability and the fact that larger particles mask the detection of smaller ones makes their detection and quantification challenging. Primary MPs are micron sized and the further wearing of the primary plastics result in secondary MPs including those in the nano range (Duis and Coors, 2016). To date, elimination of these incidentally created plastic NMs has not been accounted for in waste water treatment plants as in the primary treatment of waste water plants, larger solids are eliminated using filters with pore sizes of approximately 20-50 μm allowing micro and nano plastics to effortlessly pass through (Duis and Coors, 2016). Recent studies indicate the release of polyethylene terephthalate (PET) polyester MP fibres from fleece clothing during wash cycles with fibres released as high as 0.021 weight percent in the first wash and continuing to be released even after ten washes, fibres of which are then released into wastewater effluent (Pirc et al., 2016). A study of WWTP effluent found that the concentration of MPs with sizes less than 500 μm is 0.08-8.9 MP/L, of which PS was in the top 5 most abundant MPs identified (along with polyethylene (PE), polyvinyl alcohol, polyester (PES), PS and polyamide (PA)) as cited in Duis and Coors, 2016. 7% of these MPs <500 μm were not removed in the final filtration step, which must reach fresh water systems (Duis and Coors, 2016). MP litter is an important issue and has been identified in many fresh water systems. Due to their small size, MPs are bioavailable to organisms and their large surface area to volume ratio makes them a likely candidate to bind to organic contaminants and to release toxic plasticisers and therefore may be presenting potent contaminants at the bottom of the food chain (Teuten et al., 2009). Thus, the presence of micro and nano plastics in environmental waters is a growing concern, and PS NMs can be used as a dual representative of both manufactured and incidental NM characteristics and will be investigated as such in this thesis.

1.2.3 Industrially Manufactured NMs

The last type of NMs are manufactured NMs that are purposely made for industrial use. Manufactured NMs have been incorporated into a vast array of applications such as the use of rod shaped nano sized gold in cancer treatment due to their increased photothermal capacity (Letfullin et al., 2011, Jain et al., 2006) or silver NMs being used in antimicrobial products due to their ability to release toxic silver ions (Sondi and Salopek-Sondi, 2004). Table 1.1 lists the various applications that some of the main industrially manufactured NMs have been incorporated into. This is not a complete list of all NMs and is to only illustrate the diversity of NMs and their applications, rather than an exhaustive review of all NMs. Gold NMs are an industrially manufactured NM which are used in medical applications and are largely deposited into environmental waters. The effect of size, shape and surface charge of gold NMs on *D. magna* is the focus of chapter 4 and therefore is expanded upon after the table summary.

Table 1.1. Various types of industrially manufactured nanomaterials and their unique characteristics.

Nanomaterial	Industrial Application	Characteristic	Reference
gold	Medical	Photothermal capacity	(Letfullin et al., 2011)
polystyrene	Biosensors	Monodispersity	(Loos et al., 2014)
Supermagnetic iron oxide NPs	Medical Imaging	Contrast agent	(Shan, 2009)
graphene	Aeronautics	Intrinsic strength	(Lee et al., 2008)
silver	Antimicrobial (coatings, wound dressings etc.)	Dissolution of silver ions	(Sondi and Salopek-Sondi, 2004)
carbon nanotubes	Drug delivery	Hollow interior	(Bianco et al., 2005)
zinc oxide	Incorporation into textiles	UV-blocking properties	(Becheri et al., 2008)
copper oxide	Integration into concrete	Flexural strength	(Arefi and Rezaei-Zarchi, 2012)

1.2.3.1 Gold NMs

There has been a drastic increase in the use of spherical gold NMs in the field of medicine, for instance, the binding of NMs to antibodies specifically targeted for cancer cells (Letfullin et al., 2011). Gold nano-rods which differ in dimension to spherical NMs are also being tested for use in cancer therapy as they have a higher absorption efficiency (approximately 14) compared to other shaped NMs such as nano-spheres or hybrid silica-gold nano-shells whose absorption efficiencies range between 3.5-4.02 (Letfullin et al., 2011). This absorption

efficiency refers to optical absorption, an intrinsic property of a gold NM based on size and shape to convert absorbed light into heat. The higher absorption efficiencies of gold NM rods (as well as spheres and hybrid NMs) make gold NMs excellent photo absorbers, converting radiated light to heat which can be harnessed in order to eradicate cancer cells. This also indicates that change in NM shape can fundamentally affect NM characteristics. The increased use of differently shaped gold NMs in the medical field, where the annual use of gold NMs is estimated at approximately 540 kg in the United Kingdom and where the predicted environmental concentration (PEC) in surface waters is estimated to be 468 pg/L (Mahapatra et al., 2015), calls for further investigation of the effects of deposited gold NMs in the environment and their toxicological effects towards aquatic organisms.

1.3 Unique Characteristics of NMs

NMs made for commercial purposes are widely used due to their characteristically small size causing a larger number of atoms to be situated at the surface of the NM compared to the bulk form (Auffan et al., 2009). The following sections discuss size, specific surface area (SSA) and charge which have been identified as important characteristics of NMs which give them unique attributes that allow them to be extensively used in various industrial fields and considers how each of these parameters impacts toxicity towards water based organisms such as *D. magna* which will be the model organism used to assess toxicity and uptake throughout this thesis.

1.3.1 Families of NMs

There are several families of manufactured NMs, which have their own characteristics making them suitable for the field they are used in. By the same token, not all characteristics apply to every type of NM and referring to all NMs as a single group is misleading. Table 1.2 is a brief summary of some of the various NM families and the unique characteristics exhibited by that class of NM (Bhatia, 2016).

Table 1.2. Families of different types of manufactured NMs and their corresponding characteristics.

NM Family	Size (nm)	Unique features
Metal and metal oxide	<100	Large SA for functionalization
Polymer	10-100	Biodegradable and biocompatible
Dendrimer	<10	Highly branched
Carbon Nanotubes (CNT)	<5 diameter, 20-100 length	High aspect ratio, tensile strength and electrical characteristics
Liposome	50-100	Phospholipid vesicles, excellent encapsulation ability, biocompatible
Nanocrystals (Quantum dots)	<10	Semi-conductive, fluorescent, photostable

1.3.2 Size and specific surface area of NMs

As particle size decreases this may cause changes in crystal shape, thermodynamic and other properties (Auffan et al., 2009). NMs have a large SSA, which causes NMs to have a heightened surface energy which increases their reactivity due to the increased availability of atoms present for reaction. As particle size decreases there is also an exponential surge in band gap between atoms due to lattice contractions which favour specific electronic states of metal and metal oxide NMs (Kelly et al., 2003) which are not achieved with larger particle sizes. Smaller NM size also influences thermodynamic characteristics and can be seen by decreased melting points of metal NMs when the size decreases from 100 to 10 nm, due to increasing abnormalities in the lattice structure of the NMs (Auffan et al., 2009), which can also affect the magnetic properties of the NM. These heightened characteristics of NMs allow for increased efficiency in commercial products though their potential health effects on the

environment and living organisms must be considered as NMs could have heightened toxicity compared to larger bulk material.

1.3.3 Shape and charge

Generally, during the synthesis of NMs, surfactant molecules are added which bind to the NM surface, which stabilize the NM against agglomeration by a repulsive force and to also control NM growth in terms of size and shape. Depending on the type of NM and surfactant used, shape control can also be achieved by the surfactant binding to certain crystal faces in preference to others (Sperling and Parak, 2010). The use of different surfactants to control shape and stabilization is one of the challenges in comparing NMs, as different surfactants used to produce NMs of different shapes will cause the NMs to have different surface properties and thus differences in toxicity effects could be from NM shape or the surfactant itself. Quite often NMs are coated with ligands which control the size of the NM during synthesis and also limit NM agglomeration for example; the presence of the polymeric ligand, polyvinylpyrrolidone (PVP) on gold NMs providing steric stabilization (Seol et al., 2012) and the presence of citrate (CIT) on the surface of gold NMs providing charge stabilization (Tejamaya et al., 2012). A number of factors can govern repulsion such as electrostatic repulsion, steric repulsion or addition of a hydration layer. Coatings need an attractive force in order to bind to the NM such as chemisorption, electrostatic attraction or hydrophobic interaction which is commonly achieved via the head group of the ligand (Sperling and Parak, 2010). Certain types of ligands are more likely to bind to certain surfaces such as thiol groups to gold (Sperling and Parak, 2010). Some NMs are stabilized via electrostatic repulsion by charged coatings on the surface such as gold NMs being synthesised via CIT reduction where the resulting NMs acquire negatively charged CIT molecules on their surface and therefore are stabilized through electrostatic repulsion (Sperling and Parak, 2010).

The surface of NMs are usually altered with functional groups which also affect NM stability and it has been shown that positively charged gold NMs are more stable than negative in

moderately hard test water (Dominguez et al., 2015) though stability of NMs is dependent on ionic strength and stability measurements taken in deionized (DI) water may not represent the stability of NMs in medium containing different salts; of varying pH's or a combination of both in real environmental waters. It has been established that the charge at the NM surface is a major influence on toxicity, though this may be changed when interacting with other salts or ions present in biological media. Interestingly, bonds between an NM such as gold and an electron donating end group of a coating such as thiol, usually undergo a continual binding and unbinding, which means that coatings can be easily removed by mass attraction of another more dominant ligand which might alter the stability of the NMs. This is extremely important as natural biomolecules such as proteins or carbohydrates naturally existing in environmental waters may have a higher affinity for the deposited NM compared to its original coating and may replace it influencing its stability. Also in the case of environmentally acquired coatings, initially bound ligands or macromolecules in high abundance may be displaced by those of lower abundance but with higher affinity for the NM surface over time (Cedervall et al., 2007).

1.4 Effect of deposited NMs on environmental organisms

1.4.1 Deposition of NMs into the environment and its implications

With the heightened incorporation of NMs into a range of industrial processes, the release of NMs into environmental sectors is unavoidable. The small size of NMs provides them with exclusive physiochemical characteristics which make them attractive candidates for industrial processes, though it is these same properties that can prompt physiological reactions within organisms upon exposure. The projected use of NMs manufactured and used in industrial processes is estimated to be half a million tonnes by 2020 (Stensberg et al., 2011). There are various entry mechanisms for NMs to enter the environment (Mueller and Nowack, 2008) though it is challenging to evaluate concentrations of manufactured NMs

present in the environment at a specific point for several reasons; 1) NMs entering the environment at low (ng/L) concentrations (Weinberg et al., 2011); 2) characterization of NMs at these levels depends on the detection limit of instruments; 3) the high amount of already naturally existing colloids in the environment (as discussed previously in section 1.2.1) makes it difficult to distinguish manufactured NMs; and 4) the incapability of instrumental methods to separate manufactured NMs from an environmental sample without altering the original sample. Table 1.3 is a summary of commonly used NMs and their predicted environmental concentrations from their various entry pathways.

Table 1.3. Different types of NMs and their predicted environmental concentrations under various environmental entry pathways.

NM	Pathway	PEC	Reference
Au	Surface water	468 pg/L	(Mahapatra et al., 2015)
	Effluent	440 pg/L	(Mahapatra et al., 2015)
	Sludge	124 µg/kg	(Mahapatra et al., 2015)
carbon-based	Surface water	0.001–0.8 ng/L	(Mueller and Nowack, 2008)
	Effluent	3.69–32.66 ng/L	(Gottschalk et al., 2009)
	Sludge	0.0093–0.147 mg/kg	(Gottschalk et al., 2009)
Ag	Surface water	0.088–10 000 ng/L	(Mueller and Nowack, 2008)
	Effluent	0.0164–17 μg/L	(Gottschalk et al., 2009, Blaser et al., 2008)
	Sludge	1.29–39 mg/kg	(Gottschalk et al., 2009) (Blaser et al., 2008)
ZnO	Surface water	1–10 000 ng/L	(Gottschalk et al., 2009)
	Effluent	0.22–1.42 μg/L	(Gottschalk et al., 2009)
	Sludge	13.6–64.7 mg/kg	(Gottschalk et al., 2009)

1.4.1.1. NM transformations

Once NMs are released into environmental compartments (e.g. surface water, wastewater, etc.), they are highly likely to be transformed from their original pristine state as their surroundings influence factors such as stability which are no longer under their original conditions. Some of these transformations include change in surface charge resulting from differences in ionic strength of the surrounding medium, dissolution of NMs, agglomeration and interaction with biological macromolecules present in the environment. These transformations affect NM transport and toxicity, and thus for toxicity assays in particular, it is essential to understand and test the environmentally relevant, or transformed NMs rather than the as-produced or pristine NMs.

1.4.1.1.1 Ionic strength

The addition of charged groups around NMs provides stability to NMs in suspension. For example, sulphate ester groups on NM surfaces are highly acidic and dissociate at a low pH resulting in negatively charged surfaces encouraging electrostatic repulsion between the NMs and therefore improving stability (Romdhane et al., 2015). There is an opposition of forces between the attractive Van der Waals and the repulsive electrostatic forces between NMs. With NMs that have a charge, a layer of opposite charge forms in the fluid around them which is called the 'electrical double layer'. At low ionic strength (where there are a low amount of ions in the suspension), the electrical double layer is large and domineers over any Van der Waal forces causing repulsion to be the dominant force, inhibiting NM agglomeration (Badawy et al., 2010). At high ionic strengths, the electrical double layer shrinks usually resulting in NM agglomeration. In addition, pH can drastically influence ionic strength (Badawy et al., 2010) as a lower pH increases the presence of positively charged protons. In environmental waters where the pH and ionic strength can vary, NMs that are deposited into the environment have a high chance of either stabilization or agglomeration, either of which can affect toxicological and biological responses to the NMs. This is an important property to

consider as *D. magna* medium used throughout this thesis has a variety of salts within it and consequently high ionic strength and therefore the stability of all types of NMs will be assessed.

1.4.1.1.2 Dissolution

Dissolution of NMs is an important transformation that provides some metal oxide NMs with antimicrobial properties which in turn affects their toxicity. Dissolution is when ions from a solid diffuse into the surrounding medium (Misra et al., 2012). The process of dissolution can cause the release of lethal ions, which is a question to be highlighted with regards to nanotoxicology of whether toxicity of dissolving NMs is due to (i) the NM itself or; (ii) due to the ions released by the NMs or; (iii) a combination of both NMs and released ions. As a general rule it has been noted that smaller NMs are more soluble than larger particles of equivalent composition (Misra et al., 2012). The medium surrounding NMs also has an influence on NM transformation, whereby acidity of the medium, presence of salts or other ions in the medium and water hardness all effect dissolution potential and rate (Misra et al., 2012). This is important as NMs released into environmental waters, which have a range of pH and ionic strength, may be subject to transformations that will cause them to change from their pristine state. Assessing NMs under only one condition therefore may not be representative of the various transformations they may undergo in the environment. Shape and morphology also have an impact on solubility as this influences the specific surface area, whereby smaller NMs with a contingent smaller diameter have a convex curving making them more likely to be energetically unstable and more prone to dissolve (Borm et al., 2006) though also there will generally be more dissolution with smaller NMs due to a larger available surface area and proportionally more of the atoms at the surface. It is important in the case of dissolving NMs to test ionic controls so that toxicity can be attributed correctly to the NMs or the corresponding concentration of released ions. Though the contents of this

thesis investigate PS and gold NMs which poorly dissolve (Carvalho et al., 2007) though dissolution is still an important NM transformation to discuss.

1.4.1.1.3 Presence of biological matter

Natural organic matter (NOM) and biomolecules may replace surfactants or other stabilising agents which originally provided charge or coating to the NM surface in order to ensure proper dispersion (Maurer-Jones et al., 2013). The acquisition of a layer of macromolecules that originally existed in the environment is usually termed the 'eco-corona' and can change the identity of the NM, which may cause either stabilization or destabilization leading to NM agglomerates, changing the NM size which in turn affects toxicity. The presence of an eco-corona around a NM also transforms the NM surface wherein biomolecules now present on the surface of the NM may change its shape and through molecular recognition cause it to be able to interact with receptors on the surface of cells potentially instigating other responses such as internalisation, for example, 15 nm gold NMs incubated in protein contained medium had increased binding of NMs to A549 cells leading to increased uptake as well as retention within the cell. This was due to increase in protein concentration influencing NM aggregation and cell receptor compatibility and association (Albanese et al., 2014). The presence of an adsorbed corona around NMs and their subsequent effects on toxicity will be more thoroughly discussed later in this chapter.

1.4.2 Impact of NMs on cell lines and organisms

It is difficult to generalize the relationship between the characteristics of NMs and the biological responses they instigate with cell lines or organisms and therefore it is important to assess NMs on a case-by-case basis due to the diversity of available NMs. Assessing the effect of NMs on the response, uptake and transport within organisms provides key information to close the knowledge gap in this area. Numerous studies show a stark difference with respect to size of NMs on toxicity towards cell lines or organisms. For

example, gold NMs of approximately 1.4 nm have an EC_{50} of 46 μM towards HeLa cells whereas smaller NMs (with the same coating as the latter) of 0.8 nm and 1.2 nm show a decrease in toxicity towards the same cell line with EC_{50} values of 250 μM and 140 μM respectively (Pan et al., 2007). The same 1.4 nm gold NM was considerably more toxic towards mouse macrophage or mouse fibroblast cell lines compared to a much larger 15 nm gold NM (Pan et al., 2007). Thus, the toxicity of a NM is very much cell type dependent and there may be thresholds of certain sizes that cause certain pathways of toxicity that are not carried out at larger NM sizes. Another example of size dependent toxicity can be seen where 5 nm gold NMs induced the MAC-1 receptor which triggers inflammation due to unfolding of the bound fibrinogen while the larger 20 nm NMs did still bind fibrinogen but did not induce unfolding of the bound fibrinogen effect (Deng et al., 2011). Quite interestingly, these, and most toxicity studies are conducted on a mass basis though this may not be accurate when measuring NMs of different size and shape, and if recalculated on a particle number basis the toxicity trends are often quite different. Toxicity of gold NMs of different size and shape are explored on mass as well as number concentration basis and the subsequent changes in their toxicity profiles of *D. magna* are investigated in chapter 4.

NM surface charge also may have an effect on toxicity where in general terms positively charged NMs are deemed to be more toxic due to the attraction of the positive charge towards the negatively charged cell membrane as well as negatively charged cellular organelles (Fröhlich, 2012). This does not negate the fact that negatively charged NMs are able to enter cells and have the ability to create harmful cellular reactive oxygen species which can lead to cell death (Geffroy et al., 2012), so that the toxicity of charged NMs on cell lines or organism should also be assessed on an individual cell type or organism basis. Characterization of pristine NM size, monodispersity and morphology is important however these parameters are subject to change in biological medium as the presence of proteins or ions may alter results (Albanese and Chan, 2011).

Substantial research has been conducted on assessing the toxicity of NMs on cell culture lines which use serum to feed cells, which also coats any NMs, and this effect has been understood for several years. Considerably less research has been conducted on more realistic scenarios involving whole organisms, where NMs are exposed to a biological environment and all their biological constituents such as the presence of secreted proteins or carbohydrates from organisms, which inevitably transforms NMs affecting their ultimate uptake and toxicity towards organisms. The presence of naturally secreted biomolecules such as proteins mimicking more realistic exposure conditions and their influence on NM stability and toxicity towards *D. magna* is a strong theme in this thesis and will be returned to several times.

1.4.2.1 Uptake and Influence of PS NMs on cells and organisms

Degradation of plastics in environmental waters into micro and nanoscale plastics is a growing concern (do Sul and Costa, 2014). PS NMs can act as a model material mimicking both plastic and nano characteristics. Investigation has been conducted on PS NMs with various functionalization on different cell types in order to gain an understanding of their mechanisms of uptake and toxicity. Amino (NH_2) and carboxylic acid (COOH) functionalized NMs (approximately 100 nm) have been shown to be taken up by a range of cell types such as human macrophage and THP-1 cells. It was seen that uptake is cell type as well as NM ligand-group specific where macrophage cells took up PS-COOH up to four-fold more compared to THP-1 cells though THP-1 cells took up PS-NH_2 at a faster rate compared to macrophage cells (Lunov et al., 2011). The mechanisms of uptake also differ between cell type where macrophage cells predominantly uptake both types of PS NMs via phagocytosis while THP-1 cells took up NMs via endocytosis (Lunov et al., 2011). PS NMs (specifically COOH functionalized) have been shown to be taken up also by rat and human hepatocytes and the degree of uptake is influenced by several factors such as NM size, duration of exposure and the presence or absence of incubation medium (Johnston et al., 2010). It was observed by confocal microscopy that 20 nm PS-COOH accumulated within the mitochondria of certain

types of cell lines (hepatocyte carcinoma cells) and only at longer exposure times (after 60 mins) indicating this as the target organelle. There was no association of these same 20 nm NMs found with early endosomes or lysozomes. (Johnston et al., 2010). Positively charged PS NMs have been shown to damage the mitochondria (indirectly via signalling from lysosomes and by causing damage to DNA) causing cellular stress resulting in increased ROS generation and decreasing antioxidant defence mechanisms in phagocytic cells, though this was greatly influenced by the state of agglomeration when dispersed in cell medium (Xia et al., 2006).

The toxicity, uptake and excretion of PS NMs is dependent on size and it has been observed that PS NMs of different size (1000 nm and 20 nm) were removed at different rates from *D. magna*. The larger 1000 nm PS NMs were more easily removed where 90% was expelled within 4 hours whereas only 40% of the smaller 20 nm PS NMs were removed at the same time duration (Rosenkranz et al., 2009) indicating that bioaccumulation and toxicity towards whole organisms must be assessed on a NM size basis as this effects residency time within an organism. *D. magna* consume algae *C. vulgaris* of approximately 2 μm in diameter (Hoek et al., 1995) as a staple food source and preferentially ingest food based on size and texture; therefore larger NM sizes might be more toxic in the case of *D. magna* which are filter-feeders, in contrast to cells. Qualitative assessment of the uptake of the fluorescent NMs was acquired using confocal microscopy and quantitative assessment was achieved using fluorimitry. The three main methods used to assess uptake and release of fluorescent NMs are the use of a plate reader, flow cytometry and confocal imaging. All three techniques are able to provide some degree of indication of uptake though plate reader measurements are the most widely used as they can provide semi-quantitative comparisons of different NMs (Claudia et al., 2017).

1.4.2.2. Effect of gold NMs on cell lines and organisms

Gold in bulk form is usually inert, although the increased surface area provided by their small size changes the toxicity of the NM form compared to larger gold material. For example, gold NMs (20 nm, exposure time of 3 days, 20 μg/kg per body weight) have been shown to increase oxidative stress and decrease antioxidant defence mechanisms in rat brain and was determined to be the main factor contributing to toxicity (Siddiqi et al., 2012).

Surface groups on gold NMs also influence toxicity and it can be seen that different ligands of similar charge may have a different effect on *D. magna* toxicity. Positively charged 5 nm gold NMs with either cetyl trimethylammounium bromide (CTAB) or poly(allylamine) hydrocholride (PAH) were both shown to be highly toxic towards *D. magna,* and that in some cases it was either the ligand (in the case of CTAB) or the NM itself (in the case of Au NMs coated with PAH) that was the inherent source of toxicity. 25 mg/L of 5 nm CIT stabilized NMs have also been shown to cause a reduction in *D. magna* size and in reproduction (Bozich et al., 2014). It has been documented widely that the addition of a positive charge on gold NMs results in toxic effects to cell lines, algae, bivalves and fish.

1.5 Model organism *Daphnia magna*

The vast majority of animal species are invertebrates and are heavily responsible for environmental maintenance (Verslycke et al., 2007). An optimal invertebrate candidate to act as a model organism for fresh water toxicology studies is the filter feeding *D. magna*. *D. magna* fulfils a central role in fresh water ecosystems as they consume phytoplankton, which are responsible for forming organic compounds from dissolved carbon dioxide to maintain the aquatic ecosystem (Brett et al., 2009). *D. magna* also act as prey for several types of invertebrates causing *D. magna* to be a vital food source (Ebert, 2005). Considering the many roles *D. magna* govern in the aquatic systems, any alteration to their wellbeing could cause multi-trophic level changes, making them a model candidate for toxicology testing.

From a toxicological model organism viewpoint, the most ideal characteristic that *D. magna* possess is their asexual (parthenogenetic) reproduction which causes offspring to be genetically identical ultimately decreasing variation in experimental studies (Berg et al., 2001). Asexual reproduction allows female *D. magna* to propagate when their environment provides them with adequate resources such as food and space. A female produces a clutch of parthenogenetic eggs which are placed in a brood chamber underneath the carapace and is closed by the abdominal process as seen in figure 1.1.

Figure 1.1. Optical image taken of adult female *D. magna* (25 days old) with a clutch of parthenogenetic eggs in the brood chamber. The green colour at the top of the gut is autofluorescence from ingested algae. Image taken on a transmitted light microscope.

Under ideal temperature conditions, the embryos hatch from the eggs after approximately one day though remain in the brood chamber for further development and then are released (Ebert, 2005). Under optimal and normal conditions, adult females produce diploid eggs, which develop into identical daughter neonates, called the parthenogenetic cycle meaning that no fertilization is needed. In laboratory conditions, females are likely to live for longer than two months (Ebert, 2005). Adult females release a brood every 2-3 days and

experiments in this thesis used neonates that were released from the third brood onwards. After 8 weeks the adult females were discarded and fresh neonates (of the third brood onwards) were grown to adults to replace the discarded adults.

Stressful conditions, such as change in population density, scarcity in food resources or alterations in temperature, cause *D. magna* to switch to sexual reproduction in order to create genetic variability amongst their offspring which leads to male *D. magna* being produced as well as females (Berg et al., 2001). The adult female can thus also produce diploid asexual eggs which develop into sons, which is a phenomenon directly influenced by environmental factors. Another route is that the adult female produces haploid eggs that need fertilization by males which results in sexual eggs with different genetic makeup compared to the mother (Ebert, 2005). These sexual eggs hatch after the adult female undergoes diapause (a dormant period due to negative environmental circumstances) resulting in daughters that are genetically different than their mothers.

D. magna are filter feeders taking in material suspended in the water column and therefore are exposed to a wide range of natural and anthropogenic materials in the water. The most common food source for *D. magna* is algae and they usually consume algal clusters between 1-50 μm though are able to selectively uptake entities based on size and texture. Once food is taken up, it moves through the digestive system which is tubular and divided into three parts; the oesophagus, midgut and hindgut (Ebert, 2005). The midgut is lined with epithelial cells and has a bush boarder protruding into the gut lined with microvilli to increase the surface area for absorption of nutrients. Peristaltic contractions push material forward through the gut though also more importantly, the uptake of newly acquired food creates pressure to dispel already ingested material (Ebert, 2005). *D. magna* are sensitive organisms and show a response in terms of feeding rate, body size and reproduction in response to water quality. *D. magna* also undergo physiological responses to kariomones, which are signalling molecules released by predators indicating that *D. magna* are sensitive to organic

biomolecules released by other organisms. Larva *Chaoborus* preys on daphnia and releases kairomones which induce daphnia defence mechanisms. These kairomones cause a decrease in essential life cycle stages such as reproduction due to energy being relocated in order to produce crests on its neck as a resistance trait (Hanazato and Dodson, 1995).

The link between *D. magna* and other organisms highlights their importance within the food web. *D. magna* consume *C. vulgaris* which form biological compounds from dissolved carbon dioxide thereby maintaining the aquatic ecosystem. Conversely, *D. magna* are also a food source for invertebrates, and therefore occupy a central position in the aquatic food web, making them a useful organism for aquatic toxicity testing.

1.5.1 Factors influencing uptake and release of NMs by *D. magna*

D. magna are filter feeders taking up particulates present in the water column, though interestingly, there are many factors that influence the uptake and excretion. *D. magna* preferentially consume particles closer to their natural food source of approximately 1 μm (Ebert, 2005) so that agglomerated NMs may be a more preferential size for *D. magna* to uptake as a food source. *D. magna* also uptake particulates based on texture so NMs that have an adsorbed organic eco-corona around them may appear to be an organic food source and more preferential for consumption. Consumed material (or NMs) moves through the tubular gut, via peristaltic contractions to move the contents forward. Also, very importantly, the intake of newly ingested food is a major factor in creating pressure and pushing already consumed matter through the gut so that the presence of food is a major contender in the excretion of any NMs that were consumed and therefore can impact residency time of NMs within *D. magna* and the absence of food to push out NMs may lead to extended bioaccumulation. The presence of food has a direct impact on the excretion rate of particulates, where below the 'incipient limiting level' (the concentration at which the amount of food no longer impacts the grazing rate (Downing and Rigler, 1984)), the rate of feeding is proportional to the concentration of food present (Ebert, 2005). The presence of

food such as algae can also influence uptake of NMs as algae can bind to NMs carrying them into the organism and therefore the presence of food interacting with NMs before consumption can increase the uptake of NMs incidentally (Kalman 2015) and will also be further investigated in chapter 5. Therefore, the presence of food can impact the rate of excretion of NMs consumed by *D. magna* as well as also causing an increased uptake of NM, depending on when during the NM exposure the food source became available.

The rate of uptake of particulate such as NMs is also governed by the presence of food already present within the gut of *D. magna,* whereby starved *D. magna* (unfed for a short period of time though still healthy) have a much higher uptake of matter such as food compared to those with a full gut. *D. magna* is likely to be surrounded by bountiful amounts of algae and therefore is already predisposed to take in a limited amount of NM, unless algae conditions change. The work in chapter 5 focuses heavily on the factors influencing uptake and release of NMs and assesses the impact of presentation mode of NMs to *D. magna* on uptake. This pushes forward the current state of the art with regards to how natural factors have a large influence on uptake and retention of NMs by organisms that are not always considered in standardised toxicity (and uptake) studies that were initially developed for chemicals.

1.5.2 Moulting

The process of moulting is essential to *D. magna* at various stages of its life cycle, where it sheds its inflexible carapace for growth and development (Zou and Fingerman, 1997) as seen in figure 1.2.

Figure 1.2. Optical image of *D. magna* neonate (3 days old) shedding its exoskeleton in the process of moulting. Image taken on a transmitted light microscope.

Within the first 96 hours of life, *D. magna* is known to shed its carapace 1-3 times depending on the available food present (Dabrunz et al., 2011a). *D. magna* shed their exoskeleton more frequently as neonates (up to day 4) and then decrease the frequency of moults in adolescent and adult stages. Calcification of the new exoskeleton occurs just before moulting almost simultaneously to the release of the neonates from the brood chamber so that the process of calcification is linked to that of moulting (Porcella et al., 1969). Environmental factors, such as temperature, effects the moulting cycle. The process of moulting is also a defensive mechanism whereby *D. magna* is able to shed adsorbed toxins that have bound to its exoskeleton. The impact of the presence of NMs on moulting will be later discussed in section 1.5.3.3 and also investigated in chapter 3 looking at the effect of PS NMs (bare and with an adsorbed corona) and in chapter 4 with gold NMs (of different shape) and their effects on *D. magna* moulting.

1.5.3 Mechanisms of stress in *D. magna*

1.5.3.1 Reactive oxygen species formation

Oxygen is an important component for living organisms that respire aerobically (where the end product of the reaction is adenosine diphosphate (ADP) binding to an inorganic phosphate to create adenosine triphosphate (ATP) which is the energy molecule for cells) though certain derivatives of oxygen called reactive oxygen species (ROS) such as superoxide anion ($O_2^{\cdot-}$), hydrogen peroxide (H_20_2) and hydroxyl radicals ($OH^{\cdot-}$), are extremely toxic to all biological organism. ROS occur naturally and are formed from within the cell where 90% of ROS are generated by the mitochondria in the electron transport chain (ETC) (Zhang and Martin, 2014). During the last stage of cellular respiration, coenzymes such as NADH and FADH donate a proton which is pumped across the proteins from the mitochondrial matrix into the cytoplasm creating a proton gradient. The coenzymes also lose an electron (resulting in NAD^+ and FAD^+) and these electrons are moved along membrane proteins where they finally bind with molecular oxygen and protons to form water. The proton gradient created in the cytoplasm also powers ATPase to bind ADP to an inorganic phosphate to create ATP (energy for the cell). Through this natural process, electrons can escape the ETC and bind with molecular oxygen to form the free radical $O_2^{\cdot-}$. A simplistic schematic of the ETC can be seen in figure 1.3.

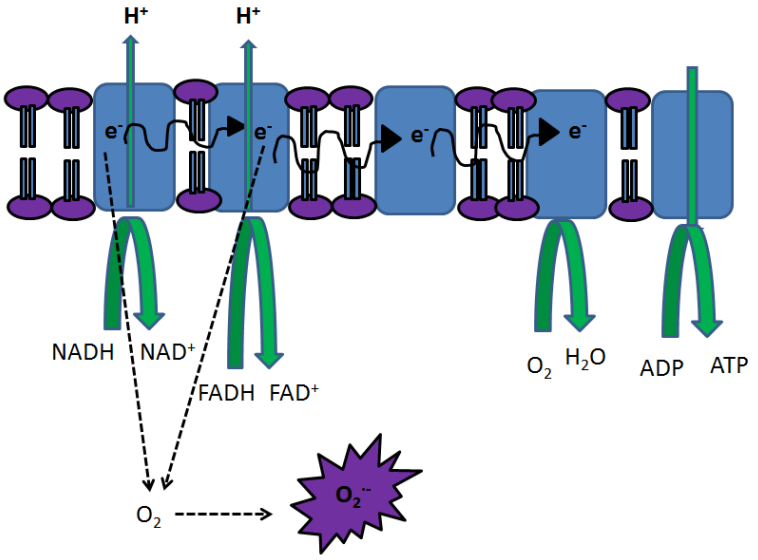

Figure 1.3 ETC within the mitochondria of a cell where escaped electrons are able to reduce molecular oxygen to form the ROS superoxide anion ($O_2^{\cdot-}$).

Given the highly reducing environment (where molecules accept an electron) of the mitochondria where many steps in the ETC involve transferring a single electron, the reduction of molecular oxygen by a single electron is extremely likely (Turrens, 2003). For every molecule of O_2 that is reduced (gains an electron) another molecule must donate this electron and become oxidized, which is usually the coenzyme NADH which is converted to NAD^+. NADH is known to be a reducing agent where it donates electrons to reduce a molecule such as O_2 and therefore become NAD^+ which is its oxidized form. The resulting superoxide anion $O_2^{\cdot-}$ can be enzymatically converted to other reactive oxygen species such as H_2O_2 via the enzyme superoxide dismutase (SOD) as seen in equation 1 which is a reduction reaction.

$$O_2^{\cdot-} + 0_2^{\cdot-} + H^+ \rightarrow H_2O_2 + O_2 \qquad \text{(Equation 1)}$$

H_2O_2 can then be further converted into a hydroxyl radical ($OH^{\cdot}$), yet another ROS, via the Fenton reaction, a simplistic diagram of which can be seen in figure 1.4.

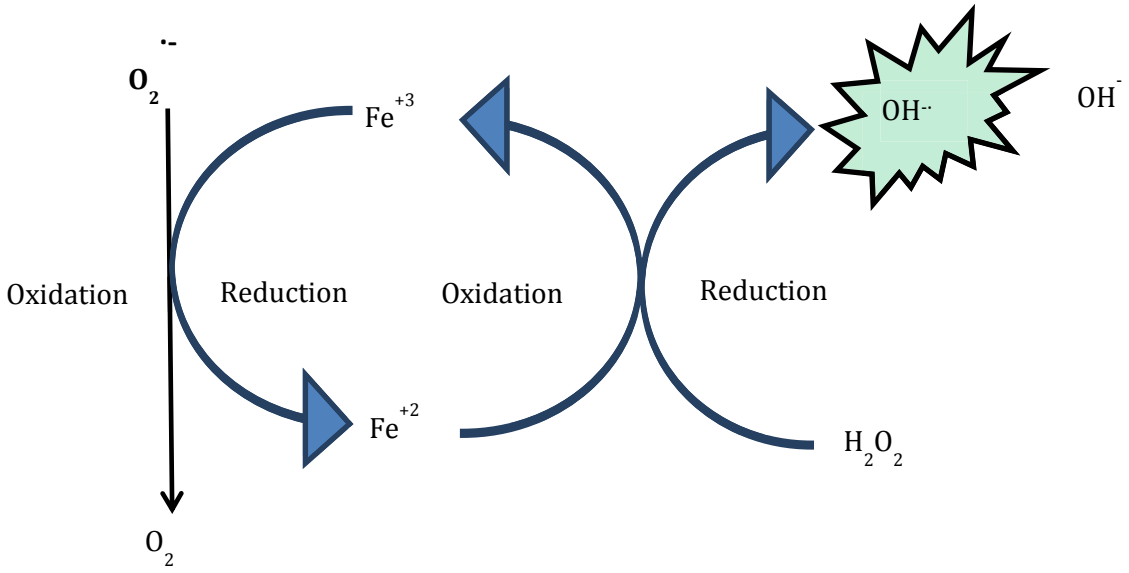

Figure 1.4. The Fenton reaction;, whereby the $O_2^{\cdot-}$ is oxidized contingently reducing Fe^{+3} to Fe^{+2} and simultaneously reducing hydrogen peroxide to the hydroxyl radical.

The generated $OH^{\cdot}$ is then converted into water via a reduction reaction so that the transition between molecular O_2 and water has a series of intermediate ROS i.e.; $O_2^{\cdot-}$, H_2O_2 and $OH^{\cdot}$. In order to counteract ROS generated intracellularly and maintain homeostasis, cells have antioxidant cellular defence mechanisms such as the enzyme glutathione peroxidase which maintains homeostasis within cells. Glutathione (GSH) is an antioxidant present within cells which donates an electron to H_2O_2 resulting in its oxidized form glutathione disulphide (GSSG) and creating two molecules of water via the enzyme glutathione peroxidase. GSSG can be converted back to its reduced form via the coenzyme NADH which donates its electron to GSSG forming two molecules of GSH. A simplistic diagram is below reaction is shown in figure 1.5.

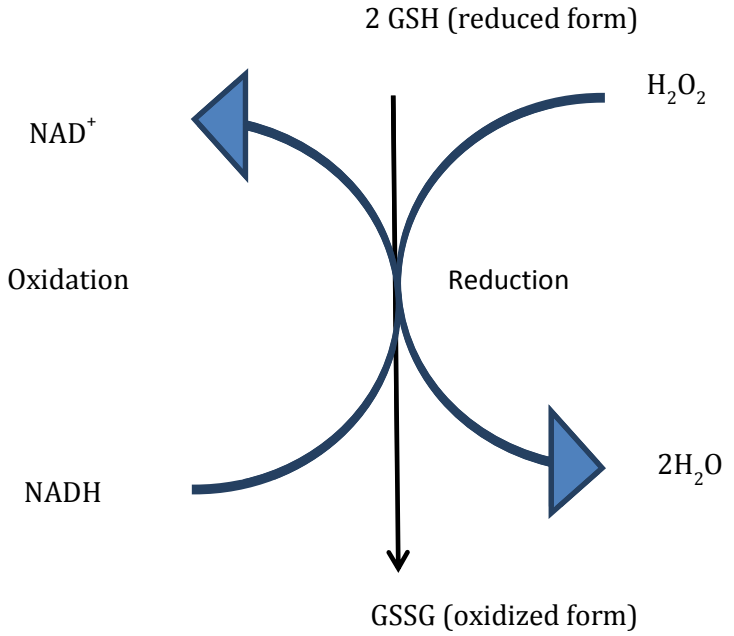

Figure 1.5 Mechanism of the antioxidant glutathione being oxidized to glutathione disulphide and simultaneously reducing hydrogen peroxide to water.

Catalase (CAT) is another antioxidant enzyme present in aerobic cells which converts H_2O_2 into water and dissolved oxygen as seen in equation 2.

$$\mathbf{2H_2O_2 \rightarrow 2H_2O + O_2} \qquad \text{(Equation 2)}$$

CAT breaks apart H_2O_2 by binding a single oxygen atom to a haeme group and releasing the remaining molecule of water. Another H_2O_2 molecule then binds to another active site on the enzyme and releases another molecule of water while the remaining oxygen from the second H_2O_2 binds with the oxygen on the haeme group to release a molecule of molecular oxygen.

ROS can also be generated due to extracellular sources such as cellular exposure to environmental toxicants or exposure to UV light and the generated ROS may cause a shift in homeostasis where antioxidant defences may not be able to cope with the amount of ROS being generated which leads to random cellular damage and impaired physiological function leading to cell death (Krumova and Cosa, 2016).

1.5.3.1.1 Effect of NMs surface charge on ROS production in *D. magna*

It is known that ROS production is influenced by charge and surface ligand groups on NMs. The gut of *D. magna* is likely to be exposed to NMs, as *D. magna* take up matter via filter feeding and the contents then move though the gut. Charge has been shown to influence toxicity across multiple organisms, though it has not been determined which type of charge causes higher toxicity (Dominguez et al., 2015). Effects of NMs may also be ligand specific. For example, negatively charged gamma-cyclodextrin coated fullerenes caused higher mortality in *D. magna* compared to positively charged ones. Oxidative stress is a commonly used marker of cellular stress due to NM exposure. It has been shown that both positive and negatively charged ligands bound to gold NMs are able to induce ROS production, though there is a much higher percentage (approximately 5 times more) of ROS produced by *D. magna* enterocytes that are exposed to positively charged CTAB coated gold NMs compared to negatively charged CIT-coated ones (approximately 1.5 times more) compared overall to the control (Dominguez et al., 2015). Positively charged NMs (coated with PAH or CTAB) also prompt an increase in glutathione transferase (*GST)* gene expression which did not occur for negatively coated NMs (coated with CIT or mercaptopropionic acid (MPA)) (Dominguez et al., 2015). At certain concentrations of exposure to NMs coated with negatively charge MPA, there was a significant up regulation of *CAT* gene expression. Also, the heat shock protein HSP70 was up regulated at an increased concentration of PAH coated NMs (Dominguez et al., 2015). Gene expression connected with cellular stress showed that stress is not only influenced by charge but also by the coating, even with different coatings of the same charge, and therefore it cannot be generalized that NMs of the same charge will cause the same degree of stress as stress appears to be coating specific.

When considering toxicity of NMs, charge must be taken into consideration. Positively charged NMs have been shown to be more toxic compared to negatively charged NMs due to their attraction towards the negatively charged phospholipid membrane. Though this has been a well-documented reason, this may only be a partial reasoning. The attraction does

indeed give positively charged NMs greater proximity to cell surfaces so that they may enter more readily.

1.5.3.2 Cellular stress caused by NM internalization

It is usually accepted that NMs should be tested to assess toxicity towards cells or organisms, though a general risk assessment does not go into detail about the mechanisms of toxicity within cells or towards organisms. ROS is an excellent indicator of cellular stress though there are other mechanisms of toxicity that can be induced by NMs other than the production of ROS. Along with size, surface modifications by adding a charge influence toxicity and it has been seen that modifications to gold NMs influence the cellular trajectory of NMs, which cause different organelles to be NM targets. Different surfactants are used to produced NMs of different shapes produce different geometries of NMs, which can influence cellular internalization of NMs by receptor mediated endocytosis, which is directly affected by NM shape (Gratton et al., 2008, Salatin et al., 2015). Rod shaped NMs have a higher effectiveness of binding to cells compared to spheres as the curvature of spheres provides only a limited number of binding sites to interact with cell receptors (Salatin et al., 2015). Figure 1.6 shows a simplistic depiction of how surfactants produce different NM shapes which can affect cellular internalization via receptor mediated endocytosis in cells.

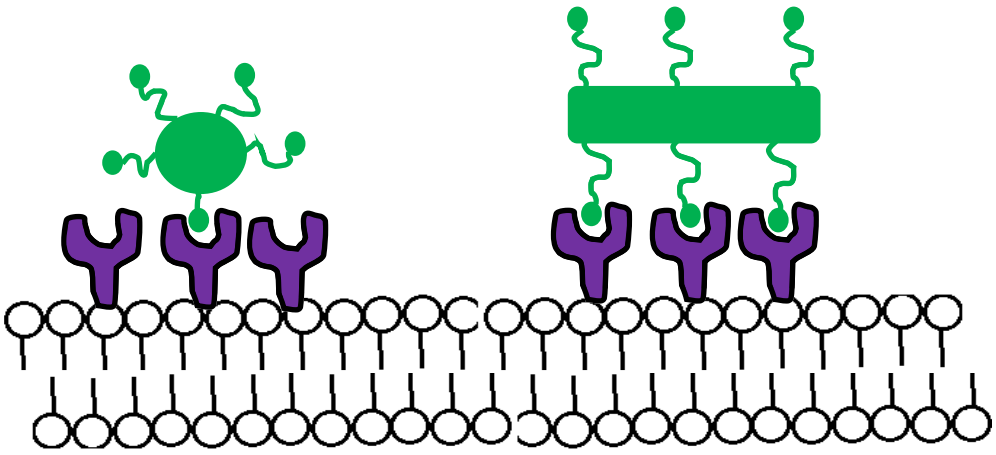

Figure 1.6. Spherical NM ligands only interacting with minimal cell receptors whereas longer NMs allowing for increased binding, resulting in receptor mediated endocytosis.

D. magna ingest molecular sized molecular contaminants and a specialized cell membrane lining the gut allows for transport of these contaminants further into the daphnid. Larger bulk contaminants are also consumed by *D. magna* and then are digested within the gut. The route of accumulation of NMs, which have a size between molecules and bulk material is unclear though several studies have shown that NMs are definitely ingested by *D. magna* though whether they pass through the gut epithelial wall is disputed. NMs have been shown to be located in areas other than the gut though whether these migrated from the gut is unknown. *D. magna* has the capability of further internalizing NMs via endocytosis at low (2 mM ~ 80 mg/L) calcium ion concentrations. High Hardness (HH) Combo is the culture medium used for *D. magna* experiments throughout this thesis and contains 110.28 g/L of calcium chloride dehydrate so that there is a substantial amount of calcium present so that endocytosis may not occur.

Damage to the mitochondria is most often the primary step in instigating cellular stress, which leads to a cascade of events in turn, resulting in cell death (Pan et al., 2009). An intrinsic indicator of mitochondrial damage is the mitochondrial permeability transition (PT), which is a phenomenon that causes the inner mitochondria to undergo a rapid increase in its permeability towards large solutes which causes water to influx in resulting in mitochondrial swelling which occurs in the initial phases of apoptosis (Pan et al., 2009). Toxicants such as NMs can activate several apoptotic mechanisms (ultimately resulting in the onset of the mitochondrial PT pathway), which have detrimental effects such as the shrinking of chromatin within the nucleus and DNA breakage, which in turn mutates the *p53* tumor suppressor gene causing an abundance of ROS to be generated as a result. The generated ROS deactivates the *bcl-2* gene coding for integral membrane proteins on the mitochondria (Kroemer, 1997) which activates the PT pathway allowing large solutes to pass through these membrane proteins resulting an influx of water causing cell death. Gold NMs (1.4 nm) have been shown to prompt a high degree of PT in HeLa cells indicating their ability to cause cellular stress through mitochondrial damage (Pan et al., 2009). As a result of damage to the

mitochondria, there is less available energy for production of ATP. PT also prompts parallel cell death pathways such as activating apoptosis related proteases, which are enzymes that degrade proteins within the nucleus and in the cytoplasm. NMs accumulate in lysosomes and result in lysosome dysfunction and deactivation of enzymes causing signaling for the degradation of cellular organelles such as the mitochondria (Neun and Stern, 2011).

The origin of generated ROS and cellular stress due to NM exposure is difficult to assess in terms of which reaction comes first as both can occur in parallel as well as a trigger each other. It was found that gold NMs create ROS by selectively oxidizing oxygen due to their high surface area to volume ratio and the specific electronic configuration of the surface gold atoms. Gold NMs are also resistant to oxidation, causing them to be effective oxidation catalysts due to their closed-shell structure (Pan et al., 2009) making them excellent ROS generators. Different types of NMs generate ROS though the exact mechanisms of how this occurs is not well understood though some postulations could be; (1) in an attempt of lysosome trying to metabolize the non-biodegradable NMs within the endosome, intermediates are created by the lysosome that are prone to reduction or oxidation reactions; (2) inflammation in organisms that cause oxyradical release by white blood cells (Pisanic et al., 2009). The produced ROS are then able react with lipids, proteins and DNA in turn generating additional ROS which have a direct impact on the function of the mitochondria, altering mitochondrial PT. Also, PT causes an increase in the superoxide anion ROS as a by-product of the ETC as well as decreasing the available GSH (Kroemer, 1997) which decreases the amount of H_2O_2 that can be successfully converted into H_2O thereby increasing the overall ROS formation within the cell which further triggers oxidation of membrane lipids (Kroemer, 1997). Overall, the formation of ROS and the increased cellular stress with the primary source being the mitochondrial PT, both occur simultaneously triggering several positive feedback mechanisms enhancing additional ROS production and cellular stress resulting in cell death.

1.5.3.3 Physical stress

NMs have an affinity to bind to biological surfaces which results in a layer of NMs (Handy et al., 2008). Due to the large surface area provided by NMs they have a high sorption capacity making the binding of NMs to the carapace of *D. magna* highly likely (Baun et al., 2008). During moulting, it has been seen that the entire bound layer of NMs was completely removed allowing *D. magna* to be NM free at the end of the moult, though the presence of NMs in the suspension caused re-adsorption of more NMs onto *D. magna* (Dabrunz et al., 2011a) and binding of NMs to the surface of an organism is known to facilitate NM consumption. The adhesion of NMs to the carapace can cause a decrease in movement by increasing the weight of each neonate and increasing the amount of physical endurance and energy required to swim (Dabrunz et al., 2011a).

1.5.3.4 Dissolution and toxicity towards *D. magna*

It is difficult to assess the main source of toxicity of NMs towards *D. magna* as several factors can influence this such as the NM characteristics but also the exposure conditions. NMs that dissolve such as copper and zinc are known to have toxic effects on *D. magna* created by the NM themselves as well as from the dissolved ions released by the NM, where low exposure concentrations were shown to have toxicity majorly exerted by the dissolved ions though at high concentrations (0.1 an 1 mg/L respectively) toxicity is predominantly provided by the NM. The dissolved ions from NMs as well as the NMs themselves have both been shown to induce a toxic effect towards *D. magna* though this is dependent on factors such as exposure concentration. It has been seen that at low concentrations of copper (50 nm) and zinc (43 nm) NMs (compared to their EC_{50}) of 0.05 and 0.5 mg/L that the dissolved ions were the main source of toxicity whereas at higher concentrations above 0.1 and 1 mg/L respectively that the NMs were the main factor contributing to toxicity (Xiao et al., 2015), indicating that exposure concentrations and NM type both affect the toxicity imposed by dissolution.

1.6 Ecological (eco)-Corona

NMs released into the environment will inevitably interact with biological milieu containing naturally secreted biomolecules which will create a biological layer around the NM called the 'eco-corona' which will consist of macromolecules such as carbohydrates, proteins and lipids (Lundqvist et al., 2011). The constituents of the corona depend on several factors such as the size of the NM as well as the composition of the NM surface and the macromolecules present in the surrounding solution or organism. Corona's can be divided into two subcategories; the hard corona which are macromolecules that are bound tightly to the NM surface and; the soft corona which are macromolecules that mildly associate with the NM surface and are recurrently substituted between the NM and the biological milieu (Lundqvist et al., 2008). The molecules that create the NM corona inevitably change the identity of the NM and are what cell receptors identify on contact with a NM. The corona can then trigger other pathways depending on its interaction with the cell or organisms.

Most corona-related work has been conducted on human blood plasma, or in cell culture medium containing bovine serum proteins, and less is known about the eco-corona. Initially, proteins which are high in abundance bind to nanoparticle surfaces and then are displaced by less abundant yet higher affinity proteins (Dell'Orco et al., 2010, Cedervall et al., 2007). It has been evidenced that human serum albumin (HSA) dominates NM surfaces and subsequently becomes displaced by higher affinity proteins such as apolipoprotein (A-I), which are present in lower abundance and have slower binding kinetics. This phenomenon can be explained by the Vroman effect which observes blood serum proteins binding to various surfaces where those with high mobility bind first and are subsequently exchanged with proteins that have a higher affinity to the NM surface (Lynch et al., 2014). This phenomenon is well established in human corona work and similar principles apply to eco corona work.

For NMs, diverse shape or composition can impact how biomolecules adhere to its surface. NMs with various curves or edges will impact what molecules can be adsorbed to them which can ultimately affect NM identity (Hung et al., 2011). Macromolecules such as proteins present in the environment or those that are secreted or released by organisms (discussed in section 1.6.1), natural organic matter (NOM) present in the water or bacteria secreting extracellular polymeric substances (EPS) may absorb to NM surfaces changing their overall identity, and may also have stabilization or destabilization effects on NMs (Nasser and Lynch, 2015). Adsorbed proteins creating the corona may cause NMs to aggregate due to proteins interacting or due to the NM surface being destabilized (Albanese et al, 2014) which ultimately effects NM size and therefore also influences its toxicity and uptake by organisms. Agglomeration is often ignored yet is a crucial part of NM identity since the change between monodisperse NMs into larger agglomerates causes changes in the presentation molecules adsorbed to the NM surface and what can interact with cell receptors on cell membranes (Albanese and Chan, 2011). Agglomeration also causes changes in NM bioavailability as agglomerates may be more or less effectively taken up compared to single particles in dispersion.

Conditioned media ultimately changes the macromolecular components that can be adsorbed into the NM corona and is a factor to be considered when incubating NMs with cells over 24 hours as it is unclear how cellular conditioning alters NM biological identity their interaction with organisms (Albanese et al, 2014). Organisms also 'condition' their local surroundings, altering the levels of proteins and other substances by releasing them into their immediate environment (Kulasingam and Diamandis, 2007).

Standard toxicity testing by the Organization for Economic Cooperation and Development (OECD) created for immobilization and reproduction (Co-operation and Development, 2012) for *D. magna* exist, though several studies have suggested that in fact, these tests are not appropriate for NM testing as the traditional OECD medium does not take into account the

complexity of natural environmental waters which contains naturally present or organism excreted biomolecules which in turn affects NM stability as well as bioavailability.

1.6.1 Conditioning of biological medium by cells and organisms

The contents of biological or environmental fluid are not consistent over time as cells and organisms continuously 'condition' their environment by releasing macromolecules such as proteins into the environment (Albanese et al., 2014). Cells secrete proteins into their surroundings for a number of reasons such as the release of hormones (Bernton et al., 1987); enzymes or antibodies for the purposes of internal regulation of the organism, cell-to-cell communication and as a defence mechanism. Organisms also condition their surrounding medium by releasing substances called kairomones which trigger defence mechanisms in their prey. A primary predator towards *Daphnia pulex (D. pulex)* is larva *Chaoborus* which secretes kairomones which cause physical and anti-predator reactions by *D. pulex*. These kairomones have been shown to reduce both development and reproduction which is most likely due to the relocation of energy within *D. pulex* which also starts to develop teeth like structures on its neck as a defence mechanism which also further reduces the available energy for regular development (Hanazato and Dodson, 1995). It has also been observed that the released kairomones decrease the ability for *D. pulex* to overcome other stresses such as a decrease in the availability of food (Hanazato and Dodson, 1995).

D. magna also release proteins into the surrounding fluid though this has never been precisely quantified. For example, the enzymes chitinase and chitiobase, which degrade the polymer chitin, which is the main component of the exoskeleton of *D. magna* is in abundance prior to moulting. These enzymes are released along with the moulting plasma into environmental waters during moulting which conditions the surrounding medium (Oosterhuis et al., 2000). *D. magna* also has the ability to condition their surroundings by releasing carbohydrates into their surrounding environment and do this as a natural process of growth and development in the process of moulting whereby the chitin-based (mainly

composed of polysaccharide) exoskeleton is released into the surrounding fluid (Anderson and Brown, 1930) and is secreted at different time points depending on the age of the daphnid. In this thesis, quantification of secreted proteins within conditioned medium by *D. magna* was performed under unstressed conditions. Assessment of the interaction of these proteins with NMs, and the influence of corona formation on stability of NMs of different charge, size, shape and composition and toxicity towards *D. magna* was also performed.

1.6.2 Impact of corona on NM stability and toxicity

The presence of an adsorbed corona alters the biological identity and affects agglomeration, so that the presence of a corona has the ability to affect NM stability and its subsequent toxicity towards organisms. Stabilization or destabilization effects may either increase or decrease the toxicity of the NM depending on the exposed organism, especially considering that *D. magna* are more likely to uptake matter closer to the size of their natural food source between 1-2 μm, so that larger agglomerates may be taken up more readily making them more toxic.

1.6.2.1. Influence on agglomeration

Biological or environmental fluids that contain proteins will cause a thermodynamically favourable exchange of biomolecules or synthetic ligands at the surface of the NM with proteins existing in the medium. This can cause a destabilization of originally monodisperse NMs causing agglomeration in the medium or conversely have a stabilization effect. Recently, it has been shown that NMs with a stabilizing shell of polyethylene glycol (PEG), which usually remain monodisperse short term, agglomerate when incubated *in vitro*, measured by aggregation index (Albanese et al., 2014) and *in vivo* measured by DLS (Rausch et al., 2010), in their corresponding mediums, indicating that the exchange of biological matter with molecules originally present on the surface of NMs will eventually cause a degree of agglomeration. In biological environments, NM doublets and triplets will initially form which

then quickly grow into large agglomerates. These larger agglomerates may be a more preferential size for uptake for *D. magna* who uptake matter closer to their natural food source and therefore these larger NM agglomerates may pose a higher toxicity as they are actively taken up by filter feeders.

1.6.3. Influence of corona on toxicity towards organisms

As mentioned, in environmental medium, NMs may interact with macromolecules such as proteins and lipids, creating an adsorbed corona around the NM, which can cause destabilization or stabilization of the NMs. Destabilization effects can cause agglomeration, altering the size of the NM compared to the original pristine NM in protein free medium, which thereby alters its toxicity. Limited research has been conducted on the effect of the corona on cell types and even less research has been conducted on the effect of the corona around NMs on toxicity towards whole organisms and it must be taken into consideration that the effect may be different on a case-by-case basis depending on the exposed organism, and its mechanisms of potential interaction with NMs. Generally, smaller NMs are said to be more toxic due to the larger available surface area to interact with the organism and smaller NMs less than 100 nm can enter cells and NMs below 40 nm can potentially enter the nucleus (Saptarshi et al., 2013), assuming that they escape from the endo-lysosomal pathway. This NM-size-dependent hypothesis is largely debated as toxicity is also highly dependent on NM type (as well as dependent on the shape and presence of charge) as previously mentioned, where gold NMs of 1.4 nm were more toxic towards HeLa cells compared to smaller gold NMs (1.2 and 0.8 nm) of the same coating though the same 1.4 nm gold were considerably more toxic compared to a larger sized gold NM of 15 nm towards fibroblast cells indicating size toxicity cannot be broadly assessed on only one cell type. Size dependent toxicity can also be organism dependent which can be seen in the resulting EC_{50}'s of 40 and 60 nm silver NMs towards crustaceans (*D.* magna) and algae (*P. subcapitata*). The EC_{50} induced by 40 nm NMs towards *D. magna* is 0.00060 mg/L (all EC values are NM specific and not ions) which has a

less toxic effect compared to the EC_{50} induced by the larger 60 nm NMs which is 0.0053 mg/L. These very same NMs have an opposite effect when exposed to *P. subcapitata* where the smaller 40 nm NMs induce an EC_{50} of 0.007 mg/L while the larger 60 nm NMs have a less toxic effect on the same organism where the EC_{50} is 0.009 mg/L (Ivask et al., 2014). These EC values are also highly dependent and contingent on the mechanism of toxicity, whereby NMs could be sticking to algae thereby blocking photosynthesis, or sticking within the gut of *D. magna* resulting in extended accumulation so that the mode of toxicity may not be directly comparable. This indicates that it cannot be generally stated that smaller NMs are always more toxic and that different sized NMs may have opposite effects on different environmental organisms and that size toxicity of NMs is organisms specific.

The presence of a corona has shown to have an impact on the uptake of 75 nm silver NMs towards the earthworm *E. fetida*. Silver NMs have shown to adsorb secreted native coelemocytes proteins to its surface and also separately adsorb non-native fetal bovine serum (FBS) proteins to its surface. Coelemocytes preferentially uptake silver NMs coated in their own native proteins compared to those with a foreign corona (Hayashi et al., 2013) Proteins present in the media may have destabilizing effects on NMs and this increase in NM size is often said to dictate a decrease in NM toxicity though this as previously discussed is organism dependent as it has been shown that organisms such as *D. magna* uptake NMs based on (large, ~ 1 micron) size and that agglomerated NMs thus represent a more agreeable food source and therefore may uptake agglomerated NMs to a higher degree than monodisperse NMs. The presence of an organic corona also causes the NM to have a more organic texture making the NM to me a more natural food source. Of course, an acquired corona may also change within the organism where an exchange of proteins originally surrounding the corona before consumption can be exchanged with other macromolecules within the digestion passage of the organism once consumed which can further alter its size as well as alter its propensity to remain within the organism therefore increasing its residency time. This is a highly unexplored area and the effects of proteins present in media

and their subsequent effects on NM stability, toxicity towards and uptake into *D. magna* forms the basis on which this current work builds. Parallel to this is the need for understanding what are the realistic testing conditions, such as the feeding regime of *D. magna,* and how these factors also alter uptake and depuration of NMs.

1.7 Idea Development

Following a thorough review of the literature regarding NMs and their toxicity towards organisms, and what factors may govern toxicity such as charge, size, presence of adsorbed proteins or presentation mode, the ideas for the composition of this thesis were then developed using the available literature as a foundation though also looking at gaps in the research that could be fulfilled. PS NMs were selected due to the increased deposition of micro and nanoplastics in environmental waters. Au NMs were also selected due to their large incorporation in medical products where both their deposition into fresh water systems and exposure to *D. magna* was highly likely, and the lack of realism in standard methods of assessing NM-organism interactions was an area in the literature that called for further investigation.

1.8 Aims and Objectives

The overall aim of this thesis is to investigate how NM characteristics such as charge, shape, the presence of secreted biomolecules experimental design parameters such as the NMs presentation mode affected *D. magna* and how this related to the observed toxicity and the mechanism of toxicity. To achieve this overall aim, each chapter has specifically designed aims with its own objectives. The novel results acquired by fulfilling these objectives are integrated and together advance the field of NM toxicity towards *D. magna.*

1.8.1 Chapter 1 Aim

To investigate the impact of an acquired protein corona on the stability of differently charged PS NMs and their toxicity towards and retention, within D. magna

The work in this chapter aims to investigate the toxicity of differently charged PS NMs and the influence of the protein corona formed from biomolecules secreted by *D. magna* as well as the incubation time of the NMs in protein contained medium, on the stability of the NMs. The effect of the changes in stability resulting from corona formation and the subsequent changes in toxicity of the NMs towards *D. magna* shall analysed. In parallel, this chapter also compares the incubation of NMs in algal *C.* vulgaris secreted proteins to assess if this affected NM stability. The quantification and identification of the proteins secreted by *D. magna* shall also carried out. The work explores the uptake and excretion of NMs over short time periods and investigates how the protein-corona affects the retention of NMs within *D. magna.* Finally, this work will investigate how once ingested, how corona bound NMs may alter the subsequent feeding of *D. magna* on algae *C. vulgaris* and how bare and corona bound NMs effects moulting as a proposed mechanism of toxicity.

1.8.2 Chapter 2 Aim

To investigate the impact of charge and shape of Au NMs on the chemical and physical toxicity towards D. magna and to assess the influence of the protein corona.

The work in this chapter aims to study the impact of differently charged and shaped Au NMs on the toxicity towards *D. magna.* Mass concentration exposure will be considered initially and then exposure will also be performed in terms of number concentration which is a more accurate dose metric when considering NMs of different size and shape. The toxicity effects of

both types of exposures will be compared. The work will also investigate how charge per surface area affects toxicity. This chapter also aims to assess the effect of charge (positive and negative) and shape (sphere, short rod, long rod) on the mechanisms of toxicity, which will be assessed at a chemical level, looking at the prompting of and recovery from reactive oxygen species as well as at a physical level, looking at the impact on moulting. This work is also intends to demonstrate how adsorption of proteins to Au NMs could alter NM stability and how this in turn may affect toxicity.

1.8.3 Chapter 3 Aim

To investigate the impact of presentation mode of differently sized PS NMs on the uptake, excretion and retention by D. magna

The work in this chapter is aimed to investigate how realistic presentation modes of NMs altered their uptake by, and excretion from *D. magna.* The chapter looks at how NMs are taken up and retained with no additional influencing factors and compared to how the presence of a food source at different time points (only present during excretion; incubated with the NMs and then presented to *D. magna;* or present before NM exposure) alters uptake and release and these findings shall be compared and contrasted. The work also aims to explore the cause of residual amount of PS that was retained within *D. magna* regardless of the presentation mode. Finally, the chapter intends to show how the presence of secreted biomolecules such as proteins and carbohydrates could cause stabilization or destabilization to NMs depending on size and undertakes the quantification of carbohydrates released and compares this to the amount of proteins released.

1.9 Thesis Layout

This thesis opens with the introduction in chapter 1, which provides an overview of NMs. The chapter then goes into detail about the deposition of NMs into the environment and their potential risks towards the fresh water organism *D. magna* as well as their behaviour and toxicity when interacting with natural components and biomolecules existing in the environment and what factors influence this. The chapter is written to present not only an overview of the environmental-nano field, but to also outline areas that are under investigated and give an understanding of the concepts that are, and should be important in NM toxicology.

The methodology utilised is then described in chapter 2 which includes technical detail of the instruments and techniques used for analysis of the data as well as biological culturing techniques.

Chapters 3-5 are results chapters. Each chapter begins with an introduction, setting the scene for the important concepts relevant to that chapter. Next are details on the aims and objectives specific to each chapter and what the chapter hopes to achieve. This is then followed by the results obtained and an interpretation of their wider relevance.

The thesis concludes with a summary of the results found in each chapter and integrates them into an overall set of conclusions (chapter 6) and also indicates how the results accomplished the original aims of the chapter and the overall thesis. The chapter also offers an insight on possible future work that would be beneficial in order to further explore some of the new insights generated here.

2

Methodology

2.1 Characterization techniques

2.1.1. Dynamic light scattering

Dynamic light scattering (DLS) is a technique used to measure the hydrodynamic diameter of NMs. A NM's hydrodynamic diameter is comprised of the NM core diameter plus any capping agents and the hydration layer absorbed to its surface. NMs in suspension undergo Brownian motion and randomly collide with solvent molecules as the NMs diffuse through the medium (Lim et al., 2013). When a laser is shone onto a NM dispersion, the light is scattered and produces a speckled pattern and the intensity reaching the detector is monitored. The intensity of the scattered light that reaches the detector will change as NMs move within the suspension, which is depicted in figure 2.1.

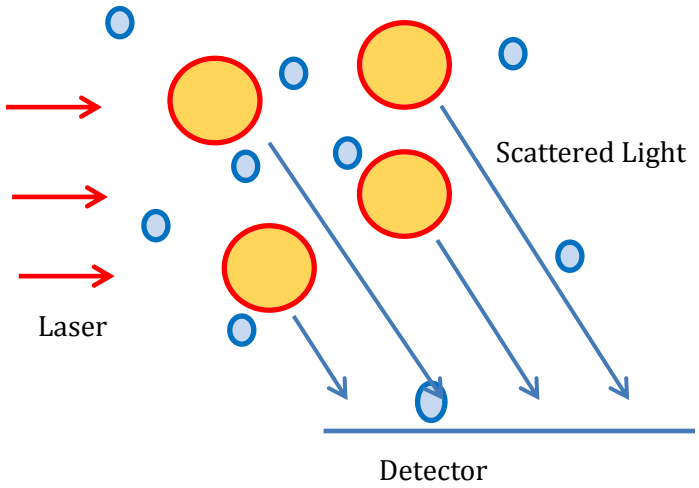

Figure 2.1. NMs (yellow) in suspension collide with solvent molecules (blue) and undergo Brownian motion. A laser beam passing through the NM dispersion interacts with the NMs causing the light to scatter, which is monitored by the detector. For illustrative purposes the detector is shown to be 90° to the scattered light though in actuality the instrument used backscattered light at 173°.

Since NMs are constantly moving, the intensity of the speckle pattern will fluctuate. Larger NMs move slower and consequently the intensity of their speckled pattern will fluctuate slowly, and oppositely, smaller NMs move faster and the intensity of the speckle pattern will fluctuate quicker (Holmberg et al., 2002). The variation of the scattered light is used to calculate the size of the NMs within the sample by measuring the relationship between intensities of light measured over a period of time. Briefly, if measurements are made right after each other, the intensities of the scattered light will be similar though the second measurement will be slightly decreased compared to the first. The longer the duration between the first and the subsequent measurements, the lower the correspondence of the intensities will be (Hassellöv et al., 2008). The autocorrelation function is measured to obtain the intensity of scattered light using equation 2.1.

$$I = I_0 \left(\frac{2\pi}{\lambda}\right)^4 \left(\frac{d}{2}\right)^6 [1cos^2\theta]/2R^2][(n^2-1)/(n^2+2)]^2 \qquad \text{(Equation 2.1)}$$

Where I is the intensity of scattered light; I_0 is the intensity of the incident light; θ is the scattering angle; R is the distance to the NM; λ is the wavelength of light; n is the refractive index of the NM; and d is the NM diameter.

The instrument uses a series of algorithms and determines an autocorrelation function, which is calculated from the intensity of the scattered light (Baalousha and Lead, 2012) from the previous equation 2.1, whereby the hydrodynamic diameter is then calculated using the Stokes Einstein equation, as seen in equation 2.2.

$$D = \frac{K_B T}{6\pi n R_H} \qquad \text{(Equation 2.2)}$$

where D is the diffusion coefficient (calculated from the decay rate); K_B is the Boltzman constant; T is the absolute temperature; n is the viscosity of the solvent; and R_H is the hydrodynamic size of the scattering entities (the NMs).

Measurements for the DLS were performed using a Malvern Zetasizer with low-volume cuvettes. Standard operating procedures (SOP) were created for each of the NM types which took into account the refractive index (RI) and the adsorption of each type of material and the parameters can be seen in table 2.1.

Table 2.1. Refractive index (RI) and absorption of NMs used for DLS analysis.

NM type	RI	Adsorption
Polystyrene	1.59	0.01
Gold	0.47	1

Samples of 650 µL were pipetted into low volume cuvettes and placed within the DLS sample holder. The corresponding SOP was chosen for the specific NM type and replicates were run at room temperature in n=3 and each measurement was the average of at least three runs.

2.1.2 Zeta-potential

Zeta potential is calculated by measuring the electrophoretic mobility of NMs which can then be applied to the Henry equation. When NMs have a surface charge, ions of opposite charge are attracted to it and surround them. This results in the formation of a layer of oppositely charged ions (compared to those at the NM surface) forming around the NMs which is termed the 'electrical double layer'. The inner layer is where ions are very attracted to the oppositely charged NM and is termed the 'Stern layer' (Hunter, 2013). The outer layer of ions are weakly attracted to the NM surface, and a description of this can be seen in figure 2.2.

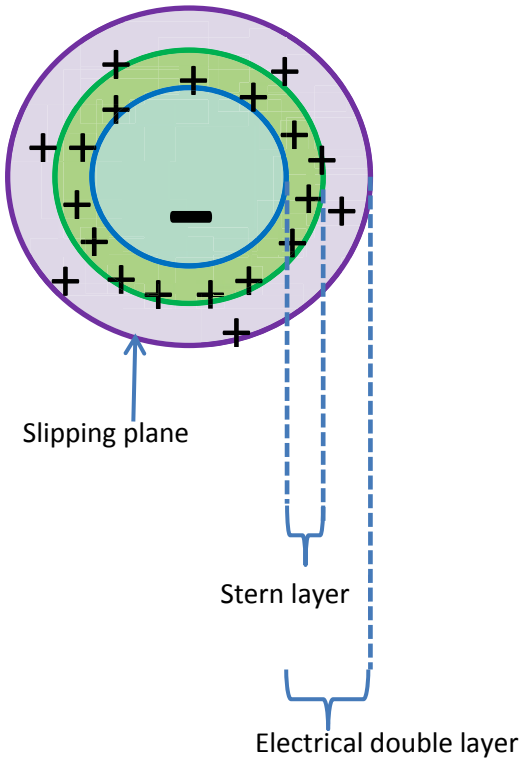

Figure 2.2. Components of the oppositely charged layers around charged NMs which contribute to their zeta-potential.

When NMs migrate, the ions that surround them also move with the NM, though any ions that are outside the double layer are not affected and do not move with the NM. This boundary between affected and non-affected ions is known as the 'slipping plane'. The voltage that exists at the slipping plane is also termed the zeta-potential and gives an indication of NM surface charge and thus electrostatic stability (Hunter, 2013).

When an electrical field is applied across a NM sample, charged NMs in the dispersion will be attracted towards the electrode of opposite charge. The viscosity of the medium will acts as a force in the opposite direction slowing the movement of the NMs, though eventually an equilibrium is reached and the NMs will begin to migrate with constant velocity, which is termed 'electrophoretic mobility' (Hunter, 2013). This can be used to calculate the zeta-potential using the Henry equation shown in equation 2.3.

$$U_E = \frac{2\varepsilon z f(ka)}{3\eta} \quad \text{(Equation 2.3)}$$

where U_E is the electrophoretic mobility, ε is the dielectric constant, z is the zeta-potential, ŋ is the viscosity and ƒ(Ka) is Henry's function which can either be 1.5 (Sze et al., 2003) for larger NMs, or 1, for NMs smaller than 200 nm.

The sample is illuminated and a detector detects the scattered light at a chosen angle. This scattered light fluctuates in intensity and the rate at which it fluctuates is directly proportional to the speed of the NMs (which is related to their size, see section 2.1.1 above). Approximately 1 mL of sample was taken up by a syringe and used to fill a capillary cell. This was done to avoid any bubbles from forming. The caps were added back and the cell was then inserted into the holder. A separate SOP was created to measure zeta potential where the same RI and absorption values were used as for DLS.

2.1.3 UV-Vis Spectroscopy

There is an electron cloud surrounding gold (metallic) NMs (Figure 2.3 a) which can be excited by illumination (b). The excited electron cloud begins to oscillate causing polarization of the NM, where the negatively charged electrons move away from the NM and a positive charge remains on the core (c) (Cao, 2004). Repolarization occurs as the electron cloud is restored and this sequence is repeated, resulting in resonance (d) which is termed surface plasmon resonance (SPR). The electron cloud around a specific sized (or shaped) NM will not oscillate unless excited by a specific wavelength. The absorption of light by the NMs creating the oscillation of electrons in turn provides a red colour to spherical gold NMs (Das et al., 2009). To simplify, NMs of a specific size absorb light of a specific wavelength which causes the oscillation of electrons (for example 25 nm gold absorbs at approximately 520 nm). This absorption can be seen on the UV-Vis spectrum at the specific wavelength. The colours corresponding to the wavelength causing the oscillation (for example 520 nm is green) are

absorbed and the dominant non-absorbed colour (red) is emitted (and thus is the colour "seen"). SPR is a useful property that can be quantified by UV-Vis to obtain an SPR band profile of the NMs which gives size and shape information.

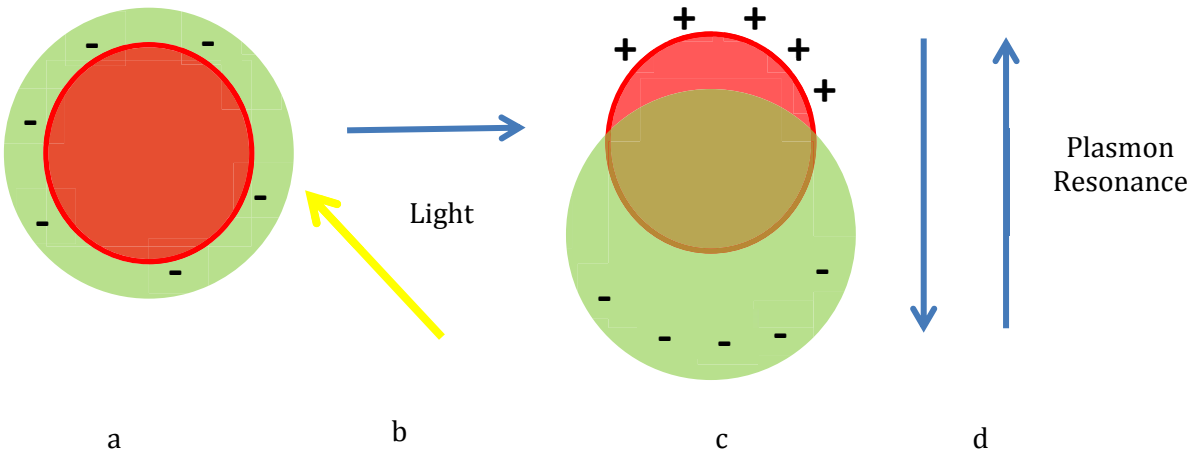

Figure 2.3. Schematic of light causing excitation of an electron cloud around a gold NM, resulting in surface plasmon resonance (SPR).

Below is a depiction of all of the components that comprise a UV-vis spectrophotometer as seen in figure 2.4

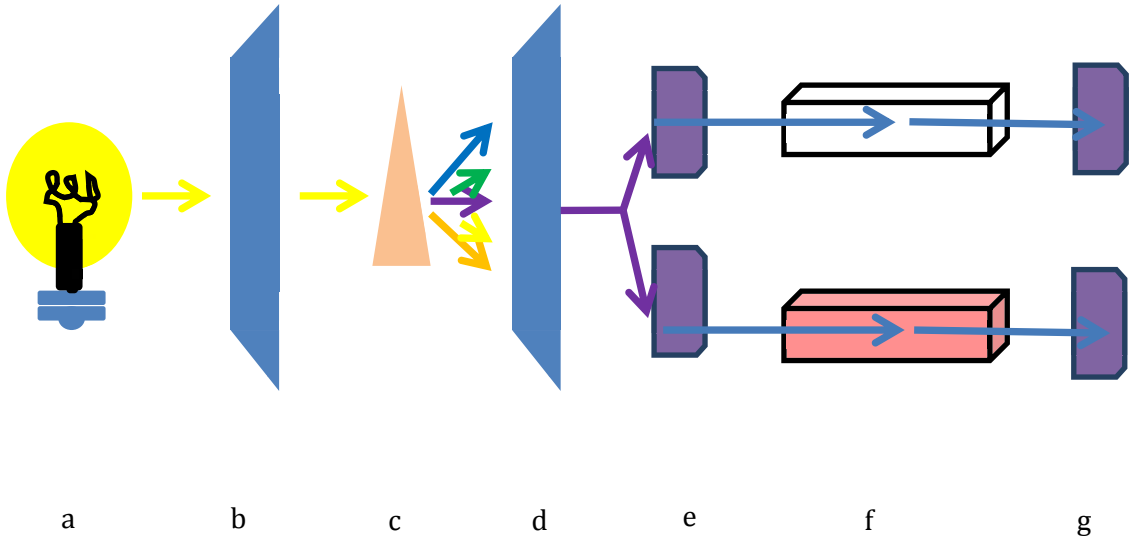

Figure 2.4. Schematic of a UV-Vis spectrophotometer.

In a UV-Vis spectrophotometer, a light source emits a light beam a) which enters a slit to ensure the light is coming out in parallel lines (b). The emerging light beam enters a monochromater (c) and the light is refracted into several beams. Only a pre-set range of wavelengths enters a second slit (d) and then is subsequently split by a beam splitter (e) which occurs when using dual beam UV-Vis, which was indeed the type used to conduct measurements. One beam enters a reference cell and another enters the cell containing the NM sample (f). When the light reaches the sample containing NMs, some of the energy is absorbed into the NM to cause the electron cloud to resonate, so that there is a decrease in intensity of the light that reaches the sample detector (g). The amount of light reaching the detector is proportional to the NM concentration.

The ratio of the intensity of light leaving the sample cell (I) to the intensity of light leaving the reference cell (I_0) is termed the % transmittance, which can be seen in equation 2.4.

$$\% \textbf{ Transmittence } = \frac{\boldsymbol{I}}{\boldsymbol{I_0}} \qquad \text{(Equation 2.4)}$$

% Transmittance (%T) is converted to absorption (A) to achieve a SPR band profile of absorbance of NMs over various wavelengths as seen in equation 2.5.

$$A = -logT \qquad \text{(Equation 2.5)}$$

Gold NM rods differ from spheres as they have two dimensions so that when light excites the electron cloud, the NM will have a longitudinal and transverse SPR and therefore will have an two absorption peaks in the infra-red region (Nikoobakht et al., 2002). Thus, the shape of the SPR can provide information about the NM shape also.

UV-Vis measurements were conducted using a Jenway 680 UV Spectrophotometer. An aliquot of gold NM suspension (made to 10 µg/mL with HH Combo medium) and reference medium

(HH Combo medium) were pipetted into the sample and reference cell (Plastiband disposable cuvettes) respectively. The wavelength was set to scan between 400-800 nm.

2.1.4 Transmission Electron Microscopy

The transmission electron microscope (TEM) allows for the visualization of objects such as NMs using a beam of electrons that interact with the sample (Kohl and Reimer, 2008). The electron microscope is a cylindrical tube completely devoid of air (vacuum) to remove any interference of air on electrons. A simplistic diagram of how a TEM works can be seen in figure 2.5.

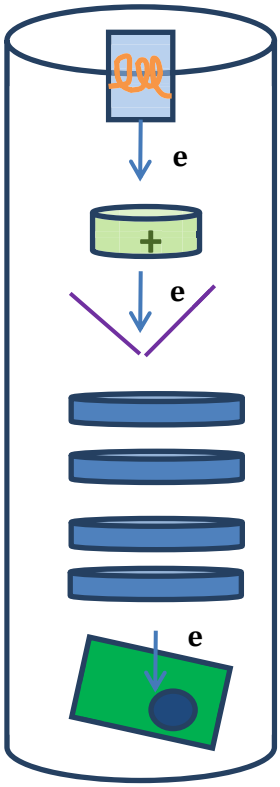

Figure 2.5. Simplistic representation of a transmission electron microscope (TEM).

The electrons are emitted by an electron gun located at the top of the tube which contains a tungsten filament acting as a cathode (source of negative charges such as electrons). A current is passed through the filament leading to thermionic emission of a field of electrons. Below the cathode is an anode plate which is positively charged and accelerates the electrons

towards it using an applied voltage of 80 KeV (Reimer, 1993). The electrons then pass through a series of apertures which forms them into a beam. Electrons are negatively charged and repel each other so a series of electromagnetic lenses (coils) are set down the length of the tube which provide a field which causes the electron beam to remain aligned (Reimer, 1993). The electron beam then encounters the sample and electrons are either absorbed, scattered or pass through the sample. As areas of the sample will be different in terms of their electron density, different amounts of electrons with different energy pass through the sample.

At the end of the tube, the electrons are collected on a phosphorus screen that creates an image of the sample. Areas that are not dense or have no sample will allow electrons to bombard the phosphorus screen which will excite a phosphorus electron and cause a photon to be emitted which is seen as a 'light' area. Areas of the specimen which are dense (contain NMs or sample) will not let electrons pass and are thus seen as 'dark' areas.

TEM samples were prepared using copper grids layered with a carbon film (Agar). 25 μL of sample was carefully pipetted on top of the grid and allowed to dry for 1 hour, covered to avoid any interference of dust. The grid was then carefully picked up by tweezers and suspended in DI water for 1 minute to remove any salts, and a second rinsing step was performed after a wait of 1 minute and then dried overnight. Samples were then analysed using a JOEL 1200 TEM.

2.1.5 Disc Centrifugation Sedimentation

Large particles (greater than 1 μm) in a liquid will sediment due to gravity, where large particles sediment first and small particles (of the same density) will settle later (Allen, 2013). Disc centrifugation sedimentation (DCS) is a technique that measures the time taken for particles to sediment through a liquid as a means to measure particle size using the previously mentioned Stokes law (equation 2.2). Small particles (less than 1 μm) such as

NMs, have a low rate of sedimentation as the Brownian motion of small NMs is too large to allow settling of NMs due to only gravity (Allen, 2013). Centrifugation provides a high g-force causing the settling of small NMs to be much faster. Stokes law is altered to accommodate the change in g-force as seen in equation 2.6.

$$D = \left(\frac{18\eta \ln\left(\frac{R_f}{R_0}\right)}{(\rho_p - \rho_f)\omega^2 t}\right)^{0.5} \qquad \text{(Equation 2.6)}$$

Where D is the NM diameter; ŋ is the viscosity of the fluid; R_f is the radius of the outside of the disc; R_0 is the radius of the inner disk; ρ_p is the density of the NM; ρ_f is the fluid density; ω^2 is the rotation speed of the disk; and t is the time needed for the NM to sediment across the distance of the disk.

A disc is rotated at high speeds to create a centrifugal force to help accelerate the sedimentation of the NMs as seen in figure 2.6.

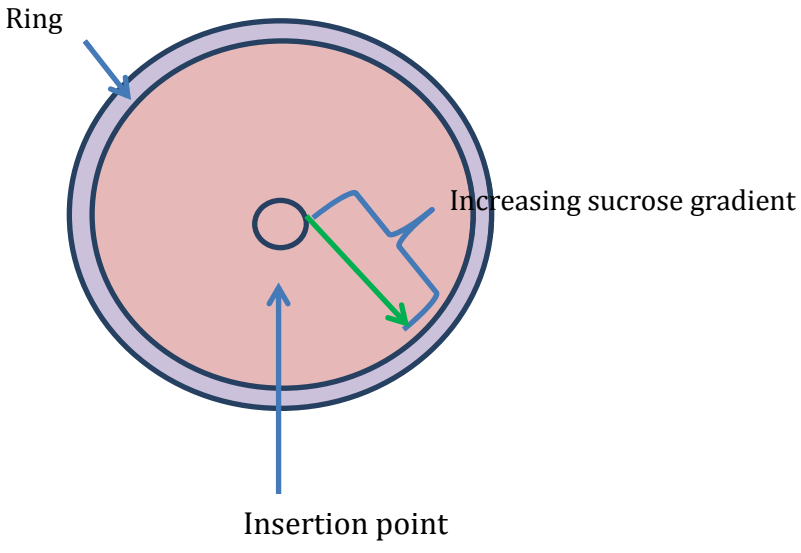

Figure 2.6. Schematic of the components of the disc centrifugation sedimentation (DCS) disk.

The disc is held in between a light source and a detector so the rings of NMs separate based on size during sedimentation. The sedimentation time can be measured by the decrease in light reaching the detector as each band goes past the light source.

When a sample of NMs denser than the fluid is placed in the disc, the NMs will not sediment according to Stokes-law but instead, the NMs will quickly sediment as a whole. The bulk 'crashing' of a sample is usually termed 'streaming' (Allen, 2013) and will not give accurate size measurements. One way to eliminate this problem is to create a density gradient of sucrose. When a sample of NMs is placed on the top of the fluid (at the injection point), the entire density of the suspension is slightly increased compared to just the pure sucrose solution, but the density of the sucrose solution just under the surface (moving towards the outside of the disk) is also marginally higher due to the density gradient and continues to increase towards the outside of the disk, so that there is no force causing bulk sedimentation of the NMs and therefore NMs sediment according to Stokes law (Allen, 2013). The density of the sucrose gradient depends on the density of the NM sample. A sample with a high density requires a longer range of the density gradient then a sample with low density, as seen in table 2.2.

Table 2.2. Sucrose gradients to be created based on NM density being analysed.

NM density	Sucrose gradient (%)
1.04-1.1	2-8
1.1-1.3	4-12
>1.3	8-24

Two stock gradients of sucrose were made separately in falcon tubes using weight/weight (w/w) depending on the density of the NMs that were being analysed to make 25 g total mass of each gradient type. Working masses used can be seen in table 2.3.

Table 2.3 Mass of sucrose (g) and water (g) to be added to create w/w concentration of 25 g of the corresponding gradient.

Percent gradient (%)	Mass of sucrose (g)	Mass of water (g)
2	0.5	24.5
8	2	23
24	6	19

An SOP for each type of NM was created entering in parameters such as density, absorption and RI which can be seen in table 2.4. The SOP allocates an optimal disk speed based on the provided parameters.

Table 2.4. Corresponding density, absorption and RI values for NM sample types.

NM type	Density (mg/L)	Absorption	RI
Gold	19.3	0.47	1
PS	1.052	1.594	0.02

An appropriate sucrose gradient was chosen for each specific type of NM based on its density, as previously seen in table 2.2. Using a 3 mL syringe, both chosen sucrose solutions were taken up in different ratios to make a final volume of 1.6 mL which was injected into the injection point. After the gradient was built, 0.5 mL Dodecane was also injected in order to prevent evaporation. The disk was allowed to spin for 40 mins before inserting the first sample in order to achieve an evenly distributed gradient of sucrose in the disk. 0.1 mL of calibration standard (0.239 PVC calibration standard CPS instruments) was then injected and followed by 0.1 mL of each sample to be assessed. The gradient was used for subsequent measurements for up to 6 hours.

2.2 Analysis techniques

2.2.1 BCA Assay for protein concentration

The BCA (bicinchoninic acid) assay is a technique to measure protein concentration using a bovine serum albumin (BSA) standard curve (Walker, 2009). The BCA assay consists of two steps; the first is the reduction of copper (Cu^{+2}) by the amino acids of proteins in the sample resulting in the reduction of Cu^{+2} to Cu^{+1} as depicted in figure 2.7.

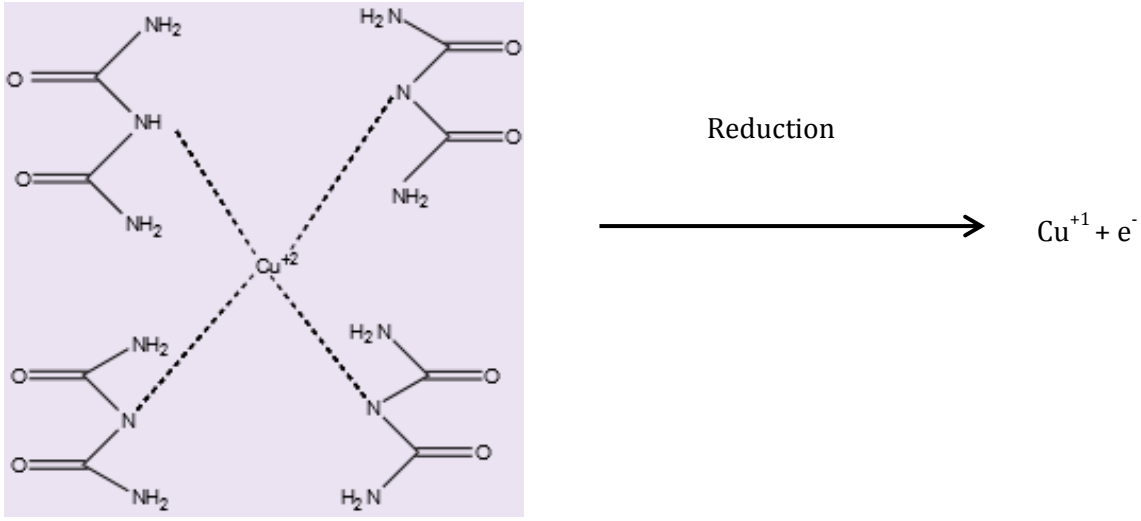

Figure 2.7. Proteins constructed of amino acids bind to Cu^{+2} to give a faint violet colour under basic conditions, Cu^{+2} is reduced to Cu^{+1}.

This results in a mildly coloured complex and is commonly known as the Biuret reaction and is sometimes used to measure protein concentration, though this technique is known to have low sensitivity and therefore may not be useful to measure samples of low protein concentration (Smith et al., 1985). BCA is known to have high specificity to complex with Cu^{+1} ions and remains stable (Smith et al., 1985) which can be seen in figure 2.8.

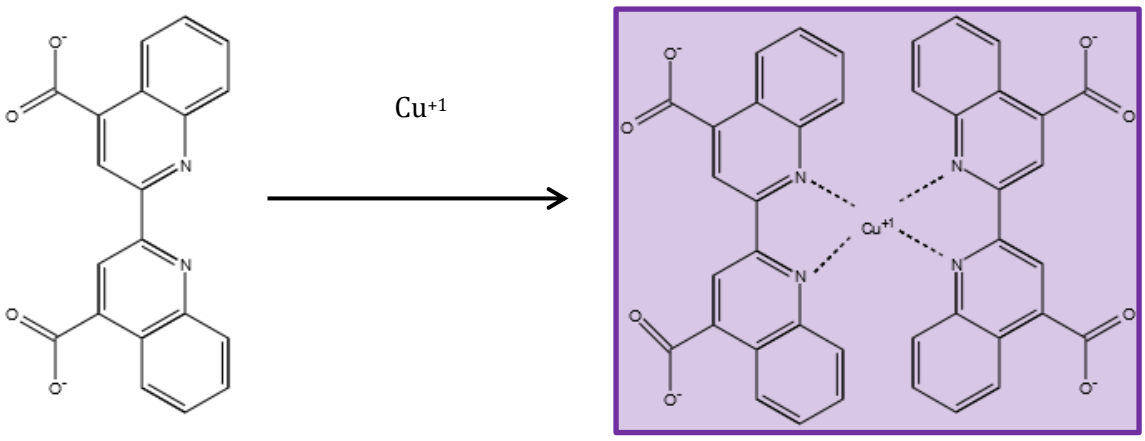

Figure 2.8. Two molecules of BCA selectively bind to Cu^{+1} resulting in a violet complex. The second step involves the reaction of each Cu^{+1} with two molecules of BCA as depicted in figure 2.8 creating a violet coloured complex which is soluble in water and has a strong absorbance at 560 nm.

For protein analysis of samples, a Peirce BCA assay kit was used. A range of dilutions were made using the known 2mg/mL BSA standard for a standard curve and 100 µL of each concentration was added to wells in a 96 well microplate (Falcon).

100 µL of samples of unknown protein concentration were added to empty wells. A 50:1 ratio of reagent A (sodium carbonate, sodium bicarbonate, sodium tartrate and the reactive ingredient BCA) to reagent B (4% cupric sulphate) was created in a falcon tube. The 4% cupric sulpfate will be reduced by the proteins present in the sample, and the BCA reacts with the reduced Cu^{+1} complex. Reagent A also contained 0.1 M sodium hydroxide to provide an alkali environment which was needed for the reaction. Enough of Reagent A and B was created to add 200 µL to each reaction well (each well can hold 300 µL of volume i.e. 100 µL of sample (or BSA) and 200 µL of reagent A:B mixture). The microwell plate was microwaved for 20 seconds (with the lid on) along with 100 mL of DI water in a beaker to act as a heat sink. The plate was analysed immediately using the absorbance function of a plate reader at 560 nm. The standard curve was plotted with absorbance versus BSA concentration and unknown protein concentrations from samples could be determined by their absorbance and the equation of the line of best fit to the standard curve.

2.2.2 CM-H_2DCFDA for ROS detection

Chloromethyl-dichlorodihydrofluorescein diacetate (CM-H_2DCFDA) is a general reactive oxygen species indicator within cells (Kristiansen et al., 2009). The mechanism of action is depicted in figure 2.10.

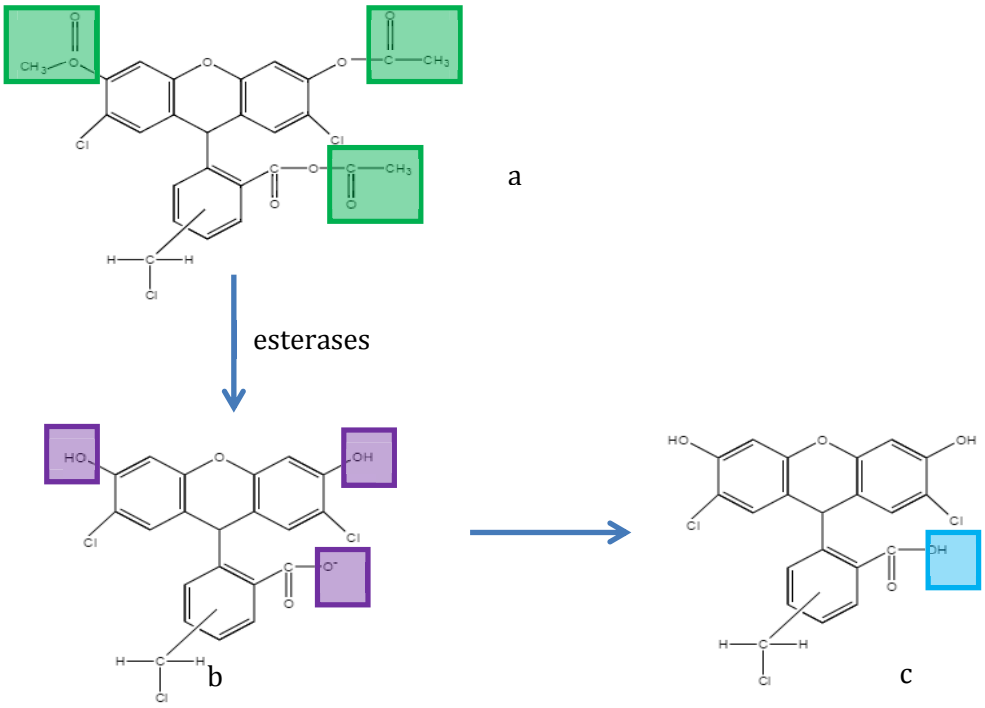

Figure 2.10. Schematic of the mechanism of action of CM-H_2DCFDA (a) which passively diffuses into the cell where esterase enzymes within the cell cleave off acetate groups exposing hydroxyl functional groups leaving the molecule in its reduced form (b); ROS within the cell oxidize the molecule (c) resulting in a fluorescent molecule which is detected by fluorescence emission at 520 nm and quantified.

CM-H_2DCFDA which is non-fluorescent, passively diffuses into cells (a) where its acetate groups (green panels) are cleaved off by esterase enzymes within the cell, which break ester bonds leaving behind exposed hydroxyl groups (purple panels) on the molecule (b), which is still non-fluorescent and in its reduced form. ROS within the cells oxidize the molecule (c) resulting in a fluorescent molecule which cannot diffuse back out of the cell (Eruslanov and

Kusmartsev, 2010). The chloromethyl (CM) group binds to cellular structures which increases its retention within the cell.

Eppendorf tubes containing 50 µg of CM-H_2DCFDA were stored in the freezer and were thawed in the dark at room temperature for approximately 15 mins immediately before use. 86 µL of absolute ethanol was pipetted into the Eppendorf tube to create a 1mM stock. A 50 µM working stock was created using the original 1 mM stock and absolute ethanol. Enough working stock was created to add 50 µL to every 250 µL sample (HH Combo medium and *D. magna* neonates) and incubated for 40 mins. ROS accumulation was assessed using the fluorescent function on the plate reader at 485-512 nm excitation/520 nm emission.

2.2.3 Fluorescence quantification of NM uptake

Fluorescence is the light emitted at a specific wavelength by a molecule after the absorption of light energy (Hibbs, 2004). Figure 2.11 is a depiction of a stokes shift and will be described below.

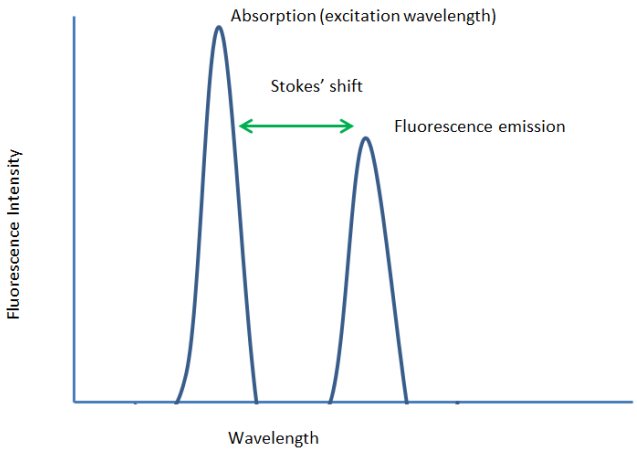

Figure 2.11. Emission of a longer wavelength photon due to absorption of a lower wavelength photon resulting in a Stokes shift.

When a molecule absorbs a photon, it gains energy and an electron jumps to a higher and more excited state. As the electron drops back down to a ground state it emits a photon

(Hibbs, 2004). Stokes fluorescence is a re-emission of longer wavelength photons by a molecule that has absorbed photons of a shorter wavelength. When the emitted photon has less energy than the absorbed photon this energy difference is a stokes shift (Brinkley et al., 1994).

Fluorescence can be quantified using a plate reader. Commonly, a tungsten-halogen lamp is used as a light source and an excitation wavelength is selected to illuminate the sample with 'excitation light'. The wavelength of the excitation and emission light are selected by the use of a monochrometer, which can use interference filters (or a prism or diffraction grating), which restrict one or more spectral bands and transmit others. Both the excitation and emission pathways are positioned with a 4-position filter wheel and emitted light is detected by a photomultiplier tube detector.

Costar 96-well microplates (flat bottom), were used for fluorescence analysis. Samples were carefully pipetted into the microplate wells (which had a maximum volume of 300 µL). Microplates were wrapped in foil while being transported to the plate reader to avoid any light from reaching the samples. The micro-well plate was inserted into the plate reader and the corresponding emission/excitation wavelengths were selected using the filters via the Omega software. The gain was adjusted and kept consistent throughout the NM uptake studies for each type of NM to allow for comparison of NM uptake based on fluorescence.

2.2.4 Mass Spectroscopy for protein identification

The sample (of *D. magna* conditioned medium) is injected into the mass spectrometer and a heated filament vaporizes the sample. The sample is a mixture of peptides which have been digested by trypsin and separated by liquid chromatography (LC).

The separated sample is injected and subjected to an electrospray ion source. This is a technique where a potential difference is applied across a liquid sample to create an aerosol consisting of ionized peptides. This will not affect the mass of the peptides, although it will

cause it to acquire a positive charge. This technique is useful to produce ions of peptide samples as it does not promote the fragmentation of the peptides after ionization. The mass spectrometer also uses collision-induced dissociation (CID) which causes breaking of molecular ions in the gaseous phase via collisions with neutral nitrogen, where the kinetic energy of the molecular ion is converted to internal energy on bombardment, causing bonds to break and the molecule to fragment, which occurs within the ion trap. It is important to fragment the molecule or only one peak of the parent molecule would be detected, giving the mass but not the structure of the molecule. Fragmenting the parent molecule allows for piecing together of the structure of the parent molecule. Both the parent and the fragments are then detected by the orbitrap analyser in m/z.

2.2.5 Epoxy-resin Embedding

To analyse uptake of NMs into the gut of *D. magna*, after exposure to a NM suspension, neonates were fixed in 2.5% gluteraldehyde solution in a 0.1 M phosphate buffer. Neonates were then dehydrated in a graded ethanol series and then embedded in an Agar100 epoxy resin. After polymerisation of the resin (which takes 48 hours at 60 ˚C), 1 µm survey sections were cut and mounted on a slide and stained with Toludene blue to locate the desired area to be further sliced. After selecting the area to be sectioned, ultrathin (80 nm) sections were cut using a diamond knife. Sections were mounted on a 100 mesh copper grid coated with Formvar/carbon. Ultrathin sections were stained using 30% Methanolic Uranyl Acetate and Reynolds Lead Citrate. Grids were examined using the Joel 1200EX TEM and images were taken between 5000-3000X magnification. Preparation of the epoxy resin samples was done with support from the centrally run electron microscopy facility.

2.2.6 Total Carbohydrate detection

A carbohydrate detection kit (Abcam) was used to quantify the concentration of carbohydrates released by *D. magna* into HH Combo medium as well as the carbohydrate

content in environmental samples. The first step uses Sulfuric acid (H_2SO_4) which causes the hydrolyzation of glyosidic bonds that hold together polysaccharides and breaks them into monosaccharide units (such as glucose) which are then converted by dehydration to the aldehyde furfural or hydroxyfurfural (Nielsen, 2010) as seen in figure 2.12.

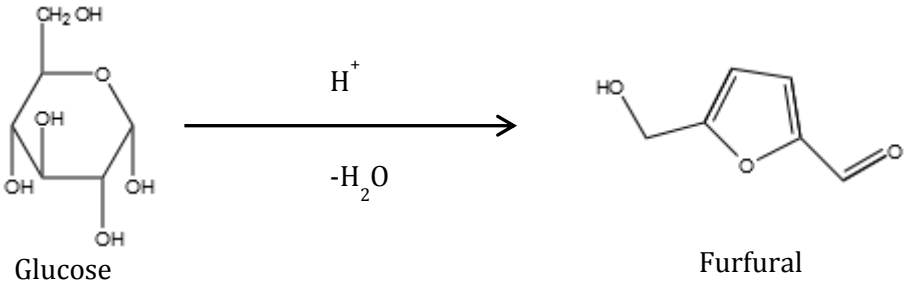

Figure 2.12. The dehydration of glucose by H_2SO_4 to form the aldehyde furfural.

The second step is where Furfural or Hydroxyfurfural reacts with two molecules o phenol naphthol, which is in the developer, in a condensation reaction to form a coloured compound which can be measured by absorbance at 490 nm as seen in figure 2.13.

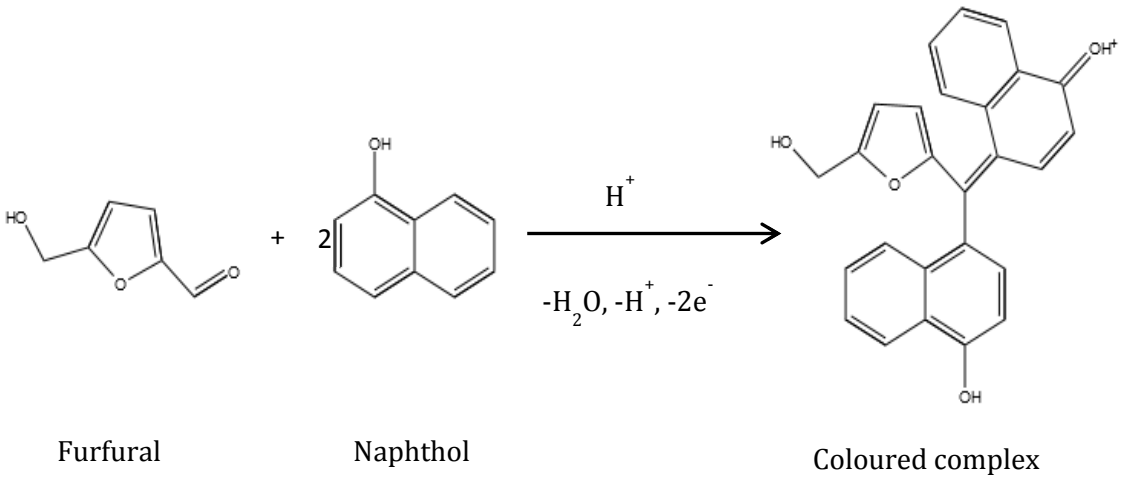

Figure 2.13. Furfural undergoing a condensation reaction with two molecules of naphthol, to form a coloured complex that can be quantified by its absorbance at 490 nm.

A glucose standard curve was created using glucose concentrations of 0-20 µg per well (volume 30 µL) adjusted using DI water. 30 µL of conditioned HH Combo medium (containing carbohydrates and other macromolecules) or environmental samples were added to separate wells in triplicate. Then, 150 µL of H_2SO_4 was added to each well and allowed to mix on a shaker for 1 min and then incubated for 15 minutes at 90 ˚C in an oven. Then, immediately upon removal, 30 µL of developer was added to each well and allowed to react whilst shaking for 5 minutes at room temperature. The absorbance was then measured at 490 nm using a plate reader.

2.2.7 Hard-Corona Isolation

NMs were incubated in conditioned media for a set incubation time. The protocol for protein-corona isolation was used and modified from Monopoli et al, 2013 (Monopoli et al., 2013). At the end of the incubation time the NM-protein mixture was centrifuged for 20 mins at 15,200 G at 4°C to separate the NM-protein complex from unbound proteins. The supernatant was aspirated off and the pellet was re-suspended in 1 mL of phosphate buffered saline (PBS). The centrifugation and re-suspension steps were repeated three more times in order to remove the soft corona leaving only the strongly bound proteins of the hard corona in the pellet. To elute the hard corona proteins from the NMs, 100 µL of SDS lysis buffer was added to the sample. The SDS lysis buffer was made volumetrically in a 100 mL volumetric flask and can be seen in table 2.5 and was stored frozen in 1 mL Eppendorf tubes.

The resulting SDS lysis buffer was a four times (4X) concentrated solution. Therefore at the time of use, 25 µL of the 4X solution was added to 75 µL of PBS to create a 1X solution to be added to each NM-hard corona sample and incubated at 95°C for 5 mins to allow for proteins to denature and be released from the NM surface. The NMs were then pelleted by centrifugation at 15,200G for 15 mins at room temperature leaving only the proteins that were present in the hard corona in the supernatant.

Table 2.5. Ingredients of the SDS denaturation buffer to create a 4X concentrated suspension.

Ingredient	Amount	Purpose
Tris-HCl (1 M and pH 6.8)	2 mL	A buffer that provides chloride ions
SDS	0.8 g	Detergent to denature and to provide overall negative charge to proteins
10% Glycerol	4 mL	Increases the viscosity of the sample
ß-mercaptoethanol	4 mL	Denatures proteins by acting as a reducing agent and reduces the disulphide bonds between amino acids
0.01 % Bromophenol blue	500 µL	Staining dye to be able to detect the sample on the gel
DI water	Top to 100 mL	To maintain an ion free volume

This step was conducted although was not necessary as once the proteins are denatured they will move through the resolving gel while the NMs (if not removed) will get retained within the stacking gel. The supernatant was gently pipetted and transferred to a fresh vial which was stored at -18°C until its use in a gel.

2.2.8 Gel electrophoresis

Sodium Dodecyl Sulphate Polyacrylamide Gel Electrophoresis (SDS-PAGE) is a commonly used method to separate molecules such as proteins based on molecular weight (Blancher and Jones, 2001). Polyacrylamide is used to form a matrix which has pores (Blancher and Jones, 2001). Protein samples are added to the top of the gel (one sample in each well), where the negative electrode is and the bottom of the gel chamber has a positive electrode. A

voltage is applied to the gel (using a power pack) so that the proteins migrate through the pores, whereby larger proteins remain at the top of the gel unable to move through the pores and smaller proteins are able to move lower down the gel so that the proteins are separated based on size, as seen in figure 2.14.

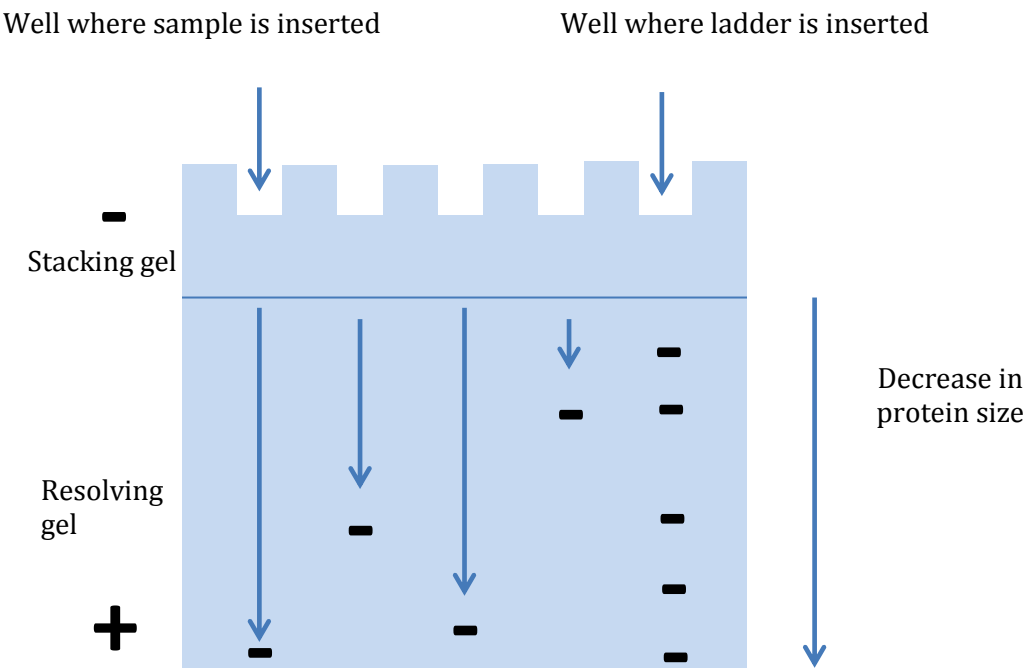

Figure 2.14. Schematic of an SDS-PAGE gel containing the stacking and resolving regions whereby proteins migrate down the gel according to their size (Molecular weight).

To create a gel for an SDS-PAGE, solutions need to be made both for stacking (4%) and resolving gels (12.5%), the contents of which can be seen in table 2.6. This percentage relates to the amount of acrylamide in the gel solution. For example, when making a 12.5% resolving gel, 20.8 mL of the acrylamide/bis-acrylamide gel solution was used of which 30% was acrylamide equating to 6.24 mL. 6.24 mL of the entire 50 mL resolving gel made equals 12.5 %. The separation of the proteins is determined by the size of the pores inside the gel. The size of the pores is determined by two factors; firstly, the amount of acrylamide within the gel (which can be adjusted by altering the ratio of acrylamide to DI water), and secondly, the amount of crosslinker could be adjusted (the ratio of bis-acrylamide to acrylamide in the solution used was 0.8%/30% equating to 2.7% which is the cross-link percentage). A higher

percentage of acrylamide or crosslinker results in a smaller pore size formed in the gel. The 12.5% was chosen based on the range of molecular weights of the proteins to be separated.

Table 2.6. Components and amounts of stacking and resolving gels for PAGE.

	4% (Stacking Gel)	12.5% (Resolving Gel)
Distilled H_2O	30 mL	16.1 mL
Tris-HCl	12.5 mL	12.5 mL
Acrylamide/ Bis-Acrylamide	6.7 mL	20.8 mL
10% SDS	0.5 mL	0.5 mL
APS	500 µL	500 µL
TEMED	75 µL	75 µL

The first four components, DI water, tris-HCl, acrylamide/bis-acrylamide and SDS were made into a solution and stored in bulk (approximately 50 mL) in a falcon tube while ammonium persulphate (APS) and tetramethylethylenediamine (TEMED) were added at the time of use as these will cause the gel to polymerize (Tang et al., 2005). Approximately 10 mL (one fifth of the stock solution) is needed per gel plate so that 100 µL APS and 15 µL of TEMED were added to a fresh falcon tube which already had the other components. The resolving gel was prepared first in a falcon tube and inverted three times to ensure homogeneity. 10 mL of the gel was then pipetted using a 10 mL graduated stripette, though only 8 mL was needed to fill the 1.5 mm gap between the two glass plates, and was left to set which took approximately 20 mins. The glass plates had previously been clipped firmly into a gel clipper which was then firmly clipped to a larger holder so that none of the gel would leak from the bottom, as seen in figure 2.15.

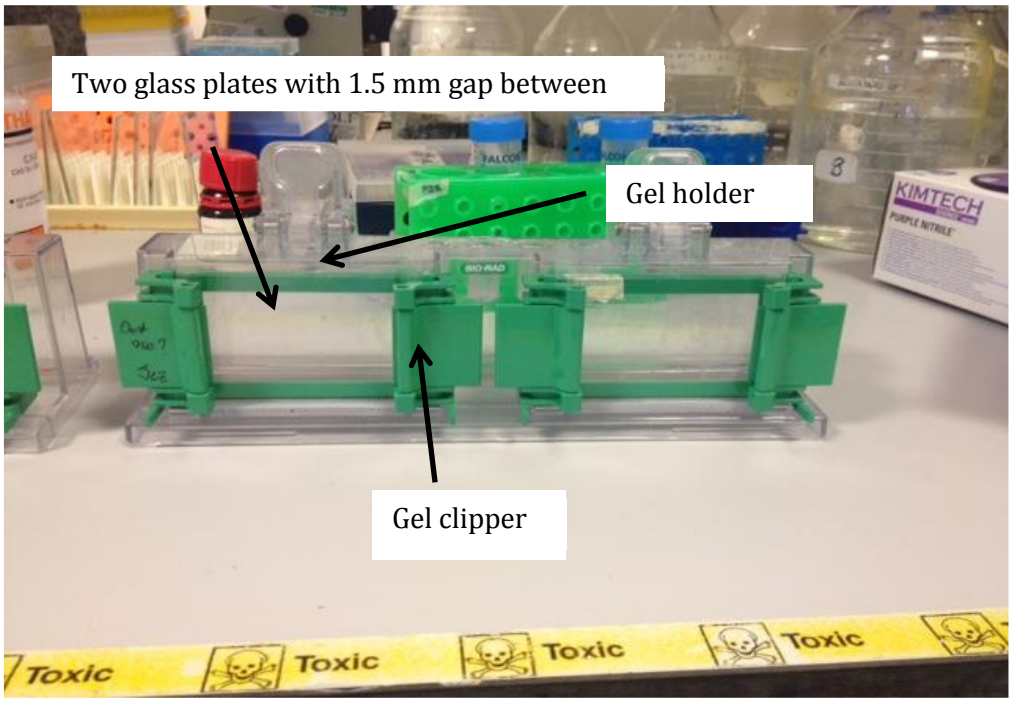

Figure 2.15. Set up for making PAGE gels: setting gel is pipetted into the gap between 2 glass plates (1.5 mm gap) held together firmly by a gel clipper and firmly held up by a gel holder.

The 2 mL remaining in the falcon tube was used as a guide to when the gel was set. A small amount of ethanol (70 %) was added on top of the resolving gel to flatten the top edge. Once the resolving gel had set (~ 20 mins), the excess ethanol was discarded. APS (100 µL) and TEMED (15 µL) were then added to create the final solution of the stacking gel (already containing 6.7 mL (of which 30% w/v is acrylamide and 0.8% w/v is bis-acrylamide crosslinker) and then was added using a stripette over the resolving gel which was already set. The comb was then inserted immediately into the resolving gel so that the resolving gel set around it. Once the resolving gel had set the glass slides with the gel inside were clipped into the gel holder and inserted into the tank with the wells facing the inside. Running buffer (1 X) was added to fill the running tank up to the '2 gel' line and the comb was then carefully pulled out. A comprehensive list of how each of the stocks were made can be found in table 2.7.

Table 2.7. Ingredients and protocol to make stock solutions used in PAGE.

Item	How it was made
Tris-HCl (for stacking gel) 0.5 M pH 6.8	78.8 g of Tris was dissolved in 1 L of DI water volumetrically. 1 M HCl was used to obtain the correct pH
Tris-HCl (for resolving gel) 1.5 M pH 8.8	236.4 g of Tris was dissolved in 1 L of DI water volumetrically. 1 M HCl was used to obtain the correct pH
10 % SDS	10 g of SDS was dissolved in 100 mL of DI water volumetrically
Running Buffer	Firstly, a 10X Running buffer was made by dissolving 144 g glycine, 30 g Tris and 4 g SDS into 1 L of DI water volumetrically and then poured into a glass bottle. A 1X running buffer was then made by diluting 100 mL of 10X running buffer into 900 mL DI water.
APS	1 g of APS was dissolved in 10 mL of DI water volumetrically, then divided into 1 mL aliquots in Eppendorf tubes and frozen until use

An important component of the running buffer is glycine, which is an amino acid that plays an important role in the protein separation by PAGE gels, as described in detail below. pH influences the pKa which is a property of an individual proton on a molecule. In acidic conditions (below pka 2.3) the amino acid is protonated and therefore positively charged. In alkaline conditions (above pka 9.6), the amino acid is deprotonated and therefore negatively charged. Between these two pH's, the amino acid is neutral (zwitterionic) as the positive and negative charges cancel out (Jensen and Gordon, 1995) as seen in figure 2.16.

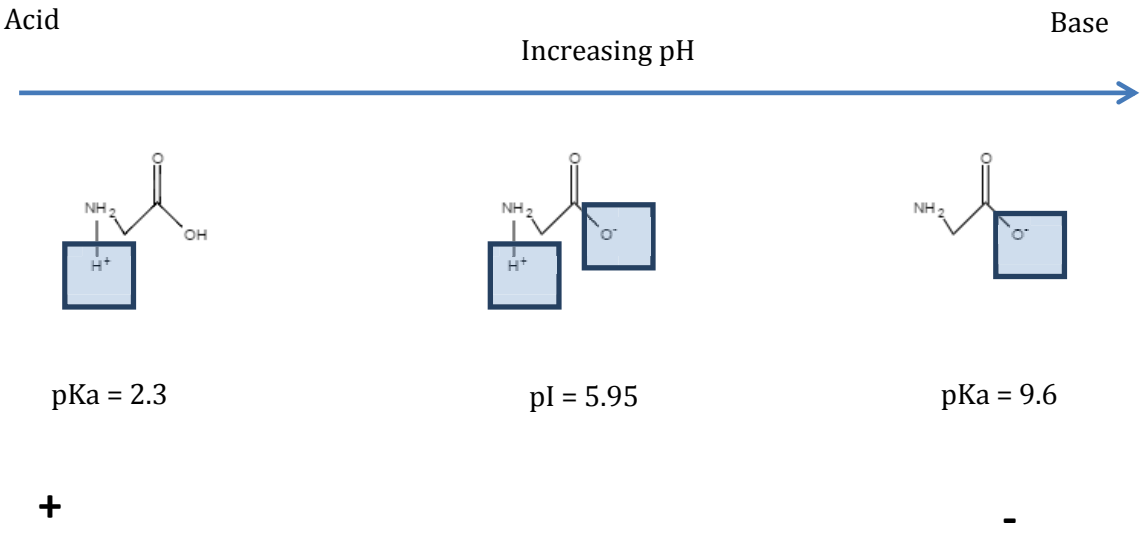

Figure 2.16. Various charge states of glycine under different pH conditions.

Between the two pKa values (2.3 < pKa < 9.6), glycine is a neutral amino acid with no overall charge at the isolectric point (pI). In the range of pH between the neutral and fully negative glycine, glycine will have a slightly negative charge and the negativity increases as the surrounding pH becomes more basic. The pH of the stacking gel is 6.8 so the glycine will migrate from the negative to the positive end of the gel, though it is only partially negative if not closer to neutral. The other two components that will migrate are the strongly negative charged Cl^- (from the tris-HCl buffer) and the negatively charged SDS-protein sample so that Cl^- will migrate first, then the SDS protein sample and finally the partially negative/neutral glycine. In a sense, the SDS-protein samples are 'stacked' in between the other two components which is why this part of the gel is termed the 'stacking gel'. When the samples enter the resolving gel, the pH is 8.8 which makes the glycine much more negatively charged. The order of the components as they move through the resolving gel is first the Cl^- then the highly negative glycine and finally the SDS-protein complexes which are 'free' to move at their own speed according to their size. This discontinuous gel system is used so that when proteins enter the stacking gel, they are stacked together and all the samples will enter the resolving gel at the same time giving comparable separation. If the samples were inserted

straight into the resolving gel, the proteins would enter at different times, reducing the separation efficiency.

8 µL of protein MW ladder (BioRad) was added to the well on the end of the gel and 25-30 µL of sample (the isolated hard-corona that had been previously heated at 95˚C for 5 mins in SDS and glycerol solution with bromophenol blue to track band progress through the gel, as described in Section 2.2.8) was added to the other wells using gel loading tips and then topped with running buffer. The voltage was set to 100 V and allowed to run for 2-3 hours until the samples could be seen to reach the bottom of the gel (the bromophenol blue in the denaturation solution allows tracking of the bands so that the proteins do not run off the gel). When the gel was complete the running buffer was poured out and the glass plates containing the gel was carefully prised apart (using a plastic priser) and the gel was peeled off and washed with DI water in a washing tray for a few minutes. Coomassie blue stain was poured over the gel until fully submerged and left on a shaker for 1 hour and then discarded. Destain was poured over the gel and left to destain for 2 hours, decanted off and then fresh destain was poured over the gel and allowed to shake overnight. Coomassie staining is a useful and relatively simple technique though is not very sensitive having a detection limit of only 100 ng so that bands present may not always show up clearly using only Coomassie (Weiss et al., 2009). Silver staining is a more sensitive technique that can be done after the Coomassie stain or without it. Gels were always done with the Coomassie stain in case bands did appear and then silver staining was done subsequently.

2.2.9 Silver Staining

Proteosilver contains silver nitrate which binds to the amino acids which comprise proteins under near neutral pH. The silver ions bound to the amino acids are then reduced by formaldehyde at basic pH to form metallic silver on the gel. Silver staining has a much higher sensitivity than the Coomassie stain (Weiss et al., 2009) though there are a few disadvantages, such as the use of formaldehyde in the process making it incompatible for

subsequent use in mass spectrometry, the length of time for development is variable making the reproducibility of the gels difficult, and the whole process is time consuming. Silver staining was conducted at room temperature on an orbital shaker at medium stetting in a clean plastic tray after the gels were destained from Coomassie overnight. The following steps were used to stain the gels using silver staining using the ProteoSilver Stain Kit (Sigma Aldrich).

I. The gel was washed with 150 mL of 30% ethanol to remove any of the fixative acetic acid from the Coomassie stain.

II. The ethanol solution was removed and the gel was then washed with 250 mL of DI water for 10 mins on a shaker.

III. The water was then removed and the gel was washed with 100 mL of the sensitizer solution for 10 mins. This was made by adding 1 mL of the ProteoSilver sensitizer to 99 mL of DI water.

IV. The sensitizer solution was then removed and the gel was then washed with 250 mL of DI water for 10 mins on a shaker.

V. The water was then removed and the gel was then washed with 100 mL of Silver solution for 10 mins. This was made by adding 1 mL of ProteoSilver solution to 99 mL DI water.

VI. The silver solution was removed and the gel was then washed with 250 mL DI water for approximately 1 minute. Care was taken not to wash the gel for longer than 1 minute as this can lead to the silver solution being removed resulting in poorer sensitivity.

VII. The water was then decanted and the gel was developed by adding 100 mL of developer solution. This was made by adding 5 mL of ProteoSilver developer 1 and 0.1 mL of ProteoSilver developer 2 to 95 mL of DI water. The development time was approximately 2-5 mins until bands appeared.

VIII. When the development was finished, 5 mL of 'stop solution' was added on top of the developer and incubated for 5 mins. A minimal amount of release of CO_2 occurred. Once the incubation was complete, the developer and stop solution mixture were removed and the gel was washed in 250 mL DI water for 15 mins and the gel could be stored in fresh DI water. Images of the gel were taken with a BioRad (GelDocEZ using the white light try).

2.2.10 Confocal Microscopy

A laser (excitation chosen depending on the fluorophore in the sample) is shone onto a set of mirrors which tilts the laser beam and the beam is then focused onto the fluorescent sample by an objective lens as seen in figure 2.17. This excitation beam from the laser excites the fluorophore present in the sample and an emission is released which goes back through the objective lens and passes through the mirrors and hits the detector system.

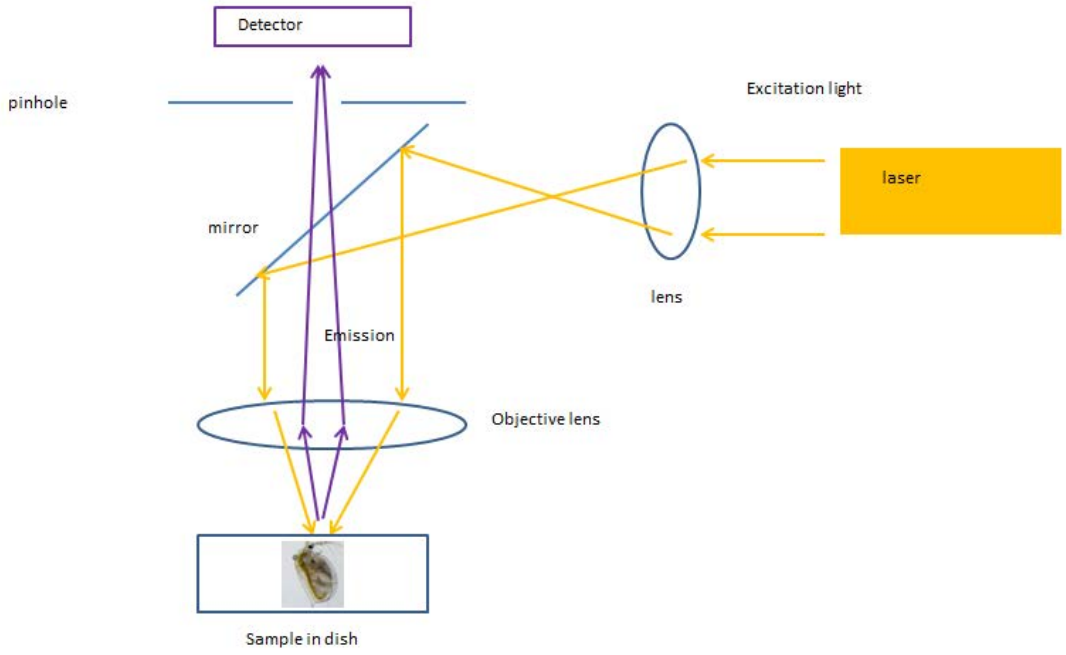

Figure 2.17. Schematic of the components of a confocal microscope and how they create an image.

Confocal imaging is a useful technique to image as only in-plane light reaches the detector making images much sharper compared to epi-fluoresence. In the detector system there is a pinhole aperture. The excitation light may illuminate other sections in different focal planes which would emit their own emissions and travel towards the detector which would produce noise. The pinhole reduces the out of focus light and only allows in-focus emitted light to pass through to the detectors. Since this will be fluorescent light, it will be different from the original laser light, and emission filters are used to isolate them from any laser light that is reflected from the sample. The emitted light from the fluorophore may be of weak intensity so a photomultiplier (PM) collects the photons that are emitted by the sample and transforms the light signal into an electrical signal which is recorded. The laser scans the sample and any photons emitted are constantly converted by the PM to give a real-time image of the specimen.

Samples of *D. magna* that had consumed fluorescent NMs were washed in fresh HH Combo medium to remove any fluorescent NMs from their exoskeleton and placed in a 35 mm round dish. The fluorescence excitation/emission pathways were chosen depending on the fluorophore. A Carl Zeiss Confocor LSM710 was used with the 458 nm laser for fluorescent PS-COOH and the 543 nm laser for RB-ITC conjugated gold NMs (see Chapter 4 for details).

2.2.11 Statistical approaches

To compare statistical relevance between two or more samples, Student's t-test was used by comparing n=3 of each sample. The purpose of the t-test is to check if the average (with several repeats) of two groups is reliably different (statistically significant difference) and does this by assessing the variance between the groups to the variance within the groups as seen in equation 2.7.

$$T = \frac{varience\ between\ gropus}{varience\ within\ groups}$$

Each T value has a corresponding p-value, which is the probability that the pattern of the data in the sample could be produced by random data and is therefore a good indication of a significant result. A p-value of 0.05 indicates there is a 5% chance there is no real difference between groups. 0.05, 0.01 and 0.001 were the p-values selected when comparing samples for statistical difference.

2.3 Biological Culturing techniques

2.3.1 High-Hardness Combo medium and *D. magna* culturing

High Hardness (HH) Combo medium was developed to be used for culturing and testing studies involving *D. magna.* The medium has been developed from the previous Combo medium which was used for soft water daphnia and modified for hard water daphnia such as *D. magna*. This medium also allows for healthy growth of algal food source (Baer and Goulden, 1998).

D. magna of the Bham2 strain were cultured in HH Combo medium with each culture vessel containing 15 individuals (originally neonates which grow into adults and produce neonates for experimental use) in 900 mL of medium, as seen in figure 2.18.

Figure 2.18. Culture vessels of D. magna in 900 mL of HH Combo medium.

Eight different stock solutions, , details of which can be seen in table 2.8, were used to create the medium, by adding 4 mL of stocks 1-7 and 8mL of stock 8 into 3500 mL of DI water in a 4 L beaker. Then, 200 µL of sodium selenite was added and the solution was topped up to 4000 mL and aerated overnight (minimum 2 hours to reach a saturated oxygen content).

Table 2.8. Ingredients in High Hardness Combo Media

	Compound	Formula	Stock (g/L)
1	Calcium Chloride, Dihydrate	$CaCl_2 \cdot 2H_2O$	110.28
2	Magnesium sulphate heptahydrate	$MgSO_4 \cdot 7H_2O$	113.5
3	Potassium phosphate dibasic	K_2HPO_4	1.742
4	Sodium nitrate	$NaNO_3$	17
5	Sodium metasilicate nonahydrate	$Na_2SiO_3 \cdot 9H_2O$	28.42
6	Boric acid	H_3BO_3	24
7	Potassium chloride	KCl	5.96
8	Sodium Bicarbonate	$NaHCO_3$	63

The pH of the medium was adjusted to between 7.6-7.8 using 1M HCl wherepon 4 mL of animate (table 2.9) and 2 mL of vitamins (table 2.10) were added.

Table 2.9. Ingredients in Animate. 1 mL of each of the stocks was pipetted into a 1 L volumetric flask containing 500 mL of DI water and the volume was then brought to 1L. The contents were decanted into a Duran bottle for use.

Compound	Chemical formula	Stock (g/100 mL)
Lithium chloride	LiCl	31
Rubidium chloride	RbCl	7
Strontium chloride Hexahydrate	$SrCl_2 \cdot 6H_2O$	15
Sodium bromide	NaBr	1.6
Potassium iodide	KI	0.33

Table 2.10. 30 mL of DI water was added to a 50 mL volumetric flask. Biotin and B12 were thawed at room temperature and 0.5 mL of each was added along with 10 mg of Thiamine HCl and toped up to 50 mL with DI water. The solution was decanted into a small bottle and wrapped in foil and kept in fridge for use for the week.

Compound	Original stock	Working stock
Biotin (*d*-biotin)	10 mg into 96 mL H_2O	Aliquot into 1.5 mL Eppendorf tubes and freeze
B12	10 mg into 89 mL H_2O	Aliquot into 1.5 mL Eppendorf tubes and freeze

Individual *D. magna* were carefully transferred to new media weekly and neonates (of third or more brood) were filtered out for experimental use. *D. magna* cultures were fed daily on *C. vulgaris* and enough food was provided as per the age of the daphnia in the culture vessel (1-2 days: 1 mL, >3 days: 1.5 mL). Cultured *D. magna* also underwent a 16:8 light: dark cycle period where optimal temperature (20 ±2 ˚ C). Adult *D. magna* were discarded after 8 weeks and 1 day old neonates were used to create new stock cultures.

2.3.2 *C. vulgaris* culturing

The strain of algae used for daphnia feeding was *C. vulgaris* and was cultured using Bolds Basal Media (BBM) which promotes algae growth (Megharaj et al., 2000). Approximately 3-5 stocks were actively being grown at each given time and the best looking stock visually was chosen to culture and to prepare the new stocks, as seen in figure 2.19.

Figure 2.19. C. vulgaris being cultured in BBM under aeration and exposed to UV light.

The stocks remained under aeration and are exposed to UV light as seen above. For algal feed preparation, algal stocks were centrifuged at 3500 rpm for 15 mins at 4°C and the pellets were re-suspended in Standard Combo Media (SCM) which promotes algal maintenance. The optical density (OD) of the suspension was checked at 440 nm and adjusted to an OD of 0.8 which is then ready for use. The algae were stored at 4°C with new stocks being cultured every few days.

2.4 Chapter specific protocols

2.4.1 Chapter 3 protocols

2.4.1.1 NM dispersions

Both amino (NH_2) and carboxylic acid (COOH) functionalized PS NMs of a stock concentration of 20 mg/mL were obtained from a previous FP7 project (QualityNano). The stock concentrations were diluted to concentrations ranging between 0.0001-1 mg/mL using HH Combo medium to a final volume of 5 mL. Ten *D. magna* neonates (1-3 days old) were then exposed to the different concentrations of NMs for 24 hours to determine the half-maximal effective concentrations (EC_{50}) levels. A concentration of 0.01 mg/mL of PS NMs, corresponding to $EC_{30\text{-}40}$ values for PS-COOH and PS-NH_2, was used for subsequent studies on uptake and retention of NMs, as this concentration had higher survival rates of neonates compared to an EC_{50} though also clearly appeared to have some effect on survivorship.

2.4.1.2 Impact of functionalised PS on *D. magna* EC_{50}

Ten *D. magna* neonates (1-3 days old) were exposed to various concentrations (between 0.0001-1 mg/mL) of either NH_2 or COOH functionalized PS NMs dispersed in HH Combo medium with final volumes of 5 mL. Neonates were exposed for 24 hours, at which time the survival rate of neonates was determined. The EC_{50}, at which 50% *D. magna* mortality observed when exposed to PS-COOH and NH_2 NMs were 0.0363 mg/mL and 0.0258 mg/mL respectively (n=3). The same study was carried out using NMs that had been incubated for either 6 or 24 hours in conditioned HH Combo medium that had previously been conditioned for 6 hours to assess the potential influence of the *D. magna* secreted eco-corona on NM toxicity.

2.4.1.3 Assessment of NM uptake and removal by *D. magna*

Fluorescently labelled PS-COOH NMs (Polysciences) were used to assess NM uptake and removal by *D. magna* neonates. Ten daphnia magna neonates (1-3 days old) were exposed to NMs for either one, two or three hours and at the end of exposure time, neonates were transferred to fresh HH Combo medium and washed three times to remove any NMs bound to the exoskeleton. Each sample of ten neonates was then put into a single well of a 96-well plate (Costar, flat bottom) in replicates of three and analysed using the fluorescence function of the plate reader (FLUOstar Omega, BMG labtech). For experiments that had a conditioning step, *D. magna* neonates conditioned the medium for six hours and then were removed leaving behind only medium containing secreted proteins. Fluorescent COOH-PS NMs were then diluted with and incubated in conditioned medium and then fresh *D. magna* neonates were exposed to the NMs for 2 hours.

To monitor the removal of NMs, after neonates had been completely exposed to the fluorescent COOH-PS NMs for the various exposure times (1, 2 and 3 hours), neonates were then placed in fresh HH Combo medium, and moved into fresh HH Combo medium every 15 mins to ensure they did not re-uptake any NMs that were expelled. Neonates were assessed for total fluorescence at 1, 3 and 6 hours of post-exposure using the previously mentioned method.

2.4.1.4 Assessment of NM size in conditioned HH Combo medium

The effect of conditioned medium on the stability of NH_2 and COOH-PS was assessed. Ten *D. magna* neonates (or 1.5 mL suspension of *C. vulgaris* OD = 0.8) were used to condition 5 mL of fresh HH Combo medium for various conditioning times (1, 3 and 6 hours) and neonates were then removed using a Pasteur pipette (algae was filtered over coarse filter paper (Whatman, 0.1 μm) allowing smaller proteins to be filtered through with the medium). PS NMs were incubated in conditioned medium for various incubation times (1, 4 and 6 hours)

at a concentration of 0.01 mg/ mL of NMs, after which time the NM size was measured using a zetasizer ZS nano (Malvern instruments).

2.4.1.5 Determination of protein concentration released by *D. magna or C. vulgaris*

A BCA assay (details in section 2.2.1) was conducted to quantify the concentration of protein released by *D. magna* neonates as a function of conditioning time using a Peirce BCA assay kit. Ten *D. magna* neonates were used to condition 5 mL of HH Combo medium for various conditioning times (1, 3 and 6 hours). The BCA assay was conducted to obtain the unknown concentration of protein within samples using a BSA standard curve.

2.4.1.6 Effect of NMs on feeding rate of *D. magna* on *C. vulgaris*

To determine if NMs remaining in the gastinointestical tract (GI) of *D. magna* cause a change in feeding rate of *D. magn*a on algae *C. vulgaris*, *D. magna* neonates were exposed for two hours to fluorescent COOH-PS NMs which had previously been incubated in six-hour conditioned medium. Neonates were then moved into fresh HH Combo medium and subsequently put into new medium every 15 mins to avoid re-uptake of NMs and this was done until 6 hours of post-exposure. Neonates were then exposed to 1.5 mL of algae *C. vulgaris* and ten neonates each were collected at different time points (0, 1, 2, 3 and 6 hours) and assessed for fluorescence (derived from the algae emission/excitation at 355 /460 nm) using the plate reader. In parallel, a control was done to monitor standard feeding behaviour of *D. magna* neonates on algae (where they had not been exposed to NMs).

2.4.1.7 Confocal microscopy imaging of uptake and retention of PS NMs in D. magna gut

Confocal microscopy was used to visualise the uptake of fluorescent COOH-PS NMs into *D. magna* neonates. Laser scanning confocal microscopy (LSCM) was conducted using a Zeiss

LSM 710 ConfoCor using the 485 nm argon laser. Neonates (1-3 days) were exposed to PS-COOH NMs at 0.01 mg/mL for 24 hours before being transferred to fresh HH Combo medium and were subsequently washed twice with fresh medium to remove any NMs bound to the exterior carapace. Fluorescent images of neonates were taken by placing a single neonate in a 35 mm glass bottom dish (MatTek) and reducing the surrounding medium to a minimum to reduce movement of the neonate and using the 10X objective lens to capture images (n=3). Both fluorescent and transmitted light images were taken and overlaid to show both parameters in a single image.

2.4.1.8 Eco-corona isolation and assessment of proteins by PAGE

Protein coronas were isolated using a well-documented method described in detail by (Docter et al, 2014). NMs were incubated for 24 hours in 6 hour conditioned medium at a concentration of 0.0001 mg/mL. At the end of the incubation period, NMs were isolated using the previously discussed corona isolation method (section 2.2.7) and run on a 12.5% gel using PAGE (2.2.8) to detect bands present in the hard-corona.

2.4.1.9 Effect of PS NMs and protein corona on moulting of *D. magna*

The influence of PS-NH_2 NMs (0.001 mg/mL; final volume 5 mL) corresponding to the EC_{20}, on *D. magna* moulting was assessed by exposing neonates (<6 hours) for at least 84 hours (time taken for control neonates to fully complete their second moulting succession). Positively charged PS NMs were tested due to their higher toxicity compared to negatively charged PS NMs. Each jar (n=20) contained only one neonate to assess the moulting of each individual organism. The shedding of the exoskeleton was recorded every 6 hours until control cultures had completed their second moulting cycle (which occurred at 84 hours), and was assessed by visual observation (and could also be seen on an optical microscope). To encourage effective moulting and healthy neonates, each individual neonate was fed 20 µL of *C. vulgaris* (equivalent to 10 µg carbon) 1 hour prior to PS-NH_2 NM exposure. To assess the

impact of the NMs corona on moulting, 10 neonates were allowed to condition 5 mL of HH Combo medium for 6 hours (this was done 20 times for each sample) and were then removed leaving behind only conditioned HH Combo medium. NM suspensions were diluted with the conditioned medium to reach a concentration of 0.001 mg/mL (the EC_{20} concentration) with a final volume of 5 mL and were incubated for 1 hour to allow for NM-protein interaction. One fresh neonate was then added to each jar and the same aforementioned technique was used as above.

2.4.2 Chapter 4 protocols

2.4.2.1 NMs selected for toxicity studies

Gold NMs of various charge (positive and negative) and shape (sphere, short rod and long rod) were purchased from NanoPartz and volumetrically dispersed in DI water to make a 50 µg/mL working stock where both the mass and number concentration could be calculated. A summary of the various types of NMs used is given in table 2.11.

Table 2.11 Dimensional characteristics of the Au NMs used in experiments. Note: no long positively charged rod was available.

Type	Shape	Diameter (nm)	Length (nm)	Charge
COOH-Au	Sphere	25	-	Negative
COOH-Au	Short Rod	25	60	Negative
COOH-Au	Long Rod	25	146	Negative
NH_2-Au	Sphere	25	-	Positive
NH_2-Au	Short Rod	25	60	Positive

On a side note, the work in this chapter aimed to explore the difference in toxicity due to shape using both positive and negatively charged spheres and short rods. Adding another

dimension of a longer rod was meant to broaden the scope of the work, although positively charged long rods were unavailable for purchase and thus are not included in the study. Considering the high toxicity of positively charged NMs compared to negative ones it was deemed that it would still be interesting to add negatively charged long rods to the NM library in order to gain an understanding of effect of shape on toxicity to *D. magna*.

2.4.2.2 Assessing NMs effect on *D. magna* survivorship

Twenty *D. magna* neonates were exposed to a range of mass concentrations 0.001-0.05 μg/mL (positively charged NMs) and 1-50 μg/mL (negatively charged NMs) and in a separate experiment to a range of number concentrations of 2.5 x 10^6 -1.3 x10^8 NMs/mL (positively charged NMs) and 1.5 x 10^9 - 5.5 x10^{10} NMs/mL (negatively charged NMs) diluted with fresh HH Combo medium for a final volume of 5 mL. These concentrations were chosen after exposing *D. magna* to a wide range of mass concentrations and a suitable concentration range was obtained spanning of a spectrum mortalities. These concentrations were chosen as positively charged NMs were considerably more toxic than negative and the chosen concentrations displayed a range of y-axis (mortality) responses. Exposures were conducted for 24 hours as separate experiments (by mass or by particle number). After the 24h exposure the percent mortality was determined by counting the number of living organisms. The EC_{50} of each NM was then determined.

2.4.2.3 Assessment of charge per surface area by electropotential titration

NMs were placed in a beaker at a concentration of 5 μg/L with a final volume of 50 mL. The number of NMs present in 50 mL was calculated based on the original concentration of the stock suspension. The total surface area (SA) present in each 50 mL sample was then calculated and the equivalent amount of moles (n) present in each sample determined. Known aliquot volumes of potassium chloride (KCl) at a concentration of 0.01 mM was titrated into the sample under mild stirring. The zeta potential of the sample was measured

at intervals (< 5 mins) to monitor the change in the surface charge until 0 mV was reached. The total moles of KCl needed to neutralize the moles of NMs and total charge per SA was calculated.

2.4.2.4 Impact of different shaped and charged Au NMs on ROS production in *D. magna*

Twenty *D. magna* neonates were exposed to nominally high (EC_{40}) and low (EC_5) number concentrations of Au NMs for positively charged NMs and high (EC_{10}) and low (EC_3) number concentrations for negatively charged NMs in a final volume of 5 mL for 24 hours. These EC values were chosen based on the survivorship of *D. magna* at a range of different number concentrations, in order to give a cross comparison of ROS generation at the same degree of survivorship within each set of charges. At the end of the exposure period living neonates were placed in fresh HH Combo medium for a recovery phase, with recovery assessed at different time points (0, 3, 6, 8 and 24 h) during recovery. At the end of the recovery period, living neonates of each sample were put into a well in a 96-well plate with approximately 250 µL of HH Combo medium. ROS presence was detected using CM-H_2DCFA. 50 µg of CM-H_2DCFA (stored at -20°C) was thawed for approximately 15 mins. Ethanol (absolute) was added to the aliquot to create a 1 mM stock solution. A 50 µM working stock was created from the stock by diluting with ethanol and enough working stock was created to add 50 µL to every 250 µL sample containing twenty neonates. Plates were incubated for 40 mins at room temperature covered in foil. ROS levels were assessed using the fluorescence function on a plate reader at 485-512 nm excitation/ 520 nm emission. Exposures were skewed so that all recovery periods ended at the same time so that ROS presence could be assessed at the same time for all experiments.

For experiments with a previous conditioning step, ten *D. magna* neonates were allowed to condition 5 mL of HH Combo medium (this was done for each sample) for 24 h. NMs were incubated in the conditioned HH combo medium at a 'high' concentration (EC_{40} for positively

charged NMs and EC_{10} for negatively charged NMs, the rational to why these concentrations were chosen is explained below). Twenty *D. magna* neonates were then exposed for 24 hours using the method outlined in the previous paragraph to quantify ROS generation at 0, 3, 6, and 24 hours of post-exposure (recovery).

EC values were chosen as appropriate 'high' and 'low' values based on the mortality results from positively and negatively charged NMs, using a NM number concentration where all NMs of the same charge would be comparable. Number concentrations compare the same number of NMs in a certain (fixed) volume. Thus, converting from the mass concentrations to number concentrations meant that for the spheres there was an order of magnitude more particles than for rods at the same mass. Thus, to select the NM number concentrations for comparison across a set of similar charged particles, this had to be done on the basis of the NM with the lowest number concentrations (for the X axis), which limited the Y-axis response. For the negatively charged NMs, which were low toxicity, and thus never reached EC_{40} concentration at the number concentrations evaluated, the EC_{10} concentration was chosen as the "high" concentration and EC_3 as the "low" concentration, as these span the range of effects observed. Note that there was no attempt to compare positive with negative charged NMs as the chosen 'high' and 'low' values were different, but rather effect of shape and charge density within a specific charge were compared.

2.4.2.5 Influence of medium conditioning by *D. magna* on NM stability

Ten *D. magna* neonates were put into 5 mL of fresh HH Combo medium and allowed to condition the medium for 6 hours. At this point, neonates were removed, leaving only the conditioned medium. Suspensions of NMs were created at the EC_{15} value for number concentration using NM stock suspensions and the conditioned HH Combo medium, and NMs were incubated in conditioned medium for 0, 3, 6 and 8 hours at which point a sample of NMs (0.1 mL) was taken and size was assessed using DCS.

DCS was chosen as the characterisation method as it is suitable to assess the size of both spheres and rods. The disc centrifuge method is built on differential sedimentation using Stokes' law which measures the settling velocity of NMs accelerated in fluids as a function of diameter (Nadler et al., 2008). DCS is able to assess non-spherical NMs with a cylindrical or rod shape by assuming sedimentation according to Stokes' law where the dimensions of a cylinder can be directly related to an equivalent spherical diameter using equation 4.1.

$$d_{st} = d_c\sqrt{\ln(2\beta)} \qquad \text{(Equation 4.1)}$$

where d_{st} is known as the rod NM's equivalent spherical diameter, also known as its Stokes' diameter, d_c is the diameter of the rod NM and β is the aspect ratio of the rod NM. Using Stoke's law, it can be seen that the diameter of the sphere depends directly on the diameter of the cylinder but very slightly on its length and therefore the resulting diameter of rods will always be closer to that of its diameter and gives reliable results.

2.4.2.6 Effect of Au NMs on moulting of *D. magna*

This experiment is similar to that described in section 3.2.9 with alterations to the NM concentration. To summarize, the influence of positively charged spherical and short rod Au NMs (5.3 x10^6 NMs/ mL; final volume 5 mL) on *D. magna* moulting was assessed by exposing neonates (less than 6 hours) for 84 hours (length of time it took control neonates to successfully and fully complete a second moulting succession) to both types of NMs alongside a control (no NM exposure). Positively charged NMs were tested due to their higher toxicity compared to negatively charged NMs. Each jar (n=20) contained only one neonate to monitor moulting on an individual level. Ecdysis was noted every 6 hours until control cultures had completed their second moulting cycle (which occurred at 84 hours), and was monitored visually (though could also be verified by an optical microscope). To stimulate moulting and ensure healthy neonates with sufficient energy to moult, each individual neonate was fed 20 µL of *C. vulgaris* (equivalent to 10 µg carbon) 1 hour prior to NM exposure.

2.4.2.7 Confocal imaging of localization and retention of Au NMs in *D. magna gut*

Confocal microscopy was used to visualize the uptake of spherical NH_2-Au NMs into *D. magna* neonates. Laser scanning confocal microscopy (LSCM) was conducted using a Zeiss LSM 710 ConfoCor using the 543 nm laser. Positively charged Au NMs were conjugated to the dye Rhodamine B Isothiocyanate (RhB-ITC) using the NH_2 group on the NM, where enough dye molecules were used to be able to conjugate to half the NH_2 surface groups. This value was chosen to have a large proportion of dye molecules conjugated to the Au NMs but to also reduce the presence of any free dye. Neonates were exposed to RhB-ITC-NMs for 1 hour exposure time and then washed twice with fresh HH Combo medium. Fluorescent images of *D. magna* neonates were taken by placing a single neonate on a 35 mm glass bottom dish and reducing the surrounding medium to a minimum to avoid movement, using the 10x objective lens to capture images (n=3). Both fluorescent and transmitted light images were recorded and overlaid. Reflectance confocal imaging of the uptake of Au NMs was also tried, though the keratin comprising the carapace was also highly reflectant, rendering these measurements unsuccessful as a means to confirm Au NM uptake, as the controls were as reflectant as the NM exposed neonates due to the organisms ingesting the shed carapase.

2.4.2.7.1 Calculation of conjugating of RhB-ITC to positively charged spherical NMs

RhB-ITC was conjugated to NH_2-Au NMs by adding 5 mL of 50 µg/mL of Au NMs to 5 mL of RhB-ITC to create a final 10 mL of 25 µg/mL Au NMs where half the NH_2 groups were conjugated to RhB-ITC. Below is the calculation used to determine the amount of RhB-ITC needed.

The number and mass concentration of the stock were known, so that it was determined that in a 25 µg/mL working stock, there was 2.67×10^{11} NMs/mL.

2.67×10^{11} NMs in 1 mL x 5 mL = 1.335×10^{12} NMs in 5 mL

1.335 x10^{12} NMs x 5889 ligands (determined from the charge titration in section 4.2.2) on 1 positively charged NM= 7.862 x10^{15} total ligands

$\frac{7.862 \times 10^{15}}{2} = 3.93 \times 10^{15}$ is the number of RhB-ITC molecules needed to bind to half the NH_2 groups

$$\frac{3.93 \times 10^{15}}{6.022 \times 10^{23}} = 6.53 \times 10^{-9} mol\ of\ RhB - ITC$$

$n = \frac{m}{M}; \quad m = nM;\ 6.53 \times 10^{-9} mol \times 536.08 \frac{g}{mol} = 3.499 \times 10^{-6} g$ = 3.5 x 10^{-3} mg RhB-ITC

3.5 mg of RhB-ITC was weighed and volumetrically made up to 1 L. 1 mL of this was then taken and added to a new 1 L volumetric and made up to 1L. 5 mL of this was then added to 5 mL of 50 μg/mL of NH_2-Au spherical NMs where there was enough RhB-ITC to conjugate to half the NH_2 groups on the Au NMs so that the ligands on the Au NMs were in excess, resulting in a low likelihood for any free dye to be left unbound.

2.4.3 Chapter 5 protocols

2.4.3.1 NM dispersions

PS-500 and PS-50 NMs (Life Technologies) were received as 2% (in 10 mL stock) and 5% (in 1 mL stock) respectively. Percentages were converted into grams/litre, with PS-500 as an example below:

2% solids in 10 mL stock

$$\frac{2}{100} \times 10\ mL = 0.2\ mL\ is\ solid$$

Density of PS = $1 \frac{g}{cm^3}$

0.2 g in 10 mL therefore 20 g/L is the concentration of the stock.

The stock was diluted with DI water to create 2 mL of a 0.2g/L (or 0.5 g/L for PS-50) working stock. The working stock was then used to make 2 mL samples of 0.001 g/L (non-lethal concentration) PS using HH Combo (or in the case of mode 3, PS NMs incubated in algae). Stock and working stock suspensions were covered in foil and stored in the fridge in the dark until use.

2.4.3.2 Uptake and release of NMs *by D. magna*

2.4.3.2.1 HH Combo medium with no feeding (Mode 1)

Ten *D. magna* were exposed to 0.001 g/L of either PS-500 or PS-50 for 1 hour in a volume of 2 mL which was dispersed in fresh HH Combo medium. After the 1 hour exposure to NMs, neonates were moved to fresh HH Combo medium to excrete NMs, and were subsequently moved into fresh HH Combo medium every 30 mins in order to avoid neonates re-taking up any expelled NMs. Fluorescence readings were taken during uptake: 0, 0.5 and 1 hours and during post-exposure (depuration) at: 0.5, 1, 3 and 6 hours.

2.4.3.2.2 With feeding on algae *C. vulgaris* during release phase (Mode 2)

To assess the impact of feeding on depuration of PS-500 and PS-50 from *D. magna* following exposure via the water phase (Mode 1 as described above), a similar experiment was conducted to that in section 5.2.2.1 with the additional measure that during the release stage, neonates were moved into fresh HH Combo medium that contained 10 μL of fresh algae *C. vulgaris* as a food source and algae was also present in each subsequent move to fresh medium.

Note, for experiments dealing with feeding on *C. vulgaris,* a test was conducted to ensure that algal fluorescence did not interfere with the results of the PS fluorescence (as PS and algae emit at sufficiently different wavelengths) and results show that the algal fluorescence

emitted at the emission and excitation of the PS NMs was negligible and not significantly different from the controls (only *D. magna* neonates), indicating that any fluorescence was solely due to PS NMs.

2.4.3.2.3 NMs incubated in algae *C. vulgaris* (Mode 3)

Both PS-500 and PS-50 were dispersed in fresh algae (OD= 0.08) with a final concentration of 0.001 g/L and were incubated for 3 hours in falcon tubes (volume of 42 mL comprising of 4.18 mL algae + 37.61 mL HH Combo medium + 210 μL of PS NMs (500 or 50 nm) working stock to make 42 mL of 0.001 g/L PS NM dispersed in 0.08 OD of algae *C. vulgaris*) whilst gently rotating to ensure proper dispersion. The incubated NMs in algae were then separated into 2 mL volumes in tubes (7 time points with 3 replicates) and 10 neonates were then added to each tube for exposure with a similar protocol to that of section 5.2.2.1.

2.4.3.2.4 Feeding of *D. magna* on algae *C. vulgaris* prior to NM exposure (Mode 4)

To assess the impact of having been just fed on the uptake and depuration of PS-500 and PS-50 by *D. magna*, 10 neonates per sample were placed into 2 mL of fresh HH Combo medium and were fed 10 μL of fresh algae and allowed to consume for 24 hours. This allocation of food is appropriate for this quantity of neonates in this volume for this specific time length and was chosen in order to avoid stress from over feeding. Immediately after feeding, neonates were moved into 2 mL of 0.001 g/L of PS-500 or PS-50 and a similar protocol was used to that of section 5.2.2.1 for uptake and depuration.

2.4.3.3 Confocal imaging of uptake and release of NMs by *D. magna*

Confocal microscopy was used to visualise the uptake of PS-500 and PS-50 NMs into *D. magna* neonates using the same method described in section 3.2.7.

2.4.3.4 Determining impact of conditioning and incubation on NM agglomeration

The effect of conditioned medium on the stability of PS-500 and PS-50 NMs was assessed. Ten *D. magna* neonates were used to condition 2 mL of fresh HH Combo medium for various conditioning times (1, 3 and 6 hours). Neonates were then removed using a Pasteur pipette leaving behind only conditioned medium. Both types of NMs were incubated in conditioned medium for various incubation times (1, 4 and 6 hours) at a concentration of 0.001 g/L, at which time NM size was measured using a zetasizer ZS nano (Malvern instruments) described in section 2.1.1.

2.4.3.5 Quantification of release of carbohydrates by *D. magna*

Carbohydrate release from *D. magna* was determined using a total carbohydrate detection kit (Abcam). A glucose standard curve was created by diluting D-glucose with fresh HH Combo medium and adding 30 µL to each well. 10 *D. magna* neonates were also allowed to secrete carbohydrates into 2 mL of HH Combo medium for specific time points and were then removed at the end of the time point leaving behind 'conditioned medium' containing carbohydrates. 30 µL of samples of unknown carbohydrate concentration were added to the sample wells. 150 µL of 98% H_2SO_4 were also added to each well containing either standard or sample and were mixed on a shaker for 1 min and then set to incubate at 90˚C for 15 mins. After the incubation, 30 µL of developer was added to each well and mixed on a shaker for 5 mins at room temperature and a light orange colour formed in the wells. Absorbance was determined at 490 nm using a plate reader. The standard curve was used to quantify concentrations of carbohydrates in the samples.

2.4.3.6 Eco-corona isolation and assessment of proteins by PAGE

Protein coronas formed on the PS-50 and PS-500 NMs in the conditioned medium were isolated using a well-documented method described in detail by Docter et al, 2014 (with the

elimination of the sucrose cushion step). Isolated proteins were run on a 12.5% PAGE and bands were stained using Coomassie blue and silver stain. A full method for this can be found in section *3.2.8.*

2.4.3.7 TEM imaging of NMs within *D. magna* gut following exposure via presentation mode 1

Ten *D. magna* neonates were exposed to 0.001 g/L of PS-500 for 1 hour dispersed in HH Combo medium in a volume of 2 mL. At the end of the exposure, neonates were washed with fresh medium to remove any NMs bound to the carapace. Neonates were then prepared for epoxy resin embedment for TEM imaging, details of which can be found in section 2.2.5.

3

Secreted protein eco-corona mediates uptake and impacts of polystyrene nanomaterials on *Daphnia magna*

Parts of this chapter have been published as:

F Nasser* and I Lynch. Secreted protein eco-corona mediates uptake and impacts of polystyrene nanoparticles on *Daphnia magna*. **Journal of Proteomics** (2016) 137; 45-51.

These results have been presented at **SETAC' 2015**

3.1 Introduction

In parallel to the growth of applications of NMs, there has been a substantial increase in the use of MPs, either manufactured to be microscopic (< 5 mm) in size or resulting from the degradation of larger plastic fragments whose further wearing will likely result in nanoscale entities. The presence of MPs in aquatic systems makes it extremely likely that these MPs will be consumed by organisms and as the potential detrimental effects are uncertain it is therefore important to study the impact of MPs on the environment. PS beads over 1 μm have been used as a model to mimic MPs and their effect on ingestion and feeding by copepods was investigated, where the EC_{50} of 500 nm PS was found to be 23.5 μg/mL and the much smaller and more toxic 50 nm PS had an EC_{50} of 2.15 μg/mL. Here, the focus of this chapter is specifically on the role of the eco-corona on uptake, retention and toxicity of nanoscale PS.

Micro and nano-plastics deposited into environmental waters are highly likely to be available to *D. magna* as these filter feeders are known to consume suspended particles. The

Organization for Economic Cooperation and Development (OECD) has created standard tests to monitor toxicity using both *D. magna* which are also relevant to test the toxicity of NMs. The OECD has deduced that the protocols (OECD 2009) used for assessing bulk chemicals are in general suitable for evaluating the safety of NMs (Rasmussen et al., 2016) though many studies have noted that there are several reasons that the OECD guidelines are not appropriate for NM testing such as;

1) the lack of feeding effecting NM removal in short-term studies, the importance of which is discussed in section 1.5.1 where feeding pushes out previously ingested material so that the protocol does not allow for the realistic quantification of bioconcentration when studying NMs (Skjolding et al., 2014).

2) OECD test waters also do not take into account the secretion of proteins and other macromolecules released by aquatic organisms, which is not relevant for bulk chemical assessment as there is limited potential for binding as there is no binding surface available, though these are considerations relevant for NM exposure and;

3) NMs have high surface energies (Nanda et al., 2003) and if they are not moderated by bound macromolecules, this may also result in non-realistic stickiness of the NM to organism appendages leading to physical effects (Lovern et al., 2007) that would probably not occur under real conditions.

The presence of micro-plastics in natural waters, which can be further degraded into nano structures, calls for an investigation of how the proteins released by aquatic organisms under normal and stressed conditions adsorb to the nanoparticle surface creating an 'eco-corona' around the NMs. The eco-corona around NMs can change the overall identity of the NM and influence its toxicity and interaction with organisms (Albanese and Chan, 2011, Lundqvist et al., 2008). It has also been suggested that the eco-corona around NMs influences the distribution of NMs within living organisms (Lundqvist et al., 2011) and therefore it is important to assess how secreted molecules may adsorb to NMs and cause changes in uptake

and persistency inside aquatic organisms once ingested. As stated in section 1.5.1, *D. magna* take up particulates based on size and texture so that organic corona-coated NM agglomerates would be preferentially taken up based on size and texture. Based on work conducted on human blood/lung coronas, the same principles can be applied to assess how proteins secretion from *D. magna* can affect NM stability and how in turn this affects toxicity, retention and uptake.

3.1.1 Aims and Objectives

The aim of this chapter was to investigate the effect of an eco-corona formed from the proteins and biomolecules secreted by Daphnia under their normal conditions on the impact and toxicity of NH_2/COOH-functionalised PS NMs on *D. magna*. This was achieved through the following objectives.

1. Quantification of the effect of *D. magna* conditioned medium on the stability of PS NMs
2. Determination of the impact of protein-corona around PS NMs on the survivorship of *D. magna* compared to the 'bare' PS NMs
3. Investigation of the impact of a secreted protein corona on the uptake and release of PS NMs by *D. magna*
4. Examination of the impact of *D. magna* feeding on *C. vulgaris* after uptake of PS NMs with surrounding protein-corona.
5. Assessment of proteins comprising the hard corona around PS NMs
6. Exploration of the impact of 'bare' and corona-bound PS NMs on *D. magna* moulting

3.2 Results and Discussion

3.2.1 Stability of COOH and NH_2-functionalised PS NMs in HH Combo Medium

A concentration of both COOH and NH_2-PS NMs needed to be chosen that promoted survivorship though also showed to have an effect on *D. magna* neonates, see figure 3.1. Neonates were exposed to a range of concentrations (0.0001-1mg/mL) of PS NMs and EC_{50} values were calculated to ensure an optimal concentration was chosen for all subsequent experiments.

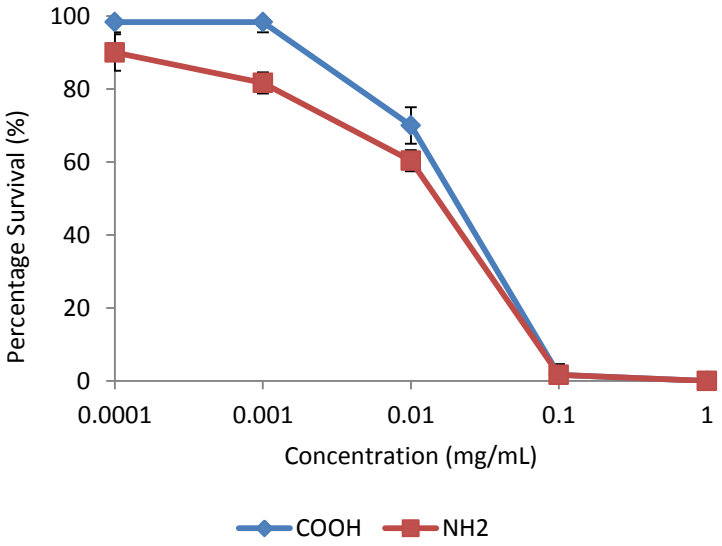

Figure 3.1. Survival curves of *D. magna* neonates exposed to COOH or NH_2-PS NMs for 24 hours.

It was shown for both COOH and NH_2 -PS NMs, concentrations greater than 0.1 mg/mL were lethal and that there were no surviving neonates. COOH-PS NMs were shown to have an EC_{50} value of 0.0363 mg/mL and NH_2-PS NMs had an EC_{50} value of 0.0258 mg/mL indicating that NH_2-PS NMs had an increased toxicity compared to COOH-PS NMs. This result was expected due to the positively charged NH_2 group being attracted to the negatively charged phospholipid bilayer on cell membranes. It is well recorded that the attraction of the negative charge on cells and positively charged NMs is responsible for increased toxicity of positively

charged NMs relative to similar materials with neutral of negative charges (Bozich et al., 2014, Hauck et al., 2008). However, this may be a relatively simplistic view, as positively charged NMs, once consumed, may also be interacting with intracellular components such as negatively charged DNA or interacting with the mitochondria which could result in increased cellular or oxidative stress contributing to an increase in mortality. A concentration of 0.01 mg/mL was chosen as a suitable concentration showing a high degree of survivorship as well as showing to have an effect from NM exposure for both NMs (corresponding to $EC_{30\text{-}40}$ values).

Studies in this chapter focus on assessment of NM agglomeration due to proteins released by *D. magna* interacting with PS NMs. *D. magna* are cultured and grown in HH Combo medium and therefore it was important to assess PS stability in medium to ensure there was no agglomeration due to the components in the medium which can be seen in figure 3.2. Stability of COOH and NH_2 -PS NMs was monitored over 4 hours at a concentration of 0.01 mg/mL. Both types of NMs were shown to be stable in HH Combo medium and hydrodynamic size was measured by DLS. PS-NH_2 remained monodisperse with a hydrodynamic diameter of 87 ± 13 nm and PS-COOH also remained monodisperse with a hydrodynamic diameter of 200 ± 13 nm; both NMs had very low polydispersity index (PDI) and the curves had only single peaks and stability was also monitored after 7 days (see also the example included in figure 3.3).

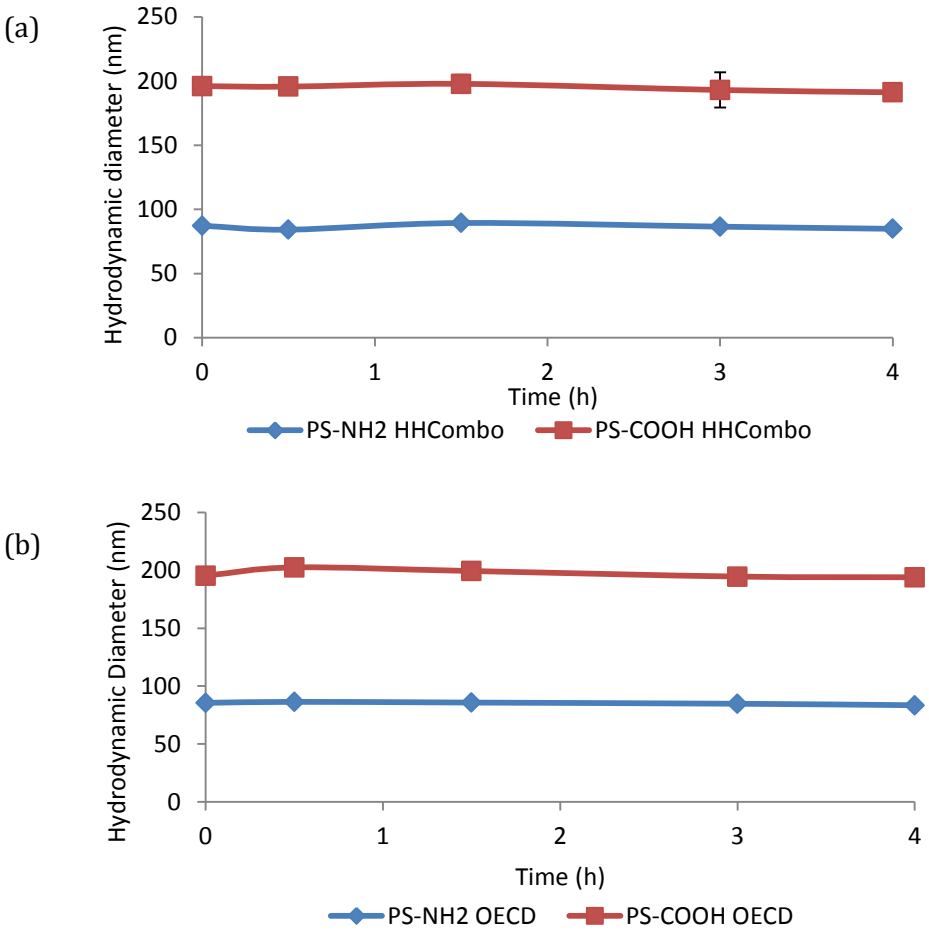

Figure 3.2 Hydrodynamic diameters of COOH or NH_2-PS NMs in a) HH Combo medium and b) OECD medium.

It was confirmed that the sizes of the NMs remained stable for up to 24 hours in HH Combo medium with no change in statistical significance (verified by Student's t-test). This confirmed that HH Combo medium components did not cause agglomeration of the PS NMs at 0.01 mg/mL and that any agglomeration observed in subsequent experiments is due to other experimental factors. Monitoring the stability of the NMs in HH Combo medium was essential as usually medium of high ionic strength can cause a decrease in the electrical double layer separating the NMs, which may cause agglomeration, although this is also influenced by pH. It was confirmed that the salt components in the medium did not cause any agglomeration between pH 7.6-7.8.

In order to maintain genetically identical neonates and non-stressful conditions, growth of neonates must be kept at 20˚C and therefore it is important to assess the stability of PS NMs at this temperature, which was assessed with storage at 20°C (ambient), and for comparison at 4°C (typical storage conditions for PS NM stock solutions) and -20°C (frozen) temperatures for seven days which can be seen in table 3.1. Though NMs were never stored in frozen conditions, the study was added to gain a complete picture of how storage conditions affect stability.

Table 3.1 Effect of temperature on the hydrodynamic size (z-average) of a) COOH-PS NM stability b) NH_2-PS NM stability in HH Combo medium at 0.01 mg/mL measured in nm.

(a)

Day	Hydrodynamic size at 20 °C (nm)	SD ± (nm)	Hydrodynamic size at 4 °C (nm)	SD ± (nm)	Hydrodynamic size at -20 °C (nm)	SD ± (nm)
0	203.7	4.70	197.2	5.80	197.4	7.64
1	215.4	3.42	205.6	2.01	204.7	7.92
2	208.9	11.00	207.3	1.31	197.7	1.45
3	208.8	9.29	205.1	11.02	206.8	3.79
4	200.0	5.48	206.4	0.45	201.6	3.68
5	206.5	5.69	202.0	7.76	203.6	1.57
6	209.5	3.44	207.7	8.21	198.5	2.38
7	210.3	6.32	206.6	1.50	196.7	8.15

(b)

Day	Hydrodynamic size at 20 °C (nm)	SD ± (nm)	Hydrodynamic size at 4 °C (nm)	SD ± (nm)	Hydrodynamic size at -20 °C (nm)	SD ± (nm)
0	99.0	1.91	96.8	1.95	96.2	0.049
1	98.4	1.62	94.8	0.053	95.1	3.409
2	98.8	2.66	96.5	2.82	92.4	2.16
3	97.4	1.47	94.8	1.93	96.1	1.28
4	94.8	0.83	95.4	3.76	94.3	0.92
5	98.4	0.94	95.4	0.92	92.7	1.52
6	98.7	1.88	94.8	0.42	98.4	2.05
7	99.7	0.03	95.3	1.94	94.7	0.20

The growth of *D. magna* in HH Combo medium is maintained at a temperature of 20˚C with controlled humidity with a 16: 8 hr light to dark cycle. Under optimal conditions *D. magna* produce neonates as clones, although any form of stress such as change in temperature, humidity or alterations in food levels can cause a change in reproductive behaviour causing them to produce genetically different offspring in an attempt to increase variability and

survivorship. It was determined that growth of *D. magna* at an ambient temperature of 20˚C also allows for NM stability and does not cause any agglomeration, as DLS plots only show the presence of a single peak as seen in figure 3.3.

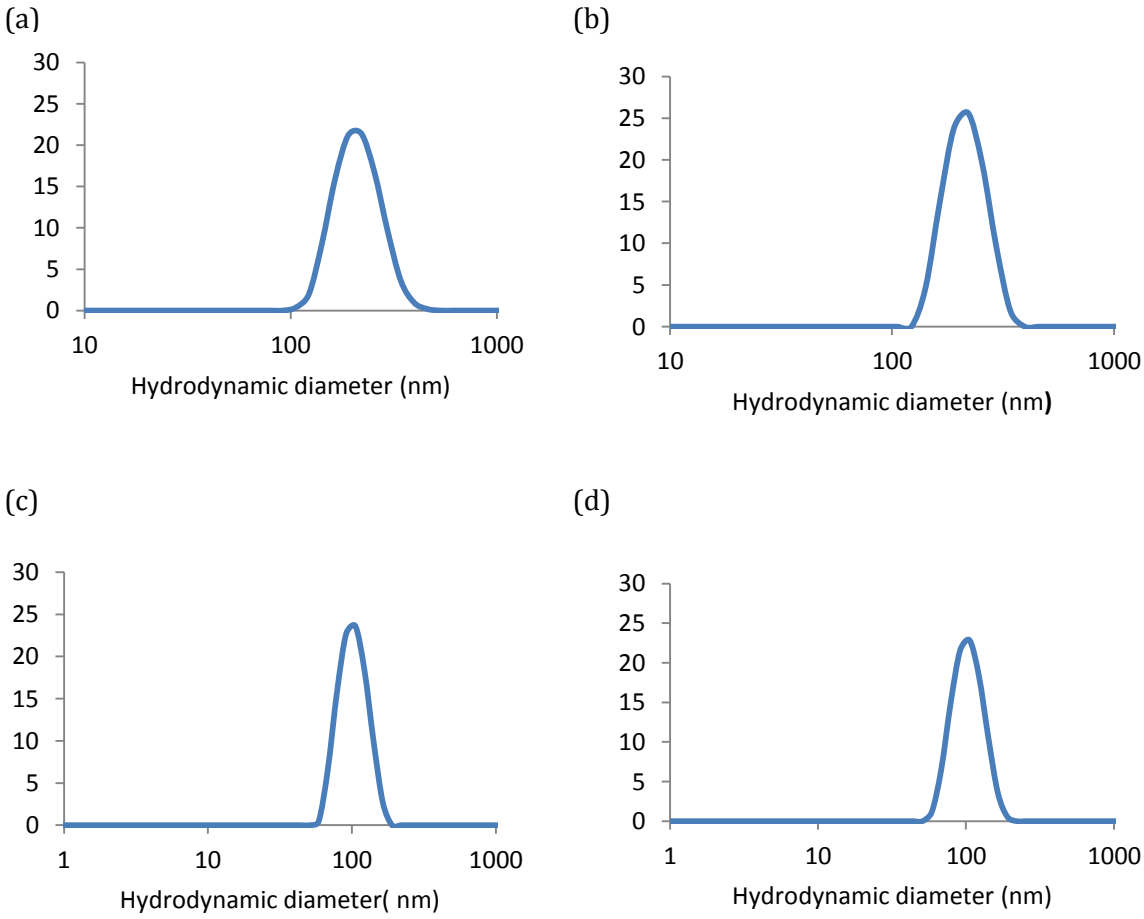

Figure 3.3 Hydrodynamic diameter of PS-COOH NMs dispersed in HH Combo medium at a) 0 days, b) 7 days; and PS-NH2 NMs at c) 0 days; and d) 7 days, with dispersions stored at ambient temperature (20 °C).

At ambient temperatures, at time point 0 hours PS-COOH NMs show a single peak at 203.7 nm (with a low PDI of 0.033) and does not show agglomeration even after 7 days at ambient temperature with a size of 210.3 (PDI 0.034) as seen in figure 3.3 (a) and (b) of which the slight change in size is statistically insignificant at $p > 0.05$ confidence level. PS-NH_2 NMs also do not appear to agglomerate at ambient temperatures with an original single peaked hydrodynamic diameter of 99.0 nm (PDI 0.062) at 0 days and 99.7 nm (PDI 0.031) at 7 days

as seen in figure 3.3 (c) and (d), also any slight change in size is statistically insignificant at $p > 0.05$. This confirms that temperature is not a factor contributing to NM agglomeration in subsequent studies.

3.2.2 Effect of medium conditioning and NM incubation time on NM stability

Proteins released by *D. magna* neonates have the ability to interact with NMs and it is important to understand how the adsorbed eco-corona affects NM stability and subsequent toxicity to *D. magna*. Figure 3.4 (a) shows that when neonates were allowed to condition HH Combo medium for six hours an increase in medium concentration of secreted proteins up to 435 μg/mL as quantified by BCA assay was found, and therefore, it can be concluded that as conditioning time increases so does the concentration of proteins present in the medium. It was shown that there was a considerable increase in protein over time up to 6 hours, though proteins being secreted by *D. magna* eventually plateaued at 24 hours where there was only a slight increase in concentration from 435 μg/mL to 470 μg/mL from 6 to 24 hours indicating that *D. magna* does not release proteins in a linear fashion or at the same rate so that protein concentrations cannot be predicted purely on assessment of proteins secreted in the first hour. When NH_2 and COOH-PS NMs were incubated in the conditioned medium (conditioned for 1, 3 or 6 hours), both NM size and polydispersity increased slightly as shown in Figure 3.4 (b) and (c).

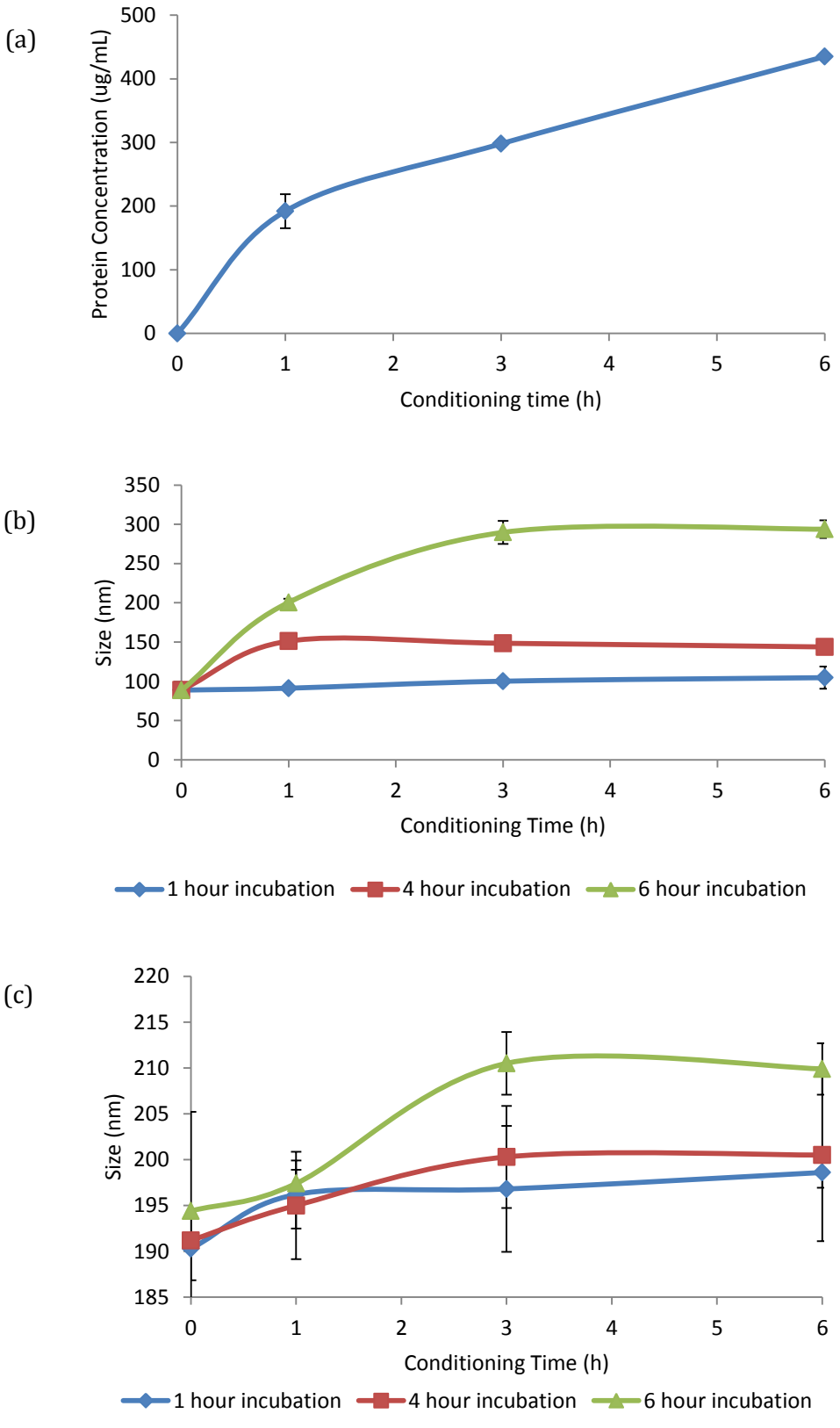

Figure 3.4 a) Concentration of proteins secreted by *D. magna* neonates into HH Combo medium over 6 hours quantified by BCA assay; Changes in hydrodynamic diameter of b) NH_2 –and c) COOH- PS NMs with different incubation times (1, 4 or 6 hours) in *D. magna* conditioned HH Combo medium.

The assessment of protein secretion could also be limited due to the volume of medium available to condition by *D. magna*. Realistic exposures in fresh water will not be volume limited leading to greater dispersal of secreted proteins, *D. magna* are constantly moving through their surroundings, and there may be contributions from other organisms which will result in variable protein concentrations.

In the case of one hour incubation of the NMs in the conditioned HH Combo medium, the increase in size can be attributed to a layer of bound proteins and not agglomeration, irrespective of the media conditioning time (protein concentration). It can also be concluded that NM incubation time affects NM size and that longer incubation times lead to some agglomeration, as it is highly unlikely that a protein layer surrounding a NM would cause an increase of 150 nm above its original size. Clearly some exchange or rearrangement of the proteins adsorbed to the NM surface is occurring during the longer (4 and 6 hour) incubation times, which is contributing to increased agglomeration by bridging or clustering of NMs. It is believed that there is a rearrangement of proteins rather than a slow subsequent binding. Earlier studies focussing on human corona formation have established there is a reorganisation of proteins that are adsorbed to NM surfaces (Lynch and Dawson, 2008). Initially, proteins that are higher in abundance bind to NM surfaces and then are later displaced by less abundant yet higher affinity proteins. This phenomenon can be explained via the Vroman effect which observes proteins with high mobility binding to NMs first and later being displaced by proteins with higher affinity though slower kinetics (Rahman et al., 2013). Results indicate that as both conditioning and incubation times increase so does agglomeration of NH_2 - and COOH-PS NMs, and suggests that the proteins released by *D. magna* neonates are acting as a destabilizer for these NMs dispersed in HH Combo medium.

D. magna consumes algae, which is also abundant in fresh water systems, as a part of its diet and therefore is always in close proximity to algae. It is therefore also important to consider if proteins released by algae cause any changes in NM stability. *C. vulgaris* were allowed to

condition HH Combo medium for six hours and were then removed by filtration leaving behind only conditioned HH combo medium as seen in figure 3.5.

Figure 3.5. *Left*: Algae *C. vulgaris* in HH Combo medium. *Right*: filtration and removal of algae leaving behind only the conditioned medium.

It was quantified that *C. vulgaris* increase the concentration of proteins present in HH Combo medium to 89 μg/mL after 6 hours of conditioning time, as seen in figure 3.6 (a), which is considerably lower than the amount of proteins secreted by *D. magna*. Figure 3.6 (b) and (c) shows that the minimal amount of proteins released by *C. vulgaris* did not cause any size changes to PS-NH_2 or to PS-COOH NMs that were incubated in the conditioned medium and indicates that any instability in NM size is primarily due to proteins secreted by *D. magna.* Algae may also be releasing various other components such as polysaccharides or lipids into the medium though regardless of which components may be being secreted, they are not affecting NM stability, while BCA assay confirms there are indeed proteins present in the medium as well. PS-NH_2 and PS-COOH NMs and their respective PDI incubated in *D. magna* (a) and (c) and *C. vulgaris* (b) and (d) conditioned medium is reported in table 3.2.

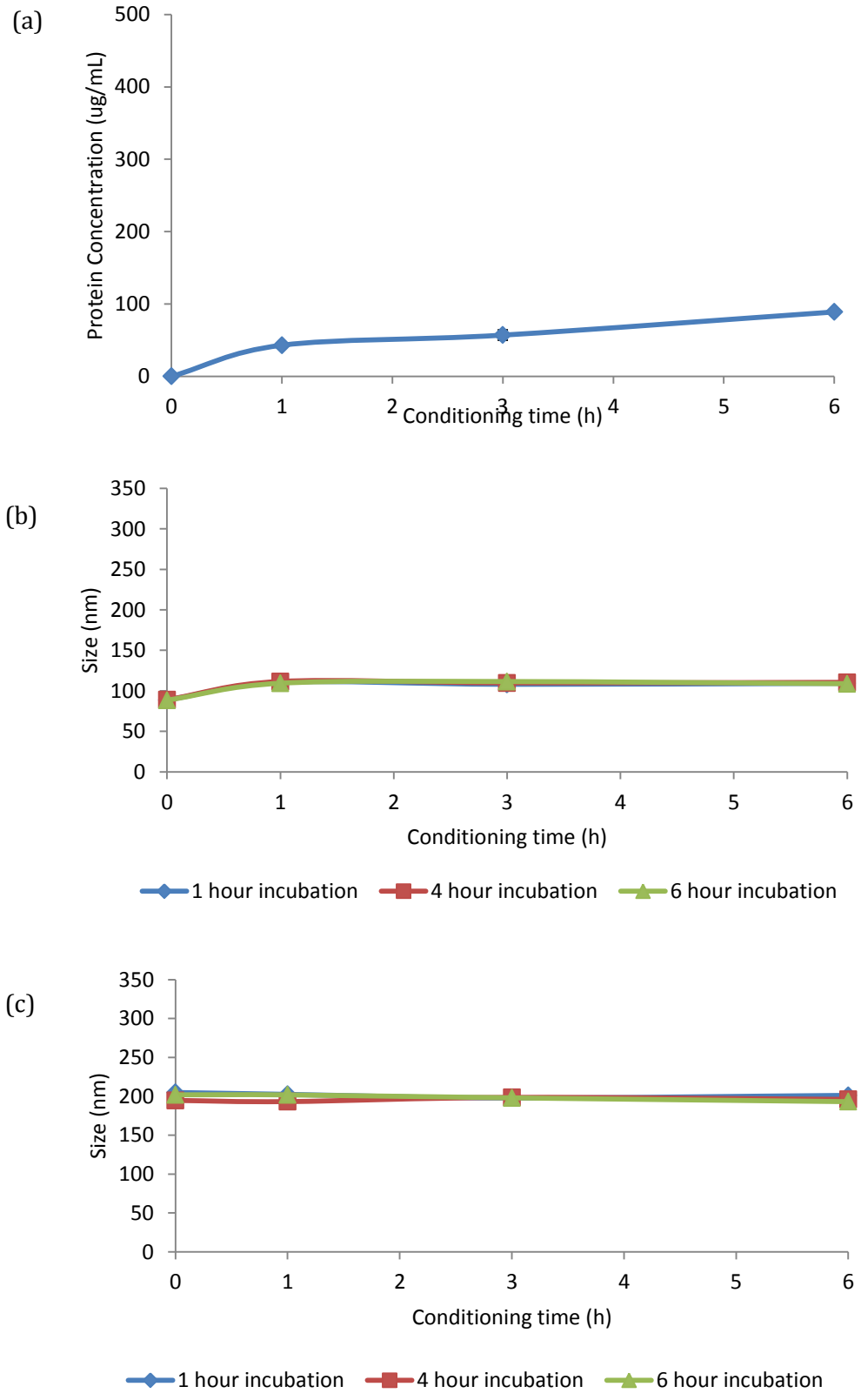

Figure 3.6 (a) Concentration of proteins secreted by *C. vulgaris* into HH Combo medium over 6 hours quantified by BCA assay; b) Changes in hydrodynamic diameter of PS-NH_2 NMs and; c) PS-COOH NMs, with different incubation times in *C. vulgaris* conditioned HH Combo medium.

Table 3.2 Hydrodynamic size and corresponding PDI of PS-NH_2 and PS-COOH NMs with different incubation times in (a) and (c) *D. magna* conditioned HH Combo medium and (b) and (d) *C. vulgaris* HH Combo medium respectively.

(a)	Incubation Time (h)					
	1		4		6	
Conditioning Time (h)	Size (nm)	PDI	Size (nm)	PDI	Size (nm)	PDI
0	88.83	0.018	89.09	0.025	85.51	0.030
1	91.26	0.169	151.2	0.318	200.5	0.034
3	100.2	0.186	148.5	0.366	289.7	0.477
6	104.7	0.12	143.8	0.323	293.8	0.510

(b)	Incubation Time (h)					
	1		4		6	
Conditioning Time (h)	Size (nm)	PDI	Size (nm)	PDI	Size (nm)	PDI
0	88.83	0.018	89.09	0.025	88.51	0.030
1	110.4	0.193	111.6	0.196	109.4	0.206
3	108.1	0.215	109.9	0.175	111.5	0.156
6	109.3	0.184	110.5	0.153	108.8	0.200

(c)	Incubation Time (h)					
	1		4		6	
Conditioning Time (h)	Size (nm)	PDI	Size (nm)	PDI	Size (nm)	PDI
0	190.3	0.084	191.2	0.090	194.4	0.092
1	196.2	0.047	195.0	0.083	197.4	0.045
3	196.8	0.073	203.3	0.025	210.5	0.081
6	198.6	0.079	200.5	0.116	209.9	0.070

(d)	Incubation Time (h)					
	1		4		6	
Conditioning Time (h)	Size (nm)	PDI	Size (nm)	PDI	Size (nm)	PDI
0	204.9	0.131	194.7	0.031	201.9	0.055
1	202.5	0.017	193.2	0.048	201.8	0.062
3	197.8	0.036	198.6	0.018	198.0	0.067
6	201.2	0.057	196.0	0.142	193.1	0.081

These findings are important as organisms naturally condition their environment and have the ability to alter NM stability and surface characteristics and consequently affect NM uptake by organisms.

3.2.3 Effect of secreted eco-corona on EC_{50} of *D. magna*

As concluded previously, proteins released by *D. magna* cause destabilization of NH_2 and COOH- PS NMs which lead to partial agglomeration of the NMs. The effect of the eco-corona on the EC_{50} to *D. magna* was then investigated. As shown in figure 3.7 (a), PS-COOH NMs that were incubated in conditioned medium for six hours had an EC_{50} of 0.0337 mg/mL, compared to 0.0363 mg/mL for PS-COOH NMs having no previous conditioning step. NMs that were incubated for 24 hours had an even lower EC_{50} of 0.0095 mg/mL. These results are significant as they indicate that conditioning causes the proteins released by *D. magna* to adsorb to the NM surface which results in the NMs having a detrimental effect on the neonates. A longer NM incubation time leads to a greater amount of destabilization of NMs causing an increase in NM size. Literature notes that although *D. magna* are filter feeders and are exposed to all substances in the water column, they are still able to selectively uptake food based on factors such as size and consistency (Ju-Nam and Lead, 2008). The larger size of NMs caused by the destabilization by proteins and partial agglomeration could thus potentially make NMs a more attractive size as a food source for *D. magna*. Also, the proteins adsorbed to the surface of the NMs could make the agglomerated PS NMs appear to be a more organic food source, and it can be concluded that NMs coated by an eco-corona are more readily taken up compared to bare and monodisperse NMs. PS-NH_2 NMs had a similar trend and can be seen in figure 3.7 (b). Incubation of PS-NH_2 NMs in conditioned medium for six hours caused a decrease in EC_{50} to 0.0189 mg/mL compared to those with no conditioning step which had an EC_{50} of 0.0258 mg/mL. NMs that were incubated for 24 hours had an even greater decrease in EC_{50} to 0.0081 mg/mL. It was also shown that amino functionalised NMs

were generally more toxic than carboxylic functionalised ones, regardless of having a conditioning step or not.

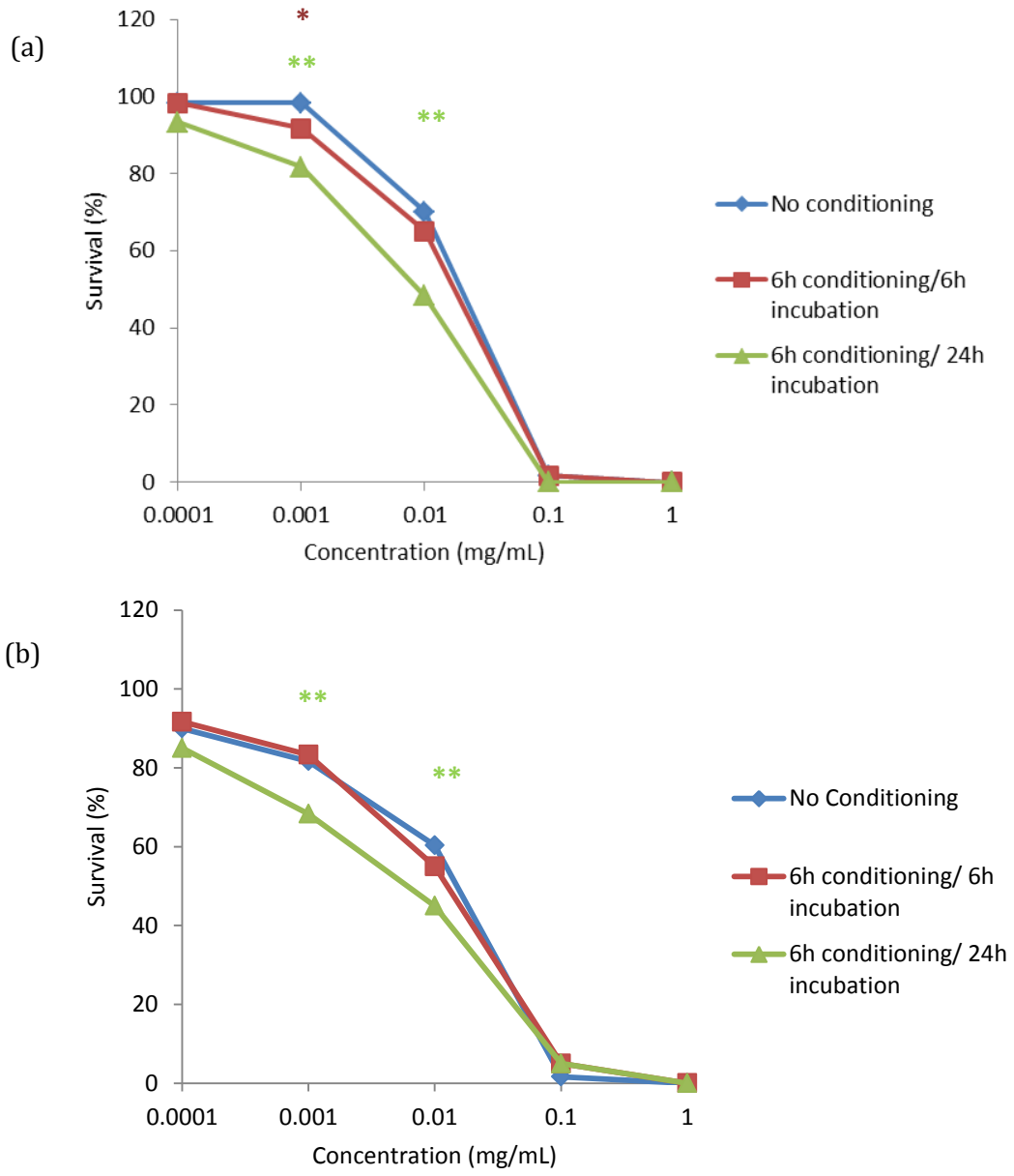

Figure 3.7. Survival curves of *D. magna* neonates exposed to a) PS-COOH NMs and b) PS-NH_2 NMs with either 6 hour conditioning/6 hour incubation or 6 hour conditioning/24 hour incubation. Statistical significance is indicated using a 2-tailed Student's t-test with p-values of 0.05, 0.01 and 0.001 with *, **. *** indicating the respective significances in the data.

These results are important as they indicate that the proteins that are released by *D. magna* neonates in fact adsorb to the surface of the NMs and ultimately have a detrimental effect on neonate survival. Longer incubation times of NMs in conditioned medium lead to a greater amount of proteins being adsorbed to the NM surface which can then be subsequently rearranged which leads to an increase in size. Assessment of the specific proteins bound to the NMs incubated for 24 hours in HH Combo medium conditioned for 6 hours by 12.5% PAGE was conducted with both Coomassie blue and silver stains to confirm the presence of proteins deriving from the *D. magna* secretions and forming the hard-corona around COOH and NH_2 -PS NMs as seen in figure 3.8.

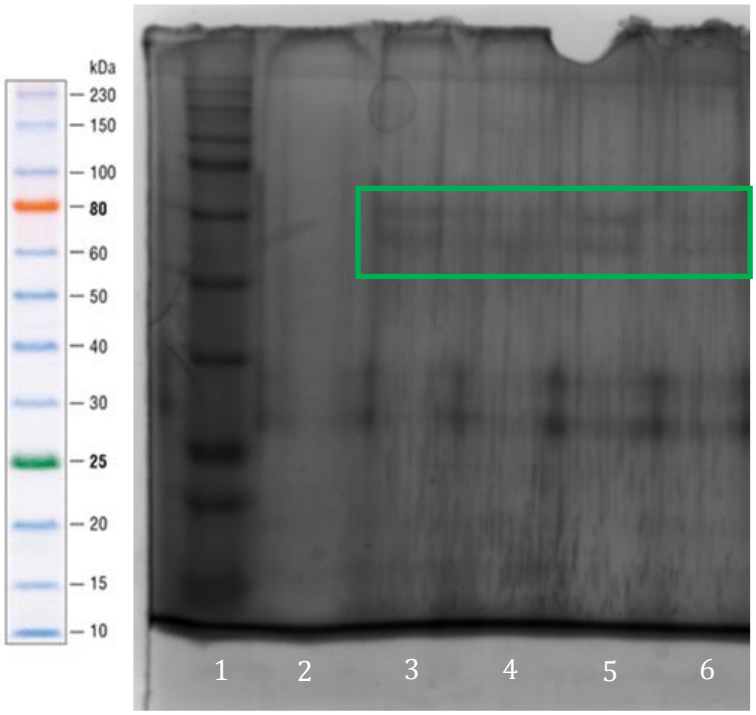

Figure 3.8. Lane 1: Ladder; Lane 2; blank (no sample therefore lack of bands); Lane 3: Protein corona around PS-NH_2; Lane 4: Repeat of lane 3; Lane 5: Proteins around PS-COOH and; Lane 6: Repeat of Lane 5.

Bands appear between 50-80 kDa indicating the presence of proteins such as Type VI secretion system (74.8 kDa) which is a known as a stress-response protein and QseC sensor protein often used for cell-to-cell communication in *D. magna*. Both proteins were identified in the list of proteins secreted by the *D. magna* during conditioning a 6 hour conditioning

time, as determined form the mass spectrometry results, done on the conditioned medium, with the full list in Table 3.3, all of which are available to interact with the NMs in suspension to create the eco-corona. Bands seen across all the lanes between 30-40 kDa are from ß-mercaptoethanol from the SDS-denaturation buffer or may indicate the presence of residual keratin from *D. magna*.

Table 3.3 List of proteins identified in *D. magna* conditioned medium by mass spectrometry, after 6 hours of conditioning.

Description	Molecular Weight (kDa)
Elongation Factor	43.2
Glucose-6-phosphate Isomarase	51.2
Glycerol-3-phosphate binding periplasmic protein	46.3
Sensor protein QseC	50.4
Bifunctional Aspartokinase	88.3
Photoporphyrinogen IX dehydrogenase	20.6
Polyribonucloetide nucleotidyltransferase	79.2
Type VI secretion system	74.8
Murein DD-endopeptidase	49.0
Paraquat inducible protein B	61.0
Pyruvate carboxylase	128.3
Pyruvate kinase	62.9
Helicase (magna)	84.6

3.2.4 Rates of uptake and rates of removal of PS NMs after exposure to *D. magna*

As incubation time of unconditioned PS-COOH NMs increases, so does the NM uptake into *D. magna* neonates as shown in Figure 3.9. The decrease in the fluorescence of the medium and the increase of the fluorescence inside *D. magna* neonates is not symmetrical as *D. magna* is well known to adsorb molecules to their carapace and have developed the mechanism of moulting to remove toxic substances. Fluorescent NMs bound to the carapace of *D. magna* were washed three times so that the detected fluorescence most likely only represented NMs

that were ingested by *D. magna* and it appears that a proportion of NMs were bound to the carapace and were washed off during this process.

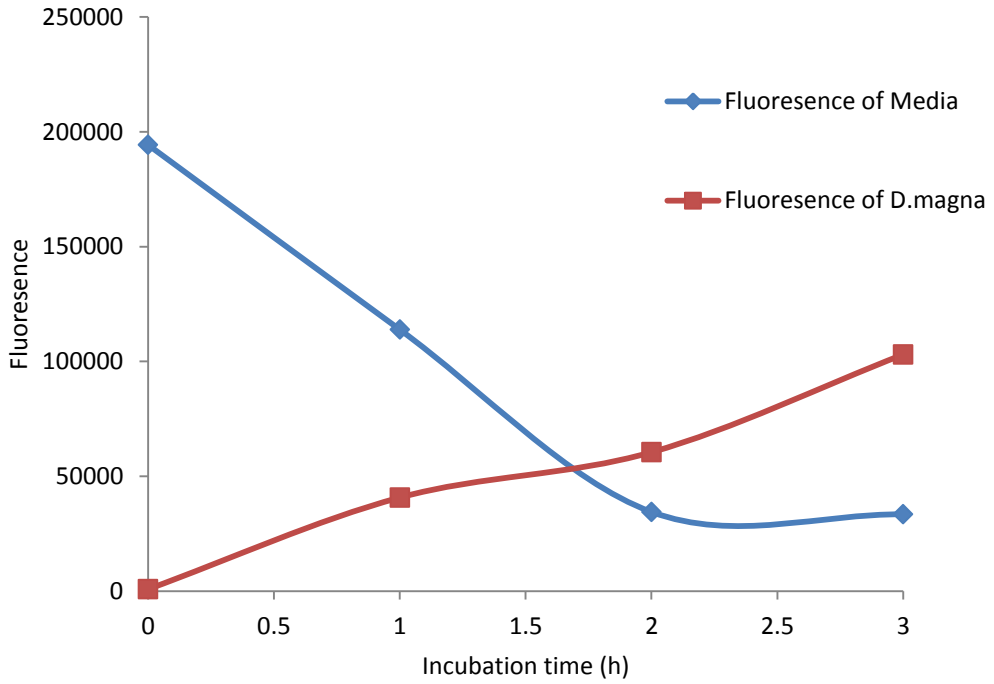

Figure 3.9 Increase of fluorescent PS-COOH NMs into *D. magna* neonates and the contingent decrease of NMs from HH Combo medium in 3 hours.

It is also important to understand the rate of removal of NMs from the *D. magna* gut to assess the full body burden of NMs on neonates in order to properly understand the effects. Considering that *D. magna* is a central organism in fresh water systems, its inability to properly remove NMs from its system can lead to long term effects and alterations to the aquatic ecosystem. As seen in figure 3.10 (a), (b) and (c), as exposure time of *D. magna* to PS-COOH NMs, increases so does the uptake of the NMs into neonates.

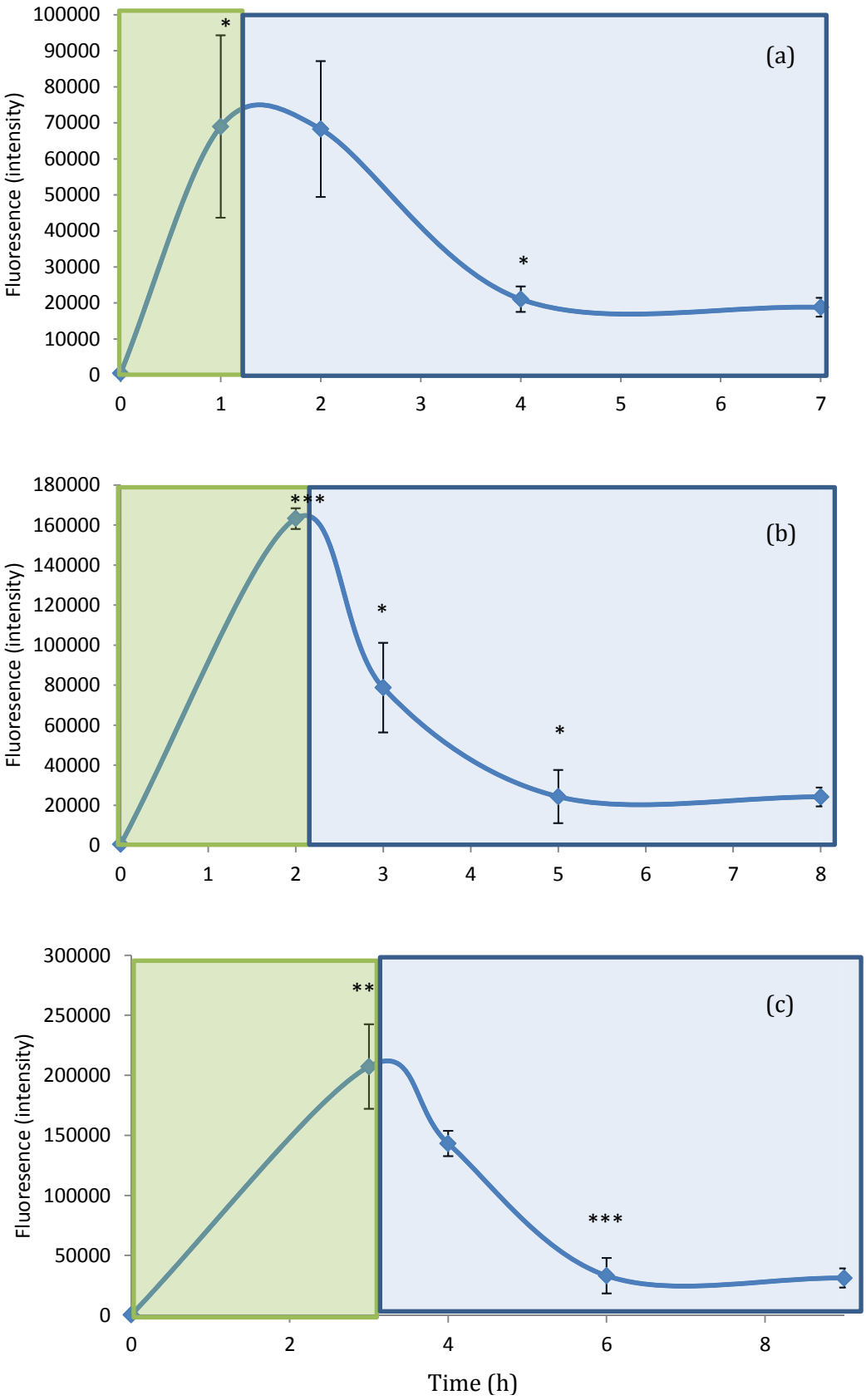

Figure 3.10 Exposure of fluorescent PS-COOH NMs to *D. magna* for a) 1 b) 2 c) 3 hours (green panels) and their subsequent rates and amounts of removal (blue panels).

It can also be observed that neonates are steadily able to remove NMs from their system during post-exposure regardless of the length of exposure time and that longer exposure time (up to three hours compared to one hour) does not affect the neonates ability to remove NMs. It was calculated that even after six hours of post-exposure, approximately 15% of NMs still remain in the gut of the neonates and that the rate of removal starts to level off after three hours of post-exposure in the absence of further feeding. The accumulation of NMs in the gut of the neonates can lead to physiological consequences to these filter-feeders especially in regions where NMs are routinely added into the environment leading to multiple exposures.

It is difficult to quantify NM number concentration within *D. magna* using the NM fluorescence, as the gut of *D. magna* has regions of varying pH, and pH is a major factor influencing fluorescence. A second factor to consider is that when *D. magna* consume fluorescent NMs, the particles are confined in space in the gut, whereby fluorescent molecules are likely to quench each other resulting in a decrease in fluorescence which is not representative of how many NMs are actually present. Both of these factors indicate that external calibration of fluorescent NMs in medium is not sufficient for internal measurements which is a limitation that was considered using fluorescent NMs. Other methods of quantifying NM uptake are ICP-OES though this would be useful to quantify metal NMs and not PS as this is carbon based, though this too has its own limitations, such as not differentiating between NMs or ions. The figures pertaining to uptake and release of fluorescent NMs are acceptable as they compare internalised NM fluorescence after different exposure and deputation times.

It is also imperative to consider other influences on NM uptake such as *D. magna* movement (swimming) which influences kinetics and increases collision between particles and *D. magna*. In natural fresh waters there will be a constant change in movement and shaking of water from the environment though fresh water ponds are generally still though movement

may derive from natural flow, rain and wind as well as movement from surrounding organisms which may have an impact on uptake as the presentation of NMs to *D. magna* is changing and therefore important to asses a spectrum of exposure conditions. It was determined that shaking (0, 80, 240, 320 rpm) of the environment of *D. magna* definitely changes the rate of uptake of NMs as seen in figure 3.11, although too much disturbance (shaking) dramatically reduced uptake.

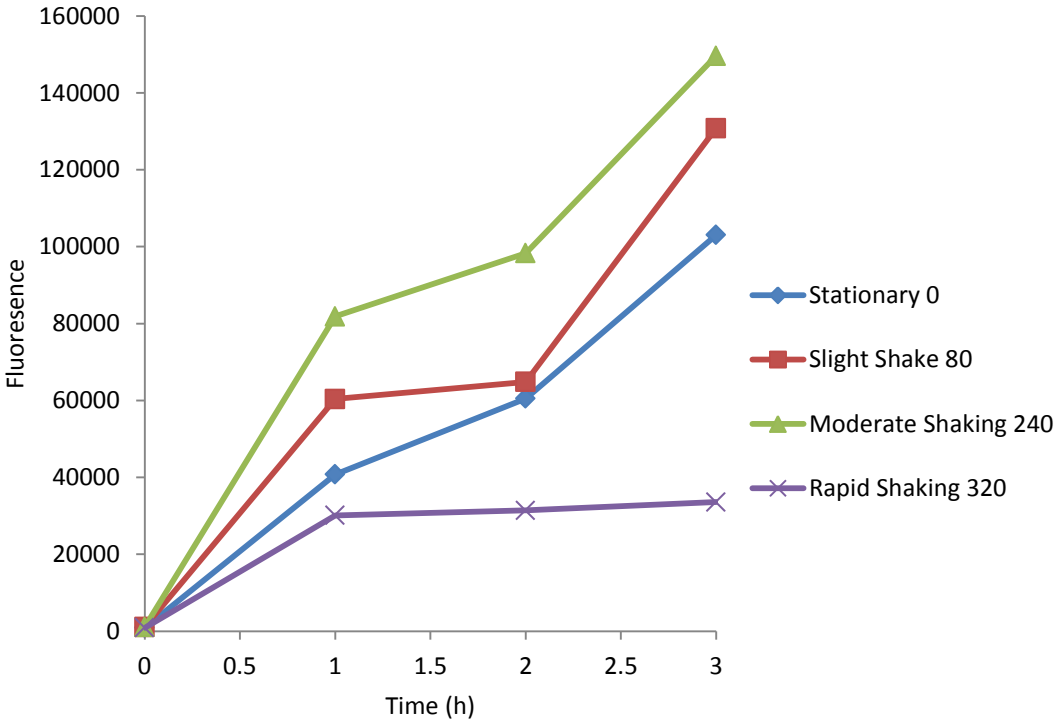

Figure 3.11 Uptake of PS-COOH NMs into *D. magna* neonates with different shaking conditions.

Though there is no settling of NMs even without shaking, it was determined that a slight shaking at 80 rpm increased the rate of uptake PS-COOH NMs as the *D. magna* neonates were consistently being presented with new NMs from the increased kinetic energy. Moderate shaking at 240 rpm increased the rate of uptake to an even greater extent from an even higher increased presentation of new NMs.

Conditioning of medium that the NMs are incubated in also has a different yet resounding effect on rate of NM removal. NMs that were incubated in conditioned medium and then allowed to be taken up by neonates showed that the rate of removal of NMs was not as smooth or consistent as those without a conditioning step as seen in figure 3.12.

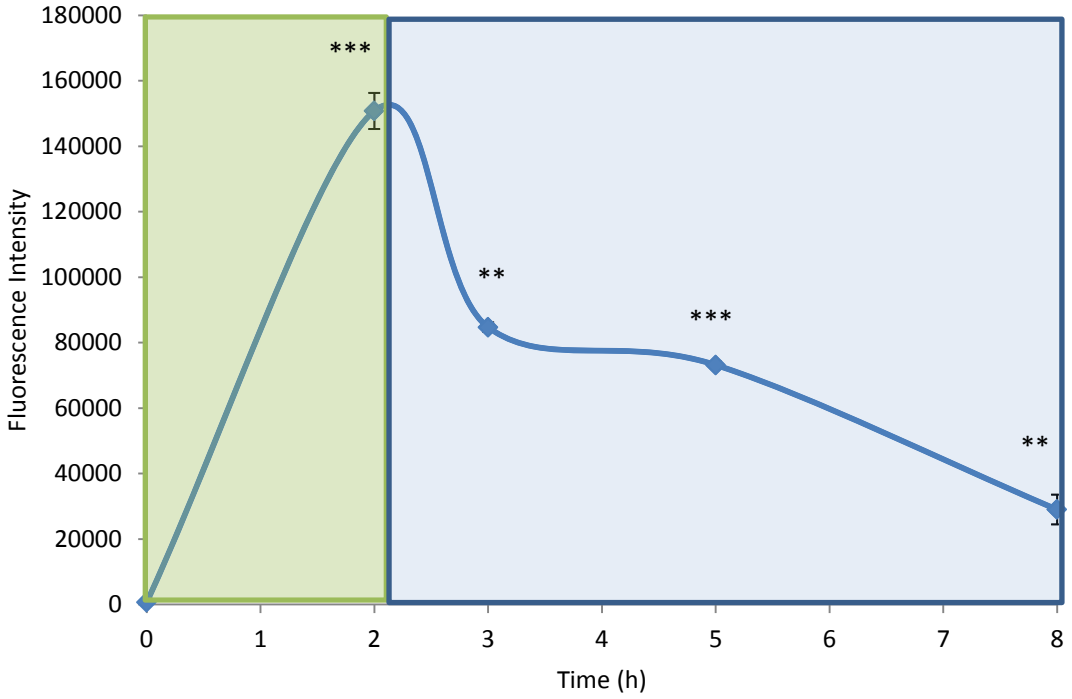

Figure 3.12 Exposure of conditioned PS-COOH NMs for 2 hours and 6 hours post-exposure to assess NM excretion and retention.

At six hours post-exposure, 20% of the eco-corona coated PS-COOH NMs still remained in the gut of *D. magna* neonates, which could be attributed as being the cause of the decrease in EC_{50} as a result of a higher amount of NMs that are retained within the neonates. NMs that have an eco-corona are taken up slightly less than those without an eco-corona though remain longer within the neonates and are not filtered out as effectively as NMs without any adsorbed surface proteins. Confocal images were taken to confirm that retained bare PS-COOH NMs were confined solely to the gut of the neonates as seen in figure 3.13 and that even after a full 24 hours of continuous exposure, no NMs have translocated to other tissue.

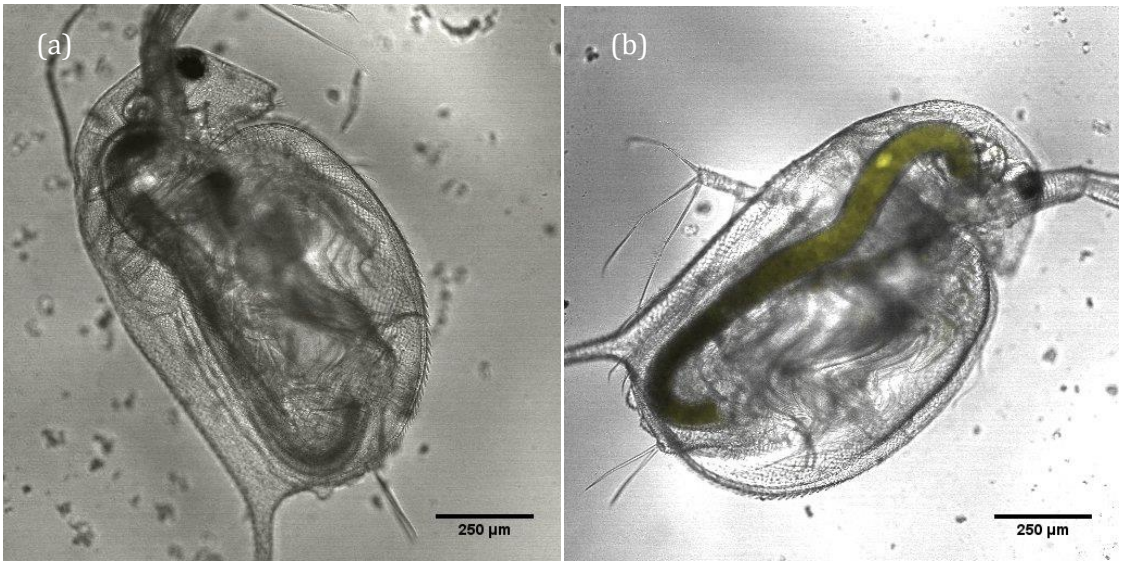

Figure 3.13 a) control *D. magna* neonate in NM free HH Combo medium and b) *D. magna* neonate exposed to PS-COOH NMs after 24 hours with no further feeding.

Chapter 5 will assess the effect of NM size and presentation mode of feeding on NM uptake and retention within *D. magna*.

3.2.5 Ability of *D. magna* to effectively feed on *C. vulgaris* after NM accumulation

Algae *C. vulgaris* is a main food source for *D. magna* and is abundant in fresh water systems. It has been recorded that the feeding rate of *D. magna* depends on what is already pre-existing in the gut (MacMahon and Rigler, 1965). As concluded in the previous figures, a proportion of corona-coated (or bare) NMs remain in the gut of *D. magna* after six hours of post exposure and it is important to assess if this affects the rate of subsequent grazing on algae *C. vulgaris* as the presence of food in the gut is known to limit subsequent food intake (MacMahon and Rigler, 1965) though newly acquired food is also known to push out previously ingested food. As seen in figure 3.14 due to the presence of NMs with an adsorbed eco-corona retained in the gut even after only 6 hours of post-exposure, subsequent feeding rate does indeed decrease though the amount is not statistically significant by 6 hours; however, if this trend is followed, it could become significant over a longer span of time. This issue of feeding during or after exposure to NMs is addressed further in Chapter 5.

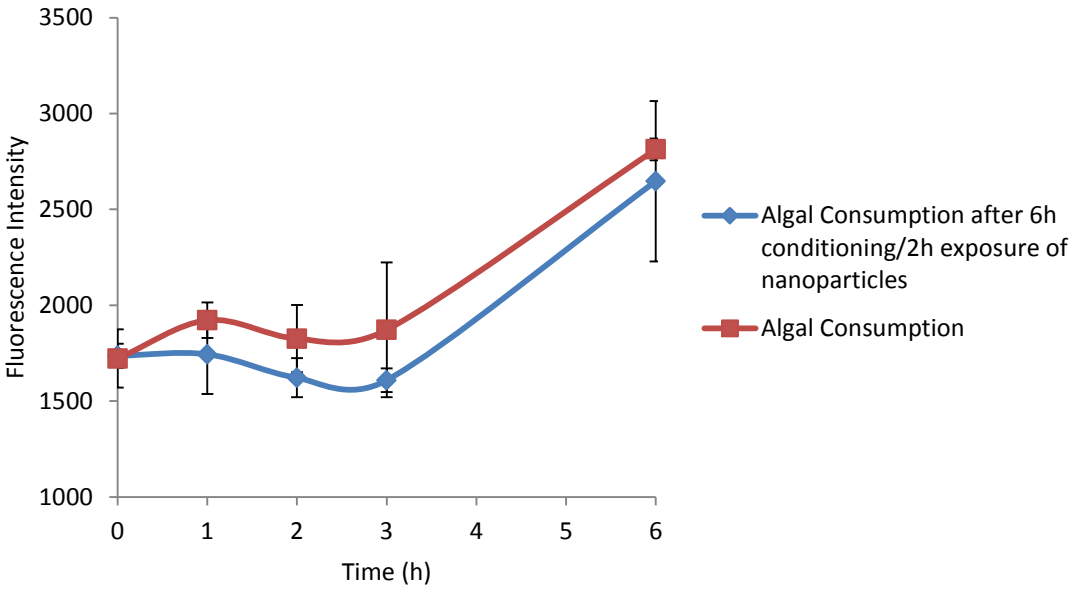

Figure 3.14. Comparison of feeding rates of (*C. vulgaris*) of control *D. magna* neonates (red) and *D. magna* neonates that have retained 20% of corona-bound NMs (blue).

The feeding rate of neonates is an important factor as *D. magna* acts as a regulator of algae levels which in turn are responsible for creating organic compounds for use by other organisms and also provide chlorophyll which is a much needed component for photosynthesis and the maintenance of dissolved oxygen for aquatic organisms. Alterations of the *D. magna* feeding rate on *C. vulgaris* could cause multi-trophic level changes. *D. magna* are consumed by many invertebrate predators and changes to their survival could cause a decrease in levels of food for many organisms. It is also important to note that *D. magna* that have NMs retained within them and are consumed by predators could cause secondary transfer to other organisms. Clearly then, it is important to understand how proteins released by organisms' impact the eco-corona, which in turn can affect bioaccumulation in, *D. magna* guts and subsequent toxicity, as well as the impact of the feeding regime and exposure conditions on the toxicity of NMs which will be explored in Chapter 5.

3.2.6 Effect of PS NMs and corona on *D. magna* moulting

D. magna neonates that are exposed to PS-NH_2 appeared to jolt on immediate exposure to the NMs and therefore it could be that NMs are binding to surface structures on *D. magn*a which may affect moulting. *D. magna* shed their carapace as a method to remove any toxic contaminants such as NMs bound to their exterior. Results indicate that all living *D. magna* that were exposed to 0.001 mg/mL (EC_{20} concentration) of PS-NH_2 are able to successfully complete their first moulting cycle (approximately 16 out of 20 exposed neonates completed their first moult which equates to 100% successful moult of the living neonates) as seen in figure 3.15. Exposed neonates have no delay in completing their first moult cycle which occurs at 42 hours compared to at 36 hours for control *D. magna,* which is statistically insignificant ($p > 0.05$). Binding of NMs to the filtering apparatus of *D. magna* happens rapidly and neonates remove the bound NMs during their first moulting cycle (Dabrunz et al., 2011b). The process of synthesizing a new exoskeleton begins in the brood chamber so that the process of moulting begins even before freshly released neonates are ever exposed to the NM suspension leading to a successful first moult. The completion of the second moult cycle for *D. magna* that are exposed to PS-NH_2 NMs is not delayed compared to the controls ($p > 0.05$) where 100% of the controls (all 20 neonates) finish their moulting cycle at 84 hours. Thus, the exposed neonates successfully complete their moulting cycle at 90 hours, where 16 out of the 16 living neonates, equating to a 100% successful moult (there was no additional death). This indicates that at the EC_{20} concentration that bare PS-NH_2 NMs do not affect moulting of *D. magna*.

D. magna neonates that were exposed to PS-NH_2 that had been incubated for 1 hour in 6 hour conditioned HH Combo medium successfully completed their first moult cycle at 42 hours which showed no delay compared to controls ($p > 0.05$). Neonates that were exposed to PS-NH_2 incubated in conditioned HH Combo medium also successfully complete their second moulting cycle with 16 out of 16 living neonates equating to a 100% successful moulting

cycle with no further death. The second moulting cycle was also not delayed compared to the controls ($p > 0.05$).

D. magna neonates exposed to both bare PS-NH_2 or corona bound PS-NH_2 NMs were not delayed in their second moulting cycle compared to controls ($p > 0.05$) which indicates that the mechanism underpinning the increased toxicity of corona-PS-NH_2 compared to bare PS-NH_2 NMs was not related to moulting or and a result of NMs adhering to the exoskeleton.

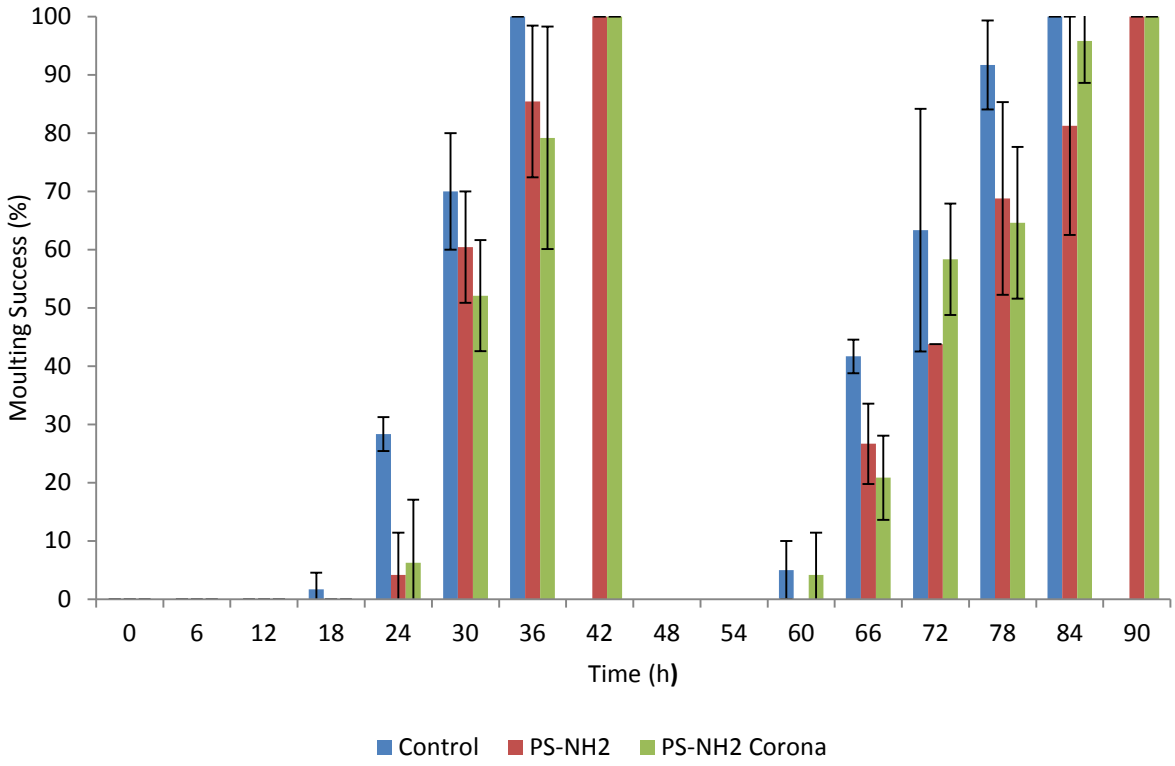

Figure 3.15. Moulting success of D. magna exposed to 0.001 mg/mL with a final volume of 5 mL (EC_{20}) of bare and corona bound (6 hour conditioning with 10 neonates; 1 hour incubation) PS-NH2 NMs.

3.3 Summary and conclusions from Chapter 3

As a well-established model for toxicity assessment, *D. magna* is an important indicator species and is known to engage in numerous predator-prey responses via secreted macromolecules. Coupling this with the propensity of NMs to bind to proteins to form a corona, there is an urgent need to understand the role of secreted proteins in mediating NM

toxicity towards *D. magna*. The work presented in this chapter is the first step to addressing this pressing issue and conclusions have been reached in order to address each original objective.

1. Conditioning of the dispersion medium by *D. magna* neonates resulted in a release of proteins which quickly coated NH_2/COOH-PS NMs forming a protein corona. The corona causes destabilization of NMs over 6 hours, observed as an increase in particle size indicative of particle agglomeration, whereas the NMs were mono-dispersed in the unconditioned medium.
2. The presence of a protein corona around NH_2/COOH-PS NMs caused a decrease in the EC_{50} compared to equivalent unconditioned NMs towards *D. magna* and longer incubation times in conditioned medium lead to a more detrimental effect (lower EC_{50}) towards *D. magna.*
3. *D.* magna were able to uptake and release PS-COOH NMs, though 15% remain within the gut after 6 hours of post exposure, compared to 20% retention of the protein corona-coated PS-COOH NMs, indicating that the corona-NMs were less effectively removed from the gut of *D. magna.*
4. The corona-coated PS-COOH NMs remaining in the gut (20%) of *D. magna* affected its ability to feed on *C. vulgaris* over the subsequent 6 hours.
5. Proteins released by *D. magna* adsorbed to the surfaces of PS NMs creating a hard protein-corona. Of the various secreted proteins, two (as Type VI secretion system and QseC sensor protein) were preferentially bound to both types of NMs, suggesting core rather than charge drives composition of corona in this case.
6. Bare PS-NH_2, or those that have been incubated in conditioned medium do not appear to affect moulting of *D. magna.*

Data presented in this chapter confirms the important role of secreted proteins in modulating NM toxicity towards *D. magna* as well as confirming that uptake and removal of NMs from the gut are affected by the presence of a protein corona. As such, both corona and

retention of NMs need to be considered as part of determination of the bioaccumulated dose for toxicity assessment. Conditioning of medium, ability for proteins to adsorb to NM surfaces which changes their stability and how this effects retention and toxicity, as well as the lack of additional food sources to push out ingested NMs, are all factors not currently considered a part of OECD standard tests and represents a significant modification of the tests that is needed to improve and ensure their appropriateness for assessment of NM toxicity under conditions that are relevant for their behaviours in real environments and exposure conditions.

4

Shape and charge of Gold nanomaterials and presence of protein corona influences survivorship, oxidative stress and moulting in Daphnia magna

Parts of this chapter have been published as:

F Nasser et al. Shape and charge of gold nanomaterials influences survivorship, oxidative stress and moulting of *Daphnia magna*. **Nanomaterials** (2016) 6(12).

This paper was awarded the Michael K. O'Rourke PhD Best Publication Award 2017 for the College if Life and Environmental Science (LES) from the **UoB** Westmere Graduate School.

These results have been presented at **ISMC' 2016**

This work was awarded the Sir Eric Rideal award for work with colloids by the **RSC.**

4.1 Introduction

Different shapes and morphologies of NMs provide improved properties such as hollowness for use in drug delivery for the transport of drugs, and it is therefore important to assess the impact of shape on NM toxicity. There has been extensive progress towards the incorporation of spherical gold (Au) NMs into medical applications, for example, by using Au NMs to bind to antibodies specifically targeted for cancer cells (Letfullin et al., 2011).

Au in bulk form is known to be an inert material, whereas Au NMs, due to their small size, have an increased reactivity especially with the addition of surface charge. Positively charged particles are known to be more toxic than negatively charged Au particles (Bozich et al., 2014), and may trigger biological effects such as prompting increased mortality in *D. magna* (Bozich et al., 2014). The addition of surface charge to NMs during synthesis is common as it

provides charge stabilization to NMs resulting in monodispersity. The addition of charge can also be harnessed in medical applications such as drug delivery where Au NMs bearing a positive charge are more likely to be removed by macrophages while negative or neutral Au NMs have a longer circulation time (Blanco et al., 2015) and therefore have an increased likelihood of providing the correct drug dosage. Circulation of NMs used in drug delivery is also profoundly influenced by shape where filamentous polymer NMs have a long circulation time of over one week due to the NMs ability to align with blood flow compared to spherical NMs which have a maximum circulation time of three days (Geng et al., 2007).

It has been documented that 10 nm spherical Au NMs are taken up by *D. magna* and reach steady-state concentrations (whereby uptake and excretion rates are equal) in *D*. *magna* in 10 h but are not readily excreted back into the surrounding environmental waters even after 48 h in the absence of feeding (Skjolding et al., 2014) , although this is not a realistic scenario as feeding is part of the normal excretion process for *D. magna* Exposure of *D. magna* to Au NMs (negatively charged 14 nm, 0.5-20 mg/L chronic exposure for 14 days, with feeding on *P. subcapitata* with every media change) has also been shown to prompt physiological effects such as increased moulting, which is an important regulatory mechanism for *D. magna* to shed their exoskeleton as a means to regulate internal metal concentrations (Botha et al., 2016) implying that ingested metal Au NMs cause physical effects to *D. magna*.

Due to the increased surface area provided by NMs compared to larger materials, they have been shown to generate harmful reactive oxygen species (ROS), which are an indicator of oxidative stress in *D. magna* (Becker et al., 2011). The charge of surface groups on NMs can effect toxicity though results have not been consistent as to which type of charge causes the greatest effect as effects can be organism specific (Dominguez et al., 2015). For example exposing zebrafish to negatively charged Au NMs induces genes associated with mitochondrial dysfunction (Geffroy et al., 2012) which directly leads to ROS accumulation, whereas exposing clams to positively charged Au NMs caused oxidative stress by increased

levels of *CAT* (enzyme previously discussed in chapter 2). Depending on the NM size, surface charge and shape, different proteins may adsorb to the surface of Au NMs (Cai and Yao, 2014) and may affect NM stability and toxicity in different ways, making NM shape and charge important parameters to assess.

4.1.1 Aims and Objectives

The aim of this chapter is to assess how shape and charge of Au NMs impact upon the physical (survivorship and moulting) and chemical (reactive oxygen species formation) factors in the response of *D. magna* to the NMs and to evaluate the effects of the protein corona. This will be achieved through the following objectives:

1. Investigation of the impact of Au NMs shape and charge on the survivorship of *D. magna.*
2. Assessment of reactive oxygen species formation in response to low and high exposures to Au NMs
3. Quantification of charge to surface area ratio of Au NMs and the ranking of NMs toxicity towards *D. magna* on this basis
4. Exploration of the effect of a protein corona on NM stability and toxicity towards *D. magna* as a function of shape and charge
5. Investigation of the exposure of different shaped Au NMs on *D. magna* moulting.

4.2 Results and Discussion

4.2.1 Characterization of Au NMs

Differently shaped NMs provide unique characteristics due to their different sizes, morphology and shape that are not present in simple, spherical NMs and therefore are important to assess in terms of potential toxicity. The following studies utilise NMs of different charge, shape and length to determine impact of dimensional and charge

characteristics on NM toxicity. Au NMs used were characterized using multiple methods including DLS, UV-vis and TEM to ensure adequate characterization.

4.2.1.1 DLS

Spherical Au NMs were measured for hydrodynamic diameter using DLS. The z-average hydrodynamic size of positive spherical Au NMs was 53.45 ± 1.38 with a PDI of 0.195, and the hydrodynamic size of spherical Au NMs was 51.04 ± 0.65 with a PDI of 0.179 as seen in figure 4.1. The relatively low PDI values show that both NMs are monodisperse upon immediate dispersion in HH Combo medium. There is no difference in the z-average hydrodynamic sizes between the two ($p > 0.05$).

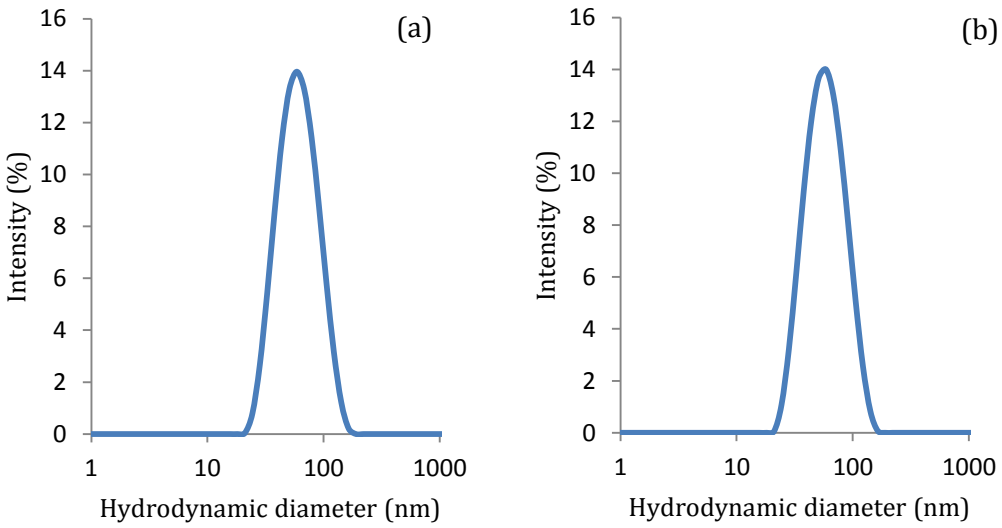

Figure 4.1 DLS graphs indicating hydrodynamic diameter of spherical (a) positive and; (b) negatively charged Au NMs.

4.2.1.2 UV-Vis

Colloidal suspensions of Au NMs have a unique characteristic of having different colours and therefore difference UV-Vis absorbance's as seen in figure 4.2 compared to larger bulk material.

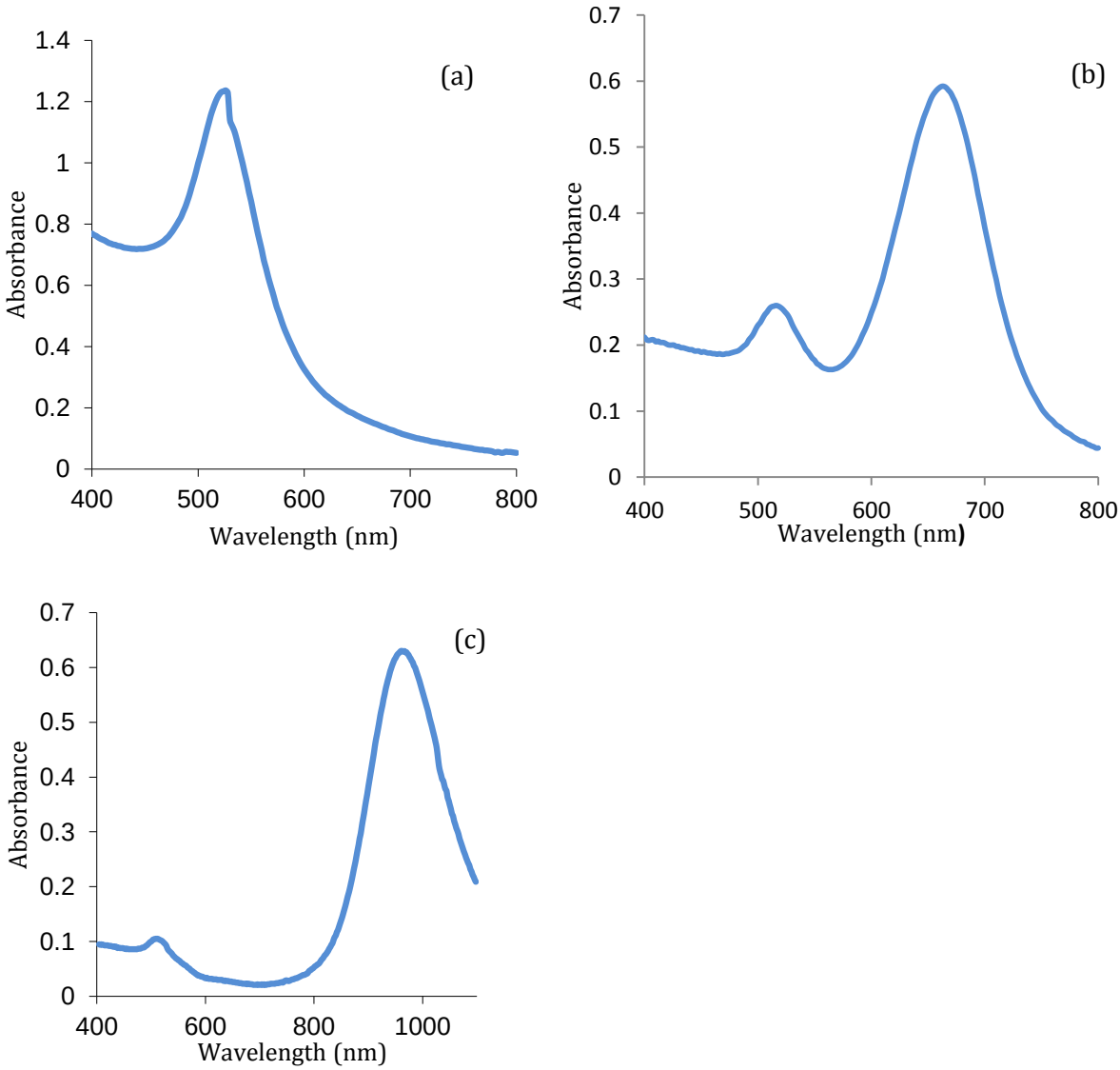

Figure 4.2. UV-Vis spectra of different shaped negatively charged Au NMs dispersed in HH Combo medium. (a) sphere (b) short rod and (c) long rod Au NMs. Positively charged NMs will have the same UV characteristics as these are inherent to the material rather than surface charge.

The absorption of light by spherical Au NMs, which causes the oscillation of electrons resulting in an SPR band at approximately 550 nm, can be seen in figure 4.2 (a) and is what gives rise to the red colour of Au NMs (Das et al., 2009). Au NMs that have a second dimension, such as rods have a second peak which is red-shifted to the right, with longer diameters resulting in a farther red-shift which can be seen in figure 4.2 (b) and (c). This

second peak is due to the movement of electrons resonating in two directions resulting in two SPR bands.

4.2.1.3 TEM

Characterization of NMs was completed in fresh HH Combo medium, except for TEM images which were prepared in DI water as seen in figure 4.3.

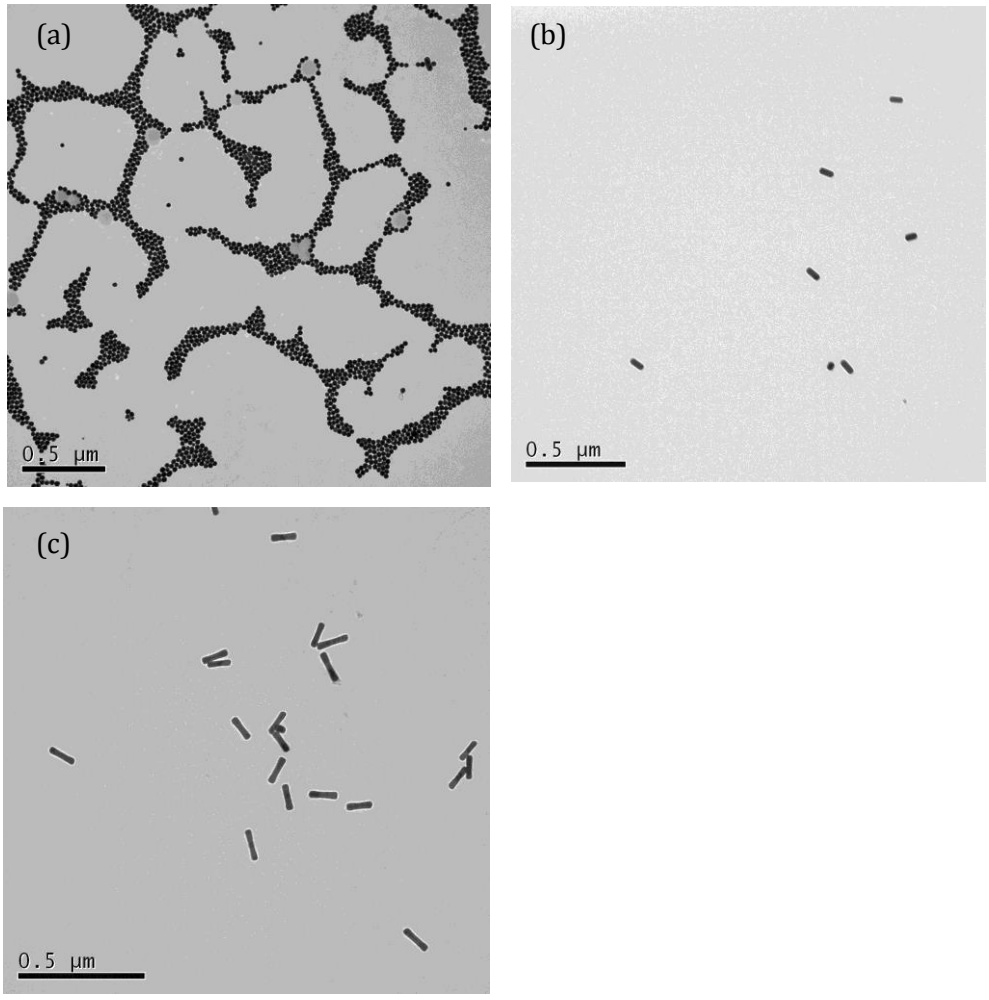

Figure 4.3 TEM images of (a) spherical, (b) short rod and; (c) long rod negatively charged Au NMs in DI water.

TEM images were taken of spherical, short rod and long rod negatively charged NMs to gain an understanding of shape and size. Positively charged NMs will have identical cores to the negatively charged NMs so that it was not necessary to image.

4.2.2 Effect of different shaped and charged Au NMs on *D. magna* survival

D. magna were exposed to a range of mass concentrations of Au NMs in order to assess survivorship, as shown in figure 4.4. It was observed that positively charged NMs, regardless of shape, were up to three orders of magnitude more toxic compared to negatively charged NMs with respect to mass concentration, as seen in figure 4.4 (a). The EC_{50} for positively charged spheres and short rods were 0.0061 and 0.018 μg/mL respectively indicating that positively charged spheres are more toxic compared to positively charged short rods with respect to mass concentration. Differences in mortality between positively charged spheres and short rods were statistically significant at concentrations between 0.005 and 0.01 μg/mL with $p < 0.01$ and 0.001, respectively, as determined by a Students t-test. The high toxicity of positively charged NMs can be attributed to the positive charge on the NM being attracted to the negative charge on the phospholipid membrane of organisms, increasing their interaction compared to negatively charged NMs (Bozich et al., 2014). A similar trend can be observed with negatively charged Au NMs (figure 4.4 (b)) where toxicity decreases as NM size increases, where spheres appear to be most toxic, followed by short rods and then by longer rods although there is no EC_{50} value even at concentrations as high as 50 μg/mL indicating the much lower toxicity of negatively charged NMs, though not detracting from the fact that smaller sized NMs appear to be more toxic with respect to mass concentration. Negatively charged spheres were not significantly different in toxicity compared to negatively charged short rods, though were statistically significantly different in toxicity compared to negatively charged long rods at 10 and 50 μg/mL with $p < 0.05$ and 0.01, respectively.

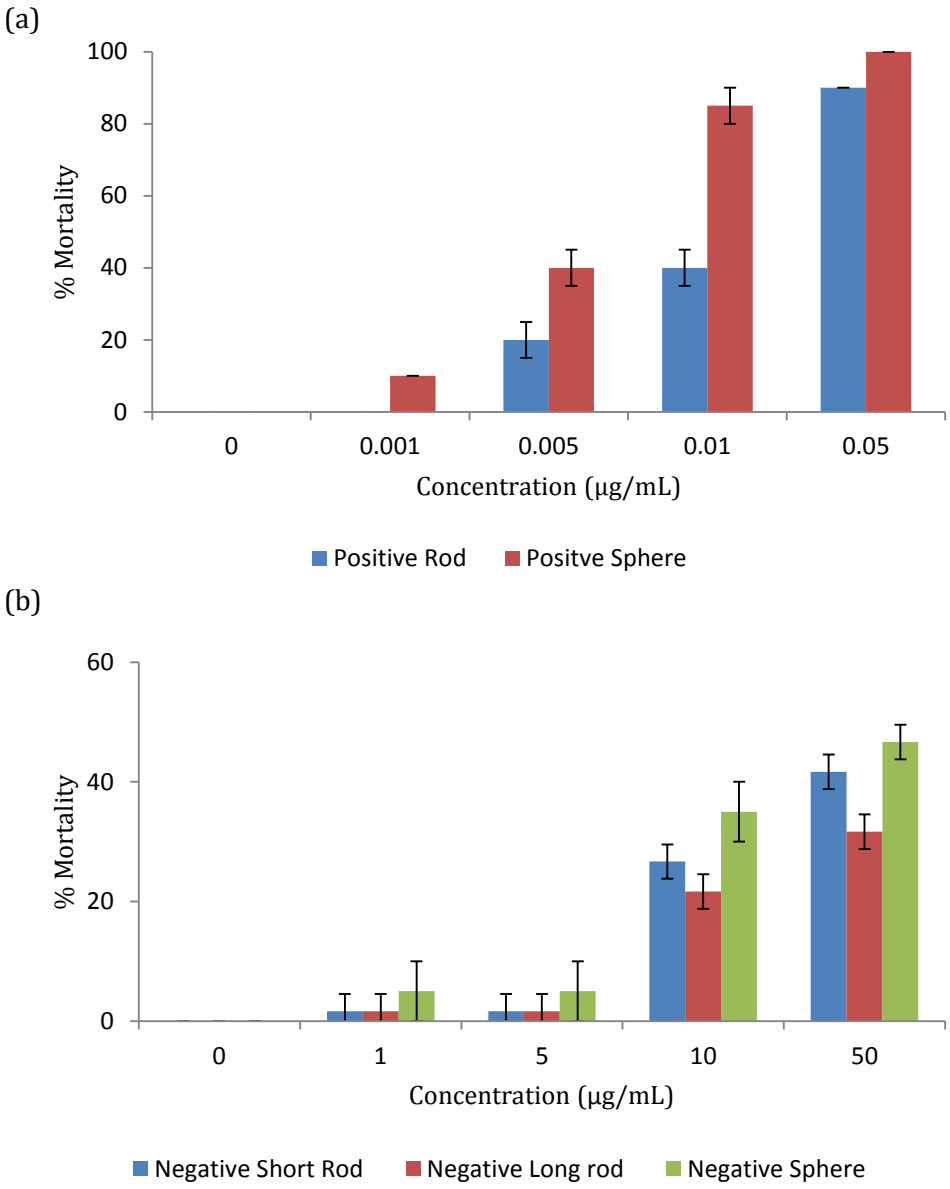

Figure 4.4 Mass concentration based survival curves of *D. magna* neonates exposed to (a) positively charged and (b) negatively charged Au spherical, short rod and long rod Au NMs.

Particle number concentration is an important comparison basis to consider for dose-metrics of NMs, where mass concentration is not an optimal comparison, especially when considering NMs of different sizes and shapes, as larger NMs will occupy more room in the same volume as smaller NMs and the numbers of particles can differ by orders of magnitude at the same mass. Toxicity of NMs is not always size dependent and NM number or surface area exposure have been demonstrated as more optimal choices for NM comparison (Huk et al., 2014). Au NMs of various number concentrations were exposed to *D. magna* neonates and as expected,

regardless of the dose-metric used, positively charged NMs were three orders of magnitude more toxic than negatively charged NMs. Interestingly, with respect to number concentration, long rods were found to be most toxic, followed by short rods and finally spheres, as seen in figure 4.5 (a) and (b) for both positively and negatively charged NMs, respectively.

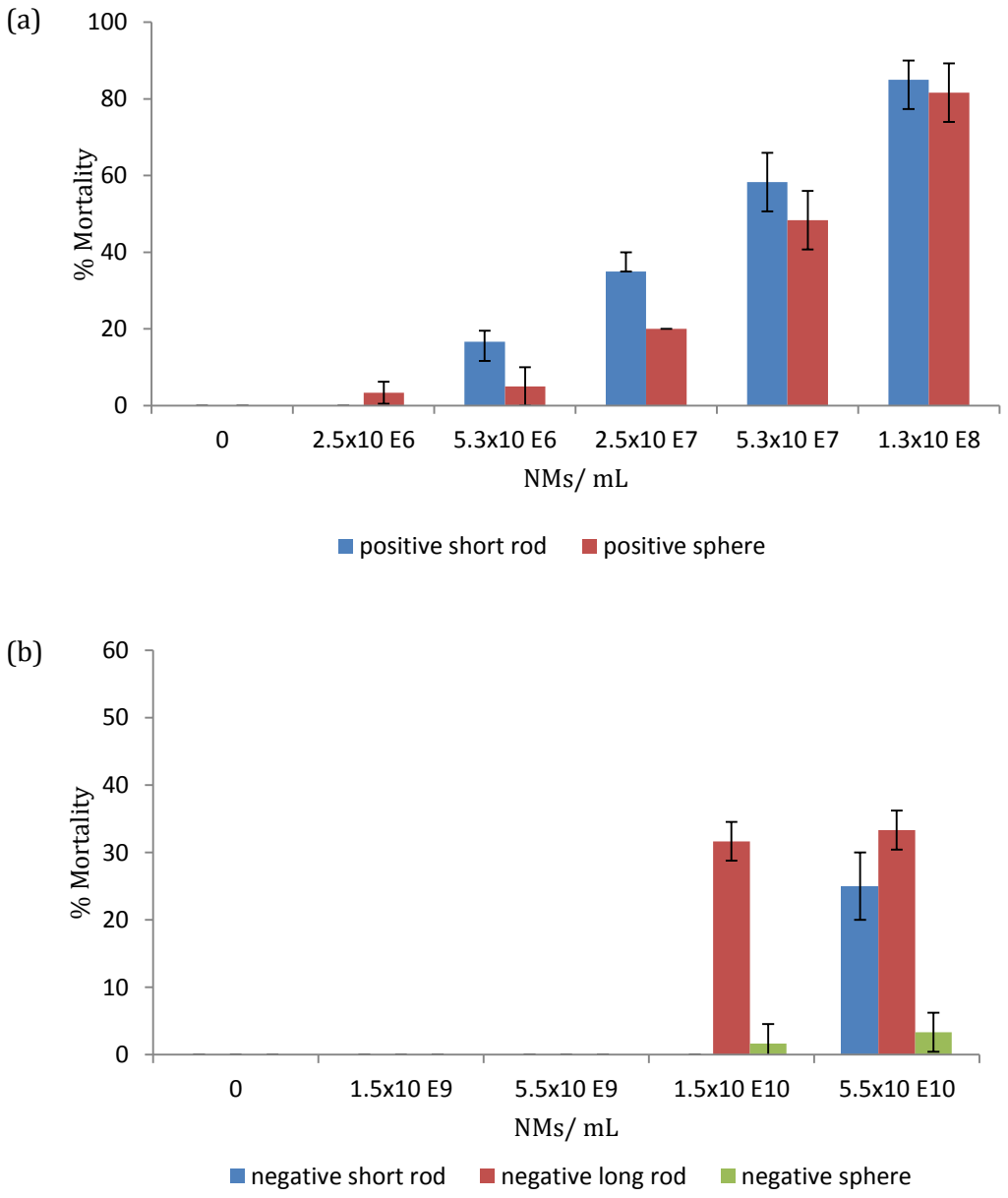

Figure 4.5 Number concentration based survival curves of *D. magna* neonates exposed to (a) negatively charged and (b) positively charged of spherical, short rod, and long rod shaped Au NMs.

When considering number concentration, which is a more comparable unit compared to mass concentration, there is a different trend in regards to the effect of NM size on toxicity. This is because when exposing *D. magna* to the same mass concentration of different sized NMs, a different particle number was being exposed. For example at a mass concentration of 1 μg/mL, 1.052 x 10^{10} NMs/mL of spherical, 2.76 x10^{9} NMs/mL short rod and 1.12 x10^{9} NMs/mL of long rod negatively charged Au NMs were actually being exposed, so that a much higher particle number of smaller NMs were being exposed to *D. magna* at the same mass concentration causing smaller NMs to appear to have a higher toxicity, with the toxicity ranking in mass concentration being spheres > short rods > long rods.

Spherical and short rod shaped NMs that were exposed to neonates at the same number concentration have a different amount of surface area exposed to *D. magna* depending on the type of NM. This can explain why positively charged short rods appear to be more toxic than positively charged spheres as they have a larger surface area available for interaction (5,694 nm^2) compared to spheres (1,963 nm^2) as can be identified in table 4.1. Though a different mass concentration is being exposed when using number concentration (for example, 1.5 x10^{9} NMs/mL equates to 0.143 μg/mL of spheres; 0.53 μg/mL of short rod and 1.34 μg/mL of long rod Au NMs), this is still a more reliable and comparable unit as the same number of NMs exist within sample for a more comparable exposure and assessment of the relative toxicity. The EC_{50} values for the positively charged NMs for spheres and short rods with respect to number concentration are 5.69 x10^{7} NMs/mL and 4.30 x10^{7} NMs/mL respectively, indicating that rods were more toxic due to having more available surface area per particle for interaction. For negatively charged NMs, there was no EC_{50} concentration even at exposures as high as 5.5 x10^{10} NMs/mL which corresponded to 20 μg/mL (short rod), 50 μg/mL (long rod) and 5.2 μg/mL (sphere) none of which none caused an EC_{50} when exposed as mass concentration, as previously seen in figure 4.4 (b).

Table 4.1. Summary of surface areas and other dimensional properties of each of the different Au NM shapes (values apply to both positive and negatively charged NMs).

	Radius (nm)	Length (nm)	Surface Area (nm^2)	Volume (nm^3)	SA/V ratio
Sphere	12.5	-	1,963	8,181	0.239946
Short Rod	12.5	60	5,694	29,452	0.193332
Long Rod	12.5	146	12,448	71,667	0.173692

When calculating number concentration, the mass and number concentration of the stock was used to calculate the number concentration of the working stock which can be seen in table 4.2, which was then used to calculate the number concentration in each exposure.

Table 4.2 Conversions of mass concentration of NMs to number concentration of working stock (50 µg/mL).

	Number concentration of stock (NMs/mL)	Mass concentration of stock (mg/mL)	Number concentration of 50 µg/mL working stock (NMs/mL)
Negative Short Rod	6.9×10^{12}	2.5	1.38×10^{11}
Negative Long Rod	2.8×10^{12}	2.5	5.6×10^{10}
Negative Sphere	2.63×10^{13}	2.5	5.26×10^{11}
Positive Short Rod	6.9×10^{12}	2.5	1.38×10^{11}
Positive Sphere	2.67×10^{13}	2.5	5.34×10^{11}

Toxicity of NMs may also depend on their ability to agglomerate as *D. magna* are more prone to taking up larger entities compared to smaller ones. It was determined that NMs remained stable in HH Combo medium for 24 hours with no statistically significant change in zeta-potential values which is an indication of stability over time as shown in table 4.3.

Table 4.3. Zeta potential for various charged and shaped Au NMs dispersed in fresh HH Combo medium indicating no significant agglomeration over 24 hours.

NM type	Zeta potential at 0 hours (mV)	Zeta potential at 24 hours (mV)	Statistical Significance of size change
Negative sphere	-27.6	-28.4	None
Negative short rod	-25.0	-25.4	None
Negative long rod	-12.4	-15.5	None
Positive sphere	+20.4	+20.7	None
Positive short rod	+27.2	+26.9	None

The zeta-potential measurements indicate that the NMs remain stable over time in HH Combo medium. Slight polydispersity can be due to the high ionic strength from the salts within the HH Combo medium though previous DLS data indicates a fairly low PDI showing relatively stable NMs with no additional agglomeration over time.

Though an increased surface area could explain an increase in toxicity, this would only hold true if the charge per surface area on each of the NMs types were the same and therefore charge per surface area must also be taken into account to verify the potency of the NM toxicity.

Considering that all the tested NMs are of different sizes and shapes, a different amount of surface area is being exposed to *D. magna* depending on the type of NM. A series of titrations were conducted using 0.01 mM KCl to neutralize the charge on the Au NMs in order to determine how many moles of KCl was needed to neutralize the same amount of moles of Au NMs. It was determined that 270 µL and 430 µL of 0.01 mM KCl was needed to neutralize the charges on positively charged spheres and positively charged short rods respectively, as can be seen in figure 4.6 which corresponds to 2 positive charges/nm^2 on spheres and 3 positive charges /nm^2 on short rods.

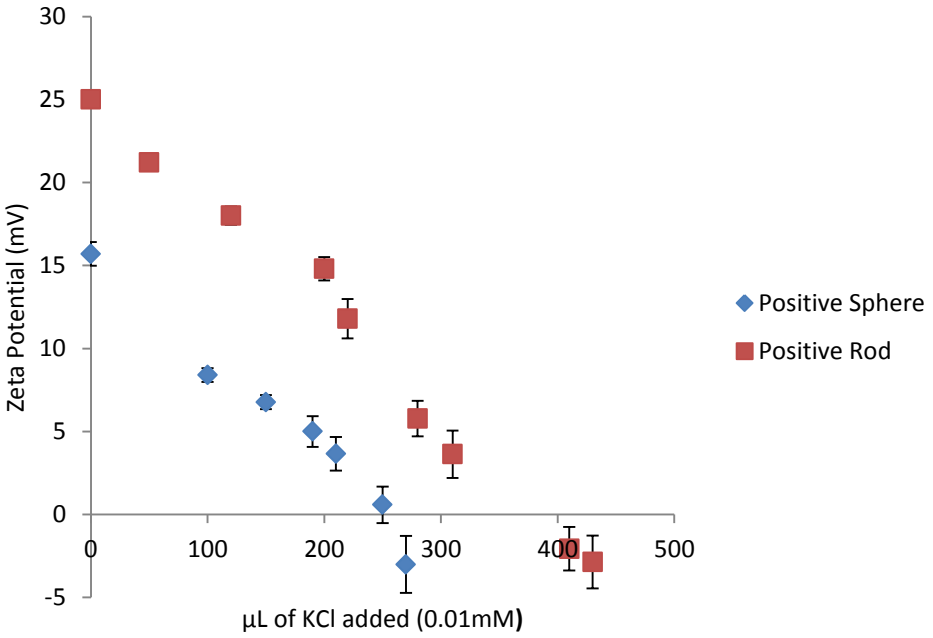

Figure 4.6 Titration of 0.01 mM KCl into 5 µg/L positively charged spherical and short rod Au NMs and subsequent change in zeta-potential.

A sample calculation for charge per surface area is shown below for positively charged spheres:

$$\frac{5.34\ x\ 10^{7} \times NPs}{mL}\ x\ 50mL = 2.67\ \times 10^{9}\ \text{particles in 50 mL}$$

$$2.67\ \times 10^{9}\ NMs\ x\ 1963\ nm^{2*} = 5.24\ \times\ 10^{12}\ nm^{2}\ total\ SA$$

*surface area calculated from the diameter of the NM

Total charges = unknown.

$$5\ \frac{\mu g}{L} = 5 \times 10^{-6}\ \frac{g}{L}$$

$$D = \frac{m}{V};\ m = DV\ \ m = \left(5\ \times\ 10^{-6}\frac{g}{L}\right) \times 0.05\ L = 2.5\ \times 10^{-7} g$$

n= $\frac{m}{M} = \frac{2.5 \times 10^{-7} g}{197\ g/mol} = 1.296 \times 10^{-9} mol\ of\ gold$

c= $\frac{n}{V}$; n= CV n= $(0.00001M) \times (250 \times 10^{-6} L) = 2.5 \times 10^{-9} mol\ KCl\ used$

$$\frac{2.5 \times 10^{-9}\ mol\ KCl}{1.295 \times 10^{-9}\ Gold} = 1.98 \sim 2$$

$$\frac{Total\ Charge}{Total\ SA} = \frac{(5.24 \times 10^{12}\ nm^2) \times 2}{5.24 \times 10^{12}\ nm^2} = 2\ charges/nm^2$$

where m is mass of particles, D is density of particle, M is molar mass of KOH etc.

Analysis of the charge per surface area can begin to explain the toxicity effects of positively charged NMs on *D. magna* as short rods have a much higher surface area compared to spheres, as well as a higher number of positive charges per nm^2 compared to spheres, which in turn provides a substantially higher amount of overall positive charge to be available to interact with *D. magna*. Therefore positive short rods appear to have a dual toxic effect of a larger surface area and a higher charge to surface area ratio compared to the positive spheres. It was determined for negatively charged long rods, short rods and spheres, that the charge per surface area corresponded to 2, 2, and 3 charges/ nm^2 as seen in figure 4.7.

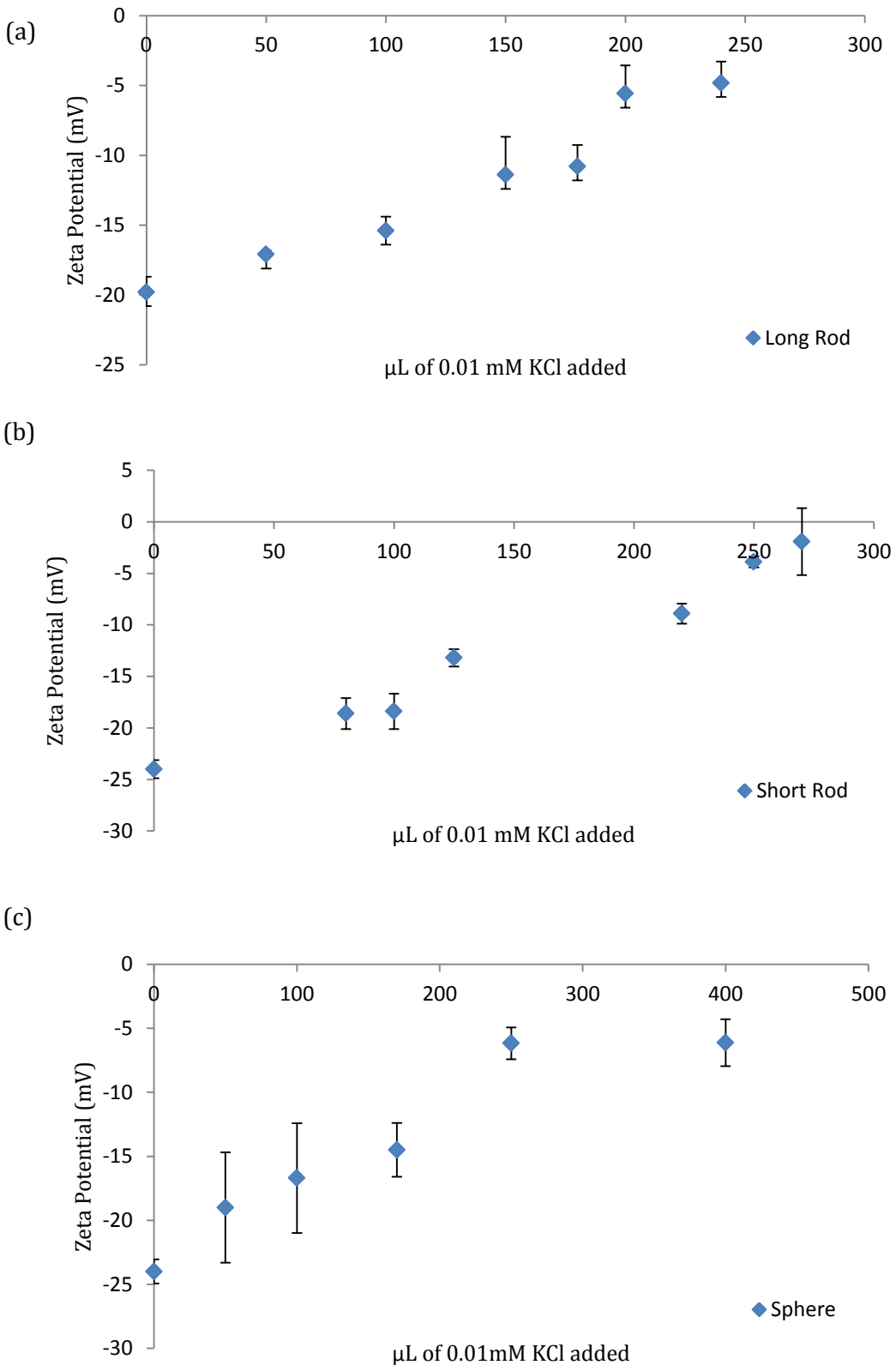

Figure 4.7 Titration of 0.01 mM KCl into 5 µg/L negatively charged (a) short rod, (b) long rod, and (c) spherical Au NMs and subsequent change in zeta-potential.

When considering number concentration, it can be concluded that positively charged Au NMs are considerably more toxic than negatively charged NMs. To summarize, positively charged short rods are more toxic than spheres due to the increased available surface area and the added toxicity added by having a greater number of positive charges per nm^2. For negatively charged NMs there is a similar trend with respect to size where long rods are the most toxic, followed by short rods and then spheres, though regardless of the number of charges all negatively charged Au NMs are still significantly less toxic than positively charged Au NMs. A summary of charge per surface area and toxicity can be seen in table 4.4.

Table 4.4. Summary of charge per surface area of each of the different shaped and charged Au NMs and their corresponding total charge and toxicity ranking based on number concentration EC_{50} values.

NM type	Charge per Surface Area (charge/nm^2)	Total charge per NM (charge/NM)	Ranking of Toxicity based on EC_{50}
Positive Short Rod	3	17,082	1
Positive Sphere	2	3,926	2
Negative Long Rod	2	24,896	3
Negative Short Rod	2	11,388	4
Negative Sphere	3	5,889	5

Interestingly, the manufacturers' specifications indicated that all NMs regardless of shape or charge have 2 charges per nm^2 although results show that this was not true for at least two of the NMs tested. This brings to light the importance of characterization of NMs before testing as there is likely to be batch-to-batch variation amongst manufactured samples which can lead to a substantial difference in terms of toxicity.

Confocal imaging was used to confirm the localisation of the ingested NMs within the gut of *D. magna* as shown in Figure 4.8. In the confocal images in Figure 4.8, NMs do not appear to

translocate any further than the gut, illustrating its effectiveness as a barrier. Fluorescence was added via conjugation of a fluorescent tag to approximately 50% of the $-NH_2$ groups on the surface of the positively charged spherical NMs. Given that the NMs remain in the gut, lumen cells and microvilli along the bush border are exposed to NMs, and the observed toxicity could be due to selective interaction of NMs with intracellular organelles (mitochondria or DNA) of lumen cells and microvilli.

As Au NM are inherently reflectant, use of reflectance confocal microscopy as a means to quantify uptake and localisation was also attempted. However, *D. magna* tend to consume their shed carapace (in the absence of more attractive food sources) and the keratin protein that constitutes the carapace is itself highly reflectant, such that control organisms that were not exposed to any Au NMs were also showing reflectance within the gut and could not be differentiated from the reflectance given by the NMs, which is why fluorescence was used as a more optimal method.

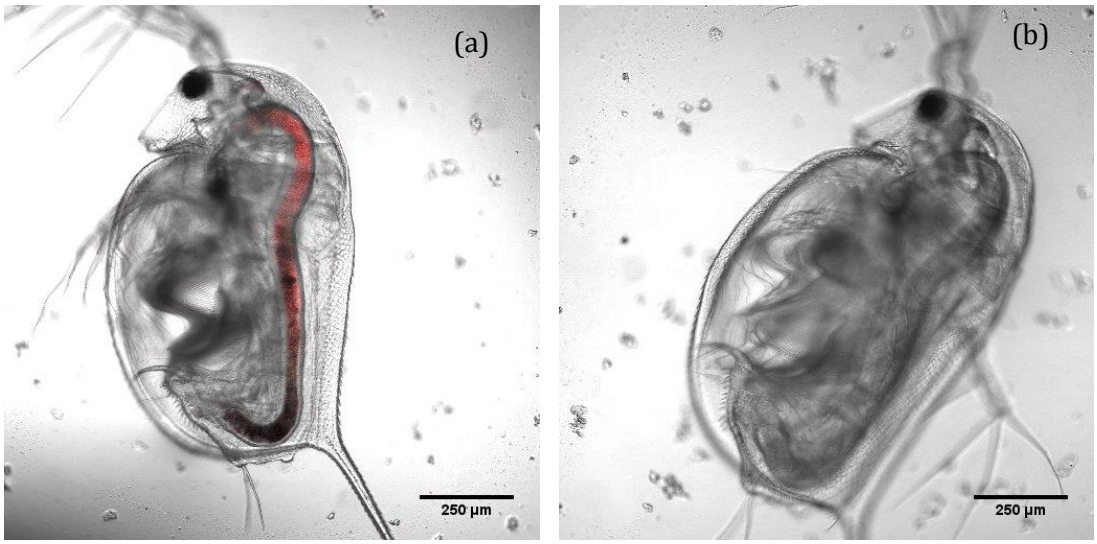

Figure 4.8 Fluorescent confocal image of *D. magna* neonate retaining NH_2-Au spherical NMs conjugated with RhB-ITC (a) and control (b) with n=3.

4.2.3 Effect of charge and surface area on ROS production in *D. magna*

It was determined that regardless of their shape or charge Au NMs influence *D. magna* survival and therefore an analysis of the toxicity mechanism was performed. It is widely recorded that *D. magna* produce ROS as an indicator of stress (Barata et al., 2005). The production of ROS within organisms is an excellent indicator of stress at a biochemical level and can take the form of superoxide anion radical, hydrogen peroxide and hydroxyl radical, each of which are known to be produced by *D. magna* (Barata et al., 2005). The mechanism(s) for formation of these ROS were detailed in section 1.5.3.1. As seen in figure 4.9 (a) negatively charged Au spheres prompted minimal ROS production in *D. magna* exposed to either high (EC_{10}) or low (EC_3) number concentrations, while positively charged Au NMs (spherical and short rods) prompted significant ROS production in *D. magna* exposed to either high (EC_{40}) or low (EC_5) number concentrations, as shown in figure 4.9 (b) and (c) for spheres and rods respectively. This is complementary to the survivorship results, as negatively charged Au NMs were shown to be substantially less toxic compared to positively charged Au NMs.

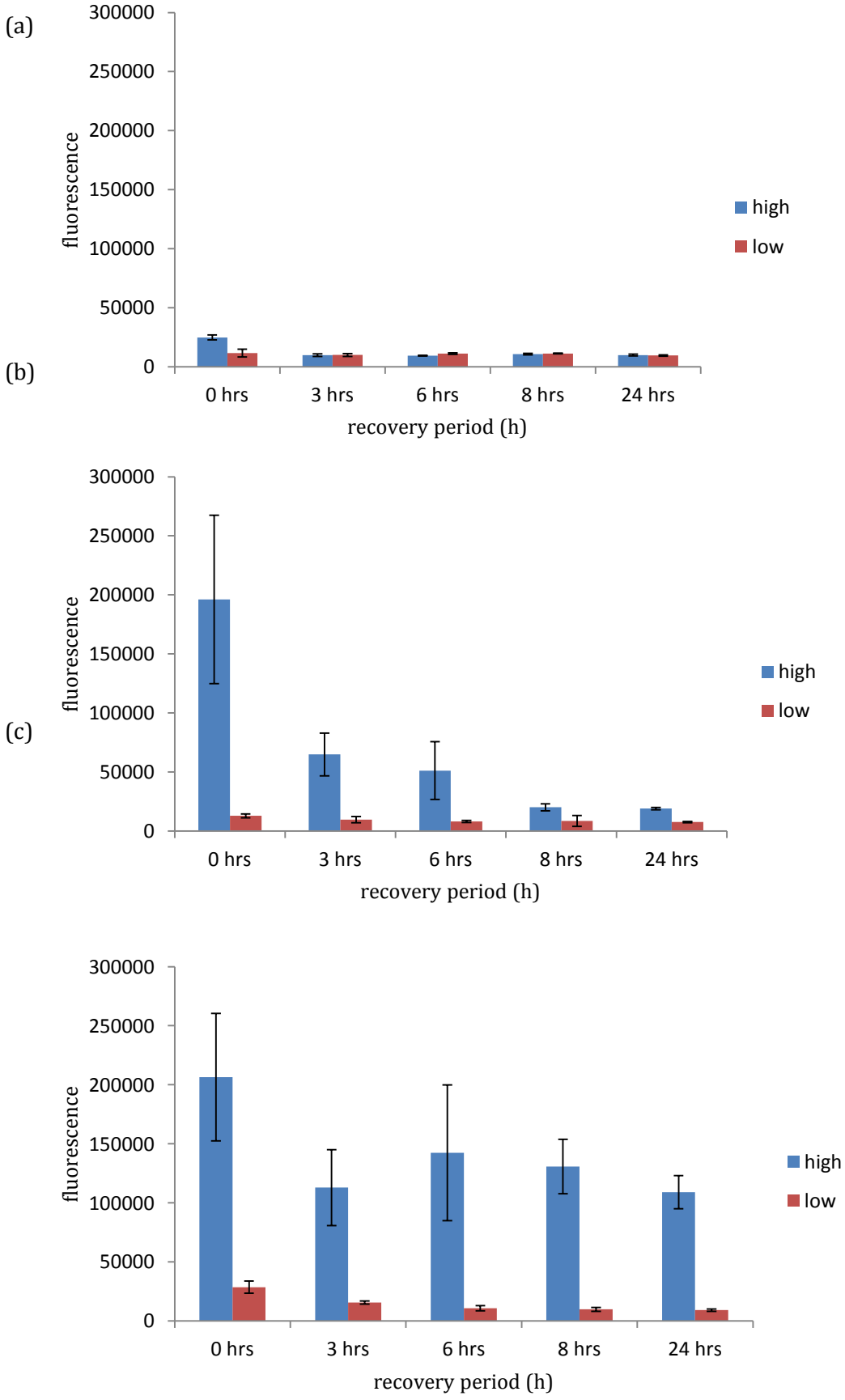

Figure 4.9 Reactive oxygen species generation and recovery (0-24 hours) in response to high and low number concentration exposures to (a) negatively charged Au spheres, (b) positively charged Au spheres and (c) positively charged short Au rods.

As shown in figure 4.9 (b), positively charged spheres prompt a high degree of ROS generation (determined immediately after the exposure period, at 0 hours recovery) at the high exposure dose although the accumulated ROS is reduced by approximately 65% within the first three hours of the recovery period and reaches steady state levels (approximately 10% of the initial ROS concentration) after 8 hours of recovery (insignificant t- test $p > 0.05$)This is in line with survivorship results as high concentrations of positive spherical Au NMs can cause a high generation of ROS where coping mechanisms are not able to fully overcome the ROS produced, resulting in increased *D. magna* mortality. ROS generated by positive and negatively charged spheres when exposed to high and low concentrations of NMs are significantly different at 0 h recovery (significant Students t-test $p < 0.05$ and $p < 0.001$ respectively) and statistically significant at low exposure concentrations at 24 hour recovery ($p < 0.05$). Positively charged rods also prompt a high degree of ROS generation of a similar level to positive spheres (insignificant difference between ROS generation at 0 h) showing that both types of positively charged Au NMs trigger similar levels of ROS, although *D. magna* coping mechanisms appear to be unable to fully recover from the stress in this case, unlike with positively charged spheres. This inability to recover could be attributed to rods having an increased surface area as well as a higher surface area to charge ratio, thus causing them to induce a higher degree of toxicity or ROS activation, as seen in figure 4.9 (c). It was observed that *D. magna* were unable to successfully remove accumulated ROS even after a 24 hour recovery period when exposed to high Au positive rod concentrations, as demonstrated by *D. magna* only able to remove approximately half of the accumulated ROS during the 24 hours of recovery. This can be due to decreasing levels of anti-oxidant enzymes and reduced anti-buffering capacity where there is insufficient enzyme available to handle ROS production, and therefore a ROS spike occurs at 8 hours into the recovery post exposure. This prompts the *de novo* synthesis of anti-oxidant enzymes to handle the excess ROS, and can be seen as ROS levels start to decrease again. Of course, the production or ROS is not the only factor influencing NM toxicity, whereby both ROS and high toxicity could correlate with

cellular stress, with damage to the mitochondria potentially causing a decrease in cellular respiration and ATP depletion. Cellular stress caused by damage to DNA can result in cells undergoing unregulated necrotic cell death. Upon exposure to cellular stress, homeostasis between net growth and death is altered, whereupon cells may employ a protective cellular response. However, if cellular stress is too high this will result in the activation of cell death pathways (Fulda et al., 2010) with ROS functioning at all stages of this process, either as an initiating event or as a symptom of cellular stress.

4.2.4 Formation of protein-corona around Au NMs from proteins secreted by *D. magna*

Proteins released by *D. magna* have the ability to adsorb to NM surfaces and it is crucial to understand the impact of these proteins on the surface properties of the NM and any subsequent stabilization or destabilization of the NM, as this can influence uptake and toxicity. Negative sphere, short rod and long rod Au NMs were incubated in HH Combo medium that had been previously conditioned for 6 hours by *D. magna* and the size of the NMs were monitored at various incubation times (0, 3, 6 and 8 hours) by DCS. Negatively charged Au NMs were chosen in order to use a range of NM sizes (as positively charged NMs only would provide two sizes) to obtain an understanding of the effect of shape on NM stability. It was determined that the proteins present in the HH Combo medium caused significant destabilization and agglomeration of spheres and short rods, causing an increase in size from 20.3 nm to 181.3 nm in spheres and from 33.3 nm to 156.9 nm in short rods, equivalent to a nine and five-fold increase in size respectively, as seen in figure 4.10. Long rods were able to remain somewhat stable over the incubation period.

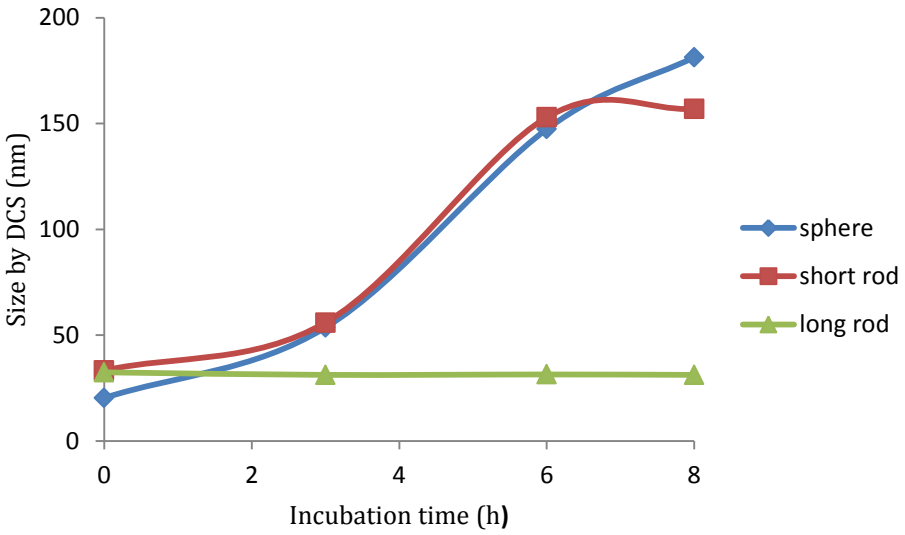

Figure 4.10 DCS monitoring of change in size of different shaped Au NMs incubated for various times in 3 hour *D. magna* conditioned media.

These NMs have shown to be stable in non-conditioned media, as shown previously in table 4.3, so that the presence of secreted proteins appears to have a destabilizing effect on smaller sized spheres and short rods. Long rods, however were able to remain consistently stable over the various conditioning times. Other studies have indicated that NM shape can influence it's interaction with proteins as well as agglomeration (Lundqvist et al., 2008) and it has been determined that smaller 15 nm gold NMs have the propensity to agglomerate faster and to a greater degree compared to larger 90 nm NMs in cell conditioned medium (Albanese et al., 2014) which is consistent with present results. This can be related to our results as it indicates that proteins in conditioned media can influence NM stability suggesting that conditioning and proteins present in the medium is responsible for agglomeration and that NM size, shape and surface chemistry as well as conditioning time are all factors that impact agglomeration, as each type of NM was able to remain stable for 24 hours when incubated in unconditioned fresh HH Combo medium, with no change in zeta potential as previously shown in table 4.4, which confirms that incubation of NMs in medium containing secreted proteins stabilizes (for long rods) or destabilizes (for spheres and short rods) Au NMs.

Interestingly, it was found that conditioning of medium by *D. magna* and incubation of various sized Au NMs had a great influence on NM toxicity. As previously seen, positively charged spheres at the 'high' EC_{40} concentration prompted a high generation of ROS at 0 hour recovery though *D. magna* coping mechanisms were able to effectively reduce the amount of ROS to steady state levels within 8 hours. By contrast, *D. magna* exposed to positively charged spheres that had been incubated in conditioned media did not even reach the recovery phase, whereby within 8 hours of the exposure period, 90% of the daphnia had died and thus recovery data is absent in figure 4.11 for positively charged spheres. The incubation of spherical Au NMs in conditioned media causes agglomeration and an increase in size of the NMs which are closer to that of a natural food source for *D. magna,* possibly leading to an increase in their uptake by *D. magna*. This increased uptake appears to cause accumulation of the NMs within *D. magna* resulting in increased toxicity and mortality in as little as 8 hours exposure (i.e., substantial death occurred before the end of the 24-hour exposure period where only 40% of the organisms exposed in the absence of the corona had died, hence the EC_{40} concentration).

Positive rods that had been incubated in conditioned media appear to have the same toxicity as those that had not been conditioned and generate similar amounts of ROS as the non-conditioned NMs, as can be seen in figure 4.11. Though it may appear that positively charged rods prompt less ROS when incubated in conditioned HH Combo medium compared to unconditioned medium, as seen by the lower y-axis values compared to previous results in figure 4.9 (c), the decrease in fluorescence is statistically insignificant as verified by t-test ($p > 0.05$).

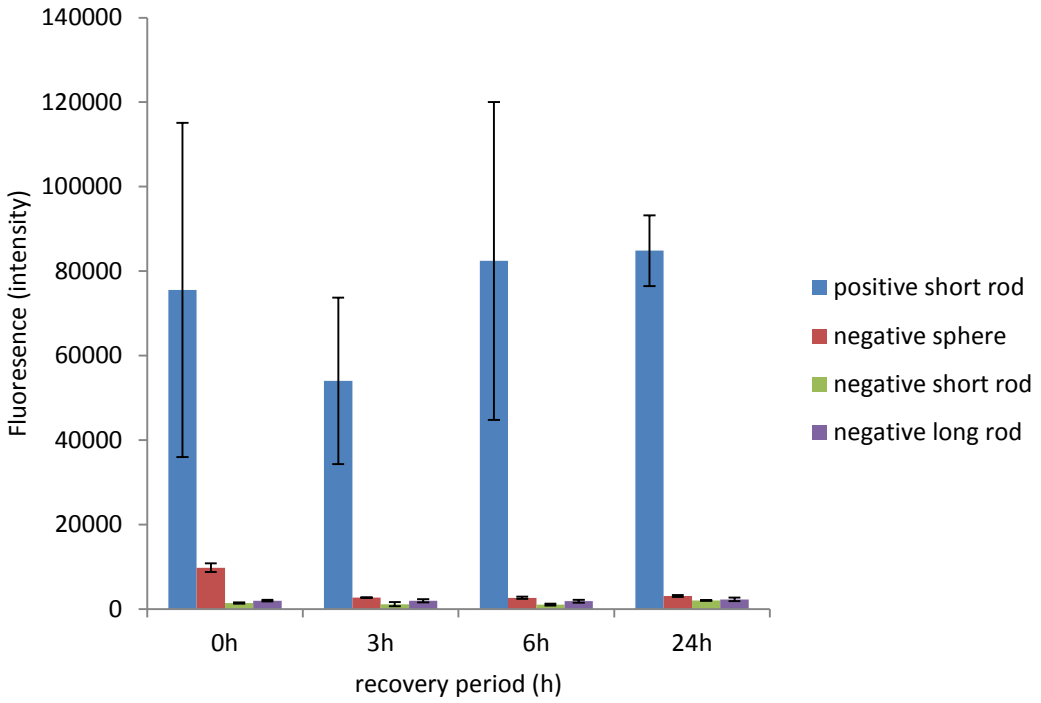

Figure 4.11 ROS formation prompted by exposure of *D. magna* to different shaped/charged Au NMs incubated in conditioned HH Combo medium. Positive spheres are absent from the figure as *D. magna* exposed to these did not survive the exposure period and thus no recovery period was possible.

NMs that were incubated in conditioned 24 hour HH Combo medium had acquired a protein corona which had either stabilizing or destabilizing effects depending on the size and shape of the NM. The hard corona was isolated using a corona isolation method and PAGE analysis was conducted using Coomassie and silver stains which showed bands between 30-150 kDa indicating the presence of proteins on the NM surfaces, as shown in figure 4.12 and confirming the formation of NM coronas in all cases (negative spheres, short and long rods).

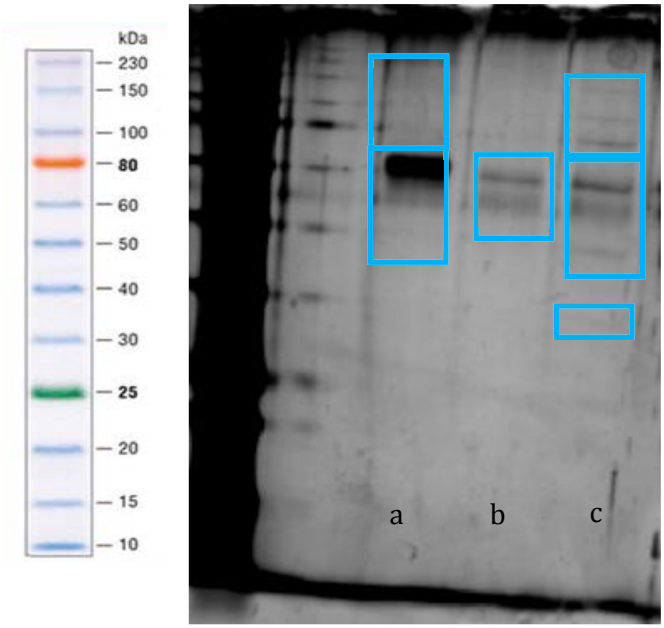

Figure 4.12 PAGE of proteins existing in the hard corona around negatively charged sphere (lane a); short rod (lane b) and; long rod (lane c). The first lane indicates the MW protein ladder. Blue boxes are a guide to the eye for visualisation of the bands to indicate the differences between the three differently sized NMs.

The proteins that comprise the hard-corona were present in the original 24 hour conditioned HH Combo medium. Mass spectrometry results indicate that a number of proteins are secreted within 24 hours, of which several range from 30-150 kDa, the most abundant of which are listed in table 4.5. The blue boxes in the gel highlight the various bands seen with the use of silver staining. Silver staining was needed in order to observe bands as the Coomassie stain used originally has a higher detection limit and therefore it was necessary to use silver stain (a much lower detection limit) though the use of silver staining (which includes formaldehyde in the development stage) rendered the excision of each individual band from the gel incompatible for mass spectrometry.

Table 4.5 List of most abundant proteins found in 24 hour conditioned HH Combo medium by *D. magna* neonates, between 30-150 kDa.

Description	Molecular Weight (kDa)
Actin	41.8
Arginine Kinase	39.9
2-phospho-D-glycerate hydrolase	39.6
Haemoglobin	38.2
Translational elongation factor	81.1
Elongation factor	39.7
Signal transduction histidine protein kinase	113.2
Phosphoenolpyruvate-protein phosphotransferase	82.9
Glucose-6-phosphate isomerase	49.1
TDP-N-acetylfucosamine:lipid II N-acetylfucosaminyltransferase	40.8
Homoserine O-succinyltransferase	35.5
Methionine synthase	136.0

Proteins from the conditioned medium secreted by *D. magna* are those that may be bound to the different NM types to create the bands seen in the gel (figure 4.12). All three types of NM shapes have bands present between 60-80 kDa which may be representative of proteins such as translation elongation factor (81.1 kDa) or Phosphoenolpyruvate-protein phosphotransferase (82.9) which can be common proteins comprising each hard corona around each NM type. Unique bands include those of low molecular weight around 30 kDa around long rods which can be Homoserine O-succinyltransferase (35.5 kDa) which may aid their size stabilization. Bands of larger molecular weight around spheres or long rods may be represented by proteins such as methionine synthase (136 kDa) or Signal transduction histidine protein kinase (113.2 kDa).

4.2.5 Effect of Au NMs on *D. magna* moulting

When *D. magna* neonates were exposed to positively charged Au NMs at concentrations as low as an EC_5, frequently neonates would appear to halt in mid-swim, an effect which was also observed during exposure to PS NMs as discussed in chapter 3, section 3.3.6. *D. magna* quickly returned to their natural swimming pattern, which prompted the question of whether NMs were adhering to the surface of *D. magna* and if this was affecting the shedding of the carapace, thereby hindering further development of the organisms. Although it was shown in Chapter 3 that positively charged PS NMs (including those that had been incubated in conditioned medium) did not in fact inhibit or increase moulting, those particles were inherently non-toxic as evidenced by their high EC_{50} values (0.0258 mg/mL for 100 nm PS-NH_2 compared to 0.0061 μg/mL for positively charged Au spheres and 0.018 μg/mL for positively charged rods. Note: EC_{50} values for gold are given as mass concentration for ease of comparison to PS). Given the much more significant toxicity in the case of the Au NMs, it is important not to make generalized hypotheses including all types of NMs, and thus it was separately assessed whether Au NMs impact on moulting ability of *D. magna*. Here, the impact of differently shaped Au NMs of the same charge on moulting is assessed. During the first moulting, which occurs approximately 24 hours after birth, *D. magna* shed their exoskeleton, and this is known to be a mechanism for removing metal pollutants, so it was postulated that any adhered Au NMs would also be shed. Results indicate that all living *D. magna* neonates that were exposed to positively charged Au NMs (regardless of shape) at a concentration of 5.3 x 10^6 NMs/mL (equating to EC_{15} for short rods and EC_5 for spheres) successfully complete the first round of moulting at 36 hours, as seen in figure 4.13. The concept of adsorption of NMs to organisms has been well established, as has the fact that the presence of environmental stressors induces difficulties in moulting (Coors et al., 2004). Coating of *D. magna by* NMs leads to NMs adhering to the filtering apparatus of *D. magna* confirmed by optical microscopy (Dabrunz et al., 2011a) resulting in an increased chance of uptake by filter feeding.

Results shown in figure 4.13 indicate that exposure to Au NMs plays a major role in the decrease of moulting ability *of D. magna*. The results clearly indicate that an 84 hour exposure to 5.3 x10^6 NMs/ mL of spherical and rod shaped Au NMs significantly reduces the success rate of a second moulting compared to 100% moulting success in the control group (**, $p< 0.01$ for spheres) and (**, $p< 0.01$ for short rods), as seen in figure 4.13. This indicates that positively charged spheres and rods induce the same degree of physical toxicity via moulting inhibition although they prompted different levels of chemical toxicity via ROS generation. The coating of the exoskeleton by Au NMs would increase both the weight and the physical stamina required by each neonate to shed the heavier carapace, which consequently increases the energy demand of each neonate. For neonates also struggling with high ROS levels, it was postulated that the required energy for moulting is unavailable due to the high demand for energy used in an attempt to remove accumulating ROS for neonates exposed to positively charged spheres or short rods. Further work is needed to confirm the adsorption of Au NMs to the carapace, e.g. via TEM imaging or inductively coupled plasma mass spectrometry (ICP-MS).

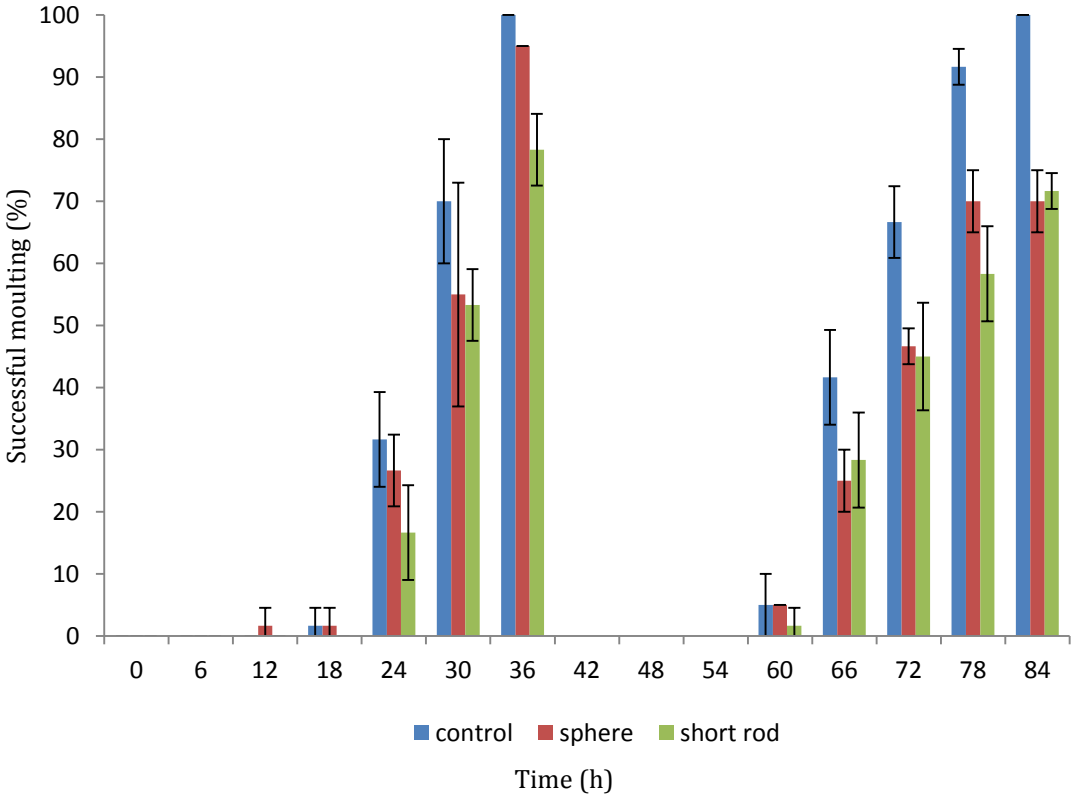

Figure 4.13. Moulting success of *D. magna* neonates (< 6 hours) exposed to 5.3 x10^6 NMs/mL of spherical and short rod Au NMs for 84 hours.

According to previous mortality results, at an exposure of 5.3 x10^6 NMs/mL, 5% (1 out of 20 neonates, actual percentage: 5 ± 5%) of *D. magna* exposed to positively charged spheres did not survive and approximately 15% (3 out of 20 neonates, actual percentage: 16.7 ± 2.9%) that were exposed to positively charged rods did not survive after 24 hours. All the rest of the living *D. magna* were able to successfully complete their first molting cycle which occurred at approximately 36 hours. During the elapsed time from 36 to 84 hours, another two neonates exposed to positively charged spheres did not survive and there was no additional mortality in neonates exposed to positively charged rods. At the end of the second moulting cycle at 84 hours, for *D. magna* that were exposed to positively charged spheres 15% (3 out of 20 did not survive after an 84 hour exposure - 1 in the first 24 hours of exposure and 2 in the remaining timespan). Out of the remaining 17, only 14 successfully completed their moulting cycle which equates to 82% moulting success of the living 17

neonates that were exposed, though 100% of the control group successfully completed their second moulting cycle and there was 100% survival. Similarly, after an 84 hour exposure to positively charged short rods, 15% (approximately 3 out of 20 did not survive, which all occurred in the first 24 hours) and out of the remaining 17, only 14 successfully completed their moulting cycle equating to 82% moulting success of the living neonates. In the previous chapter 3, when looking at the effect of positively charged bare PS NMs on moulting, an EC_{20} concentration still allowed for 100% moulting success for all living neonates with no delay in their second moulting cycle ($p > 0.05$). Contrastingly, the neonates that were exposed to positively charged Au NMs (both spheres and rods) which did not moult, did not eventually moult even after monitoring for an additional 24 hours which eventually resulted in their death. The inability of *D. magna* to moult combined with accumulated ROS generation resulted in *D. magn*a immobility and mortality. Interestingly, both positive rods and spheres induced similar degrees of physical toxicity though strikingly different levels of ROS generation (chemical toxicity) at identical particle numbers, so that the mechanism of toxicity is inflicted by both NM types though shape (or possibly more accurately the surface charge per nm^2) of the NM has a much higher effect on chemical toxicity once internalized, and thus the degree and mode of toxicity is shape dependent.

4.3 Summary and conclusions from Chapter 4

D. magna is a crucial indicator species to assess the toxicity of NMs due to its position in the fresh water system. The work presented in this chapter is paving the way to understanding and addressing this issue, focussing on the role of NM shape and surface charge and how these factors are important when assessing NM toxicity towards *D. magna* on a chemical (generation of ROS) and physical (effect on moulting) level. The chapter also takes note of exposure conditions where number concentration proves to be a more reliable method for comparison compared to mass concentration which gives strikingly different results. Surface charge density also plays a role, along with shape, as drivers of interaction with natural

biomolecules such as proteins existing in environmental waters which can affect toxicity. The work presented in this chapter is the first step to addressing this important area of work and conclusions have been reached in order to address each original objective, although more research is needed in places.

1. With respect to particle number concentration, which is a more accurate representation of dose-response, larger NMs were more toxic compared to smaller NMs with the order of toxicity ranking being long rods, short rods and finally spheres (for both positive and negative NMs), due to a larger available surface area to interact with *D. magna*. Also, positively charged NMs are orders of magnitude more toxic compared to negatively charged NMs regardless of number or mass concentration exposure.
2. Positively charged spheres at a high concentration prompted a large degree of ROS generation though *D. magna* was able to recover and return to steady-state levels. Interestingly, at a high concentration, positively charged short rods also prompted a large degree of ROS though *D. magna* were unable to fully recover from these levels resulting in a higher degree of toxicity induced by rods compared to spheres, which was consistent with mortality results. Low concentrations of positively charged NMs resulted in minimal levels of ROS generation and negatively charged spheres which were shown to be less toxic compared to positively charged NMs also prompted very low levels of ROS even when exposed at high concentrations.
3. Charge per surface area appeared to be an important modulator of toxicity along with shape and charge. For positively charged NMs, it was quantified that the larger short rods were more toxic than spheres due to not only having a larger surface area available for interaction but also a higher amount of positive charges per nm^2 of surface area compared to spheres. For negatively charged NMs, there was a larger charge per surface area on spheres compared to short or long rods though the larger

NMs still had a higher toxicity due to having a larger available surface area and more charge overall per NM.

4. Negatively charged spheres, short rods and long rods had various degrees of stability in conditioned HH combo medium where smaller NMs (spheres and short rods) quickly agglomerated and longer incubation times lead to a larger degree of agglomeration, though larger NMs (long rods) remained stable in conditioned medium. This coincides with toxicity results as agglomerated positively charged spheres resulting from incubation in conditioned medium resulted in a dramatic increase in mortality compared to those exposed to *D. magna* in unconditioned medium.
5. Both positively charged spheres and short rods, caused partial inhibition of moulting at the same particle number exposure, indicating that physical stress is a co-contributor to NM toxicity alongside chemical stress.

The results in this chapter indicate that both shape and charge are important factors in determining NM toxicity towards organisms and that these characteristics may be acting on an individual or a combined level to instigate chemical changes, such as oxidative stress, or physical changes such as moulting inhibition, which are key parameters in maintaining cellular balance and normal development in *D. magna.* The deposition of various shaped and charged NMs into environmental waters that contain secreted biomolecules such as proteins has the potential to cause physiological and developmental changes to *D. magna* that may not be picked up by traditional OECD tests which do not take into account the complexity of shape and morphology of NMs or how an adsorbed protein corona has the ability to influence agglomeration which can alter their uptake and toxicity. Thus, a comparison of NM on mass concentration exposure alone misses important subtleties resulting from non-equivalent surface areas and charge per surface areas. Assessing only mortality also misses important details such as the ability to recover from oxidative stress up to specific thresholds, or physical effects such as moulting inhibition.

5

Influence of presentation mode on uptake and release of differently sized polystyrene nanomaterials by *D. magna*

These results have been presented at **SETAC'17** as a spotlight poster presentation

A paper of the results from this chapter is in preparation bound for ES:Nano

5.1 Chapter synopsis

A substantial amount of research has been conducted on the applications of various types of NMs as discussed in chapter 1, although considerably less research has been done on investigating the implications of NMs on environmental organisms. Alongside the increase in use of NMs in industrial applications, there has also been an increase in the release of MPs resulting from the wearing of bulk plastic.

For the purpose of this thesis, we define presentation modes of NMs as how organisms are presented to NMs (e.g. via the water phase, via their food) and the factors associated with the presentation (e.g. parallel or pre/post feeding, and the presence or absence of a protein corona) which may influence the amount and form of the NMs taken up by the organisms. It is important to consider presentation mode of different sized PS NMs to organisms such as *D. magna* and to investigate how various natural environmental factors such as lack or presence of food at different times during the feeding cycle, fullness of the gut of *D. magna* or the presence of natural biomolecules such as proteins or carbohydrates secreted from organisms in aquatic systems, could potentially influence uptake and egestion of NMs from *D. magna. D. magna* consume food (or other entities) by filter feeding, and the uptake and excretion of the

consumed material is governed by several factors, which are highlighted in section 5.1.1. Figure 5.1 is a representation of the NM presentation modes investigated in this chapter.

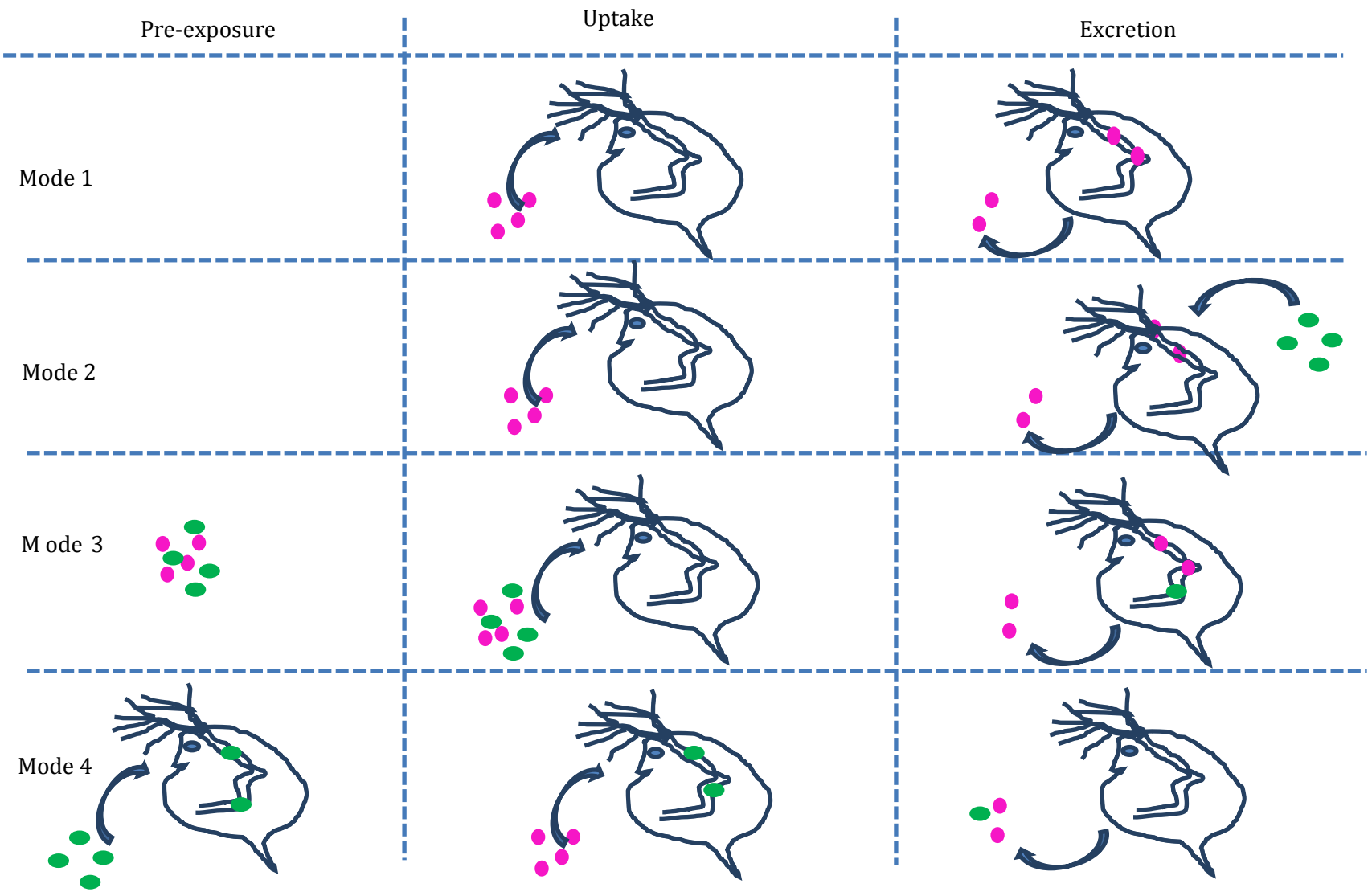

Figure 5.1 Schematic representation modes of NMs to *D. magna* used in this chapter represented by modes 1-4. Pink spheres represent PS NMs and green spheres represent algae *C. vulgaris.*

Given the range of factors that influence NM uptake, and retention, there is a need to systemically investigate /compare uptake via water or with the presence of food in order to understand important factors that influence uptake and excretion to help design more realistic exposure studies. This chapter looks at four different presentation modes of NMs towards *D. magna,* as seen in figure 5.1, and investigates how the absence/presence of food at different stages during feeding influences uptake and excretion. These presentation modes will be referred to as modes 1-4 throughout this chapter:

1. Mode 1- in medium with no feeding (standard OECD test);
2. Mode 2 - NMs presented in medium but with feeding during the excretion phase as would be normal in the environment;
3. Mode 3 - NMs presented in parallel with algal food source which is a more realistic exposure scenario;
4. Mode 4 - NMs presented in medium to pre-fed *D. magna.*

D. magna are a staple food source for a wide variety of higher trophic organisms so that NMs that are not fully excreted have the potential to be transferred to higher level organisms. Understanding how different naturally occurring factors can alter the residency time of PS NMs within *D. magna* will help to close the knowledge gap between deposition of NMs into environmental waters and their effect on organisms, which are factors that are not usually considered by standard testing procedures designed for molecular chemicals.

5.1.1 Introduction

There are several important factors that govern the uptake and depuration of NMs. Although *D. magna* are able to take up a wide range of particulate sizes, they selectively take up entities based on size and texture, often preferring entities closer in size to that of their natural food source and texture (MacMahon and Rigler, 1965) so that uptake is said to be size and consistency specific.

Peristalsis moves food through the gut but more importantly the pressure from newly ingested material pushes food through (Ebert, 2005), indicating that the presence of food in the local environment around *D. magna* is an important factor in the egestion of NMs that have been taken up.

The presence of food such as *C. vulgaris* can act as a contamination sink for NMs, which may adsorb to algal surfaces and therefore presence of algae may facilitate the unintentional uptake of NMs by *D. magna* when they consume algae (Kalman et al., 2015). Thus, the presence of food may consequently increase NM uptake although as noted above additional food also facilitates depuration. The rate of uptake has also been shown to be affected by the presence or absence of food already within the gut; for example, starved *D. magna* took up increased food compared to fed *D. magna* (MacMahon and Rigler, 1965) and therefore *D. magna* that have been consistently grazing on algae may have a decreased uptake of newly presented NMs. This chapter systematically investigates how these factors influence uptake and excretion of PS NMs as previously depicted in figure 5.1.

Many toxicological studies have shown that NMs are considerably more toxic compared to larger materials of similar composition, which has led to a commonly assumed hypothesis that smaller entities such as NMs with their larger surface area to volume ratio are more reactive and therefore are more toxic compared to their bulk counterparts (Karlsson et al., 2009). This is not completely correct to assume and there are several factors to be taken into account which are not widely addressed. One way NMs overcome their enhanced reactivity is to agglomerate by binding biomolecules so that NMs are not always available to organisms as individual NMs. The increased reactivity exhibited by NMs does not always translate to being more toxic as the correct NM size needs to be available in order to exert toxicity and this may be different for cells and between different organisms. Contrastingly, filter feeders are more likely to be able to selectively take up larger particles closer to that of their natural food source, indicating that correlating size of NMs with toxicity is dependent on several factors.

Due to the high surface free energy of NMs there is an increased tendency of NMs to adsorb biomolecules to their surface from biological environments (Lundqvist et al., 2011). There are various studies with opposing results on whether a protein corona increases or decreases NM toxicity, although likely this depends on the system (organism or cell) and NMs studied. It has been observed that NM cellular uptake in protein-free medium is higher compared to protein-rich medium (Patel et al., 2010) due to the adsorbed proteins decreasing the overall free-energy of the bound NM thus decreasing their reactivity and reducing the tendency of the NMs to damage cellular membranes which facilitates NMs entry. Due to the novelty of this field, the majority of current studies looking at the impact of protein corona's around NMs focus on cell lines *in vitro,* whereas there can be strikingly different results with whole organisms especially those that filter feed and take up particles based on size and textureThe influence of a food source at different time points during the feeding cycle is further investigated here via modes 2, 3 and 4.

5.1.2 Aims and Objectives

The aim of this chapter is to investigate the effect of presentation mode (directly via the water phase, or in parallel with food at different time points) on uptake and release of two different sized PS NMs (50 (PS-50) and 500 (PS-500) nm) under various feeding conditions (which are highlighted in figure 5.1 showing modes 1-4). This is achieved through the following objectives.

1. To assess the impact of various presentation modes (in only HH Combo medium with no feeding (mode 1); feeding only during release stage (mode 2); NMs incubated in the food source *C. vulgaris* (mode 3) and; *D. magna* having already fed (mode 4)) of different sized PS-50 and PS-500 NMs on the uptake and release by *D. magna* and to compare them to mode 1 which incorporates no additional factors and is representative of current OECD standard toxicity testing for *D. magna*.

2. To investigate the impact of conditioning and incubation time on the stability of different sized PS NMs.
3. To quantify the secretion of carbohydrates by *D. magna* to understand their role in the biomolecule corona and stabilisation of NMs.

5.2 Results and Discussion

5.2.1 Characterization of PS-500 and PS-50 polystyrene NMs

PS-500 and PS-50 NMs were characterized using various methods such as DLS, zeta-potential and TEM. DLS and zeta-potential measurements were taken in fresh HH Combo medium and TEM samples were dispersed in DI water in order to avoid drying effects from salts present in the medium. Table 5.1 indicates the characterization of size using the different methods.

Table 5.1 Characterization of PS-500 and PS-50 NMs by different techniques.

	PS-500		PS-50	
Technique	Value Average	SD (n=3)	Value Average	SD (n=3)
DLS	z-average: 515 nm *(PDI 0.097)*	20 nm	z-average: 51.8 nm *(PDI 0.062)*	0.75 nm
Zeta-potential	-19.7 mV	0.27	-19.8 mV	1.2
TEM	490 nm	15 nm	45 nm	7.5 nm

Characterization of PS-500 and PS-50 indicate that the hydrodynamic size (from DLS) is slightly larger than the core size (from TEM) due to the adsorbed layer of water around the NMs. The low PDI indicates that both types of NMs are stable and mono-disperse in HH Combo medium indicating that the salts present in the medium do not cause any

agglomeration and any agglomeration observed in subsequent experiments would be due to other factors, such as released biomolecules. Zeta potential results show that NMs are stable and also negatively charged due to the conjugated COOH groups on the NM surface. Representative DLS and TEM images can be seen in figure 5.2.

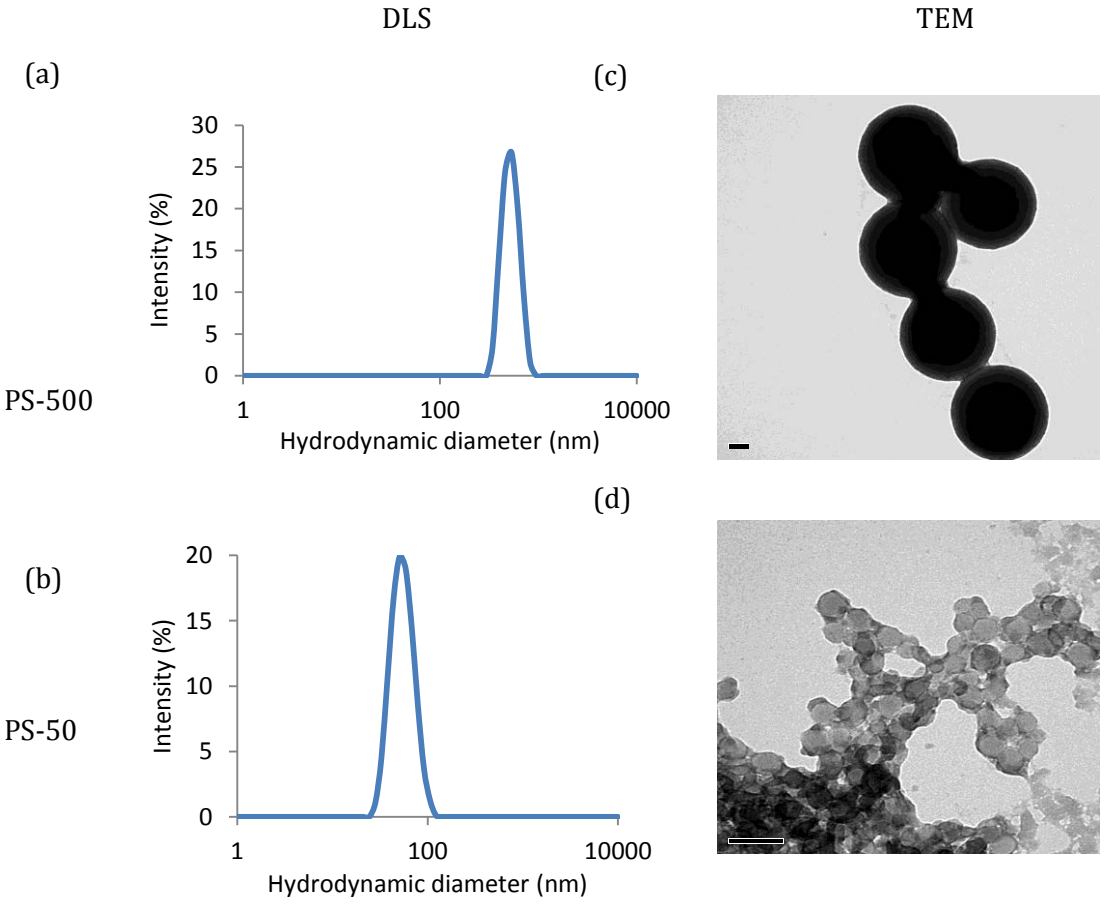

Figure 5.2 Characterization of PS-500 and PS-50 NMs by DLS (a and b) and TEM (c and d) (scale bar: 100 nm).

Table 5.2 below presents a summary of the various presentation modes of PS-500 and PS-50 towards *D. magna* and their corresponding percentages of NMs remaining within the gut at 1 and 6 hours of post-exposure, and the corresponding clearance based on the total uptake (fluorescence) after the 1 hour exposure. The table is intended a summary and provides a simplistic description as well as key highlights. A more detailed analysis of the presentation

modes, uptake, release and a comparison of these factors between the different sized NMs can be found in the subsequent sections 3.5.2.1 to 3.5.2.4.

Table 5.2 Comparison of uptake and release of PS-500 and PS-50 with different presentation modes

Presentation Method	Original NM Size in HH combo medium	Total fluorescence/ uptake (intensity)	Remained within gut at 1 hour post exposure (%)	Clearance at 1 hour post exposure (%)	Remained within gut at 6 hour post exposure (%)	Clearance at 6 hour post exposure (%)	Key Highlights
Without external any factors (in basic HH Combo medium)	500	4273	62	38	9	91	-Rapid clearance of larger PS-500 in 6-hours post exposure compared to PS-50
	50	3125	60	40	46	54	
With Feeding on algae *C. Vulgaris* during release phase	500	3855	28	72	13	87	-Increased clearance of PS-500 compared to mode 1 at 1 hour-post exposure. Minimal amount of PS-500 remains in gut at 6-hour post exposure even with feeding during release phase. -Slightly less PS-50 remains within the gut at 6 hour-post with the feeding step compared to mode 1.
	50	748	44	56	39	61	
Exposure of NMs that were incubated in algae *C. vulgaris* (no feeding during release phase)	500	7663	34	66	12	88	-Increased uptake of both PS-500 and PS-50 incubated in *C. vulgaris* compared to without algae in mode 1 - increased amount of PS-50 removed at 6 hours compared to mode 1
	50	5814	32	68	14	76	
Exposure to *D. magna* that had already been grazing on *C. vulgaris* for 24 hours prior	500	2600	46	54	12	88	-Full gut of *D. magna* results in decrease in uptake of PS-500 compared to those with no feeding -residual amount of PS-500 remains in gut regardless of full gut -no significant increase or decrease in uptake of PS-50
	50	3073	34	66	23	77	

5.2.2 Uptake and release of PS-50- and PS-50 NMs by *D. magna*

5.2.2.1 HH Combo medium with no feeding (mode 1)

D. magna were exposed to 0.001 g/L of PS-500 and PS-50 NMs for 1 hour and their release was monitored for 6 hours post-exposure without any feeding on algae *C. vulgaris*. It was quantified that *D. magna* steadily took up both sized NMs during the 1-hour exposure period, though there was a significantly higher uptake ($p < 0.01$) of the larger PS-500 compared to PS-50, indicating that *D. magna* more readily takes up larger NMs compared to smaller ones, as seen in figure 5.3, and consistent with the results in Chapter 3 where agglomeration of 100 nm particles to approximately 300 nm in *D. magna* conditioned medium increased their uptake.

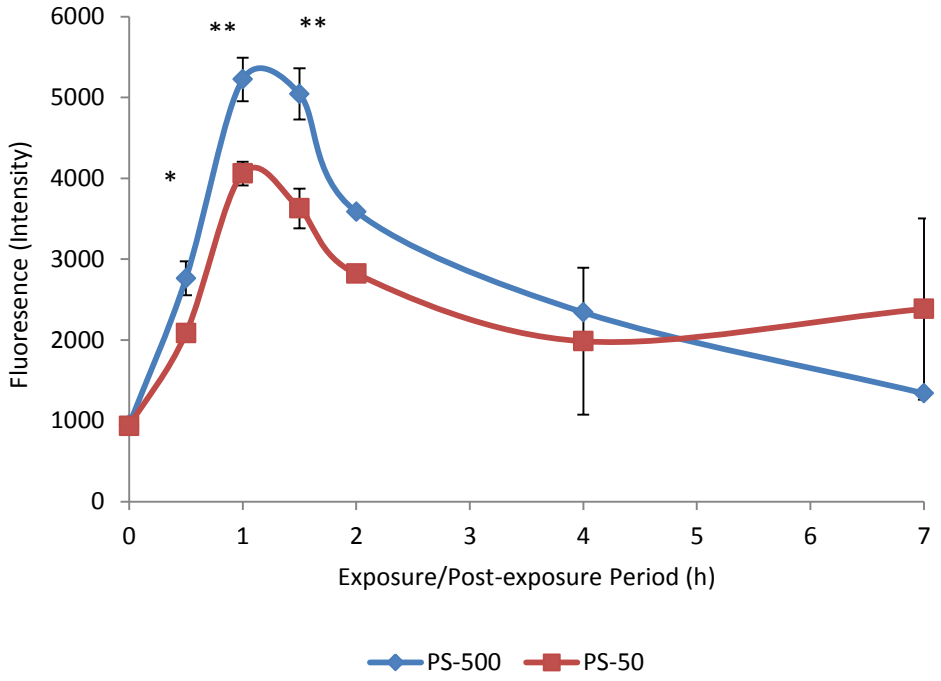

Figure 5.3 Uptake of PS-500 and PS-50 NMs during a 1 hour exposure period to 0.001 g/L of NMs and their release over a 6 hour post-exposure period in HH Combo medium.

After 1 hour post-exposure *D. magna* were able to successfully clear 38% of the internalised PS-500 NMs from their gut though 62% of NMs remained. After 6-hour post-exposure, *D.*

magna were able to clear the majority of PS-500 NMs with a clearance of 91% with only 9% remaining within the gut. By contrast, clearance of PS-50 NMs after 6 hours of post-exposure was only 54% of NMs of the total internalised NMs. This indicates that larger NMs are more readily taken up by *D. magna* and also have a relatively rapid clearance rate compared to smaller NMs over short time periods. Though a 6 hour-post exposure is a relatively short time period to assess, even within this limited timeframe, it could already be determined that larger NMs were excreted more efficiently cleared compared to smaller NMs bringing about the idea that smaller NMs may have an overall extended residency time which could lead to potential bioaccumulation upon continual exposure.

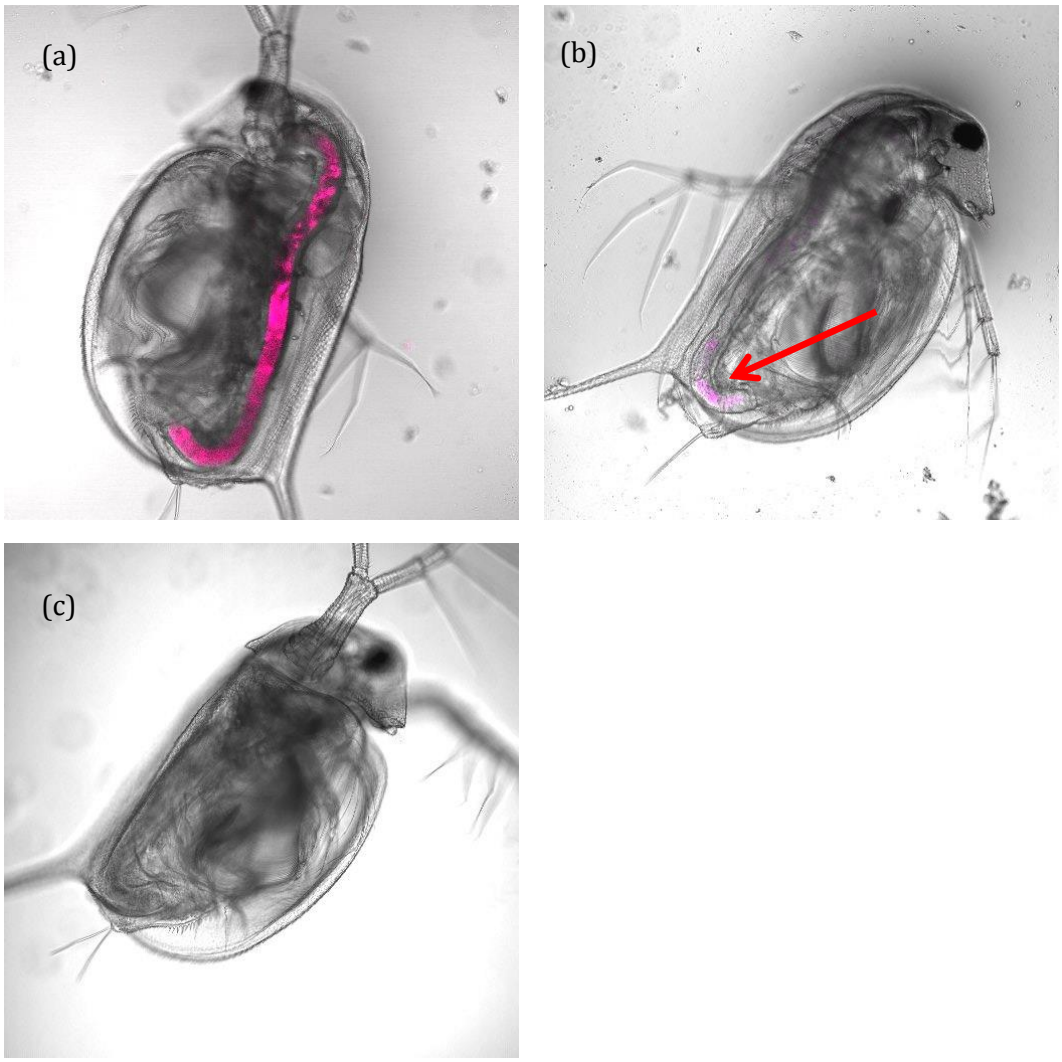

Figure 5.4 *D. magna* exposed to 0.01 mg/L PS-50 NMs after (a) 1 hour of exposure; (b) 24 hours of post exposure in HH Combo medium and (c) control (no NM exposure).

It was determined by confocal microscopy that even at 24 hours of post-exposure, there is still indeed a detectable amount of PS-50 remaining within the gut as seen in figure 5.4 indicating that there complete gut clearance could not be achieved even in 24 hours in only HH Combo medium, in the absence of feeding.

The likelihood of *D. magna* being exposed to only PS NMs in its natural environment, with no other factors influencing it such as the availability of food, is highly unlikely. Currently, many testing procedures do not take into account factors such as food that are more likely to represent realistic scenarios. It is widely recorded that consumed materials move through the gut passage of *D. magna* due to peristaltic contractions but also more importantly due to being pushed along by more recently ingested food material (Ebert, 2005) and therefore the clearance rate of a material has the potential to be affected by the availability of food and must be taken into account when assessing gut-clearance in a natural environment.

5.2.2.2 Effect of feeding on *C. vulgaris* during release phase on clearance (mode 2)

To assess the effect of feeding of *D. magna* on *C. vulgaris* depuration of PS-500 and PS-50 NMs, neonates were fed fresh *C. vulgaris* during the release phase and can be seen in figure 5.5. After a 1-hour post exposure with feeding, *D. magna* were able to successfully clear 72% of the internalised PS-500 NMs from their gut as seen in figure 5.5, compared to only 38% (statistically significant difference $p < 0.05$ *) when not being fed during the release phase (mode 1). This indicates that the presence of food does indeed increase the removal rate of PS-500 NMs from the gut, and should be considered in standard regulatory testing methods. After a 6 hour post-exposure, 13% of PS-500 NMs still remain within the gut of *D. magna* compared to 11% remaining without feeding in mode 1, which is statistically insignificant ($p >0.05$), showing that at small depuration times (6 hours), regardless of presentation mode, that there is still a minimal amount of PS-500 NMs that still remain within *D. magna* and that

the presence of food during the release phase still did not cause complete depuration of the larger PS-500 NMs from within the gut within this time period. After a 1-hour post-exposure 44% of PS-50 remain within the gut compared to 60% without feeding in mode 1 (statistically significant difference with $p < 0.001$ ***) and after a 6-hour post-exposure 39% of PS-50 remain in the gut compared to 46% without feeding, indicating that regardless of the size of NMs, the presence of food is a key factor in increasing the clearance rate of material from the gut at least at short times though after 6 hours of post-exposure there was a no difference ($p > 0.05$) in the amount of PS-50 NMs remaining within the gut exposed in only HH Combo medium with no food (mode 1) compared to those that had been presented with food during the release phase (mode 2). Interestingly, even with the presence of food, over the 6-hours of post-exposure, smaller PS-50 NMs are generally not as easily cleared compared to larger PS-500 NMs, although the presence of continual food supply (as would be expected in natural environments) may increase this clearance over time, but may also lead to enhanced uptake of the particles.

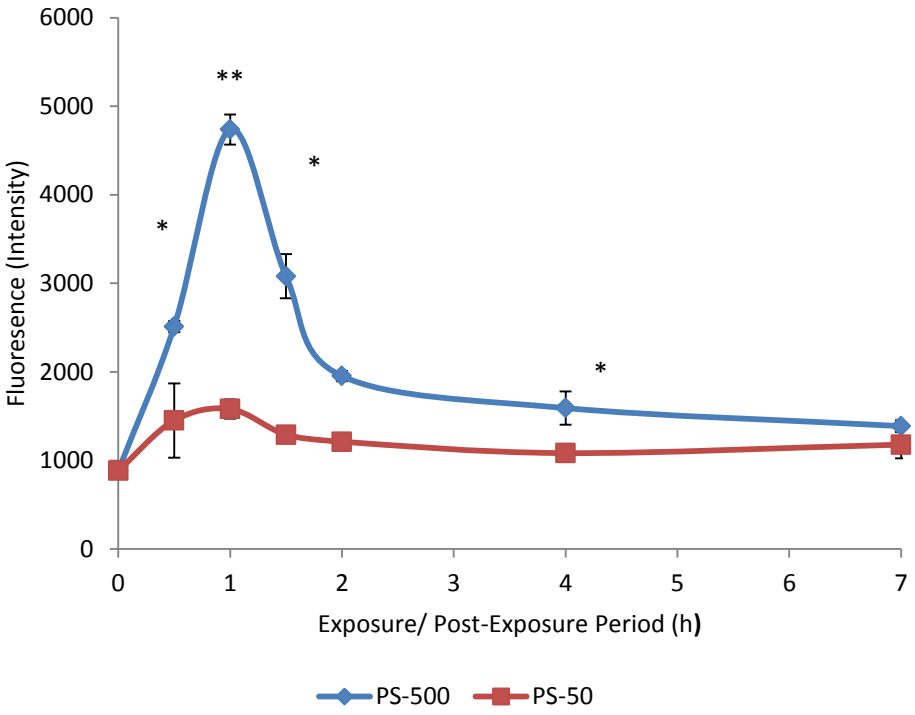

Figure 5.5 Uptake and release of PS-500 and PS-50 NMs after a 1 hour exposure period to 0.001 g/L of NMs and a 6 hour post-exposure period with feeding on algae *C. vulgaris* during release period (mode 2).

These results also conclude that PS-500 is still more effectively cleared compared to PS-50 even with feeding during the release phase. Graphically it may appear that PS-50 is taken up less at the 1 hour exposure period in mode 2 compared to mode 1 (assessed only in medium) though this exposure has statistically remained unchanged. Looking merely at percentage removal indicates that the smaller PS-50 is less effectively cleared, though in absolute terms, less PS-50 is originally taken up compared to PS-500 so that the higher percentage of retained PS-50 may still be lower than the amount of PS-500.

5.2.2.3 Exposure of NMs previously incubated in algae *C. vulgaris* (mode 3)

The excretion of NMs from *D. magna* is not the only factor that should be considered in assessing bioaccumulation potential and toxicity of NMs, as there are many factors that could influence uptake also. The following two presentation modes assess how different presentation modes factors influence NM uptake (as well as looking at release). Algae *C.*

vulgaris are an important food source for fresh water organisms and are therefore likely to be co-exposed with NMs under realistic exposure scenarios. Any impact to this primary food source may impact higher trophic levels. Algae has been known to enable the uptake of NMs when NMs bind to algae, causing unintended ingestion of NMs when organisms are feeding (Kalman et al., 2015). A summary of uptake of PS-500 and PS-50 when incubated in *C. vulgaris* compared to no prior incubation step can be seen in table 5.3 with a more detailed description and analysis below.

Table 5.3 Comparison of uptake by *D. magna* of PS-500 and PS-50 NMs incubated in *C. vulgaris* compared to exposure only in medium (mode 1).

PS NM	Type of uptake by *D. magna* after incubation in *C. vulgaris* compared to without incubation (0.5 hour exposure)	Statistical significance	Type of uptake by *D. magna* after incubation in *C. vulgaris* compared to without incubation (1 hour exposure)	Statistical significance
500	Increase	$p < 0.01$ **	Increase	$p < 0.01$ **
50	Increase	$p < 0.05$ *	Increase	$P < 0.001$ ***

The results shown in figure 5.6 (mode 3) compared to figure 5.1 (mode 1) indicate that *D. magna* take up significantly higher ($p < 0.01$ **) amounts of PS-500 when the NMs were previously incubated in *C. vulgaris* and co-exposed with the algae (mode 3), compared to those only exposed to NMs in medium (mode 1) at both 0.5 and 1 hour uptake time-points. Results indicate that *D. magna* also take up PS-50 significantly higher at 0.5 hour ($p < 0.05$ *) and 1 hour ($p < 0.001$ ***) exposure when pre-incubated in *C. vulgaris* and co-exposed with

the algae compared to those with no prior incubation/no algae present (comparing modes 1 and 3). These results show that regardless of NM size, when incubated with a food source, there is an increased uptake of NMs by *D. magna* as NMs bind to the food source and are incidentally ingested along with the *C. Vulgaris.* Overall, PS-500 NMs are also taken up to a statistically significant higher degree ($p < 0.05$ *) compared to PS-50 NMs at 0.5 and 1 hour exposure times when pre-incubated in/co-exposed with *C. vulgaris*.

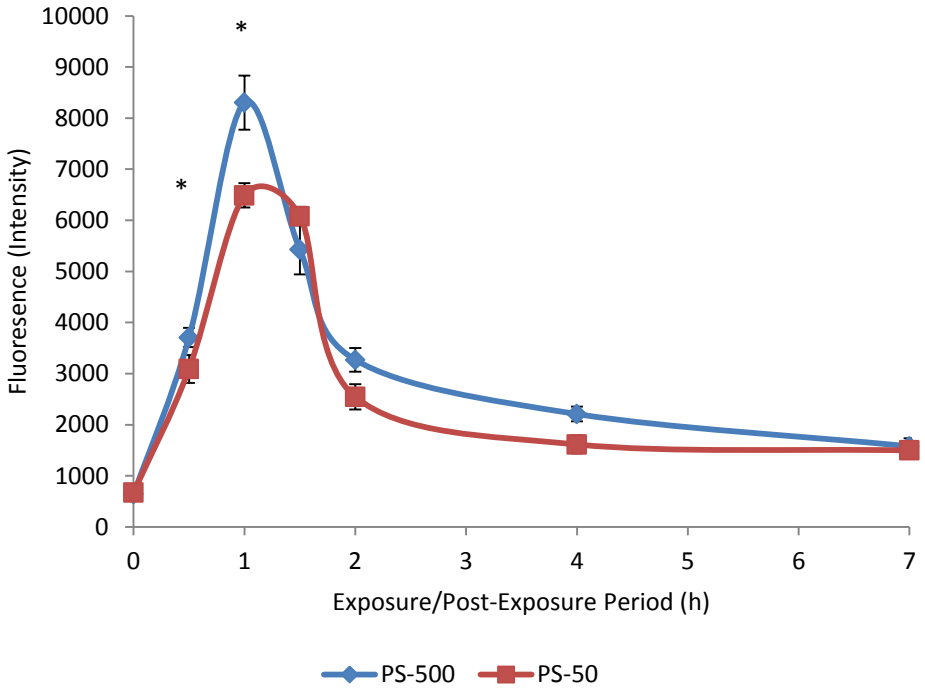

Figure 5.6 Uptake of PS-500 and PS-50 NMs (0.001 g/L of NMs previously incubated in *C. vulgaris* for 3 hours) after a 1 hour exposure period and release during a 6 hour post-exposure period in the absence of algae (mode 3).

The degradation of microplastics in environmental waters is a growing concern as suspended organic matter such as algae can act as a contamination sink enhancing exposure for filter feeders such as *D. magna.* The presence of food can facilitate toxicity by making contaminants more bioavailable which includes the process of rapid physical adsorption (less than 10 mins) of contaminants to food sources (Taylor et al., 1998). Contaminant induced changes to algae as a primary food source could prompt changes to *D. magna* structure as well as their

function including their ability to filter water and regeneration of nutrients which could lead to changes to several trophic levels (Taylor et al., 1998).

With regards to depuration, after a 1 hour post-exposure period, 34% of PS-500 NMs remain within the gut compared to 62% that remain without any additional factors (mode 1), as interestingly, even though there is a higher uptake of PS-500 by *D. magna* when incubated in algae, there is still a greater clearance rate of these NMs from within the gut at 1 hour-post exposure as PS-500 is intertwined within the algae and is therefore less likely to stick to the gut wall of *D. magna* and more likely to be egested along with the algae. There is still a higher percentage of PS-500 remaining within the gut at 1 hour post-exposure in mode 3 (i.e. 34%) compared to only 28% remaining when *D. magna* are allowed to feed on algae during the release phase (mode 2, section 5.2.2.2 above) as the newly acquired food in mode 2 pushes previously ingested material out. At 6 hours post-exposure, only 12% of PS-500 remained within the gut which is a similar percentage to NMs that remain within the gut when *D. magna* were fed on *C. vulgaris* during the release phase (mode 2), which was 13%. This indicates that there is still a residual amount of NMs that remain within the gut at a 6 hour post-exposure despite either being consumed along with a food source or having a food source available to subsequently cause depuration. This would suggest that there is some degree of stickiness to these NMs and a certain proportion are binding to the lumen of the gut wall causing increased residency time of NMs within *D. magna*.

TEM imaging of PS-500 NM exposed *D. magna* (mode 1) embedded in epoxy resin clearly shows that PS-500 NMs are sticking to the lumen of the gut (indicated with arrows) as seen in figure 5.7 (a). TEM images also clearly show a defined bush border containing microvilli protruding from the gut epithelium wall, which pushes material along the gut as well as absorbs nutrients. PS-500 NMs can be seen to be heavily taken up into the gut though there is no noticeable permeation of these NMs diffusing into the gut epithelial cells, clearly confirming that NMs remain solely within the gut, consistent with previously obtained data in

chapters 3 and 4. PS-500 NMs can also be identified stuck to the tips of the microvilli (b) and having moved further into and becoming embedded into the bush boarder (c) though there is no penetration of these NMs any further than this or into epithelial cells. Quite interestingly, PS-500 NMs can also be located within the gaps of the bush boarder (d) which cannot be easily reached by microvilli during their sweeping movements to be cleared away, essentially leaving these NMs trapped within these spaces and therefore with a higher potential to remain present for a longer duration of time leading to a residual amount of NMs remaining long term within the gut, which is complementary to quantitative fluorescent and qualitative confocal results. PS NMs getting stuck within the bush border raises questions of longer term effects such as the potential for stiffening of the bush boarder over time resulting in a lower degree of sweeping movements of food taken up.

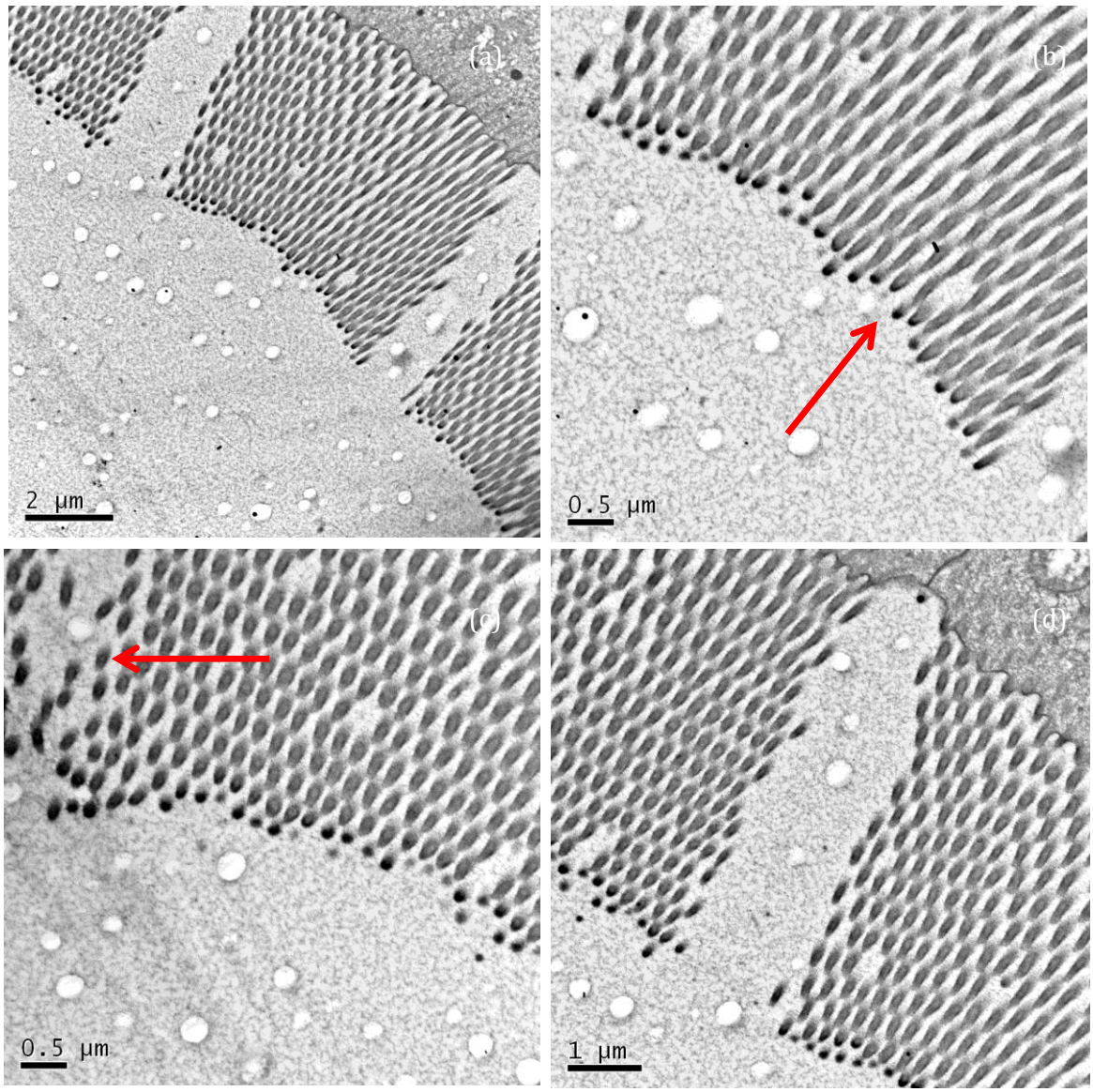

Figure 5.7 PS-500 NMs within the gut of *D. magna* adhering to microvilli and found within gaps of the bush border.

Interestingly, when PS-50 NMs that were pre-incubated in algae and had a post-exposure of 6 hours, only 14% remained in the gut compared to 54% with no feeding (mode 1). The 14% value is much closer to the residual amounts that have been consistently seen to be remaining within the gut in all modes of presentation for the larger PS-500 NMs, and suggests that incubated with the algae and being co-consumed, lessens the chance of the smaller NMs binding to the gut wall as they are already bound to the algae, causing their passage through the gut to be facilitated as they are cleared along with the algae to which

they are bound. However, there is bound to be PS-50 NMs that do interact with the gut resulting in some NMs being stuck within the gaps of the bush boarder, leading to the residual amount of NMs remaining within the gut as previously seen with other presentation modes.

5.2.2.4 Immediately after *D. magna* feeding on algae *C. vulgaris* (Mode 4)

There has been evidence to suggest that the rate of uptake of food by *D. magna* is conditional on what is already pre-existing within their gut (MacMahon and Rigler, 1965) so that the rate of uptake of NMs may be influenced by how recently *D. magna* have been fed. Figure 5.8 is a transmitted light image and shows a *D. magna* neonate that has been grazing on *C. vulgaris* for 24 hours and shows the fullness of their gut containing the green algae *C. vulgaris*.

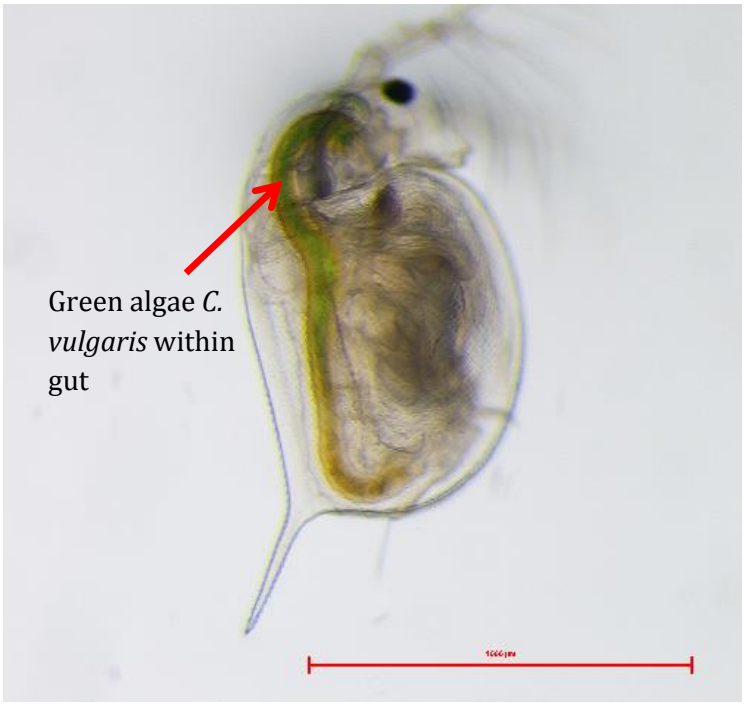

Figure 5.8. Transmitted light image of *D. magna* neonate that had been grazing on green *C. Vulgaris* for 24 hours.

Some studies suggest that *D. magna* can alter and decrease their feeding pattern when disagreeable food is present and if they have not been starved (Meise et al.). Previous results,

as seen in section 3.3.5, showed that *D. magna* that already had a partially full gut including with NMs grazed less on algae *C. vulgaris* when subsequently re-fed. Results shown in figure 5.9 indicate that *D. magna* that have been fed consistently for 24 hours on *C. vulgaris* take up significantly less of the larger PS-500 compared to those that had not been fed at all (mode 1) at both 0.5 and 1 hour uptake ($p < 0.01$ **) times, indicating that the presence of food already within the gut decreases subsequent uptake of additional particulates of an ideal food size (usually approximately 2 µm)(Hoek et al., 1995). Results also indicate that *D. magna* that have been fed consistently for 24 hour on *C. vulgaris* show no significant increase or decrease in the uptake of PS-50 NMs compared to those with no feeding. This indicates that *D. magna* that have been fed still process water and smaller NMs may be able to enter through the water column as they are substantially lower than the sizes of their natural food source and these may ingested from merely just being present in the water column. Uptake and depuration results can be seen in figure 5.9, and note the higher relative uptake of PS-50 in this case compared to PS-500.

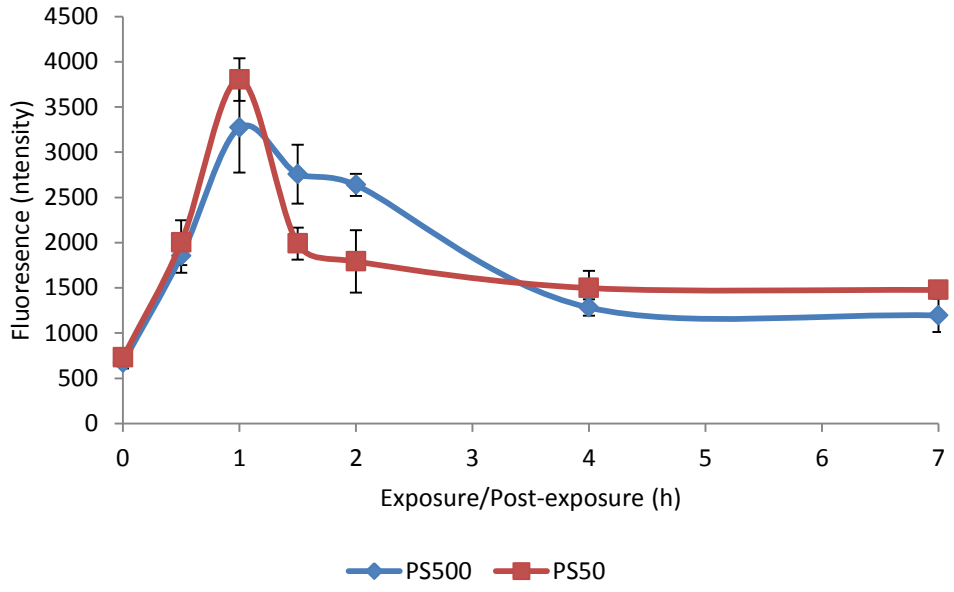

Figure 5.9 Uptake of PS-500 and PS-50 NMs by *D. magna* that had been previously fed on *C. vulgaris* for 24 hours after a 1 hour exposure period to 0.001 g/L of NMs and release during a 6 hour post-exposure.

D. magna that have been continually fed for 24 hours and then exposed to 0.001 g/L of PS-500 and then moved to fresh media to assess the release post-exposure for 6 hours, have 20% of NMs remaining within their gut after 6 hours, though this is only in comparison to how much was taken up by neonates, which was significantly less compared to neonates that had not been previously fed (mode 1). In real terms, where results can be compared to those neonates with no feeding (mode 1) (section 5.3.2), comparatively only 12% truly remain within the gut of *D. magna* which is a consistent value found for all three of the other types of exposure scenarios of PS-500 NMs i.e., no feeding (mode 1), feeding only during release phase (mode 2) and exposure to PS pre-incubated in algae (mode 3). This indicates that there is a similar residual amount of PS that remains within *D. magna* at least at 6 hours post-exposure regardless of presentation mode, and suggests there is some degree of binding of the PS NMs to the lumen of the gut passage whereby excretion is hindered.

In order to ensure increased fluorescence was due to increased uptake and not due to additional fluorophore on one NM compared to the other, fluorescence of PS-500 and PS-50 were measured at the same mass concentration. It was concluded that PS-500 was marginally more fluorescent though a simple correction factor could be applied to the PS-500 results so that the fluorescence of both types of NMs could be comparable with regards to uptake and release. This was done by taking the fluorescence of both NMs at 0.001 g/L (n=5) which showed that PS-500 was slightly more fluorescence (by approximately 12%). All PS-500 values obtained in the experiments were divided by this factor so that fluorescence of the two sized NMs was comparable in terms of monitoring retention and not due to a higher intensity of fluorophore.

5.2.3 Impact of conditioning and incubation time on NM stability

Understanding the interactions between secreted proteins by *D. magna* with NMs of different sizes is important to understand the influence of the proteins on the stabilization or destabilization of NMs in suspension. It has already been established in chapter 3 (section

3.3.2) that as conditioning time of *D. magna* increases, so does the concentration of proteins in HH Combo medium, tested up to 24 hours, due to neonates having a longer time to secrete proteins. As seen in figure 5.10, smaller PS-50 NMs agglomerate in conditioned medium when incubated for longer incubation times (6 hours), and the longer conditioning times lead to increased agglomeration only when incubated for a long enough time period (6 hour incubation (with 6 hours of conditioning) is significantly agglomerated $p < 0.05$ compared to 1 and 4 hour incubation). PS-50 NMs remain stable at shorter incubation times (1 and 4 hours) even in conditioned medium and therefore the length of time that NMs are incubated in a protein contained medium is a critical factor influencing NM agglomeration.

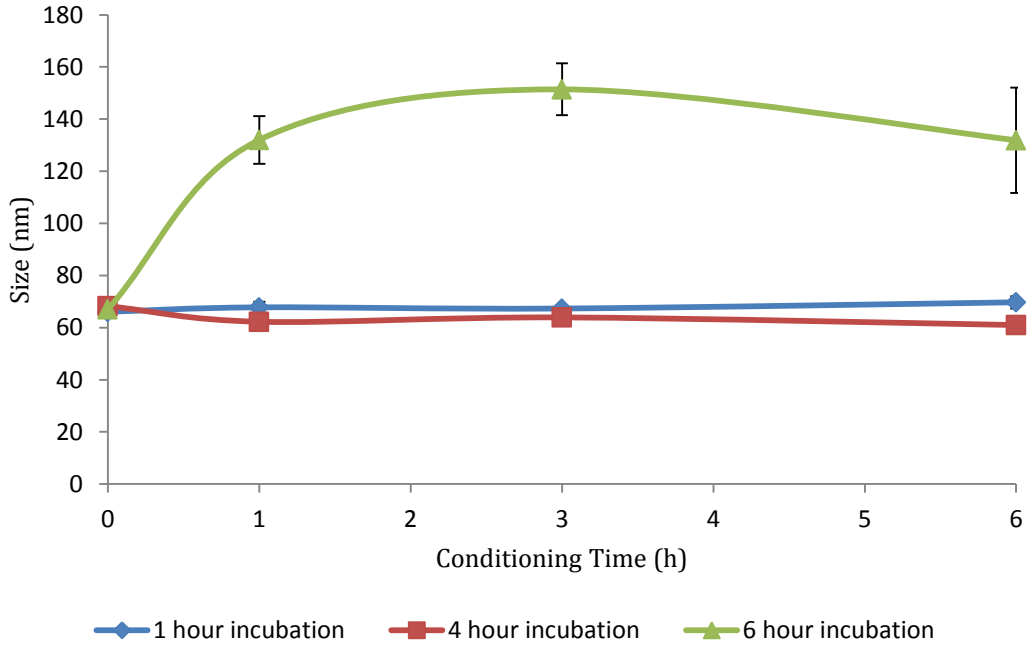

Figure 5.10. Stability of PS-50 NMs incubated for various times in *D. magna* conditioned HH Combo medium (n=3).

The incubation times used in this study were relatively short, though despite this, differences were already seen and this information helps to outline the significance of how natural substances may influence NM stability. Short incubation times were used here to be consistent with the experiments from chapters 3 and 4. The Vroman effect may have some influence in NM destabilization. This indicates that it is the proteins that have the highest

affinity to the NM that are bound to NMs at longer incubation times and are the proteins responsible for the PS-50 agglomeration. At shorter incubation times, these proteins may not be the same proteins bound to the NM, as higher abundance but lower affinity proteins typically bind first, and therefore do not cause the same degree of destabilization.

To assess this, PS-50 NMs were incubated in 3 hour conditioned medium for both 1 and 6-hour incubation times (where the amount of agglomeration was shown to be statistically significant). After incubation, the hard-corona was isolated and proteins were identified by mass spectroscopy. Results show that proteins adsorbed to NM surfaces at the 1 hour incubation were very different compared to those adsorbed after a 6 hour of incubation as can be seen in table 5.4. This confirms that as NMs are incubated in protein-contained medium, that there is a rearrangement of proteins at the NM surface and it is these proteins that either cause stabilization or destabilization effects to NMs.

Table 5.4. Most abundant proteins identified by mass spectrometry in the hard-corona around PS-50 NMs from 3 hour conditioned medium after 1 or 6 hours of incubation.

	Proteins identified in hard corona around PS-50 from 3 hour conditioned medium after 1 hour incubation	Proteins identified in hard corona around PS-50 from 3 hour conditioned medium after 6 hour incubation
Unique Proteins	Signal transduction histidine Protein kinase Glucose-6-phosphate isomerase Metallo-beta-lactamase Superfamily protein Isoleucine tRNA ligase Sulfurtransferase Putative succinyl-CoA:3-ketoacid Transferase Chaperonin Cytosine permease Transposase	ATP Synthase Ferredoxin- type protein Chaperone protein Actin Acetoactate synthase isozyme
Common Proteins	Trypsin 2-domain haemoglobin	Trypsin 2-domain haemoglobin

Contrastingly, larger PS-500 incubated for different time lengths in conditioned medium did not show any significant agglomeration, as seen in figure 5.11.

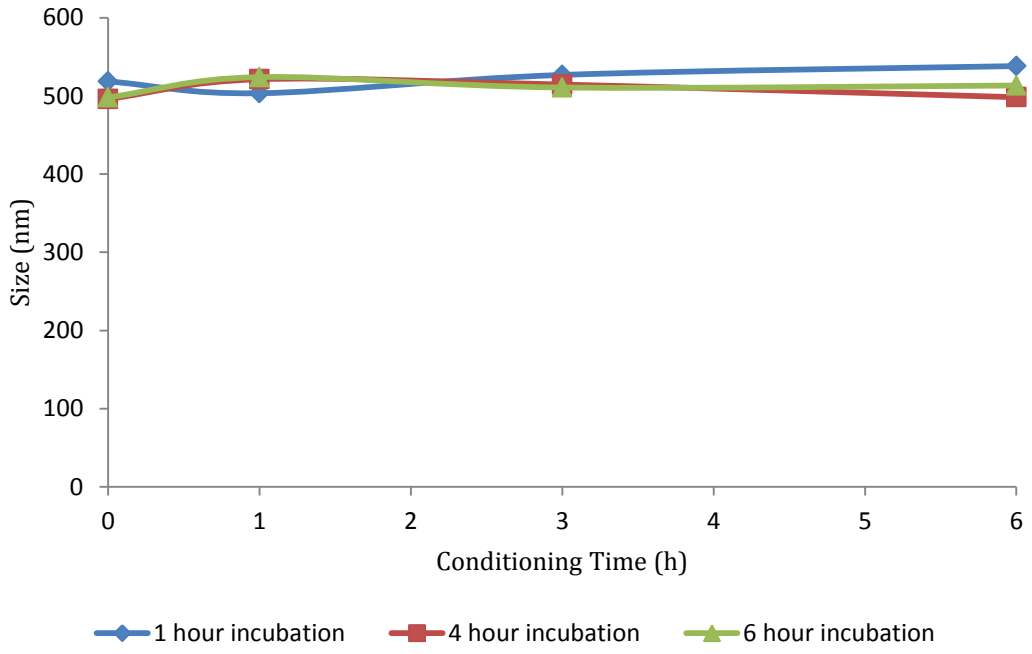

Figure 5.11 Stability of PS-500 NMs incubated for various times in *D. magna* conditioned HH Combo medium conditioned for increasing lengths of time (n=3).

This can be explained by the fact that there is a significant decrease in surface energy with increasing NM size (Holec et al., 2014). Smaller NMs have a higher surface energy and tend to agglomerate or bind to available biomolecules which may cause agglomeration in order to reduce this high energy whereas larger NMs with a lower surface energy are more stable and show less agglomeration.

5.2.4 Assessment of proteins in PS NM hard corona

Assessment of proteins existing in the hard coronas indicate that conditioning of proteins by *D. magna* leads to the adsorption of proteins to both PS-500 and PS0-50 NM surfaces. A 12.5% PAGE was conducted using Coomassie blue and silver staining in order to highlight the presence of hard corona proteins associated with PS-500 and PS-50 after 24 hour conditioning and 24 hour incubation. Significant bands appear between 25-150 kDa around PS-50 and PS-500 NMs, indicating the major protein sizes comprising the hard-corona as seen in figure 5.12.

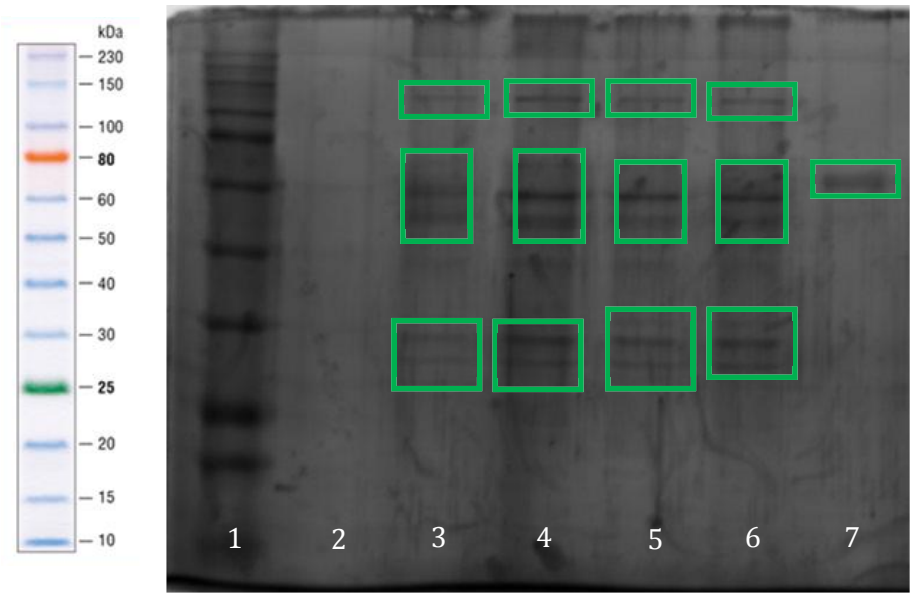

Figure 5.12 PAGE of hard-corona proteins surrounding PS-500 and PS-50 incubated for 24 hours in medium conditioned for 24 hours by *D. magna.* Lane 1 - protein ladder, lane 2 – spacer, lanes 3 and 4 replicates of proteins isolated from hard corona around PS-50, lanes 5 and 6 replicates of proteins isolated from hard corona around PS-500, lane 7 positive BSA control.

The first lane is a ladder marking the protein sizes in kDa and lane two is the negative control of fresh HH Combo medium where there are no bands present indicating the lack of any protein in the control. Lanes 3 and 4 are replicates of the proteins isolated from the hard corona-bound to PS-50 which ranges from sizes of 25-150 kDa. Lanes 5 and 6 are replicates of the proteins isolated from the hard corona bound to PS-500 which also have proteins ranging from sizes 25-150 kDa. Lane 7 is a positive control of BSA which has its fingerprint mark at 70 kDa confirming that the gel has indeed separated out proteins based on size.

5.2.5 Quantification of secreted carbohydrates

It is well established that organisms are able to 'condition' their surroundings by secreting biomolecules such as proteins into their immediate environment, and some research has been conducted on the impact of these secreted proteins on NMs stability and toxicity. *D.*

magna usually live in fresh water containing bountiful amounts of algae which are abundant in carbohydrates (Smayda, 1997) (and proteins) on which they feed, and undigested material may be excreted back into the environment as carbohydrate substances which have the ability to interact with NMs present in the local environment. *D. magna* also release chitin (a polysaccharide) into their immediate surroundings though their natural process of moulting (Anderson and Brown, 1930). Though some research has been conducted on the adsorption of proteins to NM surfaces and how this may impact their stability, relatively little research has been done on the secretion or egestion of other biomolecules such as carbohydrates or even lipids.

D. magna were allowed to condition HH Combo medium and the quantification of secreted carbohydrates can be seen in figure 5.13. Care was taken not to include any shed carapace (which can easily be done with visual observation or using an optical microscope) so these results reflect only secreted carbohydrates.

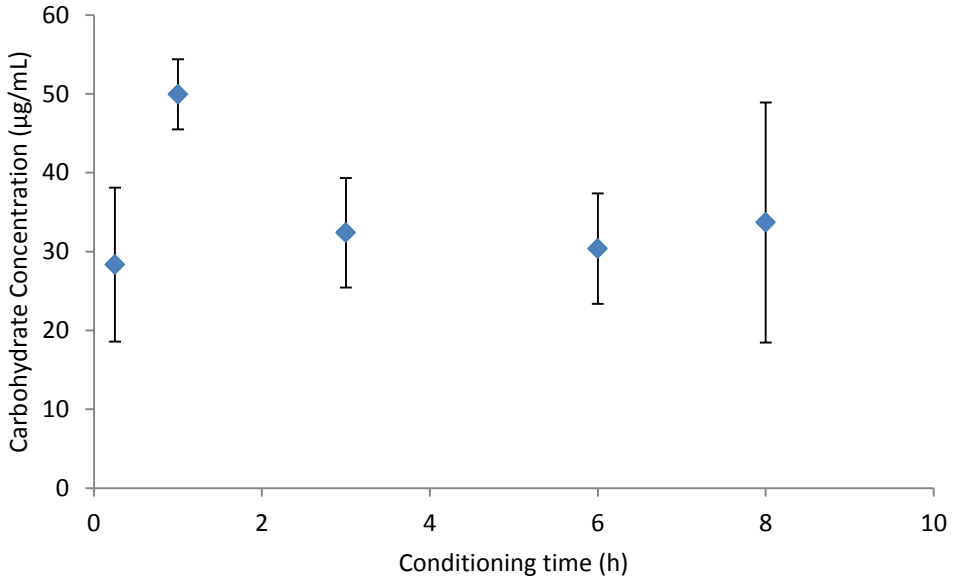

Figure 5.13 Quantification of secreted carbohydrates by *D. magna* over 8 hours with an average of average of 35 ± 8.6 µg/mL, n=3.

Results indicate that unlike the secretion of proteins by *D. magna* which increased steadily over time up to six hours as seen in chapter 3, the release of carbohydrates is much lower and follows no specific trend. Neonates shed their exoskeleton which is manly comprised of saccharide units which would be the major source of carbohydrate release by *D. magna* and it appears that other than moulting, *D. magna* secrete substantially less carbohydrates compared to proteins. The concentration range of secreted carbohydrates was between 28-49 μg/mL (average of 35 ± 8.6 μg/mL) with no significant increase or decrease in trend up to 8 hours (verified statistically) though contrastingly protein secretion increased over time and increased to 435 ±3.5 μg/mL in 6 hours as previously seen in chapter 3.

5.3 Summary

NMs will inevitably be released into the environment making monitoring of uptake and excretion of these NMs by organisms such as *D. magna* under realistic scenarios that the organism will actually be exposed to in the environment important in terms of assessing retention and bioaccumulation of NMs of different sizes. The work in this chapter aimed to explore how different presentation modes of NMs such as via the medium (mode 1) or along with a food source *C. vulgaris* (mode 3), and the effect of feeding before (mode 4) or after exposure (mode 2). Results indicated that the mode of presentation altered the feeding pattern, uptake and depuration of two differently sized (50 and 500 nm) PS NMs. In parallel, this chapter demonstrated how secreted biomolecules altered the stability of smaller NMs, which indeed has been shown in previous chapters although it is important to always assess this for each type of NM. The main findings and conclusions are summarised as follows:

1. Overall, *D. magna* take up the larger PS-500 NMs to a significantly higher degree compared to the smaller PS-50 NMs. Four modes of presentation of NM to *D. magna* were assessed. 1) In only HH Combo medium (mode 1), there was a rapid clearance of PS-500 (with a minimal residual amount remaining ~9%) compared to PS-50 at 6 hours of post exposure. 2) When *D. magna* were fed on algae *C. vulgaris* during the

release phase (mode 2), there was an increased clearance of PS-500 during the first hour of post-exposure (28% compared to 62%) compared to without feeding in mode 1. This is due to the new incoming food source pushing out the previously ingested NMs. At 6 hours of post-exposure there is still a minimal amount of residual PS-500 within the gut (~13%). The presence of additional food during the release phase did not decrease the amount of PS-50 retained within the gut at 6 hours of post-exposure compared to those with no feeding in mode 1 (39% remain compared to 46%). Overall, the larger PS-500 were cleared more effectively than the smaller PS-50 NMs. 3) Incubation of PS-500 or PS-50 in algae *C. vulgaris* increased the uptake of both types of NMs by approximately 60% more into *D. magna* as *D. magna* incidentally ingest the NMs along with the food source, compared to mode 1 with no pre-incubation step. A residual amount of PS-500 still remains within the gut after 6 hours of post exposure even in mode 3. There is an increased removal of PS-50 at 6 hours of post-exposure (mode 3) where only 14% remains compared to 46% remaining with no previous incubation step (mode 1), as the NMs may have remained bound to the algae and thus are less likely to be stuck in the gaps of the bush border. 4) *D. magna* that had previously been fed on *C. vulgaris* (mode 4), and thus had a full gut, take up a significantly decreased amount of approximately 62% of PS-500 compared to those that had not been previously fed (mode 1), indicating that the presence of food within the gut alters the subsequent feeding pattern. Having a full gut neither increases nor decreases the amount of PS-50 taken up compared to the amounts consumed by *D. magna* exposed with no feeding (comparing mode 1 and 4) suggesting that the smaller particles are passively entering the gut. The residual amount of PS NMs remaining within the gut under all conditions appears to be NMs stuck within the gaps of the bush border that are not easily cleared by the sweeping motion of the microvilli. A simple schematic of the comparison of the uptake and

excretion of the different sized NMs in each presentation mode (2-4) compared to mode 1 can be seen in figure 5.14.

PS-500	Uptake at 1 hour	Retained @ Post-Exposure 1 hour	Retained @ Post-Exposure 6 hours
Mode 2 (with feeding during release stage)	Same	↓	Same
Mode 3 (incubated and co-exposed with algae)	↑	↓	Same
Mode 4 (exposed to pre-fed daphnia)	↓	↓	Same
PS-50	**Uptake at 1 hour**	**Post-Exposure 1 hour**	**Post-Exposure 6 hours**
Mode 2 (with feeding during release stage)	Same	↓	Same
Mode 3 (incubated and co-exposed with algae)	↑	↓	Same
Mode 4 (exposed to pre-fed daphnia)	Same	↓	Same

Figure 5.14 Schematic and comparison of uptake and retention of PS NMs with different presentation modes (2-4) compared to presentation mode 1 (OECD standard).

2. Conditioning of HH combo medium by *D. magna* and incubation of each of the types of NMs did not appear to impact the stability of the larger PS-500 NMs. Smaller PS-50 NMs were also able to remain stable for shorter incubation times (1 and 4 hours) though started to agglomerate with longer incubation times which can be accounted for by different types of proteins being adsorbed to the surface at each of these time points causing different degrees of instability. This can be linked to presentation mode as pristine and monodisperse NMs initially deposited into the environment may agglomerate and become larger NMs, which have been shown to be more actively taken up by *D. magna* (modes 1-3) compared to smaller NMs.
3. *D. magna* release carbohydrates into their immediate surroundings, though there is no defined increase of carbohydrates over time up to 8 hours. There is also substantially less (approximately 35 μg/mL of carbohydrates secreted into the medium compared to 435 μg/mL of proteins in 6 hours- an order of magnitude more). The minimal amount of carbohydrate released is not likely to be a significant driver of the effects observed with uptake and excretion in each presentation mode.

The data in this chapter confirms the importance of applying realistic environmental scenarios when considering NM accumulation as the presentation mode of NMs considerably impacts NM uptake, retention and depuration by *D. magna.* Currently, it is not widely practiced to assess NM retention using environmentally relevant conditions and data obtained without this consideration may not represent how NMs act once actually deposited into the environment. It can also be noted that the work in this chapter is the initial step into investigating why considering feeding regimes are important though there may be a combination of presentation modes acting simultaneously as environmental compartments are dynamic and there may be additional factors also affecting uptake. This work also shows how natural biomolecules existing in the environment may affect NM stability which has previously been shown to impact NM toxicity though it would be recommended to assess this on each type of specific NM to avoid generalizations.

6

Conclusions

This chapter ties together the important conclusions that arise from all of the results achieved throughout the chapters and demonstrates that the research performed fulfils the aims set out for the thesis.

The first aim was to investigate the impact of the protein corona on the stability of differently charged PS NMs and their toxicity towards and retention within D. magna

Positively charged PS NMs were found to be more toxic than negatively charged PS NMs with corresponding EC_{50} values of 25.8 and 36.3 μg/mL respectively. It was found that *D. magna* steadily condition medium and release proteins which reach up to 435 μg/mL in 6 hours. Both types of PS NMs were incubated in conditioned medium, which caused destabilization of both types of PS NMs resulting in agglomeration whereby longer incubation times caused increased agglomeration. With regards to toxicity, the larger NM sizes caused by the destabilization of proteins resulting in agglomeration made both types of PS NMs a more attractive food size, resulting in a decrease in EC_{50} of positively charged PS NMs to 0.0189 mg/mL (6 hour conditioning and 6 hour incubation) and a further decrease with a longer incubation time to 0.0081 mg/mL (6 hour conditioning and 24 hour incubation). A similar trend occurred with negatively charged PS NMs, which had a decreased EC_{50} of 0.0337 mg/mL (6 hour conditioning and 6 hour incubation) and a further decrease of EC_{50} to 0.0095 mg/mL with 6 hour conditioning and 24 hour incubation. In parallel, as *D. magna* consume the algae *C. vulgaris* as a food source and both organisms are in close proximity, the release of proteins by *C. vulgaris* was also determined, but was minimal (89 μg/mL) compared to those

released by *D. magna*. Both types of PS NMs were also incubated in *C. vulgaris* conditioned medium for various conditioning and incubation times and no agglomeration took place, indicating that the destabilization of NMs was due to the proteins released by *D. magna* only.

It was also determined that *D. magna* take up negatively charged PS NMs steadily when exposed for 1, 2 or 3 hours and also release them at a steady rate for up to 6 hours of post-exposure, with approximately 15% of the internalized NMs remaining within the gut at this time-point indicating a steady rate of filtration. NMs that had been incubated in conditioned medium and then had been exposed to *D. magna* for 2 hours were not excreted as efficiently during post-exposure and 20% remained within the gut at this time point resulting in higher retained dose causing a higher toxicity of protein corona-bound PS NMs. Confocal imaging showed that ingested NMs remained solely within the gut and did not translocate to other tissue.

Subsequently, *D. magna* were allowed to feed on *C. vulgaris* after a two-hour exposure to PS NMs that had been incubated in conditioned medium. Results show that the feeding rate of *D. magna* decreases with the presence of corona-bound NMs already present within the gut.

This work provides an important insight into how naturally released biomolecules such as proteins drastically impact the stability, toxicity and retention of NMs that are released into environmental waters towards *D. magna*. This can result in extended bioaccumulation and subsequent effects such as reduced grazing, ultimately altering population levels in the environment. Currently, standardized toxicity testing does not place a high importance on the presence of natural biomolecules, which should be taken into account given NMs large surface area and well documented tendency to adsorb biomolecules from their surroundings.

The second aim was to investigate the impact of charge and shape of Au NMs on their chemical and physical toxicity to D. magna and to assess the influence of the protein corona

Positively charged Au NMs were found to be orders of magnitude more toxic to *D. magna* compared to negatively charged NMs. When exposed to a mass concentration, the EC_{50} of positively charged spheres and short rods were 0.0061 and 0.018 μg/mL respectively indicating the higher toxicity of spheres. An EC_{50} could not be obtained for negatively charged NMs regardless of shape, even at concentrations as high as 50 μg/mL though the rank in toxicity of negatively charged NMs was from smallest to largest, where spheres were most toxic, then short rods followed by long rods. Considering this work was investigating the toxicity of NMs of different size and shape, it became clear that assessing toxicity based on number concentration was a more appropriate measure of exposure. When exposed on the basis of number concentration, the EC_{50} of positively charged spheres and short rods were 5.69×10^7 NMs/mL and 4.3×10^7 NMs/mL respectively indicating a change in toxicity trends compared to mass concentration where actually the larger short rods were more toxic compared to spheres. The same trend occurred with negatively charged NMs where the long rods were most toxic, and then short rods followed by spheres though no EC_{50} could be obtained for negatively charged NMs in this case also. Regardless of mass or number concentration exposure, positively charged NMs were more toxic compared to negatively charged NMs.

With regards to toxicity, it was also important to assess charge per surface area as the work dealt with NMs of different size and shape. Our initial assumption, and indeed the manufactuer's information indicated that all forms should have similar charge density, but this turned out not to be the case. For positively charged NMs it was determined that positively charged short rods had 3 charges/ nm^2 whereas spheres only had 2 charges/ nm^2. The increase in toxicity of positively short rods can be attributed to not only short rods

having a greater surface area available for interaction but also having more positive charges per surface area providing a much higher total positive charge per NM overall. Negatively charged long rod, short rod and sphere had 2, 2 and 3 charges/ nm^2 respectively, which, when considering total surface area results in long rods bearing the highest total charge and the spheres the lowest.

Toxicity of the Au NMs was also assessed on a chemical level, looking at ROS formation, and on a physical level, looking at changes in *D. magna* moulting. *D. magna* were exposed to high or low concentrations of NMs (these were assigned based on the survivorship results discussed above). Positively charged spheres at a high exposure concentration (EC_{40}) prompted a high degree of ROS formation though *D. magna* were able to recover to steady-state ROS levels after 8 hours. Positively charged short rods at a high exposure concentration (EC_{40}) also prompted a similar high degree of ROS formation although here the *D. magna* coping mechanisms were unable to fully recover from the stress due to the increased level of toxicity induced by an increased surface area or charge per surface area. These results complement the survivorship / toxicity results. Both types of positively charged NMs exposed at a low concentration (EC_5) prompted only minimal ROS production. Negatively charged spheres prompted a low degree of ROS overall. *D. magna* were also exposed at high concentrations to NMs that had been incubated in conditioned medium. Negatively charged NMs incubated in conditioned medium still only produced low amounts of ROS. Positively charged rods incubated in conditioned medium produced a similar amount of ROS compared to those that had no previous incubation step. Interestingly, *D. magna* exposed to positively charged spherical NMs that had been incubated in conditioned medium did not even reach the recovery phase as the majority of *D. magna* had died during the exposure period. This can be due to the increase in size of spherical NMs in conditioned medium causing these NMs to become a more attractively sized and textured food source for *D. magna* contingently increasing their uptake and localized toxicity.

Toxicity of the more toxic positively charged Au NMs was also investigated in terms of a physical mode of toxicity via moulting. Both positively charged spheres and short rods caused a similar degree of partial inhibition of moulting (delayed by 24 hours eventually resulting in death). This result indicates that the mechanism of Au NM toxicity is both physical and chemical though dynamic differences can be seen at a chemical level.

This work provides significant information on the importance of exposure method when investigating toxicity of NMs of different shape and size and how charge per surface area can influence toxicity. This work also highlights the mechanisms of toxicity imposed by differently charged and shaped Au NMs and how the presence of an adsorbed protein corona which is likely to occur in natural water-based environments can influence toxicity, although this factor is not widely looked at in fresh-water toxicity studies.

The third aim was to investigate the impact of presentation mode of differently sized PS NMs on the uptake, excretion and retention by D. magna

Presentation mode was found to affect uptake and excretion of large and small PS NMs by *D. magna*. Four presentation modes of the PS NMs were investigated. Firstly, NMs were presented in only medium with no other impending factors (mode 1). Here *D. magna* were able to successfully clear the majority of the larger PS NMs by 6 hours post-exposure, though a minimal amount of the larger PS NMs remained after 6 hours of post exposure. TEM imaging indicates the presence of a minimal amount of the larger PS NMs stuck between the gaps of the bush boarder so that the microvilli cannot easily brush them through the gut passage, which explains the residual amount of remaining PS within the gut. The majority of the larger PS NMs are in the lumen.

Secondly, when *D. magna* are fed the food source *C. vulgaris* during the excretion phase (mode 2), there is a higher clearance of the larger PS NMs by 1 hour post-exposure compared

to without the presence of a food source during the excretion phase (mode 1), due to the incoming food pushing out the previously ingested NMs. The presence of the food source still does not result in total clearance of the larger PS NMs from the gut as there is still a residual amount of the larger PS NMs remaining (stuck in the bush border gaps) at 6 hours post exposure.

The presence of the food source during the excretion phase (mode 2) increased the depuration of the smaller PS NMs at 1 hours post-exposure compared to without a food source (mode 1) although at 6 hours post-exposure a large amount (similar to mode 1) still remains. What can be concluded from this is that the majority of the larger NMs are located within the lumen (as seen from TEM) and are able to be pushed along by the incoming food source, increasing the clearance, with only a minimal amount unable to be pushed out by the food as they are trapped in the gaps in the bush border. Contrastingly, the majority of the smaller NMs must be trapped in the gaps and only a small amount remains in the lumen. The NMs in the lumen are able to be pushed out by the incoming food source so that there is an increase in the amount of NMs cleared at 1 hour post exposure (compared to mode 1 with no incoming food), though any new incoming food after the lumen NMs are cleared is not able to push out the majority of the smaller NMs trapped within the gaps, so that overall, the larger PS NMs were cleared more effectively than the smaller ones due to their location primarily in the gut lumen.

Thirdly, incubation of either large or small PS NMs in the food source *C. vulgaris* increased the uptake of both types of PS NMs compared to no incubation in a food source. This is due to the NMs binding to *C. vulgaris* and being taken up incidentally when *D. magna* consume their food source. There is also an increased removal of the smaller NMs from *D. magna* that were originally incubated with the food source (mode 3) compared to without a prior incubation (mode 1) as the NMs are trapped within the intertwining food and get carried along the gut, with a lower likelihood of getting trapped within the gaps of the bush border (as they did in

modes 1 and 2). There is still a residual amount of both the larger and smaller PS NMs present at 6 hours post-exposure as seen with previous presentation modes.

Fourthly, *D. magna* that had previously been fed (mode 4) took up less of the larger PS NMs compared to those with no prior feeding step (mode 1) indicating that the presence of food already within the gut influences the rate of uptake of subsequent particulates though a similar amount of the smaller PS NMs were taken up compared to with no prior feeding (mode 1) indicating smaller PS NMs are taken up passively.

Incubation of both types of PS NMs within conditioned HH combo medium caused agglomeration of smaller PS NMs but only at longer incubation times. Larger PS NMs remained stable in conditioned medium over the assessed incubation times.

D. magna also release carbohydrates into their surroundings though there is no clear increase in concentration over time as seen with proteins. *D. magna* also release substantially less carbohydrates ranging from 28-49 μg/mL compared to proteins.

The work in this chapter highlights the importance of presentation mode of NMs to organisms and how this affects their uptake. Importantly, the alternative scenarios investigated here are potentially more representative of real-world exposures and shed important light on how exposure conditions can be modulated to better reflect those found in natural environments. Many standardized testing procedures investigating uptake and depuration do not take into account these factors which greatly influence retention and bioaccumulation and thus should be considered in any future revision of the test guidelines for use with NMs.

To conclude overall, this project investigated how various factors such as NM charge, shape, size, chemical composition, the presence of secreted biomolecules and presentation mode affected the toxicity and uptake of NMs towards the organism *D. magna.* This study brings to light the importance of assessing different factors that affect toxicity and uptake studies that

are not always considered imperative in fresh-water toxicity testing, and demonstrates that multiple mechanisms of effect might be progressing in parallel including both chemical and physical changes in the organisms.

7

Future Work

After the completion of a thesis it is important to consider what future work would be useful to be conducted in order to further the work initiated in this thesis and to reflect upon the idea, 'if I knew then what I know now'.

The first chapter looked at how the presence of an adsorbed corona bound to negatively charged PS NMs caused a decrease in the subsequent feeding of *D. magna* on *C. vulgaris*. This was only assessed over short time periods so that the decrease was not significant though it would be useful to assess this over a longer time period >24 hours to monitor if this decrease in feeding does eventually become significant and result in developmental or toxicity effects due to lack of energy.

In the second chapter, confocal imaging of the uptake of Au NMs was originally assessed via reflectance confocal microscopy though the carapace of *D. magna* was highly reflectent itself so that the control cultures had substantial reflectance within their gut from consuming parts of their own shed carapace in the absence of food. Now knowing this, harvesting the shed carapace and incubating fluorescent NMs would be indicative of whether *D. magna* uptake NMs via carapace ingestion. This would be useful to know as *D. magna* are constantly moulting, and shedding of carapace is a known mechanism for removal of toxicants such as metals, so that there would be a constant mechanism of enhanced entry if NMs were incidentally ingested along with the carapace in the absence of a more nutritious food source. This work could also be enhanced by quantitatively assessing the amount of Au NMs taken up and excreted by *D. magna* by ICP-OES or single-particle ICP-MS in order to assess the gold content adhered to the carapace compared to the total consumed gold. A subsequent piece of work could be to neutralize a proportion of charges on the NM surface to see if this effects

ROS generation. Epoxy resin embedment of the *D. magna* exposed to spherical and rod shaped NMs would enhance the knowledge base regarding gold NM retention to identify if differently shaped NMs align themselves differently within the gut bush boarder, and whether the more toxic NMs exert their effects through damage of the gut and subsequent access to other tissues. Further mechanistic work could also be conducted to determine why the corona-coated spherical NMs were considerably more toxic along with measuring gene expression to assess if stress genes were upregulated so that all energy was diverted, leading to a decrease in moulting.

The third chapter looked at presentation modes of differently sized PS NMs and how this affected uptake and retention within *D. magna*. Although this was a comprehensive assessment, in all likelihood, there will be a combination of factors and presentation modes affecting *D. magna* in the environment, such as accidental releases and spills where local high concentrations may exist for short times, and continuous low exposures via the food chain, for example. Assessment of uptake and retention using a combination of methods simultaneously, as well as sequentially, will help to further develop the picture of how *D. magna* would uptake and retain NMs. Method development for converting the fluorescence of NMs retained within the gut to number concentration would be an important next step, bearing in mind that fluorescence within the gut is likely to be influenced by varying pH along the gut as well as compaction of NMs resulting in quenching. Thus, pH sensitive NMs could be used as a probe of gut pH and used to quantify how fluorescence changes along the gut.

8

References

ALBANESE, A. & CHAN, W. C. 2011. Effect of gold nanoparticle aggregation on cell uptake and toxicity. *ACS nano,* 5**,** 5478-5489.

ALBANESE, A., TANG, P. S. & CHAN, W. C. 2012. The effect of nanoparticle size, shape, and surface chemistry on biological systems. *Annual review of biomedical engineering,* 14**,** 1-16.

ALBANESE, A., WALKEY, C. D., OLSEN, J. B., GUO, H., EMILI, A. & CHAN, W. C. 2014. Secreted biomolecules alter the biological identity and cellular interactions of nanoparticles. *Acs Nano,* 8**,** 5515-5526.

ALLEN, T. 2013. *Particle size measurement*, Springer.

ANDERSON, B. & BROWN, L. 1930. A study of chitin secretion in Daphnia magna. *Physiological Zoology,* 3**,** 485-493.

AREFI, M. R. & REZAEI-ZARCHI, S. 2012. Synthesis of zinc oxide nanoparticles and their effect on the compressive strength and setting time of self-compacted concrete paste as cementitious composites. *International journal of molecular sciences,* 13**,** 4340-4350.

AUFFAN, M., ROSE, J., BOTTERO, J.-Y., LOWRY, G. V., JOLIVET, J.-P. & WIESNER, M. R. 2009. Towards a definition of inorganic nanoparticles from an environmental, health and safety perspective. *Nature nanotechnology,* 4**,** 634-641.

BAALOUSHA, M. & LEAD, J. 2007. Size fractionation and characterization of natural aquatic colloids and nanoparticles. *Science of the total environment,* 386**,** 93-102.

BAALOUSHA, M. & LEAD, J. 2012. Rationalizing nanomaterial sizes measured by atomic force microscopy, flow field-flow fractionation, and dynamic light scattering: sample preparation, polydispersity, and particle structure. *Environmental science & technology,* 46**,** 6134-6142.

BADAWY, A. M. E., LUXTON, T. P., SILVA, R. G., SCHECKEL, K. G., SUIDAN, M. T. & TOLAYMAT, T. M. 2010. Impact of environmental conditions (pH, ionic strength, and electrolyte type) on the surface charge and aggregation of silver nanoparticles suspensions. *Environmental science & technology,* 44**,** 1260-1266.

BAER, K. N. & GOULDEN, C. E. 1998. Evaluation of a high-hardness COMBO medium and frozen algae forDaphnia magna. *Ecotoxicology and environmental safety,* 39**,** 201-206.

BARATA, C., VARO, I., NAVARRO, J. C., ARUN, S. & PORTE, C. 2005. Antioxidant enzyme activities and lipid peroxidation in the freshwater cladoceran Daphnia magna exposed to redox cycling compounds. *Comparative Biochemistry and Physiology Part C: Toxicology & Pharmacology,* 140**,** 175-186.

BAUN, A., HARTMANN, N. B., GRIEGER, K. & KUSK, K. O. 2008. Ecotoxicity of engineered nanoparticles to aquatic invertebrates: a brief review and recommendations for future toxicity testing. *Ecotoxicology,* 17**,** 387-395.

BECHERI, A., DÜRR, M., NOSTRO, P. L. & BAGLIONI, P. 2008. Synthesis and characterization of zinc oxide nanoparticles: application to textiles as UV-absorbers. *Journal of Nanoparticle Research,* 10**,** 679-689.

BECKER, D., BRINKMANN, B. F., ZEIS, B. & PAUL, R. J. 2011. Acute changes in temperature or oxygen availability induce ROS fluctuations in Daphnia magna linked with fluctuations of reduced and oxidized glutathione, catalase activity and gene (haemoglobin) expression. *Biology of the Cell,* 103**,** 351-363.

BERG, L., LSSON, S. & LASCOUX, M. 2001. Fitness and sexual response to population density. *Freshwater Biology,* 46**,** 667ą677.

BERNTON, E. W., BEACH, J. E., HOLADAY, J. W., SMALLRIDGE, R. C. & FEIN, H. G. 1987. Release of multiple hormones by a direct action of interleukin-1 on pituitary cells. DTIC Document.
BHATIA, S. 2016. Nanoparticles Types, Classification, Characterization, Fabrication Methods and Drug Delivery Applications. *Natural Polymer Drug Delivery Systems.* Springer.
BIANCO, A., KOSTARELOS, K. & PRATO, M. 2005. Applications of carbon nanotubes in drug delivery. *Current opinion in chemical biology,* 9**,** 674-679.
BISWAS, P. & WU, C.-Y. 2005. Nanoparticles and the environment. *Journal of the Air & Waste Management Association,* 55**,** 708-746.
BLANCHER, C. & JONES, A. 2001. SDS -PAGE and Western Blotting Techniques. *Methods Mol Med,* 57**,** 145-62.
BLANCO, E., SHEN, H. & FERRARI, M. 2015. Principles of nanoparticle design for overcoming biological barriers to drug delivery. *Nature biotechnology,* 33**,** 941-951.
BLASER, S. A., SCHERINGER, M., MACLEOD, M. & HUNGERBÜHLER, K. 2008. Estimation of cumulative aquatic exposure and risk due to silver: contribution of nano-functionalized plastics and textiles. *Science of the total environment,* 390**,** 396-409.
BORM, P., KLAESSIG, F. C., LANDRY, T. D., MOUDGIL, B., PAULUHN, J., THOMAS, K., TROTTIER, R. & WOOD, S. 2006. Research strategies for safety evaluation of nanomaterials, part V: role of dissolution in biological fate and effects of nanoscale particles. *Toxicological Sciences,* 90**,** 23-32.
BORM, P. J. & MÜLLER-SCHULTE, D. 2006. Nanoparticles in drug delivery and environmental exposure: same size, same risks? *Nanomedicine,* 1**,** 235-249.
BOTHA, T. L., BOODHIA, K. & WEPENER, V. 2016. Adsorption, uptake and distribution of gold nanoparticles in Daphnia magna following long term exposure. *Aquatic Toxicology,* 170**,** 104-111.
BOZICH, J. S., LOHSE, S. E., TORELLI, M. D., MURPHY, C. J., HAMERS, R. J. & KLAPER, R. D. 2014. Surface chemistry, charge and ligand type impact the toxicity of gold nanoparticles to Daphnia magna. *Environmental Science: Nano,* 1**,** 260-270.
BRETT, M. T., KAINZ, M. J., TAIPALE, S. J. & SESHAN, H. 2009. Phytoplankton, not allochthonous carbon, sustains herbivorous zooplankton production. *Proceedings of the National Academy of Sciences,* 106**,** 21197-21201.
BRINKLEY, J. M., HAUGLAND, R. P. & SINGER, V. L. 1994. Fluorescent microparticles with controllable enhanced stokes shift. Google Patents.
BUFFLE, J., WILKINSON, K. J., STOLL, S., FILELLA, M. & ZHANG, J. 1998. A generalized description of aquatic colloidal interactions: the three-colloidal component approach. *Environmental Science & Technology,* 32**,** 2887-2899.
CAI, H. & YAO, P. 2014. Gold nanoparticles with different amino acid surfaces: Serum albumin adsorption, intracellular uptake and cytotoxicity. *Colloids and Surfaces B: Biointerfaces,* 123**,** 900-906.
CAO, G. 2004. *Nanostructures and nanomaterials: synthesis, properties and applications*, World Scientific.
CARVALHO, I. C., MEZZAPESA, F. P., KAZANSKY, P. G., DEPARIS, O., KAWAZU, M. & SAKAGUCHI, K. 2007. Dissolution of embedded gold nanoparticles in sol–gel glass film. *Materials Science and Engineering: C,* 27**,** 1313-1316.
CEDERVALL, T., LYNCH, I., LINDMAN, S., BERGGÅRD, T., THULIN, E., NILSSON, H., DAWSON, K. A. & LINSE, S. 2007. Understanding the nanoparticle–protein corona using methods to quantify exchange rates and affinities of proteins for nanoparticles. *Proceedings of the National Academy of Sciences,* 104**,** 2050-2055.
CLAUDIA, M., KRISTIN, Ö., JENNIFER, O., EVA, R. & ELEONORE, F. 2017. Comparison of fluorescence-based methods to determine nanoparticle uptake by phagocytes and non-phagocytic cells in vitro. *Toxicology*.
CO-OPERATION, O. F. E. & DEVELOPMENT 2012. *Test No. 211: Daphnia Magna Reproduction Test*, OECD Publishing.

COLE, M., LINDEQUE, P., HALSBAND, C. & GALLOWAY, T. S. 2011. Microplastics as contaminants in the marine environment: a review. *Marine pollution bulletin,* 62**,** 2588-2597.
COORS, A., HAMMERS-WIRTZ, M. & RATTE, H. T. 2004. Adaptation to environmental stress in Daphnia magna simultaneously exposed to a xenobiotic. *Chemosphere,* 56**,** 395-404.
DABRUNZ, A., DUESTER, L., PRASSE, C., SEITZ, F., ROSENFELDT, R., SCHILDE, C., SCHAUMANN, G. E. & SCHULZ, R. 2011a. Biological surface coating and molting inhibition as mechanisms of TiO2 nanoparticle toxicity in Daphnia magna. *PLoS One,* 6**,** e20112.
DABRUNZ, A., DUESTER, L., PRASSE, C., SEITZ, F., ROSENFELDT, R., SCHILDE, C., SCHAUMANN, G. E. & SCHULZ, R. 2011b. Biological surface coating and molting inhibition as mechanisms of TiO 2 nanoparticle toxicity in Daphnia magna. *PLoS One,* 6**,** e20112.
DAS, R., NATH, S., CHAKDAR, D., GOPE, G. & BHATTACHARJEE, R. 2009. Preparation of silver nanoparticles and their characterization. *Journal of nanotechnology,* 5**,** 1-6.
DELL'ORCO, D., LUNDQVIST, M., OSLAKOVIC, C., CEDERVALL, T. & LINSE, S. 2010. Modeling the time evolution of the nanoparticle-protein corona in a body fluid. *PloS one,* 5**,** e10949.
DENG, Z. J., LIANG, M., MONTEIRO, M., TOTH, I. & MINCHIN, R. F. 2011. Nanoparticle-induced unfolding of fibrinogen promotes Mac-1 receptor activation and inflammation. *Nature nanotechnology,* 6**,** 39-44.
DO SUL, J. A. I. & COSTA, M. F. 2014. The present and future of microplastic pollution in the marine environment. *Environmental Pollution,* 185**,** 352-364.
DOMINGUEZ, G. A., LOHSE, S. E., TORELLI, M. D., MURPHY, C. J., HAMERS, R. J., ORR, G. & KLAPER, R. D. 2015. Effects of charge and surface ligand properties of nanoparticles on oxidative stress and gene expression within the gut of Daphnia magna. *Aquatic Toxicology,* 162**,** 1-9.
DOMINIKA DYBOWSKA, A., LUCIENE MALTONI, K., PIELLA, J., NAJORKA, J., PUNTES, V. & VALSAMI-JONES, E. Naturally occurring clay nanoparticles in Latosols of Brazil central region: detection and characterization. EGU General Assembly Conference Abstracts, 2015. 8056.
DOWNING, J. A. & RIGLER, F. H. 1984. A manual on methods for the assessment of secondary productivity. *Fresh Waters,* 2.
DUIS, K. & COORS, A. 2016. Microplastics in the aquatic and terrestrial environment: sources (with a specific focus on personal care products), fate and effects. *Environmental Sciences Europe,* 28**,** 1.
DUNPHY GUZMAN, K. A., TAYLOR, M. R. & BANFIELD, J. F. 2006. Environmental risks of nanotechnology: National nanotechnology initiative funding, 2000-2004. *Environmental Science & Technology,* 40**,** 1401-1407.
EBERT, D. 2005. Ecology, epidemiology, and evolution of parasitism in Daphnia.
ERUSLANOV, E. & KUSMARTSEV, S. 2010. Identification of ROS using oxidized DCFDA and flow-cytometry. *Advanced protocols in oxidative stress II***,** 57-72.
FRÖHLICH, E. 2012. The role of surface charge in cellular uptake and cytotoxicity of medical nanoparticles. *Int J Nanomedicine,* 7**,** 5577-91.
FULDA, S., GORMAN, A. M., HORI, O. & SAMALI, A. 2010. Cellular stress responses: cell survival and cell death. *International journal of cell biology,* 2010.
GEFFROY, B., LADHAR, C., CAMBIER, S., TREGUER-DELAPIERRE, M., BRÈTHES, D. & BOURDINEAUD, J.-P. 2012. Impact of dietary gold nanoparticles in zebrafish at very low contamination pressure: the role of size, concentration and exposure time. *Nanotoxicology,* 6**,** 144-160.
GELDERBLOM, H. R. 1996. Structure and classification of viruses.
GENG, Y., DALHAIMER, P., CAI, S., TSAI, R., TEWARI, M., MINKO, T. & DISCHER, D. E. 2007. Shape effects of filaments versus spherical particles in flow and drug delivery. *Nature nanotechnology,* 2**,** 249-255.

GEWERT, B., PLASSMANN, M. M. & MACLEOD, M. 2015. Pathways for degradation of plastic polymers floating in the marine environment. *Environmental Science: Processes & Impacts,* 17**,** 1513-1521.
GOTTSCHALK, F., SONDERER, T., SCHOLZ, R. W. & NOWACK, B. 2009. Modeled environmental concentrations of engineered nanomaterials (TiO2, ZnO, Ag, CNT, fullerenes) for different regions. *Environmental science & technology,* 43**,** 9216-9222.
GRATTON, S. E., ROPP, P. A., POHLHAUS, P. D., LUFT, J. C., MADDEN, V. J., NAPIER, M. E. & DESIMONE, J. M. 2008. The effect of particle design on cellular internalization pathways. *Proceedings of the National Academy of Sciences,* 105**,** 11613-11618.
HANAZATO, T. & DODSON, S. I. 1995. Synergistic effects of low oxygen concentration, predator kairomone, and a pesticide on the cladoceran Daphnia pulex. *Limnology and Oceanography,* 40**,** 700-709.
HANDY, R. D., OWEN, R. & VALSAMI-JONES, E. 2008. The ecotoxicology of nanoparticles and nanomaterials: current status, knowledge gaps, challenges, and future needs. *Ecotoxicology,* 17**,** 315-325.
HASSELLÖV, M., READMAN, J. W., RANVILLE, J. F. & TIEDE, K. 2008. Nanoparticle analysis and characterization methodologies in environmental risk assessment of engineered nanoparticles. *Ecotoxicology,* 17**,** 344-361.
HATTO, P. 2011. ISO concensus definitions relevant to nanomaterials and nanotechnologies. *4th Annual Nano Safety for Success Dialogue. ISO TC 229and BSI NTI/1 Nanotechnologies standardization committees. 29th and 30th March*.
HAUCK, T. S., GHAZANI, A. A. & CHAN, W. C. 2008. Assessing the effect of surface chemistry on gold nanorod uptake, toxicity, and gene expression in mammalian cells. *Small,* 4**,** 153-159.
HAYASHI, Y., MICLAUS, T., SCAVENIUS, C., KWIATKOWSKA, K., SOBOTA, A., ENGELMANN, P., SCOTT-FORDSMAND, J. J., ENGHILD, J. J. & SUTHERLAND, D. S. 2013. Species differences take shape at nanoparticles: protein corona made of the native repertoire assists cellular interaction. *Environmental science & technology,* 47**,** 14367-14375.
HIBBS, A. R. 2004. What is Fluorescence? *Confocal Microscopy for Biologists.* Boston, MA: Springer US.
HOCHELLA, M. F. 2002. There's plenty of room at the bottom: Nanoscience in geochemistry. *Geochimica et Cosmochimica Acta,* 66**,** 735-743.
HOEK, C., MANN, D. & JAHNS, H. M. 1995. *Algae: an introduction to phycology*, Cambridge university press.
HOLEC, D., DUMITRASCHKEWITZ, P., FISCHER, F. & VOLLATH, D. 2014. Size-dependent surface energies of Au nanoparticles. *arXiv preprint arXiv:1412.7195*.
HOLMBERG, K., SHAH, D. O. & SCHWUGER, M. J. 2002. *Handbook of applied surface and colloid chemistry*, Wiley New York.
HUK, A., IZAK-NAU, E., REIDY, B., BOYLES, M., DUSCHL, A., LYNCH, I. & DUŠINSKA, M. 2014. Is the toxic potential of nanosilver dependent on its size? *Particle and fibre toxicology,* 11**,** 1.
HUNG, A., MWENIFUMBO, S., MAGER, M., KUNA, J. J., STELLACCI, F., YAROVSKY, I. & STEVENS, M. M. 2011. Ordering surfaces on the nanoscale: implications for protein adsorption. *Journal of the American Chemical Society,* 133**,** 1438-1450.
HUNTER, R. J. 2013. *Zeta potential in colloid science: principles and applications*, Academic press.
IVASK, A., KURVET, I., KASEMETS, K., BLINOVA, I., ARUOJA, V., SUPPI, S., VIJA, H., KÄKINEN, A., TITMA, T. & HEINLAAN, M. 2014. Size-dependent toxicity of silver nanoparticles to bacteria, yeast, algae, crustaceans and mammalian cells in vitro. *PloS one,* 9**,** e102108.
JAIN, P. K., LEE, K. S., EL-SAYED, I. H. & EL-SAYED, M. A. 2006. Calculated absorption and scattering properties of gold nanoparticles of different size, shape, and composition: applications in biological imaging and biomedicine. *The Journal of Physical Chemistry B,* 110**,** 7238-7248.

JENSEN, J. H. & GORDON, M. S. 1995. On the number of water molecules necessary to stabilize the glycine zwitterion. *Journal of the American Chemical Society,* 117**,** 8159.
JOHNSTON, H. J., SEMMLER-BEHNKE, M., BROWN, D. M., KREYLING, W., TRAN, L. & STONE, V. 2010. Evaluating the uptake and intracellular fate of polystyrene nanoparticles by primary and hepatocyte cell lines in vitro. *Toxicology and applied pharmacology,* 242**,** 66-78.
JU-NAM, Y. & LEAD, J. R. 2008. Manufactured nanoparticles: An overview of their chemistry, interactions and potential environmental implications. *Science of The Total Environment,* 400**,** 396-414.
KALMAN, J., PAUL, K. B., KHAN, F. R., STONE, V. & FERNANDES, T. F. 2015. Characterisation of bioaccumulation dynamics of three differently coated silver nanoparticles and aqueous silver in a simple freshwater food chain. *Environmental Chemistry,* 12**,** 662-672.
KARLSSON, H. L., GUSTAFSSON, J., CRONHOLM, P. & MÖLLER, L. 2009. Size-dependent toxicity of metal oxide particles—a comparison between nano-and micrometer size. *Toxicology letters,* 188**,** 112-118.
KELLY, K. L., CORONADO, E., ZHAO, L. L. & SCHATZ, G. C. 2003. The optical properties of metal nanoparticles: the influence of size, shape, and dielectric environment. *The Journal of Physical Chemistry B,* 107**,** 668-677.
KOHL, H. & REIMER, L. 2008. *Transmission Electron Microscopy*, Springer.
KRISTIANSEN, K. A., JENSEN, P. E., MØLLER, I. M. & SCHULZ, A. 2009. Monitoring reactive oxygen species formation and localisation in living cells by use of the fluorescent probe CM-H2DCFDA and confocal laser microscopy. *Physiologia plantarum,* 136**,** 369-383.
KROEMER, G. 1997. Mitochondrial implication in apoptosis. Towards an endosymbiont hypothesis of apoptosis evolution. *Cell death and differentiation,* 4**,** 443-456.
KRUMOVA, K. & COSA, G. 2016. Overview of Reactive Oxygen Species.
KULASINGAM, V. & DIAMANDIS, E. P. 2007. Proteomics Analysis of Conditioned Media from Three Breast Cancer Cell Lines A Mine for Biomarkers and Therapeutic Targets. *Molecular & Cellular Proteomics,* 6**,** 1997-2011.
LEE, C., WEI, X., KYSAR, J. W. & HONE, J. 2008. Measurement of the elastic properties and intrinsic strength of monolayer graphene. *science,* 321**,** 385-388.
LETFULLIN, R. R., IVERSEN, C. B. & GEORGE, T. F. 2011. Modeling nanophotothermal therapy: kinetics of thermal ablation of healthy and cancerous cell organelles and gold nanoparticles. *Nanomedicine: Nanotechnology, Biology and Medicine,* 7**,** 137-145.
LIM, J., YEAP, S. P., CHE, H. X. & LOW, S. C. 2013. Characterization of magnetic nanoparticle by dynamic light scattering. *Nanoscale research letters,* 8**,** 381.
LOOS, C., SYROVETS, T., MUSYANOVYCH, A., MAILÄNDER, V., LANDFESTER, K., NIENHAUS, G. U. & SIMMET, T. 2014. Functionalized polystyrene nanoparticles as a platform for studying bio–nano interactions. *Beilstein journal of nanotechnology,* 5**,** 2403-2412.
LOVERN, S. B., STRICKLER, J. R. & KLAPER, R. 2007. Behavioral and physiological changes in Daphnia magna when exposed to nanoparticle suspensions (titanium dioxide, nano-C60, and C60HxC70Hx). *Environmental science & technology,* 41**,** 4465-4470.
LUNDQVIST, M., STIGLER, J., CEDERVALL, T., BERGGÅRD, T., FLANAGAN, M. B., LYNCH, I., ELIA, G. & DAWSON, K. 2011. The evolution of the protein corona around nanoparticles: a test study. *ACS nano,* 5**,** 7503-7509.
LUNDQVIST, M., STIGLER, J., ELIA, G., LYNCH, I., CEDERVALL, T. & DAWSON, K. A. 2008. Nanoparticle size and surface properties determine the protein corona with possible implications for biological impacts. *Proceedings of the National Academy of Sciences,* 105**,** 14265-14270.
LUNOV, O., SYROVETS, T., LOOS, C., BEIL, J., DELACHER, M., TRON, K., NIENHAUS, G. U., MUSYANOVYCH, A., MAILANDER, V. & LANDFESTER, K. 2011. Differential uptake of functionalized polystyrene nanoparticles by human macrophages and a monocytic cell line. *Acs Nano,* 5**,** 1657-1669.

LYNCH, I., DAWSON, K., LEAD, J. & VALSAMI-JONES, E. 2014. Macromolecular Coronas and their importance in Nanotoxicology and Nanoecotoxicology. *Frontiers of Nanoscience. Elsevier, Amsterdam*.
LYNCH, I. & DAWSON, K. A. 2008. Protein-nanoparticle interactions. *Nano today,* 3**,** 40-47.
MACMAHON, J. & RIGLER, F. 1965. Feeding rate of Daphnia magna Straus in different foods labeled with radioactive phosphorous. *Limnol. Oceanogr,* 10**,** 105-l.
MAHAPATRA, I., SUN, T. Y., CLARK, J. R., DOBSON, P. J., HUNGERBUEHLER, K., OWEN, R., NOWACK, B. & LEAD, J. 2015. Probabilistic modelling of prospective environmental concentrations of gold nanoparticles from medical applications as a basis for risk assessment. *Journal of nanobiotechnology,* 13**,** 93.
MAURER-JONES, M. A., GUNSOLUS, I. L., MURPHY, C. J. & HAYNES, C. L. 2013. Toxicity of engineered nanoparticles in the environment. *Analytical chemistry,* 85**,** 3036-3049.
MEGHARAJ, M., KANTACHOTE, D., SINGLETON, I. & NAIDU, R. 2000. Effects of long-term contamination of DDT on soil microflora with special reference to soil algae and algal transformation of DDT. *Environmental Pollution,* 109**,** 35-42.
MEISE, C. J., MUNNS, W. R. & HAIRSTON, N. G. 0 1985, by the American Society of Limnology and Oceanography, Inc. An analysis of the feeding behavior of Daphvtia pulex'.
MISRA, S. K., DYBOWSKA, A., BERHANU, D., LUOMA, S. N. & VALSAMI-JONES, E. 2012. The complexity of nanoparticle dissolution and its importance in nanotoxicological studies. *Science of the total environment,* 438**,** 225-232.
MONOPOLI, M. P., PITEK, A. S., LYNCH, I. & DAWSON, K. A. 2013. Formation and characterization of the nanoparticle–protein corona. *Nanomaterial Interfaces in Biology: Methods and Protocols***,** 137-155.
MUELLER, N. C. & NOWACK, B. 2008. Exposure modeling of engineered nanoparticles in the environment. *Environmental science & technology,* 42**,** 4447-4453.
NADLER, M., MAHRHOLZ, T., RIEDEL, U., SCHILDE, C. & KWADE, A. 2008. Preparation of colloidal carbon nanotube dispersions and their characterisation using a disc centrifuge. *Carbon,* 46**,** 1384-1392.
NANDA, K., MAISELS, A., KRUIS, F., FISSAN, H. & STAPPERT, S. 2003. Higher surface energy of free nanoparticles. *Physical review letters,* 91**,** 106102.
NASSER, F. & LYNCH, I. 2015. Secreted protein eco-corona mediates uptake and impacts of polystyrene nanoparticles on Daphnia magna. *Journal of proteomics*.
NEUN, B. W. & STERN, S. T. 2011. Monitoring lysosomal activity in nanoparticle-treated cells. *Characterization of Nanoparticles Intended for Drug Delivery***,** 207-212.
NIELSEN, S. S. 2010. Phenol-sulfuric acid method for total carbohydrates. *Food Analysis Laboratory Manual.* Springer.
NIKOOBAKHT, B., WANG, J. & EL-SAYED, M. A. 2002. Surface-enhanced Raman scattering of molecules adsorbed on gold nanorods: off-surface plasmon resonance condition. *Chemical Physics Letters,* 366**,** 17-23.
OOSTERHUIS, S. S., BAARS, M. A. & BRETELER, W. C. K. 2000. Release of the enzyme chitobiase by the copepod Temora longicornis: characteristics and potential tool for estimating crustacean biomass production in the sea. *Marine Ecology Progress Series,* 196**,** 195-206.
PAN, Y., LEIFERT, A., RUAU, D., NEUSS, S., BORNEMANN, J., SCHMID, G., BRANDAU, W., SIMON, U. & JAHNEN-DECHENT, W. 2009. Gold nanoparticles of diameter 1.4 nm trigger necrosis by oxidative stress and mitochondrial damage. *Small,* 5**,** 2067-2076.
PAN, Y., NEUSS, S., LEIFERT, A., FISCHLER, M., WEN, F., SIMON, U., SCHMID, G., BRANDAU, W. & JAHNEN-DECHENT, W. 2007. Size-dependent cytotoxicity of gold nanoparticles. *Small,* 3**,** 1941-1949.
PARDEIKE, J., HOMMOSS, A. & MÜLLER, R. H. 2009. Lipid nanoparticles (SLN, NLC) in cosmetic and pharmaceutical dermal products. *International Journal of Pharmaceutics,* 366**,** 170-184.

PATEL, P. C., GILJOHANN, D. A., DANIEL, W. L., ZHENG, D., PRIGODICH, A. E. & MIRKIN, C. A. 2010. Scavenger receptors mediate cellular uptake of polyvalent oligonucleotide-functionalized gold nanoparticles. *Bioconjugate chemistry,* 21**,** 2250-2256.
PIRC, U., VIDMAR, M., MOZER, A. & KRŽAN, A. 2016. Emissions of microplastic fibers from microfiber fleece during domestic washing. *Environmental Science and Pollution Research,* 23**,** 22206-22211.
PISANIC, T., JIN, S. & SHUBAYEV, V. 2009. Nanotoxicity: From in vivo and In vitro models to health risks. John Wiley & Sons, Ltd., London, UK.
PORCELLA, D. B., RIXFORD, C. E. & SLATER, J. V. 1969. Molting and Calcification in Daphnia magna. *Physiological Zoology,* 42**,** 148-159.
RAHMAN, M., LAURENT, S., TAWIL, N., YAHIA, L. & MAHMOUDI, M. 2013. *Protein-nanoparticle interactions*, Springer.
RASMUSSEN, K., GONZÁLEZ, M., KEARNS, P., SINTES, J. R., ROSSI, F. & SAYRE, P. 2016. Review of achievements of the OECD Working Party on Manufactured Nanomaterials' Testing and Assessment Programme. From exploratory testing to test guidelines. *Regulatory Toxicology and Pharmacology,* 74**,** 147-160.
RAUSCH, K., REUTER, A., FISCHER, K. & SCHMIDT, M. 2010. Evaluation of nanoparticle aggregation in human blood serum. *Biomacromolecules,* 11**,** 2836-2839.
REIMER, L. 1993. Elements of a transmission electron microscope. *Transmission electron microscopy.* Springer.
RENWICK, L., DONALDSON, K. & CLOUTER, A. 2001. Impairment of alveolar macrophage phagocytosis by ultrafine particles. *Toxicology and applied pharmacology,* 172**,** 119-127.
ROMDHANE, A., AUROUSSEAU, M., GUILLET, A. & MAURET, E. 2015. Effect of pH and ionic strength on the electrical charge and particle size distribution of starch nanocrystal suspensions. *Starch-Stärke,* 67**,** 319-327.
ROSENKRANZ, P., CHAUDHRY, Q., STONE, V. & FERNANDES, T. F. 2009. A comparison of nanoparticle and fine particle uptake by Daphnia magna. *Environmental Toxicology and Chemistry,* 28**,** 2142-2149.
SALATIN, S., MALEKI DIZAJ, S. & YARI KHOSROUSHAHI, A. 2015. Effect of the surface modification, size, and shape on cellular uptake of nanoparticles. *Cell biology international,* 39**,** 881-890.
SAPTARSHI, S. R., DUSCHL, A. & LOPATA, A. L. 2013. Interaction of nanoparticles with proteins: relation to bio-reactivity of the nanoparticle. *Journal of nanobiotechnology,* 11**,** 1.
SEE, S. & BALASUBRAMANIAN, R. 2006. Risk assessment of exposure to indoor aerosols associated with Chinese cooking. *Environmental Research,* 102**,** 197-204.
SEOL, S. K., KIM, D., JUNG, S., CHANG, W. S., BAE, Y. M., LEE, K. H. & HWU, Y. 2012. Effect of citrate on poly (vinyl pyrrolidone)-stabilized gold nanoparticles formed by PVP reduction in microwave (MW) synthesis. *Materials Chemistry and Physics,* 137**,** 135-139.
SHAN, L. 2009. Superparamagnetic iron oxide nanoparticles (SPION) stabilized by alginate.
SIDDIQI, N. J., ABDELHALIM, M. A. K., EL-ANSARY, A. K., ALHOMIDA, A. S. & ONG, W. 2012. Identification of potential biomarkers of gold nanoparticle toxicity in rat brains. *Journal of neuroinflammation,* 9**,** 1.
SKJOLDING, L. M., KERN, K., HJORTH, R., HARTMANN, N., OVERGAARD, S., MA, G., VEINOT, J. & BAUN, A. 2014. Uptake and depuration of gold nanoparticles in Daphnia magna. *Ecotoxicology,* 23**,** 1172-1183.
SMAYDA, T. J. 1997. Harmful algal blooms: their ecophysiology and general relevance to phytoplankton blooms in the sea. *Limnology and oceanography,* 42**,** 1137-1153.
SMITH, P., KROHN, R. I., HERMANSON, G., MALLIA, A., GARTNER, F., PROVENZANO, M., FUJIMOTO, E., GOEKE, N., OLSON, B. & KLENK, D. 1985. Measurement of protein using bicinchoninic acid. *Analytical biochemistry,* 150**,** 76-85.

SONDI, I. & SALOPEK-SONDI, B. 2004. Silver nanoparticles as antimicrobial agent: a case study on E. coli as a model for Gram-negative bacteria. *Journal of colloid and interface science,* 275**,** 177-182.
SOTO, K., CARRASCO, A., POWELL, T., GARZA, K. & MURR, L. 2005. Comparative in vitro cytotoxicity assessment of some manufacturednanoparticulate materials characterized by transmissionelectron microscopy. *Journal of Nanoparticle Research,* 7**,** 145-169.
SPERLING, R. A. & PARAK, W. 2010. Surface modification, functionalization and bioconjugation of colloidal inorganic nanoparticles. *Philosophical Transactions of the Royal Society of London A: Mathematical, Physical and Engineering Sciences,* 368**,** 1333-1383.
STENSBERG, M. C., WEI, Q., MCLAMORE, E. S., PORTERFIELD, D. M., WEI, A. & SEPÚLVEDA, M. S. 2011. Toxicological studies on silver nanoparticles: challenges and opportunities in assessment, monitoring and imaging. *Nanomedicine,* 6**,** 879-898.
SZE, A., ERICKSON, D., REN, L. & LI, D. 2003. Zeta-potential measurement using the Smoluchowski equation and the slope of the current–time relationship in electroosmotic flow. *Journal of colloid and interface science,* 261**,** 402-410.
TANG, C., YIN, C., PEI, Y., ZHANG, M. & WU, L. 2005. New superporous hydrogels composites based on aqueous Carbopol® solution (SPHCcs): synthesis, characterization and in vitro bioadhesive force studies. *European polymer journal,* 41**,** 557-562.
TAYLOR, G., BAIRD, D. J. & SOARES, A. M. 1998. Surface binding of contaminants by algae: consequences for lethal toxicity and feeding to Daphnia magna Straus. *Environmental Toxicology and Chemistry,* 17**,** 412-419.
TEJAMAYA, M., RÖMER, I., MERRIFIELD, R. C. & LEAD, J. R. 2012. Stability of citrate, PVP, and PEG coated silver nanoparticles in ecotoxicology media. *Environmental science & technology,* 46**,** 7011-7017.
TEUTEN, E. L., SAQUING, J. M., KNAPPE, D. R., BARLAZ, M. A., JONSSON, S., BJÖRN, A., ROWLAND, S. J., THOMPSON, R. C., GALLOWAY, T. S. & YAMASHITA, R. 2009. Transport and release of chemicals from plastics to the environment and to wildlife. *Philosophical Transactions of the Royal Society B: Biological Sciences,* 364**,** 2027-2045.
TONG, R., HEMMATI, H. D., LANGER, R. & KOHANE, D. S. 2012. Photoswitchable Nanoparticles for Triggered Tissue Penetration and Drug Delivery. *Journal of the American Chemical Society,* 134**,** 8848-8855.
TURRENS, J. F. 2003. Mitochondrial formation of reactive oxygen species. *The Journal of physiology,* 552**,** 335-344.
VERSLYCKE, T., GHEKIERE, A., RAIMONDO, S. & JANSSEN, C. 2007. Mysid crustaceans as standard models for the screening and testing of endocrine-disrupting chemicals. *Ecotoxicology,* 16**,** 205-219.
WALKER, J. M. 2009. The bicinchoninic acid (BCA) assay for protein quantitation. *The Protein Protocols Handbook***,** 11-15.
WEINBERG, H., GALYEAN, A. & LEOPOLD, M. 2011. Evaluating engineered nanoparticles in natural waters. *TrAC Trends in Analytical Chemistry,* 30**,** 72-83.
WEISS, W., WEILAND, F. & GÖRG, A. 2009. Protein detection and quantitation technologies for gel-based proteome analysis. *Proteomics: Methods and Protocols***,** 59-82.
WINKELMANN, K. & BHUSHAN, B. 2016. Global Perspectives of Nanoscience and Engineering Education. *Science*.
XIA, T., KOVOCHICH, M., BRANT, J., HOTZE, M., SEMPF, J., OBERLEY, T., SIOUTAS, C., YEH, J. I., WIESNER, M. R. & NEL, A. E. 2006. Comparison of the abilities of ambient and manufactured nanoparticles to induce cellular toxicity according to an oxidative stress paradigm. *Nano letters,* 6**,** 1794-1807.
XIAO, Y., VIJVER, M. G., CHEN, G. & PEIJNENBURG, W. J. G. M. 2015. Toxicity and Accumulation of Cu and ZnO Nanoparticles in Daphnia magna. *Environmental Science & Technology,* 49**,** 4657-4664.

XING, B., SENESI, N. & VECITIS, C. D. 2016. *Engineered Nanoparticles and the Environment: Biophysicochemical Processes and Toxicity*, John Wiley & Sons.
YANG, Y. X., SONG, Z. M., CHENG, B., XIANG, K., CHEN, X. X., LIU, J. H., CAO, A., WANG, Y., LIU, Y. & WANG, H. 2014. Evaluation of the toxicity of food additive silica nanoparticles on gastrointestinal cells. *Journal of Applied Toxicology,* 34**,** 424-435.
ZHANG, Y. & MARTIN, S. 2014. Redox proteins and radiotherapy. *Clinical Oncology,* 26**,** 289-300.
ZOU, E. & FINGERMAN, M. 1997. Effects of estrogenic xenobiotics on molting of the water flea, Daphnia magna. *Ecotoxicology and environmental safety,* 38**,** 281-285.